U.PORTO

Doutoramento

Ciências Biomédicas

Immune response to biomaterials:
modulating inflammation towards improved performance of medical devices

Daniel M. Vasconcelos

D

2017

Daniel Fernando Marques de Vasconcelos

Immune response to biomaterials: modulating inflammation towards improved performance of medical devices

Tese de Candidatura ao grau de Doutor em Ciências Biomédicas, submetida ao Instituto de Ciências Biomédicas Abel Salazar da Universidade do Porto.

Orientador – Professor Doutor Mário A. Barbosa

Categoria – Professor catedrático

Afiliação – Instituto de Ciências Biomédicas Abel Salazar (ICBAS), Instituto de Investigação e Inovação em Saúde (i3S) e Instituto de Engenharia Biomédica (INEB), Universidade do Porto

Coorientador – Doutora Meriem Lamghari

Categoria – Investigadora Auxiliar

Afiliação – Instituto de Ciências Biomédicas Abel Salazar (ICBAS), Instituto de Investigação e Inovação em Saúde (i3S) e Instituto de Engenharia Biomédica (INEB), Universidade do Porto

Coorientador – Doutora Susana G. Santos

Categoria – Investigadora Auxiliar

Afiliação – Instituto de Investigação e Inovação em Saúde (i3S) e Instituto de Engenharia Biomédica (INEB), Universidade do Porto

This PhD thesis was financially supported by the FCT PhD fellowship SFRH/BD/87516/2012.

This work was financed by FEDER - Fundo Europeu de Desenvolvimento Regional funds through the COMPETE 2020 - Operacional Programme for Competitiveness and Internationalisation (POCI), Portugal 2020, the project (NORTE-01-0145-FEDER-000012), supported by Norte Portugal Regional Operational Programme (NORTE 2020), under the PORTUGAL 2020 Partnership Agreement, through the European Regional Development Fund (ERDF) and by Portuguese funds through FCT - Fundação para a Ciência e a Tecnologia/ Ministério da Ciência, Tecnologia e Inovação in the framework of the projects: “Y1 receptor based therapy for local bone repair: antagonist behavior and delivery in challenged bone microenvironment” (PTDC/BIM-MED/1047/2012); “Incorporation of inflammatory signals in the development of biomaterials for bone repair/regeneration: an integrated approach” (PTDC/SAU-BEB/099954/2008) and "Institute for Research and Innovation in Health Sciences" (POCI-01-0145-FEDER-007274).

U.PORTO

FCT Fundação para a Ciência e a Tecnologia
MINISTÉRIO DA CIÊNCIA, TECNOLOGIA E ENSINO SUPERIOR

COMPETE
PROGRAMA OPERACIONAL FACTORES DE COMPETITIVIDADE

QREN QUADRO DE REFERÊNCIA ESTRATÉGICO NACIONAL
PORTUGAL 2007.2013

European Union
European Regional Development Fund

Agradecimentos

Não será por acaso que a secção dos agradecimentos vem no início. Ao longo dos anos que estive no INEB foram muitos os que contribuíram para o trabalho que agora aqui publico. O doutoramento, à semelhança de uma caminhada, foi-se revelando. O plano foi-se alterando fruto dos caminhos e das gentes com quem me fui cruzando. Estou convencido que é assim que aprendemos: a perguntar, a pensar, e a tentar, de preferência juntos. Parece-me que a vida é demasiado curta para errarmos sozinhos demasiadas vezes. Acredito que, mais do que as tecnologias que aplicamos e criamos, foram as ligações que fui estabelecendo que determinaram o sucesso deste doutoramento. Sem dúvida nenhuma que parte disto é vosso.

Gostaria de agradecer ao Professor Mário pela sua orientação, por acreditar sempre em mim e por me apoiar em todos os momentos e escolhas. Lançou-me o desafio, eu aceitei e fomos bem sucedidos. Obrigado por me inspirar, por trabalhar comigo e pela amizade.

A par do Prof. Mário, a minha orientação contou com a preciosa ajuda da Meriem e da Susana, às quais estou muito grato. Obrigado Meriem pelo seu cuidado, preocupação e exigência. Ajudou-me muito a manter um bom ritmo de trabalho e a definir e cumprir os objetivos. Agradeço toda a ajuda e apoio da Susana. Muitas foram as horas que investiste a discutir e a programar experiências comigo, sem contar com as inúmeras correções às versões e revisões dos artigos.

Além dos meus orientadores, foram os membros de equipa Microenvironments for New Therapies que mais de perto acompanharam o meu trabalho. Foram muitas as sugestões, críticas, ajudas, almoços, conversas...tudo essencial para o êxito e a forma como a investigação foi levada a cabo. Por tudo isto e muito mais, obrigado Ana Lourenço (Pipa), Ana Rita Almeida, Andreia Silva, Amadeu Martins, Arantxa Blázquez, Carla Cunha, Catarina Almeida Catarina Pereira, Cristina Ribeiro, Daniela Vasconcelos, Flávia Castro, Graciosa Teixeira, Guler Ungan, Hugo Caires, Inês Almeida, Joana Antunes, Joana Caldeira (Xu), Joana Ferreira, João Brás, José Henrique Teixeira, Judite Barbosa, Maria José Oliveira, Maria Molinos, Marta Oliveira, Marta Pinto, Nuno Neves, Paula Lima, Raquel Gonçalves, Rita Ferreira, Serafim Oliveira e Tom Starke.

Não poderia deixar de agradecer ao meus colegas e amigos do “Octopus Office” e do “Sea Urchin Lab”, Ana Silva, Ana Freire, António Ribeiro, Carla Gomes, Eliana Vale, Francisca Araújo, Mariana Fernandes, Mariana Valente, Paula Lima e Sara Neves. Em 2011, todos nós iniciamos um novo ciclo. Recordo com muito carinho essa fase, recheada de muitas ocasiões felizes.

Obrigado Estrela (Neto) pelo teu carinho e por teres apostado em mim para, juntos com a Ana Silva e o Tiago Esteves, nos aventurarmos na organização do Science Club e do INEB PhD Committee. Deu trabalho, mais fizemos coisas incríveis e das quais tenho muito orgulho.

Agradeço a todos os membros do INEB, de todas as equipas e departamentos, que sempre me ajudaram com um sorriso. Muitos dos resultados aqui apresentados só foram possíveis através da participação dos serviços "Biointerfaces and Nanotechnology unit" (BN-i3S), "Animal Facility" (i3S), "Translational Cytometry" (TraCy-i3S), "Cell Culture and Genotyping Unit" (CCGen-i3S), "Advanced Light Microscopy unit" (ALM-i3S), "Histology and Electron Microscopy Service" (HEMES-i3S), Centro de Materiais da Universidade do Porto (CEMUP) e "3B's Services and Consulting".

Estou grato ao serviço de ortopedia do Centro Hospitalar de São João, em particular ao Dr. António Mateus, Dr. Silva Pereira, Dr. Carlos Dopico, Dr. Artur Antunes, e, claro está, ao "Manel Ribeiro da Silva" e ao "Nuno Neves", amigos e camaradas na luta que é o doutoramento. As cirurgias à sexta-feira revelaram-se muito mais agradáveis do que aquilo que tinha imaginado, com boa disposição e partilha de experiências. Obrigado por me deixarem contactar tão de perto com a realidade hospitalar.

Gostaria de deixar um agradecimento especial ao Prof. Rui Henrique pelo a ajuda com a análise histológica. Recebeu-me de braços abertos no IPO-Porto, sem esperar nada em troca. Um gesto sem preço.

Danke Prof. Wiltrud, Katha, Lisa, Solvig e Anja, que tudo fizeram para que me sentisse em casa, em Heidelberg, e regressasse a Portugal com ótimos resultados. Foram incansáveis e muito "stickstoff" depois, conseguimos ter sucesso. Vocês são fantásticas e tenho muito orgulho em ter estado no vosso laboratório - Research Center for Experimental Orthopaedics (Heidelberg University Hospital).

Meus amigos, Agostinho, André, Daniela, Filipe, Gonçalo, João, Maria João, Margarida, Ricardo, Sofia e Telmo, obrigado por acharem que a investigação que aqui descrevo é algo espetacular.

Obrigado minha valiosa Família, talvez os mais prejudicados com a minha ausência por dedicação ao doutoramento. Se hoje cheguei até aqui, em parte, deve-se ao vosso amor, à paz que me proporcionaram e à fé que depositam em mim. Continuaremos a caminhar juntos.

E por último, obrigado minha querida Célia, o meu grande amor e a quem dedico este trabalho. Não existem palavras para agradecer o teu apoio incondicional nem para expressar quão bom tem sido partilhar a vida a teu lado. Contigo tudo é mais fácil, tudo é mais claro, tudo vale a pena...pois juntos somos mais fortes e em ti encontro, todos os dias, a felicidade.

Publications

The work performed in the frame of this Thesis resulted in the following publications:

Daniel M. Vasconcelos, Susana G. Santos, Meriem Lamghari, and Mário A. Barbosa, "The two faces of metal ions: from implants rejection to tissue repair/regeneration". Biomaterials 2016;84:262-275. (included in the Chapter I)

Daniel M. Vasconcelos, J. Cortez and Meriem Lamghari, "Technical Standards and Legislation for Implants and Implantable Medical Devices", Reference Module in Materials Science and Materials Engineering 2016

Daniel M. Vasconcelos*, Manuel Ribeiro-da-Silva*, António Mateus, Cecília Juliana Alves, Gil Costa Machado, Joana Machado-Santos, Diogo Paramos-de-Carvalho, Inês S. Alencastre, Rui Henrique, Gilberto Costa, Mário A. Barbosa[#], and Meriem Lamghari[#] , "Immune response and innervation signatures in the hip: from osteoarthritis to aseptic implant loosening". Journal of Translational Medicine. 2016;14(1):205. * equal contribution; [#] Co-senior authorship (Chapter II)

Daniel M. Vasconcelos, Raquel M Gonçalves*, Catarina R Almeida* , Inês O Pereira, Marta I Oliveira, Nuno Neves, Andreia M Silva, António C Ribeiro, Carla Cunha, Ana R Almeida, Cristina C. Ribeiro, Ana M. Gil, Elisabeth Seebach, Katharyna L. Kynast, Wiltrud Richter, Meriem Lamghari, Susana G Santos[#] and Mário A Barbosa[#] , "Fibrinogen scaffolds with immunomodulatory properties promote *in vivo* bone regeneration", Biomaterials 2016;111:163-178. * equal contribution; [#] Co-senior authorship (Chapter III)

Daniel M. Vasconcelos, Ana R Almeida, Susana G Santos and Mário A Barbosa. "The presence of magnesium ions impairs M1 macrophage polarization: impact on the crosstalk with MSCs". Manuscript in preparation. (Chapter IV)

Abstract

The vast majority of medical devices currently applied in clinics were developed based on the classical concepts of biocompatibility and bioinert materials. These implantable biomaterials “avoid” natural responses from the host, which may include allergic reactions but also lead to tissue healing and repair. However, clinicians and manufacturers have been perceiving that this inert behavior has a deleterious effect at long-term since it leads to chronic immune responses and encapsulation of the medical device. In this sense, biodegradable materials have been developed, preventing foreign body response but presenting limited tissue healing and implant integration.

Inspired by the “lessons from the past”, a new generation of biomaterials have been engineered with the aim of providing proper biological clues, to promote the regenerative process in the host. In this context, immunomodulatory biomaterials constitute a promising strategy for both regenerative medicine and advanced therapies for diseases involving immune responses.

The doctoral dissertation presented herein was based on the paradigm shift from “fighting inflammation” to “modulating inflammation”, which is now a hot topic in the Biomaterials field. In the following chapters, original work focusing the role of inflammation in the response to orthopedic biomaterials will be reported and discussed. The research plan was defined to study the drawbacks and biological responses induced by conventional orthopedic prostheses and to explore the use of fibrinogen and metals ions as alternative immunomodulatory agents.

We have started by studying the biological response that occurs in the synovial tissues of osteoarthritis and aseptic loosening patients. Extensive histological evaluation found a particle-induced chronic inflammation driven by macrophages in the tissues retrieved from aseptic loosening patients. However, the distinct tissue response observed in osteoarthritis and aseptic loosening groups was not accompanied by differences regarding the expression of inflammatory mediators, namely the classically pro-inflammatory cytokines such as TNF-α, IL-1β and IL-6. In this context, a significant reduction of TGF-β1 mRNA levels with a changed expression pattern at protein level was locally detected in aseptic loosening. However, the differences observed at synovial tissues were not found in the bloodstream, highlighting the confinement of the pathology to the joint region.

The second part of this doctoral programme was to explore strategies for immunomodulation, namely in the context of bone healing. The first strategy consisted in a biomimetic approach based on implants of pure fibrinogen to treat femoral bone defects. This study demonstrated that fibrinogen, when stabilized in 3D structures (Fg-3D), presents

immunomodulatory properties. The *in vivo* implantation of Fg-3D implants led to early bone healing at the defect region, without interfering with the up-regulation of IL-6 and IL-8 induced by the bone injury. Moreover, Fg-3D impacted the systemic immune response, inducing changes in the proportions of T, B, NK and NKT lymphocytes and myeloid cells in blood, spleen and draining lymph nodes. Remarkably, these early changes in immune cell populations appear to be later related with complete bone repair at 8 weeks post-injury, and some of the altered proportions of B, T and myeloid cells were still detectable at this late timepoint. This work highlighted the systemic nature of the immune response to bone injury and biomaterials implantation, showing the immunomodulatory effect of fibrinogen implants and their consequences for bone healing.

A second approach based on the potential role of magnesium ions (Mg^{2+}) in the macrophage behaviour was also explored. The rational for this study relied on the increasing evidence supporting immunoregulatory effects of Mg^{2+}, allied to the importance of macrophages in both healing and response to biomaterials. The differentiation and activation of primary human macrophages were assessed in presence of supraphysiological concentrations of extracellular Mg^{2+} ions. The tested Mg^{2+} concentrations exerted a regulatory effect on pro-inflammatory M1 macrophages inducing significant decrease of CD86 expression and reducing the production of IL-8. The exposure of non-activated and M2 macrophages to Mg^{2+}-enriched media did not lead to significant changes in surface molecules and macrophage secreted cytokines. The culture of primary human mesenchymal stromal cells (MSC) with conditioned media from macrophages revealed that non-activated macrophages and macrophages exposed to high extracellular Mg^{2+} concentrations support MSC osteogenic differentiation. Therefore, our findings point out the role of Mg^{2+} in modulating biological responses involving LPS-activated macrophages.

In summary, the major contributions of this Doctoral thesis are (i) highlighting the central role of macrophages and immune mediators in the response against the degradation products of orthopedic biomaterials, (ii) *in vivo* testing of a new fibrinogen-based biomaterial with immunomodulatory and pro-regenerative properties, and (iii) providing new insights on the therapeutic potential of magnesium ions on M1 pro-inflammatory macrophages.

Resumo

A maioria dos dispositivos médicos atualmente utilizados na prática clínica foram desenvolvidos tendo por base os conceitos clássicos de materiais biocompatíveis e bioinertes. Estes biomateriais implantáveis "evitam" a resposta do hospedeiro, que pode incluir reações alérgicas, mas também pode levar à reparação e regeneração dos tecidos. No entanto, médicos e fabricantes têm vindo a perceber que este comportamento inerte tem um efeito nefasto a longo prazo, uma vez que leva a respostas imunes crónicas e ao encapsulamento do dispositivo médico. Neste sentido, têm sido desenvolvidos materiais biodegradáveis, prevenindo respostas de corpo estranho, mas apresentando ainda uma performance limitada em termos de regeneração de tecidos e integração dos implantes.

Inspirada pelas "lições do passado", uma nova geração de biomateriais tem sido projetada com o objetivo de fornecer pistas biológicas adequadas para promover o processo regenerativo no hospedeiro. Neste contexto, os biomateriais imunomoduladores constituem uma estratégia promissora tanto no contexto da Medicina Regenerativa, como em terapias avançadas para doenças que envolvam a resposta imune.

A dissertação de doutoramento aqui apresentada baseia-se na mudança de paradigma de "combater" para "modelar" a inflamação, amplamente discutida nos últimos anos, na área dos Biomateriais. Nos capítulos seguintes será relatado e discutido trabalho original que foca o papel da inflamação na resposta a biomateriais ortopédicos. O plano de investigação foi definido tendo em vista o estudo das limitações e das respostas biológicas induzidas pelas próteses ortopédicas convencionais e também explorar o uso de fibrinogénio e iões metálicos como agentes imunomoduladores.

Inicialmente estudou-se a resposta biológica que ocorre nos tecidos sinoviais de doentes quer com osteoartrite quer com descolamento asséptico. A extensa avaliação histológica revelou uma inflamação crónica induzida por partículas, e liderada pelos macrófagos**,** nos tecidos recolhidos nos doentes com descolamento asséptico. Contudo, a resposta tecidular distinta observada entre os grupos osteoartrite e descolamento asséptico não foi acompanhada por diferenças ao nível da expressão de mediadores inflamatórios, nomeadamente das citocinas pró-inflamatórias clássicas TNF-α, IL-1β e IL-6. Neste contexto, foi detetada uma redução significativa dos níveis de mRNA de TGF-β1, com um padrão de expressão alterado ao nível da proteína, nos doentes com descolamento asséptico. No entanto, as diferenças observadas nos tecidos sinoviais não foram encontradas na corrente sanguínea, destacando o confinamento da patologia à região articular.

A segunda parte deste doutoramento procurou explorar estratégias para imunomodulação, nomeadamente no contexto da reparação óssea. A primeira estratégia

consistiu numa abordagem biomimética baseada em implantes de fibrinogénio puro para tratar defeitos ósseos. Este estudo demonstrou que o fibrinogénio, quando estabilizado em estruturas 3D (Fg-3D), apresenta propriedades imunomoduladoras. Quando implantados *in vivo*, os implantes Fg-3D levaram a uma regeneração óssea mais rápida na região do defeito, sem aumentar a expressão de IL-6 e IL-8 induzida pela lesão óssea. Além disso, o Fg-3D teve impacto na resposta imune sistémica, induzindo alterações nas proporções de linfócitos T, B, NK e NKT e de células mielóides no sangue, baço e gânglios linfáticos drenantes. Notavelmente, estas alterações iniciais nas populações celulares imunes parecem estar relacionadas com a completa reparação óssea observada às 8 semanas após a lesão, período em que algumas das alterações nas proporções de células B, T e mielóides eram ainda detetáveis. Este trabalho destacou a natureza sistémica da resposta imune à lesão óssea e aos implantes, mostrando o efeito imunomodulador dos implantes de fibrinogénio e suas consequências para a regeneração óssea.

O potencial dos iões de magnésio (Mg^{2+}) para influenciar o comportamento dos macrófagos foi explorado como uma segunda abordagem. O racional para este estudo baseou-se na evidência crescente que apoia os efeitos imunorreguladores do Mg^{2+}, aliado à importância dos macrófagos, tanto na cicatrização como na resposta a biomateriais. A diferenciação e ativação de macrófagos humanos primários, foram avaliadas na presença de concentrações extracelulares supra-fisiológicas de iões Mg^{2+}. As concentrações de Mg^{2+} testadas exerceram um efeito regulador sobre os macrófagos pró-inflamatórios M1, induzindo uma diminuição significativa da expressão de CD86 e reduzindo a produção de IL-8. A exposição de macrófagos não ativados e M2 a meios enriquecidos em Mg^{2+} não conduziu a alterações significativas nas moléculas de superfície e citocinas secretadas por esses macrófagos. A cultura de células mesenquimais humanas primárias (MSC) com meios condicionados de macrófagos revelou que tanto os macrófagos não ativados como os macrófagos expostos a concentrações extracelulares mais elevadas de Mg^{2+} suportam a diferenciação osteogénica das MSC. Desta forma, os nossos resultados suportam o papel dos iões Mg^{2+} na modulação de respostas biológicas envolvendo macrófagos ativados por LPS.
Em resumo, as principais contribuições desta tese de doutoramento são: (i) destacar o papel central dos macrófagos e dos mediadores imunes na resposta contra os produtos de degradação dos biomateriais ortopédicos, (ii) o teste *in vivo* de um novo biomaterial à base de fibrinogénio com propriedades imunomoduladoras e pro-regenerativas e (iii) proporcionar novos conhecimentos sobre o potencial terapêutico dos iões de magnésio sobre os macrófagos pró-inflamatórios M1.

Table of contents

List of abbreviations

ADAMTS	A disintegrin and metalloproteinase with thrombospondin motifs
AL	Aseptic loosening
ALP	Alkaline phosphatase
ALTR	Adverse local tissue reaction
ALVAL	Aseptic lymphocyte-dominated vasculitis-associated lesions
APC	Antigen presenting cells
ARMD	Adverse reactions to metal debris
ASTM	American society for testing and materials
BBB	Blood-brain barrier
BL	Blood
BMP	Bone morphogenetic protein
CCL	C-C motif chemokine ligand
CCR	C-C motif chemokine receptor
CD	Cluster of differentiation
Ch	Chitosan
CM	Conditioned media
CoC	Ceramic-on-ceramic
COX	cyclooxygenase
CXCL	C-X-C motif chemokine ligand
DC	Dendritic cell
DMEM	Dulbecco's Modified Eagle Medium
EBV	Epstein-Barr virus
ECM	Extracellular matrix
EDS	Energy-dispersive X-ray spectroscopy
FACS	Fluorescence-activated cell sorting
FBR	Foreign body response
FBGC	Foreign body giant cell
FDA	Food and Drug Administration
Fg	Fibrinogen
FGF	Fibroblast growth factor
FTIR	Fourier transform infrared spectroscopy
GM-CSF	Granulocyte macrophage colony-stimulating factor
GT	Granulation tissue

H&E	Hematoxylin and eosin
HIF	Hypoxia-inducible factor
HLA-DR	Human leukocyte antigen-antigen d related
HSC	Hematopoietic stem cells
HUVEC	Human Umbilical Vein Endothelial Cells
ICAM	Intercellular adhesion molecule 1
IFN	Interferon
IGF	Insulin-like growth factor
IgG	Immunoglobulin G
IL	Interleukin
iNOS	Inducible nitric oxide synthase
LL	Lining layer
LN	Lymph nodes
LPS	Lipopolysaccharide
MCP	Monocyte chemoattractant protein
M-CSF	Macrophage colony-stimulating factor
MHC	Major histocompatibility complex
MIP	Macrophage inflammatory protein
MMP	Matrix-metalloproteinases
MoP	Metal-on-polyethylene
MoM	Metal-on-metal
mRNA	Messenger RNA
MSC	Mesenchymal stem/stromal cell
MSD	Musculoskeletal disorders
MT	Masson's trichrome
NALP3	NACHT, LRR and PYD domains-containing protein 3
NF-κB	Nuclear factor kappa-light-chain-enhancer of activated B cells
NK	Natural killer
NMR	Nuclear magnetic resonance
NO	Non operated
NSAID	Nonsteroidal anti-inflammatory drugs
OA	Osteoarthritis
OC	Osteocalcin
OPG	Osteoprotegerin
PBMC	Peripheral blood mononuclear cells
PDGF	Platelet-derived growth factor

PE	Polyethylene
PGC	Peroxisome proliferator-activated receptor-gamma coactivator
PGE	Prostaglandin E
PMMA	Polymethylmethacrylate
PMN	Polymorphonucleated cells
PP	Polymeric particles
PRP	Platelet rich plasma
PRR	Pattern recognition receptor
qRT-PCR	Quantitative reverse transcription polymerase chain reaction
RA	Rheumatoid arthritis
RANKL	Receptor activator of nuclear factor kappa-B ligand
RGD	Arginine-glycine-aspartic acid
RNS	Reactive nitrogen species
ROI	Region of interest
ROS	Reactive oxygen species
RPMI	Roswell Park Memorial Institute
RUNX	Runt-related transcription factor
SCID	Severe combined immunodeficiency
SEM	Scanning electron microscopy
SLL	Sublining layer
SMAD	Mothers against decapentaplegic homolog
SP	Spleen
SOX	Sex determining region-Y box
TCR	T cell receptor
TGF	Transforming growth factor beta
Th	T helper cell
THA	Total hip arthroplasty
TLR	Toll-like receptor
TNF-α	Tumor necrosis factor alpha
TRAP	Tartrate resistant acid phosphatase
TRIF	TIR-domain- containing adapter-inducing interferon-β
TRPM	Transient receptor potential cation channel subfamily M
VEGF	Vascular endothelial growth factor

CHAPTER I

General Introduction

This chapter is based on the review article published in Biomaterials 84:262-275, 2016
doi: 10.1016/j.biomaterials.2016.01.046

1 Musculoskeletal system

The human musculoskeletal system is composed by specialized supporting tissues that include muscle, bone, cartilage, and other connective tissues (Figure 1). Together, those tissues provide structural support for the rest of the body, allow motion, protect vital organs and constitute a major reservoir of growth factors, cytokines, hormones, minerals and progenitor cells [1]. Due to their specialization and distinct functions, connective tissues can be categorized in three major subsystems: skeletal, muscular and joints, ligaments and synovial bursae. Muscle, bone and cartilage are organized tissues, which structure is optimized to lead with distinct mechanical stimuli such as contraction, load and friction [2; 3].

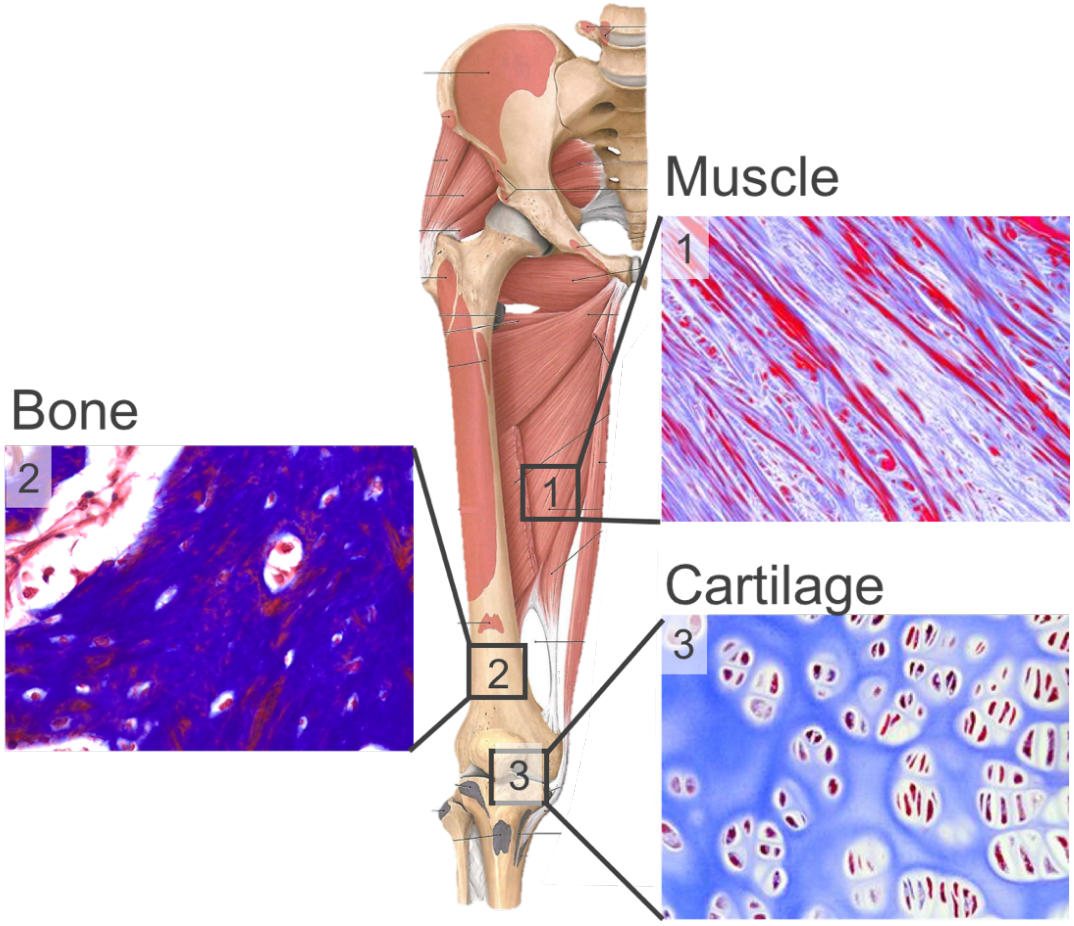

Figure 1 – Anatomical and histological structure of the musculoskeletal system. The lower limb is used as an example of the vast network of bones, muscles, tendons, ligaments and joints. The musculoskeletal system is composed by specialized tissues as illustrated by the Masson's Trichrome stained sections of muscle (1), bone (2) and cartilage (3) tissues. Differences between the collagen content (blue stain), among other proteins, may be noticed by the variation of blue and red regions (cell cytoplasm and muscle fibers). Adapted from [4].

1.1 Skeletal subsystem

1.1.1 Bone structure and biology

The adult human skeletal system comprises bone and cartilage tissues. Although bone, cartilage and muscle share the same progenitor, in embryologic terms, bone and cartilage distance from muscle tissue through their autonomous development program and interplay along ossification [5].

Bone tissue has a composite structure designed to simultaneously withstand high loads and present relative flexibility. The mechanical behavior of bone is related with its extracellular matrix (ECM), which is structurally organized by bone cells through the selective incorporation of organic and inorganic elements [6]. Type I collagen is the major organic component of bone's ECM (up to 95%), combined with other proteins such other collagens, osteocalcin, osteopontin, osteonectin, bone sialoprotein and proteoglycans. The inorganic component is formed by calcium phosphate, organized in hydroxyapatite crystals, which confer rigidity to bones [7].

Among the cell populations hosted in bone tissue, osteoblasts and osteoclasts are the most important in maintaining bone homeostasis and remodeling. Osteoblasts and osteoclasts derive from different cell lineages and present distinct functions with osteoblasts synthetizing bone ECM and osteoclasts resorbing bone.

Osteoblasts derive from mesenchymal stem/stromal cells (MSCs), a multipotent cell population originated in the mesoderm, with the potential to differentiate in to osteoblasts, chondrocytes, myocites and adipocytes [8]. During osteogenic differentiation, osteoblasts undergo metabolic and phenotypic changes regulated by growth factors and cytokines such as bone morphogenetic proteins (BMPs), platelet-derived growth factor (PDGF), fibroblast growth factor (FGF), insulin-like growth factor (IGF), transforming growth factors-β (TGF-β), interleukins (IL)-1β, IL-5 and tumor necrosis factor-α (TNF-α) [1; 9; 10]. Osteogenic differentiation is characterized by a time-dependent up-regulation of both alkaline phosphatase (ALP) and the transcription factor RUNX2, accompanied by a decreased activity of SOX9 [11; 12]. This balance between RUNX2 and SOX9 is critical for cell differentiation as RUNX2 promotes osteogenesis but it may be damped by SOX9 with induction of chondrogenesis [13]. Therefore, ALP, RUNX2 and SOX9 are considered important markers in assessing bone ossification. In bone, osteoblasts are organized in connected groups of cells to produce collagen, osteocalcin, osteopontin as well as hydroxyapatite. The lifespan of osteoblasts is approximately one month, after which suffer apoptosis or differentiate into osteocytes, a type of bone cell that is embedded in the ECM, regulates bone remodeling and translate mechanical stimuli to chemical signals [14; 15].

The progenitors of osteoclasts are the hematopoietic stem cells (HSC), which are located at bone marrow and originate both myeloid and lymphoid lineages [1]. Osteoclasts derive from the common myeloid progenitor that is also shared with other cells populations, namely the monocytes. In terms of morphology, osteoclasts are large and multinucleated cells, which is related to their bone resorption function [16]. This biological process occurs in sealed bone resorption bays created by osteoclasts, through re-organizing their actin cytoskeleton, to protect the surrounding bone tissue from the aggressive environment that is generated. Then, osteoclasts establish an interface with the bone to be resorbed named ruffled border, and through this secrete enzymes, cathepsin K and matrix-metalloproteinases (MMPs), reactive oxygen species, formed by tartrate-resistant acid phosphatase (TRAP), and HCO_3^- to dissociate hydroxyapatite. The osteoclastic differentiation involves several mediators, especially the macrophage colony-stimulating factor (M-CSF), the receptor activator of nuclear factor kappa-B ligand (RANKL), and is inhibited by osteoprotegerin (OPG). The presence of M-CSF induces the formation of osteoclast precursors through the activation of the cell surface receptor c-fms and up-regulation of RANK. Expressing RANK at their surface, osteoclast precursors became sensitive to RANKL, a pro-osteoclastogenic factor secreted by osteoblasts and other cell populations, and are able to complete their differentiation. The effect of RANKL may be inhibited by the presence of OPG, because this protein binds RANKL, blocking osteoclast differentiation [17]. Bone formation and resorption are tightly regulated processes, so that synchronized bone remodeling occurs and homeostasis is maintained.

In mammals, bone tissue has two types of organization: the compact bone and the trabecular bone, also denominated as cancellous and spongy bone, respectively [3]. In detail, the differences between compact and trabecular bone types go beyond their structure and also involve relevant changes in terms of cell composition, vascularization and biologic function, which have been previously reviewed in [1; 3].

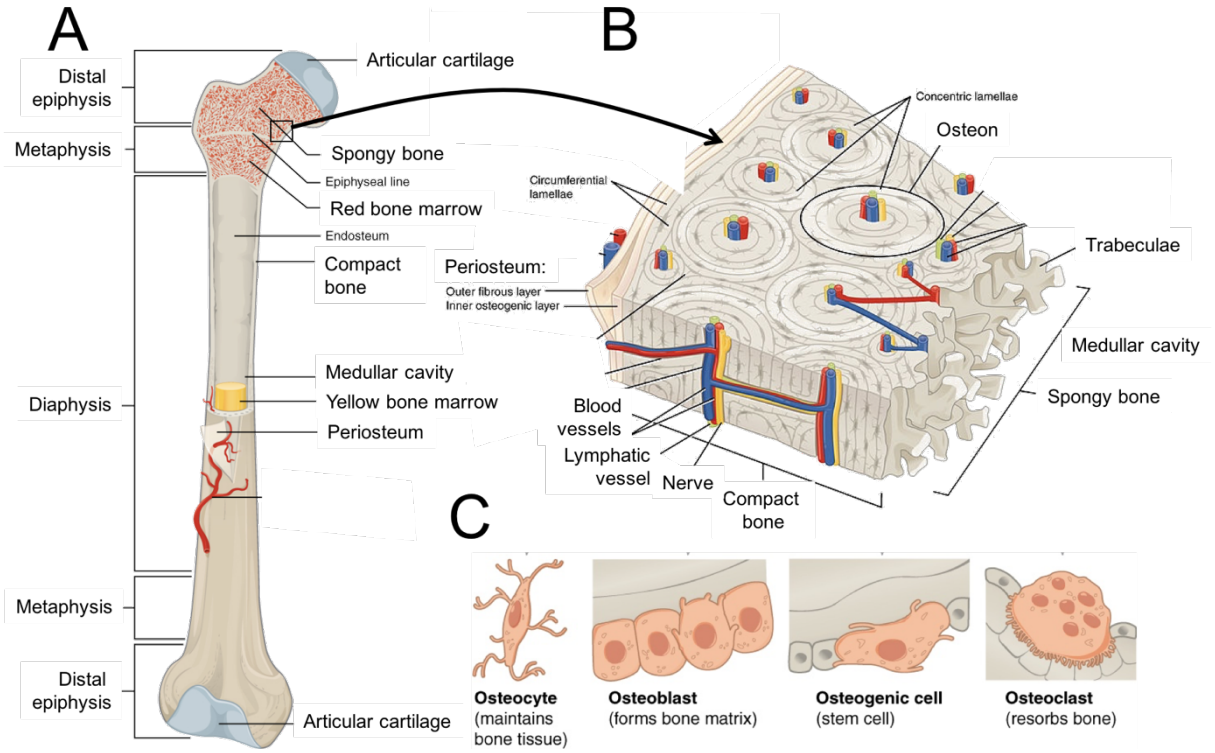

Figure 2 – Organization and composition of bone. (A) Macroscopic scheme of a long bone, which is characterized by an outer layer of compact bone, distal extremities made of spongy bone and the medullary cavity in its core where the bone marrow is hosted. **(B)** Closer view of the compact bone illustrating periosteum, the osteon with osteocytes circumventing nerve fibres and blood and lymph vessel and the transition to spongy bone and its porous structure. **(C)** Major bone cell populations: osteocytes, osteoblasts, ostegenic cells and osteoclast. Adapted from [18].

About 80% of the human skeleton is composed by compact bone, which is the denser type of bone tissue [3] As illustrated in Figure 2A, compact bone is mostly found at the external layer of bones and has the osteon as its primary functional unit. Osteon comprises osteocytes concentrically distributed around harversian canals, containing nerve fibers, blood and lymphatic vessels [19]. At the outer layer, compact bone has periosteum at the interface with soft tissues, which presents an osteogenic layer and a fibrous layer (Figure 2B). While the osteogenic layer homes progenitor cells that may differentiate into osteoblasts and lead to bone formation, the fibrous layer is constituted by fibroblasts, providing a proper attachment for muscles, bones and aponeurosis (Figure 2C).

Trabecular bone is highly vascularized and is less dense than compact bone, which creates a suitable environment for metabolically active cells. This type of bone can be observed in flat bones and at the epiphysis of the long bones. The porous structure of trabecular bone is associated with its more flexible mechanical behavior and improved deformation recovery in comparison to compact bone [20]. Bone trabeculae are dynamic structures that are constantly being remodeled to perform optimal distribution of the mechanical loads experienced by bone. Thus, bone ECM and osteocytes are organized along

stress lines by osteoblasts and osteoclasts. The inter-trabecular spaces home the red bone marrow, rich in hematopoietic progenitors, while the medullary cavities store yellow bone marrow, characterized by increased content of adipocytes. Bone marrow constitutes an important reservoir of HSCs and MSCs, giving rise to key cell populations such as leukocytes, erythrocytes and thrombocytes [1].

1.1.2 Bone healing

Bone healing may be divided in three stages: inflammation, repair, and remodeling [21], as summarized in Figure 3. The first two stages may last 4-8 weeks in rodents and 6-10 weeks in humans [22] while bone remodeling is a slower process, taking up months in rats and years in humans to be completed [23]. The inflammatory stage initiates after tissue damage, lasts about 7 days in healthy rats, and is characterized by acute inflammation with vasodilation, exudation of plasma and infiltration of leukocytes. Simultaneously, hematoma is formed at the lesion site, through the conversion of fibrinogen into fibrin, by plasmin. This new microenvironment is hypoxic, presents low pH, and both pro- and anti-inflammatory mediators are locally produced. Fracture hematoma is the primordial matrix in bone healing, housing peripheral blood-derived inflammatory cells. Polymorphonucleated cells (PMNs), mostly neutrophils migrate to bone injury in the first hours, where they accumulate and secrete CCL2 and IL-6, factors with a key role in further macrophage recruitment [24]. In bone, resident macrophages are located on endosteal and periosteal surfaces, migrating towards the bone injury [25]. Together with other innate immune cells, resident macrophages initiate a cascade of immune mediators that promote the recruitment of inflammatory immune cells, including monocytes that will differentiate into “inflammatory macrophages” at the bone injury [25]. Lymphocytes are also recruited to the hematoma/callus, where T and B cells have been reported to participate in soft and hard callus formation [26]. Soluble factors are locally produced during the inflammatory phase with known roles on the immune response (IL-1, IL-6, TNF-α, M-CSF-1, IL-10), angiogenesis (angiopoetin-1 and VEGF) and bone repair (RANKL, TGF-β1 and BMPs) [22; 27].

The orchestration of the complex process of bone healing also involves other cell populations such as endothelial cells, fibroblasts and MSCs. The formed hematoma is gradually replaced by granulation tissue, which is characterized by its highly cellular content, newly formed blood vessels and dense collagen fibers, synthetized by fibroblast. The participation of endothelial cells in the local revascularization is a key step in bone healing as it restores normoxia and establishes a suitable environment for bone healing [28]. Upon granulation tissue invasion, MSCs are attracted to the local where they exert an immunomodulatory role and further differentiate into chondrocytes and osteoblasts [21].

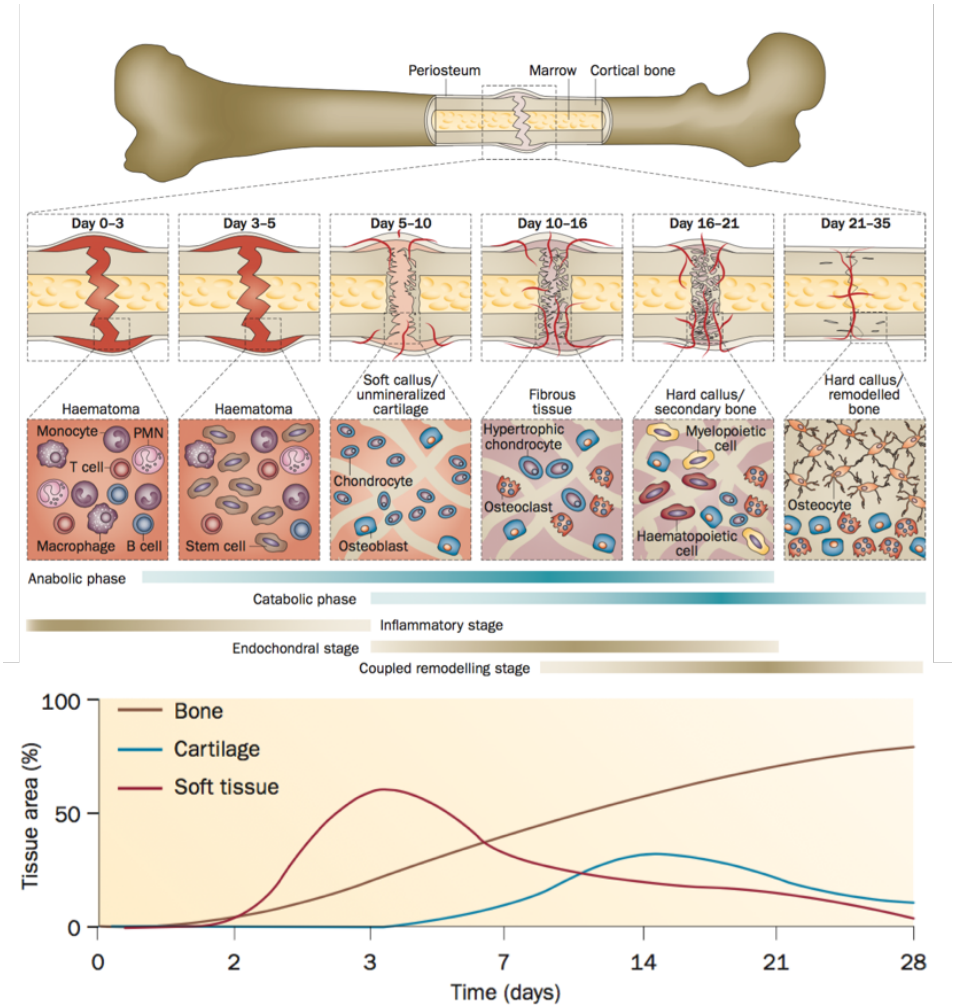

Figure 3 – Bone fracture repair. The major biological events regarding bone tissue response and the most important cell populations involved in bone healing are illustrated and organized in three main stages: inflammatory, endochondral (repair) and remodeling stages. The proportion of tissue area occupied by bone, cartilage and soft tissue along bone healing is presented. Adapted from [21] and [22].

Bone healing can be classified as primary or secondary, depending on the fracture stability [29]. Primary cortical bone healing requires almost absolute fracture stabilization (< 5% interfragmentary strain), so that new bone can be directly repaired in absence of callus formation [30]. Under these conditions, intramembranous ossification is initiated with osteoclasts resorbing dead bone tissue at fractures edges and creating channels along the fracture that support blood vessel ingrowth. With the revascularization of the fractured bone, MSCs migrate to the lesion, creating ossification centers, where they proliferate and undergo osteogenic differentiation [21]. At this timepoint, osteoblasts form the osteoid, the primary form of bone ECM mostly composed by type I collagen and where calcium phosphate crystal will be deposited [31]. With the ECM mineralization, bone spicules start to appear and by their fusion and reorganization more complex structures such as woven bone, periosteum and osteon are created, resembling the original structure of healthy bone [3]. As high fracture stability is difficult to achieve, exclusive intramembranous ossification in bone healing is rare.

This type of ossification partially occurs in bone healing, contributing for successful fracture repair.

Indirect or secondary bone healing occurs in fractures with low stability (6-20% interfragmentary strain) or impaired blood supply and involves the formation of a soft cartilaginous callus that is further converted into a bony callus. This process of bone healing is classified as endochondral ossification due to the involvement of chondrocytes and is the dominant type of bone formation [30]. Callus formation starts at the end of the inflammatory phase (3-7 days) at the periosteum. Growing from the periphery to the center of the fracture, chondrocytes drives cartilage formation at 7-10 days. At 2 weeks, the fracture gap is now bridged by cartilage tissue and chondrocytes become hypertrophic, releasing calcium and undergoing apoptosis [22]. With the fracture stabilization, new blood vessels invade the calcified cartilage, creating a pathway for monocytes and MSCs to migrate and differentiate in to osteoclasts and osteoblasts, respectively. At the end of bone repair stage, new woven bone with trabecular structures was formed and fracture stability was highly improved.

The last stage in bone healing is tissue remodeling, as the newly formed bone is structurally and mechanically weaker than mature bone [32]. Thus, during bone remodeling woven bone is converted in lamellar bone, which is characterized by collagen fibers aligned in sheets and increased structural strength with formation of osteons [3]. The remodeling stage is characterized by an overall diminishment of inflammation with decreased levels of TGF-β but high concentrations of IL-1, TNF-α and BMP-2 [23]. The callus formed during the early stages of bone healing are now reabsorbed, constituting the catabolic phase of the process where the tissue volume reduces to the one observed in homeostasis.

1.1.3 Cartilage

Cartilage is an elastic tissue with moderate strength that can be found in some joints, at ends of long bones, nose, ears, intervertebral discs, among other anatomical sites. From the three kinds of cartilage, the hyaline one is the most common and constitutes the articular cartilages while elastic and fibrocartilage are more flexible and observed in ears and in other parts of the human body. The ECM of the cartilage tissue is produced and maintained by chondrocytes and is mostly composed of collagen, proteoglycans, other noncollagenous proteins and water [2]. In articular cartilages, ECM is organized in three different zones with different content and organization. The elastic and low-friction behavior of cartilage is associated to the collagen network, mostly type II, and proteoglycans, as aggrecan. Without blood supply, nutrients reach cartilage by diffusion, namely through the synovial fluid in synovial joints. Moreover, healthy cartilage is not innervated, in opposition to other

musculoskeletal tissues, presenting very limited and confined innervation of the outer layer of articular and meniscus cartilage [33].

1.2 Joints and associated soft tissues

Bones articulate at complex structures named joints. Among the different kinds of joints (fibrous, cartilaginous), synovial joints are the main type found in the body [34]. Knee and hip are two examples of synovial joints, which allow freedom of movement in many directions. To achieve frictionless and smooth locomotion, bones, cartilage, muscles, ligaments, tendons and synovial bursae are perfectly organized in an intricate network that constitutes synovial joints (Figure 1).

Besides movement, muscles, ligaments and tendons are important anatomical structures at stabilizing the joint and limiting the extension of the motion to avoid dislocation, excessive strain or, ultimately, soft tissues rupture [35]. While ligaments stablish bone-to-bone connections (e.g. cruciate ligaments), tendons attach muscles to bone [36] (Figure 4A).

Synovial bursa delimits the joint cavity, which is externally surrounded by the articular capsule and internally contains by the synovial membrane (Figure 4B). Synovial membrane is a connective tissue organized in two layers, hosting specialized cells named synoviocytes that guarantee nutrients supply and production of synovial fluid to the intra-articular space [34]. Those cells are located at the intimal layer, also known as synovial lining, where the synovial fluid is produced and secreted to the intra-articular space. Two types of synoviocytes have been identified: macrophagic cells (type A) and fibroblast-like cells (type B) [37]. While type A synoviocytes are specialized in phagocyting debris and behave as antigen-presenting cells, type B synoviocytes are involved in the production of ECM components such as hyaluronic acid, collagen and fibronectin. The intimal layer is supported by the outer sublining layer, where the blood vessels that supply the synovial membrane are located. The joint cavity is filled with synovial fluid, which contributes to friction reduction and shock absorption due to its viscous and lubricant properties. The biomechanical properties of synovial fluid are associated to its plasma-like composition enriched in hyaluronic acid and lubricin (proteoglycan 4), which is altered in pathological conditions [38; 39].

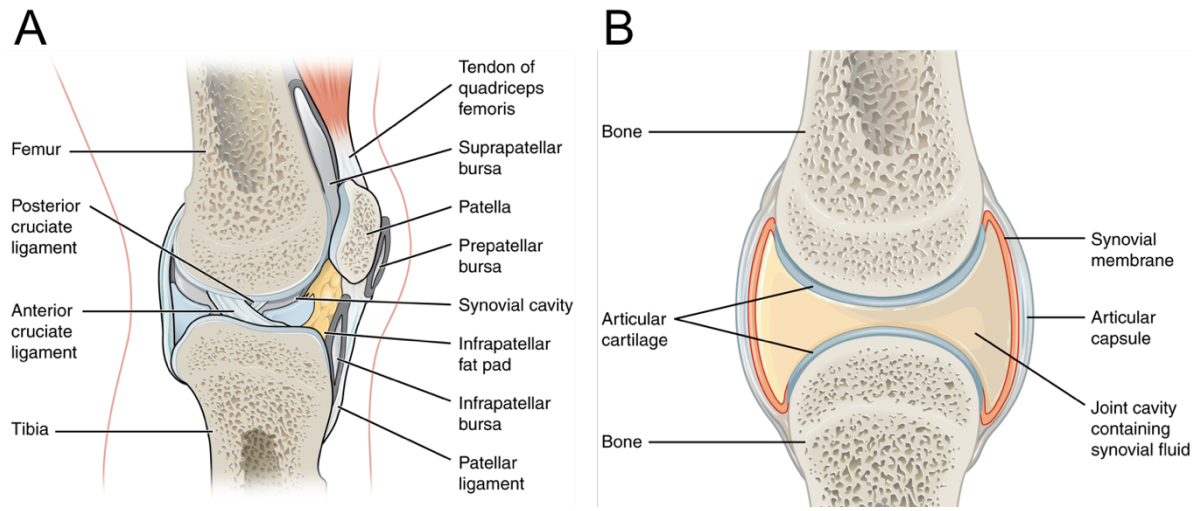

Figure 4 – Anatomy of synovial joints. **(A)** Lateral view of human knee joint where femur articulates with tibia. Various ligaments and tendons are represented and contribute for joint stability and motion. **(B)** The intra-articular space is filled with synovial fluid and is limited by synovium, which is composed by synovial membrane and articular capsule. Adapted from [40].

1.3 Musculoskeletal disorders

Musculoskeletal disorders (MSD) are a worldwide challenge for patients, healthcare systems and societies. The aging of western societies is leading to a shift in medical needs with arthritis, bone fractures and low back pain presenting as the most prevalent MSDs and leading to work disability and increased utilization of healthcare services [41]. The umbrella term MSD encompasses a wide range of diseases, traumatic injuries and syndromes characterized by pain and motion reduction. Among other risk factors, age and occupation are the major causes of MSD [42; 43].

Typically, MSD treatment options involving drugs are limited or ineffective at solving mechanical failures such as bone trauma. Although biologic and non-biologic disease-modifying antirheumatic drugs have been successfully used to reduce pain and control exacerbated inflammatory responses, those therapeutics encompass considerable side effects and are unable to avoid joint failure [44; 45]. Therefore, the application of biomaterials becomes unavoidable in the clinical management of both arthritis and bone defects caused by traumatic and non-traumatic events [46]. While metallic nails, plates and screws are applied to fix bone fractures, prostheses are implanted to replace failed arthritic joints. These two clinical scenarios will be described in the next sections, clarifying the need of using biomaterials for bone defects and osteoarthritis management, and addressing current limitations of conventional medical devices.

1.4 Traumatic and non-traumatic bone defects

Large bone defects are serious complications that are mostly caused by extensive trauma or by non-traumatic events such as tumor, infection, or congenital musculoskeletal disorders [47]. In the U.S., the 2 million bone fractures that occur annually, cost $17 billion dollars [48]. Long-bone fractures are the most common skeletal trauma and present a very high success rate of repair. However, non-unions and distal fractures impose a substantial clinical challenge in the treatment and management of orthopedic patients [47; 49]. Depending on the fractured bone, the rate of non-union, also called delayed union, may be about 5-15% [50; 51]. Patients with nonunion fractures present increased risk of additional fractures, require more surgical care and physical therapies, which doubles the costs of treating a nonunion fracture when compared to patients without nonunion [50].

As previously described, bone healing is a complex and finely tuned sequence of biological events that can be disturbed by a wide range of factors [52]. Reduction and stabilization of the fracture achieved by medical procedures influences the inflammatory phase and tissue vascularization. Poor fracture stabilization with high tissue strain and periosteal damage may lead to impaired blood supply at the injury site, creating a microenvironment with low oxygen tension that is more suitable for cartilage formation than bone repair [53]. Moreover, both local and systemic trauma severity may reduce the blood supply to the fracture region [54], impairing healing.

Other factors are not directly related to the bone fracture and highly depend on the patient, namely gender [55], age [56], lifestyle habits [57; 58], medication [59], local and systemic inflammation and other comorbidities [22; 60]. In detail, an animal study revealed that females are more affected by poor fixation than males, presenting newly formed bone with lower biomechanical properties [55]. Aging negatively influences vascularization at fracture region likely through diminished levels of key angiogenic factors (HIF-1α and VEGF) at the early response and unbalanced production of proteases MMP-9 and MMP-13 [56]. Callus revascularization may be also impaired by nicotine [58], what seems to explain the delayed chondrogenesis and impaired bone healing caused by smoking also reported by other authors [57]. Similarly, alcohol consumption was associated with decreased bone regeneration on implantable demineralized matrixes [61].

Inflammation is part of bone healing and involves various immune cell populations and both pro-inflammatory and anti-inflammatory cytokines and chemokines, as previously described. Therefore, the use of painkillers such as non-steroidal anti-inflammatory drugs to treat bone fracture symptoms has a deleterious effect on bone tissue regeneration [59]. Inhibiting the cyclooxygenase (COX) activity, an enzyme involved in the synthesis of prostaglandins, NSAIDs block angiogenesis and osteogenic differentiation of MSCs in bone

fracture [62]. Moreover, acute and chronic inflammation at systemic level affect bone healing. The impact of chronic diseases, such as rheumatoid arthritis and diabetes mellitus on bone remodelling, highlights the relationship between systemic immunity and bone architecture [60; 63]. Those diseases are characterized by augmented levels of pro-inflammatory cytokines such as TNF-α [63] and IL-6 [64], accompanied by an increased prevalence of osteoporosis [65]. Unbalanced bone turnover is induced by pro-inflammatory environments where RANKL, mostly produced by T cells, promote the activation of osteoclasts. [66]. Polytrauma patients also present increased concentration of IL-6 in serum and impaired bone healing [67]. Infectious agents lead to complications in fracture healing by modulating the immune system towards pro-inflammatory responses. The administration of LPS to rats with bone fracture induced hypertrophic callus with low bone mineral density and decreased production of BMP-2 [68]. Additionally, osteomyelitis caused by bacteria as Staphylococcus aureus lead to osteolysis with Th17-driven response and production of TNF-α and IL-1β [69]. Those findings highlight the crosstalk between local and systemic immune responses in bone healing.

1.5 Arthritis

Osteoarthritis (OA) and rheumatoid arthritis (RA) are the most common forms of arthritis and constitute major causes of pain, disability, and socioeconomic burden across the globe. Rheumatoid arthritis (RA) alone affects 1% of the adult population worldwide, is caused by chronic autoimmune response affecting joints [70]. OA is more prevalent than RA [71], with studies pointing that 10% of men and 13%-18% of women over 60 years of age are affected by this disease [70; 72]. The major risk factors for OA are age, gender, obesity, joint abnormalities, malalignments and injuries [70].

The pathological response underlying OA is perceived to be mostly confined to the joint with limited contribution of systemic inflammation. Early diagnosis of OA is extremely challenging since radiographic joint changes are often detected after the disease is already established. OA is characterized by the progressive cartilage destruction induced by the pathological overproduction of matrix proteases [73]. In healthy conditions, the architecture and ECM composition of cartilage, enriched in type II collagen, aggrecan and proteoglycans, are finely controlled, as illustrated in Figure 5A. In the context of OA, chondrocytes release inflammatory mediators (IL-1β, IL-6, TNF-α) and matrix degrading enzymes (MMPs and ADAMTSs), which may be mechanosensitive [70]. Additionally, the released ECM molecules and their degradation productions activate the innate immune system through toll-like receptors (TLRs), which are expressed by immune cells, but also by chondrocytes [74]. In this degenerative environment, chondrocytes became hypertrophic and endochondral ossification

occurs, replacing cartilage with bone tissue, and impairing proper joint function (Figure 5B). There is no consensus about chondrocytes being the primary trigger for OA. It is possible that cartilage is just amplifying a biological response that is already going on, namely in synovial tissues and/or subchondral bone. As recently proposed, alarmins, endogenous proteins rapidly secreted upon tissue damage, seem to have a major role on OA initiation and progression [75]. In OA, alarmins are thought to be released by damaged chondrocytes and necrotic osteocytes, activating pattern-recognition receptors (PRRs), like TLRs, which lead to exacerbated immune responses, both innate and adaptive immunity, and joint destruction [75].

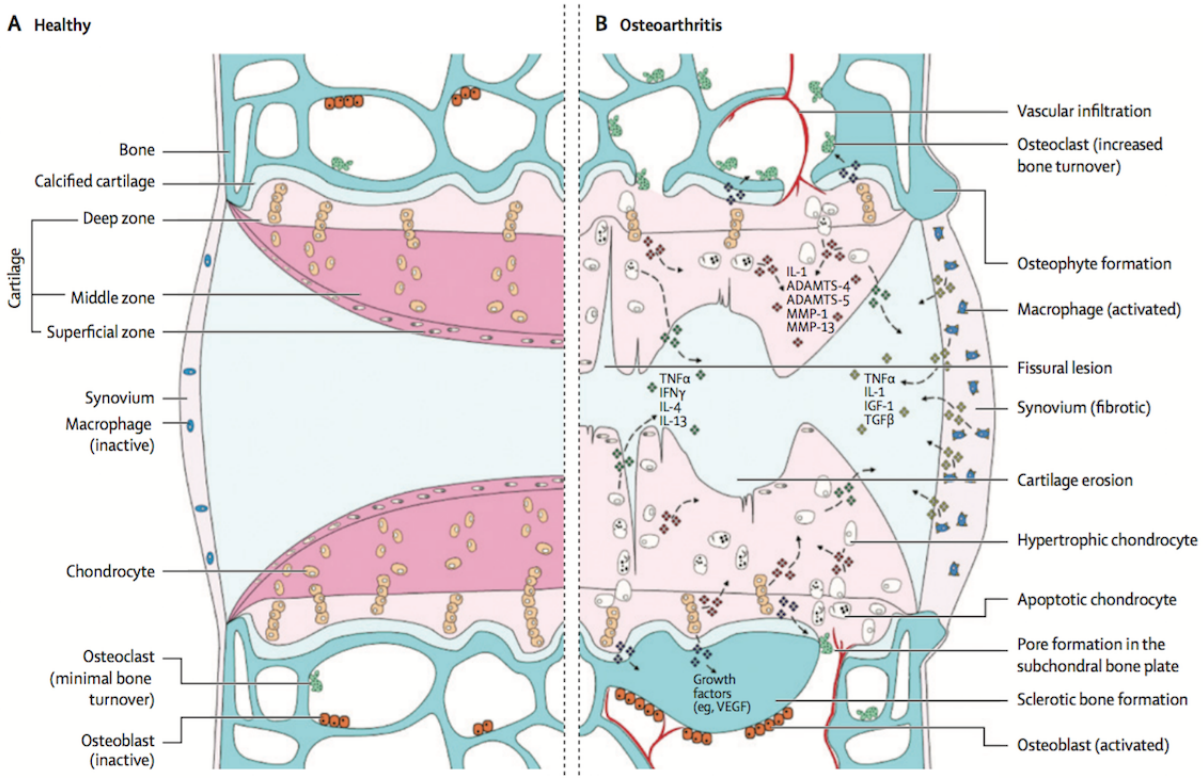

Figure 5 - Healthy and osteoarthritic synovial joint. In homeostasis, cartilage tissue is organized in three distinct layers with low cellular activity. Moreover, subchondral bone presents a minimal turnover while the synovium produces synovial fluid. Osteoarthritic synovial joints are characterized by the narrowing of the joint space as consequence of cartilage erosion and a disorganized attempt of regeneration. Additionally, subchondral bone presents augmented turnover, with formation of both bone pores and osteophytes with concomitant tissue neo vascularization and innervation. In OA, synovium undergoes inflammation with macrophage activation and production of pro-inflammatory cytokines, which contribute for the pathology progression. From [70].

2 Biomaterials in orthopedic applications

In the previous sections, two major orthopedic problems in terms of socioeconomic burden were discussed, whose treatment often involves the application of biomaterials. Bone fracture stabilization frequently requires the use of metallic fixation devices (e.g. screws, plates and nails), bone defects are filled with grafted materials and prostheses are implanted to replace non-functional joints at the end-stage of OA [46].

Although the treatment of fractures of long bones has a very high success rate, other types of fractures (e.g. tibial plateau fracture) and bone healing complications (non-union) require bone grafting [76]. In fact, about 10% of orthopedic surgeries involve bone grafting procedures using autografts, considered the gold standard, allograft or synthetic bone filler materials. The application of autografts is often successfully but 20-30% of the treated patients report chronic pain and morbidity at the donor site [77]. Allografts induce generally weaker healing responses than autografts, presenting complications, such as fracture, non-union and infection in more than 30% of bone grafting procedures. The drawbacks of both auto and allografts have prompted the development of synthetic matrices to repair and promote bone healing. Natural or synthetic biomimetic matrices are part of the orthobiologic solutions that also incorporates biological agents such as BMPs, platelet-rich plasma (PRP), and stem cells, to boost bone healing [78; 79]. Despite the interest of research and industry in orthobiologics, the majority of the orthopaedic medical devices currently used in clinical practice are still based on metal alloys.

2.1 Foreign body response to biomaterials: the key role of macrophages

Conventional materials, often resistant to degradation, frequently fail at promoting regenerative responses upon implantation, inducing instead the formation of fibrotic capsules and poor integration with surrounding tissues. As revised by Anderson *et al* [80], the foreign body response (FBR) occurs in a wide range of clinical scenarios, involving several immune cell populations and regulatory pathways. Monocytes and macrophages play a central role in FBR. Upon implantation, plasma proteins adsorb and complement system is activated on the biomaterial's surface. This reaction, of foremost importance for the further stages of the response, involves the production of chemokines, molecules that induce the recruitment of immune cells, namely polymorphonucleated cells (PMNs) and afterwards monocytes. At the injury site, monocytes differentiate into macrophages and phagocyte dead cells, bacteria and debris, they also modulate the response of other elements of the immune systems through soluble factors or direct receptor interactions. Macrophages can phagocyte particles with few

micrometers in diameter but larger fragments lead to frustrated phagocytosis. At this point, macrophages fuse to form foreign body giant cells (FBGCs), in the presence of IL-4 and IL-13. FBGCs are specialized cells, which attempt to degrade foreign materials with large dimensions, by undergoing metabolic and phenotypic changes that enable them to secrete enzymes, reactive oxygen species (ROS) and acid. Similar to the process of osteoclasts degrading bone, FBGCs adhere to the foreign particle and create an aggressive environment to digest the structure that escaped phagocytosis. When addressing implantable biomaterials such as metals, polyethylene and ceramics, designed to be corrosion-proof, FBGCs fail at degrading them and promote tissue fibrosis by crosstalk with fibroblasts. Thus, high amounts of collagen fibers are produced at the periphery of the implants, surrounding and isolating it in a fibrous tissue.

Macrophages are involved in innate immunity, playing a role of surveillance and host defense, especially by phagocytizing and scavenging cellular, bacterial and inorganic debris. Although macrophages can differentiate from circulatory monocytes, there are tissue resident macrophages in all organs. The plasticity that characterizes the wide range of functions performed by macrophages as well as the molecular mediators secreted by these immune cells, turn them a simultaneous target and ally for therapeutic applications [81]. In fact, macrophages can acquire distinct functional phenotypes in response to environmental signals, in a process designated as macrophage polarization. Depending on the stimuli, macrophages can differentiate in a continuous spectrum of phenotypes [82], which are frequently oversimplified in M1, a more pro-inflammatory population induced by classical activation and M2, more pro-healing, tissue remodeling and/or regulator phenotype, in response to alternative activation [83]. As presented in Figure 6, the various macrophages subsets are characterized by the expression pattern of surface markers, secreted cytokines and chemokines, activation of transcription factors and the production of enzymes involved in ECM degradation (e.g. MMPs) and cell metabolism (e.g. arginase-1) [82].

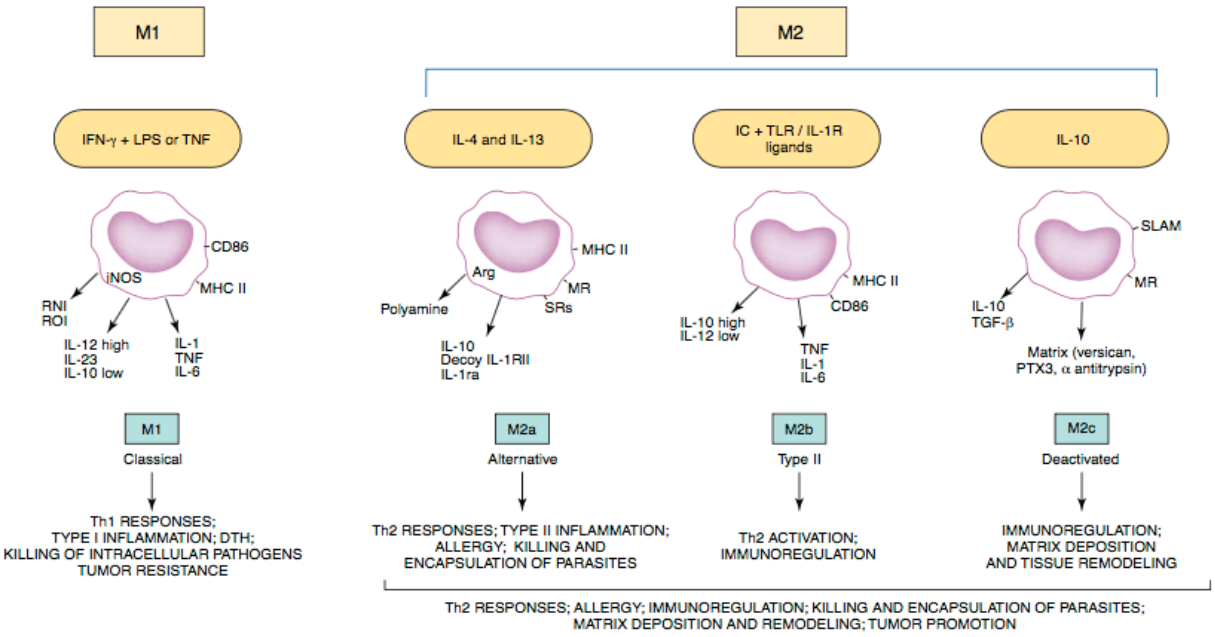

Figure 6 – Macrophage activation and polarization. Illustration of major inducers, surface receptors soluble factors and key functions involved in macrophage polarization. Classically activated M1 macrophages present a more pro-inflammatory profile in comparison to the M2 phenotypes. Depending on the stimuli, M2 macrophages may differentiate in to phenotypes more involved in tissue repair (M2a), immune regulation (M2b) or tissue remodeling (M2c). From: [84].

One of the most used and accepted markers of the human monocytic-lineage is CD14, a surface antigen that acts as co-receptor of TLR-4 in the recognition of LPS [85; 86]. Due to their high levels of expression and specificity to monocytes and macrophages, CD14 have been assessed in combination with other markers in the scope of macrophage polarization studies. Human M1 macrophages are characterized by the presence of increased levels of CD86 [84; 87], HLA-DR [87; 88], CD80 [84] and CCR7 [89] at the cell surface. It is important to state that much of the knowledge on macrophage polarization was observed in murine models and there are significant differences on the involvement of certain receptors (e.g. arginase-1) [90] and enzymes (e.g. iNOS) [91] in humans and rodents. Human M2 macrophages display on their surface CD163 (scavenger receptor) [82; 84; 87] and CD206 (manose receptor) [82; 87; 92], both considered well stablished markers. Moreover, alternative activated macrophages may be divided in three different phenotypes M2a, M2b and M2c, all expressing CD163, which may be considered a general phenotypic [93]. The M2a subset is described as an immune population specially involved in tissue repair and adaptive type II responses and together with M2c phenotype, with pro-healing and debris scavenging functions, express CD206 on the surface [84; 93]. Due to the regulatory role of M2b macrophages these cells present both pro- and anti-inflammatory functions, displaying some receptors, as CD86 and MHCII, also displayed by M1 macrophages [84; 93].

The profile of cytokines and chemokines secreted by activated macrophages is also influenced by their activation status. As expected, M1 macrophages produce mostly pro-inflammatory immune mediators such as IL-1, IL-6, IL-12, IL-15, IL-23 and TNF-α [84; 93]. Conversely, anti-inflammatory cytokines, IL-10, TGF-β1, IL-1Ra, IGF-1 and PDGF, are secreted by M2 phenotypes with some differences associated to the specific subset. As example, M2b macrophages can release, depending on the context IL-10 but also TNF-α, IL-1β and IL-6, with the chemokine CCL1 playing a main role on the maintenance of M2b phenotype [94].

Overall, monocytes/macrophages are central players in the immune response induced by biomaterials. Displaying a wide range of functions and using varied biochemical mediators, macrophages appear as interesting candidates for new therapies addressing improved integration of implantable biomaterials.

2.2 Implantable metallic biomaterials

The mechanical properties of metals have prompted their use in biomedical engineering, namely as implantable medical devices. Metals are present in almost all orthopedic devices but metal-on-metal (MoM) bearings raise the most concern, due to potential risk of adverse biological reactions elicited by excessive generation of metallic particles and ions [95-101]. In spite of widespread application of metallic components in joint replacement, these foster major concerns related to their safety, when tissues and body fluids are exposed to high levels of elements present in metal alloys [102-104].

On the other hand, it is well known that metal elements are vital for cells, where they play structural, catalytic and signaling roles. In fact, cells are able to interact with metal ions at non-toxic concentrations in the tissue microenvironment, but also at systemic level. Cells are sensitive to ions and their mechanisms and behavior may, at least in part, be modulated by these inorganic species [105-107]. Therefore, while metal ions are promising tools, a deeper understanding about the interactions between them and living systems is still needed, to identify the frontiers that limit their safe and therapeutic application.

In the last decade, metal ions have aroused attention, as tissue regeneration enhancers in bone tissue engineering strategies. These approaches promise to improve implant integration and tissue regeneration through metal ions release. A new generation of biomaterials aiming at a controlled degradation, and whose by-products induce healing processes are under intense investigation.

In this next section, both potential adverse effects and healing properties of metal ions and particles released by biomaterials applied in Orthopedic surgery, particular in hip

prosthesis, will be addressed. While clinicians mainly perceive metal ions as toxic agents, scientists start to use their biological effects to improve the interaction of medical devices with surrounding tissues and cells. Thus, we aim at bringing together the two perspectives addressing the processes behind the origin of metal ions, their systemic dissemination, interaction with immune system and involvement in tissue regeneration.

3 Biological response to the degradation products of hip implants

The current section is largely based on the review article “The two faces of metal ions: from implants rejection to tissue repair/regeneration”, published in Biomaterials Journal in 2016.

Despite advances in material design and surgical technique, a significant fraction of the high number of hip prostheses implanted every year still fail. MoM hip prostheses have raised concern among authorities and clinicians, due to the high cumulative revision rates registered at 5 years (3-6%), particularly when considering the 1.5% revision rate for metal-on-polyethylene (MoP) prostheses [95]. However, failed hip implants are an interesting model to enhance current knowledge about the biological response to the materials released by these medical devices [95]. Hip prostheses are mainly composed of metallic alloys, mostly CoCrMo (cobalt-chromium-molybdenum) and Ti_6Al_4V (titanium-aluminum-vanadium), but their bearing surface can be composed of different materials. The bearing surface refers to the superficial layer of each component at the articulation interface between the artificial femoral head and the acetabular cup [108]. The different categories of hip prosthesis are defined based on the materials that constitute their bearing surfaces. The most popular bearing surfaces used for total hip arthroplasty (THA) prostheses are MoP, MoM and ceramic-on-ceramic (CoC). Technological advances have contributed to minimize degradation of these materials. Nonetheless, wear at bearing surface is still responsible for the generation of the majority of prosthetic particles found in surrounding tissues [109]. In terms of amount, MoM bearings generate ten-fold more particles than MoP [110], and most of metallic wear particles are nanometric-sized (smaller than 100 nm) [110-115] while polymeric particles are around 100-10000 nm [116]. Thus, metallic nanoparticles are known to be more reactive as their surface area per volume is higher than polymeric particles. As the majority of hip joint bearings are based on CoCrMo alloys, the particles released are mainly chromium oxide (Cr_2O_3) with an oval to round shape [113; 115]. Also, titanium-based particles may be originated in different regions of hip implants, such as the femoral stem and/or acetabular cup [117].

Wear and corrosion are the mechanisms behind the generation of micro- and nanoparticles, as well as metallic ions. The failure of metallic prostheses is multifactorial, and likely related to adverse biological responses induced by the by-products that are released upon implantation. These agents are shed in synovial fluid, facing the synovial membrane as their first interface with the human body. Dimensions, quantity and chemical composition of the particles are important factors in assessing biological effects of wear debris, and are closely related to the biomaterial that suffers wear and corrosion. [111; 118; 119]. Particles possessing diameters up to a few micrometers are phagocytosed by macrophages [111; 120], while bigger particles can induce a foreign-body response [80]. The activation of macrophages upon

phagocytosis has been pointed out as a trigger, activating the innate immune response, which may ultimately lead to implant failure, through a pathological response sometimes referred to as “particle disease” [121; 122]. On the other hand, the physicochemical properties of metallic ions (eg. size and charge) allow these agents to reach different targets, such as DNA, producing toxic effects in a manner that is different from those caused by particles [123-125]. The local and systemic toxic effects and the mechanisms involved in the biological response against the most relevant metallic degradation products are discussed bellow.

3.1 Periprosthetic tissue response to MoM hip joints

The biological response behind aseptic loosening of hip implants is the cause of long-term failure for about 65% of hip prostheses [108] and depends on a set of immunological phenomena, including cell interactions and cytokine production. Despite MoM, MoP and CoC hip prostheses all potentially failing due to aseptic loosening, the molecular and cellular events underling those pathological response appears to be distinct. The immune response taking place around MoM hip prostheses is not as studied as the macrophage-mediated foreign body reaction to the polymeric wear particles released by MoP prostheses [126-128]. Metallosis, pseudotumors and aseptic lymphocytic vasculitis associated lesions (ALVAL) have all been associated to failed MoM hip implants [129-132]. The inflammatory response associated to the soft tissue lesions presented by some patients with MoM implants is not completely understood but thought to be related to the metal-rich periprosthetic environment. Thus, ARMD (Adverse Reaction to Metal Debris) [132; 133] or ALTR (Adverse Local Tissue Reaction) [134] have been used as umbrella terms. In spite of ARMD being often associated to MoM hip prostheses, it occurs only in about 1% of MoM patients [132] and similar histological findings may be found in periprosthetic tissues of other types of hip implants, namely where modular metal-metal interfaces or impinged metallic components are present [135-137]. Metallic wear debris and ions may be released due to wear, corrosion or tribocorrosion processes [138]. Metallic particles are deposited in periprosthetic tissues giving them a grey color, which is usually named metallosis [139]. This microenvironment may lead to adverse local tissue responses such as pseudotumors and ALVAL as presented in detail in Figure 7.

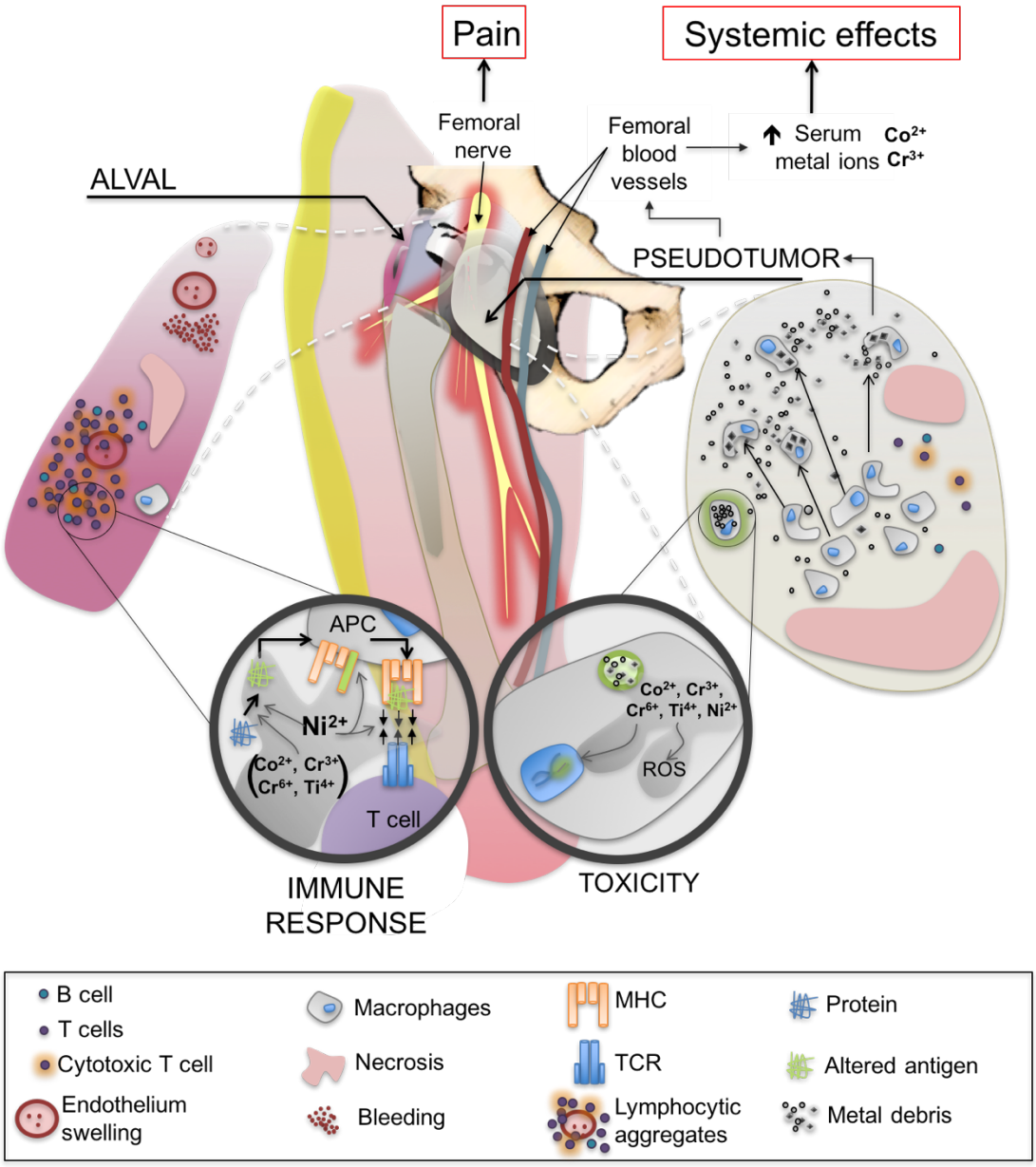

Figure 7 - Pathological responses to excessive exposure to metal particles and ions released by hip prostheses. Pseudotumors and Aseptic Lymphocyte-dominated Vasculitis-Associated Lesions (ALVAL) are the most relevant Adverse Reactions to Metal Debris (ARMD). The accumulation of high amounts of metal degradation products in hip joint space induce the formation of pseudotumors around the implant which leads to augmented serum metal ions levels. The mechanisms underlying pseudotumors formation appear to be related to the inability of macrophages to clean metal debris, despite the extensive recruitment of these immune cells induced by the prosthetic by-products. At intracellular level, high levels of metal particles and ions lead to toxic effects that ultimately result in a vicious cycle of cell death. Together with tissue necrosis, compression of femoral nerve are though to explain the pain suffered by patients with pseudotumors and ALVAL. Although ALVAL is related to metal exposure, it seems to depend more on immune system sensitivity to metal debris than on the amount of metallic particles and ions. Perivascular lymphocytic aggregates, where cytotoxic T cells (CD3+CD8+) appear to have a detrimental role, recurrent bleeding and tissue necrosis are the key events of ALVAL. In the context of delayed hypersensitivity response, several mechanisms were described regarding the influence of metal ions, namely Ni2þ, on antigen T cell activation: producing immunogenic antigens by inducing conformational changes; causing structural changes in major histocompatibility molecules (MHC) on the surface of antigen presenting cells (APC) such as macrophages and dendritic cells; and boosting T cell activation via TCR-MHC interaction (superantigen).

Pseudotumors are described as solid or cystic masses that may grow at the implant periphery. The prevalence of pseudotumors in MoM patients ranges from 20% to 61%, depending on the hip prostheses model [140; 141]. Their etiology is not completely understood and pseudotumors are diagnosed in patients with a painful hip, or even asymptomatic patients [98]. Despite the fact that pseudotumors are neither malignant nor infectious they may provoke pain, due to the compression caused by these masses on other tissues (e.g. muscles or nerves) [98; 142]. The continuous release of metallic particles may induce macrophage infiltration, which will later die (apoptosis) after phagocyting large amounts of toxic particles [132]. These particles will remain in tissues leading to new monocyte recruitment, chronic inflammatory response, and cytotoxicity, when their levels are high [143]. Thus, a stressful environment is created that may induce tissue destruction (necrosis), a significant feature in pseudotumors and failed MoM prostheses [143]. Moreover, the prevalence of pseudotumors was positively correlated with serum Co and Cr levels [144]. The excessive wear of MoM bearings is related with soft tissue lesion [132; 133; 144] but the extent of tissue destruction is not correlated with the amount of metallic particles [132]. These findings highlight the individual susceptibility of patients to metallic agents, particles and ions, which likely determines the magnitude and type of immune response. Sustained cytotoxic response, hypersensitivity to metallic degradation products, or both may be the mechanisms underlying pseudotumor formation [132; 143; 144].

Patients with ALVAL report pain as symptom [98], whose origin is reported as related to the swelling of the vascular endothelium, recurrent bleeding and extensive necrosis [145; 146]. The extension of tissue destruction seems to be related with the thickness of lymphocytic perivascular cuff [132]. The histological features observed in peri-implant tissues with a metal hypersensitivity reaction classify this immune response as ALVAL and may affect 1% of the patients with MoM bearings [98; 145; 147; 148]. It is important to state that ALVAL and pseudotumors are not directly related and may occur independently [144; 149]. ALVAL is characterized by dense perivascular lymphocytic aggregates of T cells ($CD3^+$), B cells ($CD20^+$) and some macrophages ($CD68^+$) [99; 143; 147; 150]. Among lymphocytes, CD8+ T cells (cytotoxic) seem to be the prevalent lymphocyte population [135; 143; 146]. Diffuse lymphocytic infiltrations are also detected, and are composed by T cells only [143]. The potential role of metal degradation products on ALVAL is controversial. An association between the wear rate of MoM bearings and ALVAL has been successfully established [151], but doubts remain regarding the clinical correlation between blood and urine Cr and Co ions levels and the development of ALVAL [132; 147]. Overall, the majority of pseudotumors seem to be related to excessive generation of metallic wear particles and macrophage infiltration, while cases of ALVAL are mostly correlated with unexplained pain or suspected hypersensitivity involving T cells [98].

Cases of metal hypersensitivity to implanted devices have been reported ever since their first use [152; 153]. Presently, the immune response to metal implants is still unpredictable and results provided by metal sensitivity tests are controversial [154]. The prevalence of dermal metal hypersensitivity in healthy population is reported to be about 14% and nickel (Ni^{2+}) and cobalt (Co^{2+}) are the most described offenders [154; 155]. Several reports suggest that an increasing proportion of patients, namely women, will develop hypersensitivity to metal implants, even in the absence of high wear [99; 154; 156; 157].

An immunomodulatory role of T cells in periprosthetic tissue response has been reported, but many open questions remain regarding the mechanisms behind the interactions with metallic nanoparticles and ions [99; 124; 147; 158-160]. The molecular mechanisms that influence the intensity of histologic features observed in MoM surrounding tissues are yet to be revealed [99; 124; 147]. On the other hand, the role of each T cell subpopulation on the biological response against this type of artificial joint and the influence of particulate and ionic degradation products on these immune cells are still unknown [158-160]. The increased proportions of T cells in relation to B cells in MoM periprosthetic tissues led the scientific community to believe that a type IV cell-mediated immune response was behind the lesions observed [101]. T cells may represent 10% of cells at bone-implant interface [160; 161], with the helper population ($CD3^+CD4^+$) being more frequent in periprosthetic tissues than the cytotoxic one ($CD3^+CD8^+$) [160]. T helper (Th) 1 cells seem to dominate over the Th2 population, indicating a more cell-mediated immune response, with the participation of macrophages [160; 162; 163]. At systemic level, Hart *et al* have identified in MoM patients a positive correlation between increased cobalt ions and reduced circulating CD8+ T cells [164]. In line with these findings, decreased number of circulating CD3+, CD4+ and CD8+ cells, together with increased serum interferon-gamma (IFN-γ), indicative of a Th1 response, and concomitant decrease of interleukin 4 (IL-4) levels, related to a Th2 response, were found in patients two years after large-head MoM THA [162].

The mechanisms underlying T cell hypersensitive response are thought to be related to antigen processing and presentation in the context of adaptive immunity. Conformational alterations at protein/antigens level [124; 165; 166], major histocompatibility complex (MHC) and superantigen effect [167] have been pointed as potential action mechanisms of metallic ions involved in hypersensitivity, namely to Ni^{2+}. In fact, Ni^{2+} is the most concerning allergen and its effects at major steps of antigen T cell activation have been reported [154; 155; 167; 168]. Although nickel is many times considered a trace chemical element in metals used for hip prostheses, nickel content (percentage by weight) can be up to 0.5%, 0.1% and 0.05% in CoCrMo (ASTM F75), Ti alloys (ASTM F136) and pure Ti (ASTM F67), respectively.

The microenvironment resulting from corrosion of prostheses may promote protein conformational changes and metal ions released may act as haptens, contributing to the

formation of metalloproteins [124; 165]. Haptens are small agents that can complex with "self" proteins, inducing an immune response. Since most proteins are negatively charged at physiological pH, their potential to interact with the positively charged metal ions is very high [169]. This hapten effect reported for metallic ions appears to be ion-specific and preferential molecular targets have been described. Previous studies show that serum proteins with 68 kDa and 180-330 kDa are the most frequently modified by Cr [124]. On the other hand, it has been reported that Ti binds preferentially to transferrin [125]. Also, Ti^{4+} and Co^{2+} binding sites have been identified in albumin (approx. 68 kDa) [170; 171]. While no conformational changes were associated to Ti^{4+}, it was verified that Co^{2+} binding leads to a conformational transition of albumin that exposes more binding sites for Co^{2+} ions [170; 171]. Proteins with molecular weight between 180-250 kDa, probably immunoglobulins, are associated with greater lymphocyte reactivity [124; 165]. Moreover, the association of metallic ions with plasmatic proteins may facilitate their cellular uptake [125].

The involvement of some metallic ions in antigen-driven T cell activation seems to be related to antigen presentation. It is possible that antigen presenting cells' (APCs) like macrophages and dendritic cells can internalize hapten-modified proteins, process them and present as antigens, through human leukocyte antigen molecules, such as $HLA\text{-}DR^{+}$ [159; 168; 172]. HLA-DR is a MHC class II receptor, present on the surface of APCs, together with co-stimulatory receptors CD80/CD86 and CD40, that can present antigens to T cells, activating them through their counterparts CD28, CD3 and CD40L on the surface of T cells [101]. Interestingly, a previous study has shown increased expression of CD86 and HLA-DR on peripheral blood monocytes together with a decrease of T cell markers CD3 and CD28 in patients with MoM bearings for more than 30 years [161].

3.2 Interaction of metallic particles and ions with immune cells

The findings reported at the vicinity of hip prostheses have prompted both clinical and fundamental research, aimed to clarify the interactions between metal particles (and ions) and living systems. In the following sub-sections, current evidence at research and clinical levels is discussed, focusing on cobalt chromium alloys and titanium alloys. As these families of alloys are widely applied in artificial joints, this review will address the most representative and studied prosthetic degradation products. Although when these metal alloys corrode, they release Co^{2+}, Cr^{3+},Cr^{6+} and Mo^{5+} (CoCrMo) or Ti^{4+}, Al^{3+} and V^{5+} (Ti_6Al_4V) into the human body, the literature has been mostly addressing the metallic ions present in higher percentages in those alloys. Thus, toxicity and other effects of metallic particles and ions (Co^{2+}, Cr^{3+}, Cr^{6+} and Ti^{4+}) on the immune response and bone homeostasis will be discussed below, from cellular to tissue and systemic levels.

3.2.1 Cobalt and Chromium alloys

3.2.1.1 Research evidence – in vitro and other pre-clinical data

CoCr particles and Co^{2+}, Cr^{3+} and Cr^{6+} ions are the main degradation products of CoCrMo alloys studied this far. Molybdenum (Mo^{5+}) is not so widely studied, likely due to its lower amount in CoCrMo alloys, 5-7% of the weight (ASTM F75), and mild toxicity in comparison to Co^{2+} [163]. Cobalt and chromium potential effects on biological systems are in part related with their capacity to be internalized by cells and bind vital molecules such as DNA. Competing for targets used to interact with other ions such as Ca^{2+} or Mg^{2+}, Co^{2+} and Cr^{3+} can change mechanisms that lead to cellular death [173]. The potential cytotoxic effects or the role of cobalt and chromium ions in immune system sensitization is described below. The cellular uptake of metallic ions is the first step of this interaction. Co^{2+} and Cr^{6+} -more than Cr^{3+}- can cross the cytoplasmic membrane trough a non-specific anionic transporter or via an endossomal route [169; 174-176]. Inside the cell, Cr^{6+} and Co^{2+} may exert time and concentration-dependent toxicity or even carcinogenic effects, through similar mechanisms [139; 174; 175; 177]. The reduction of these species to Cr^{3+} and Co^{3+} respectively generates reactive oxygen species (ROS) and reactive nitrogen species (RNS) [175], which saturate the cell antioxidant mechanisms and damage cytosolic proteins, lipids or even DNA. Additionally, Cr^{3+} can cross the nuclear membrane and bind to DNA [169] while Co^{3+} accumulates in cell nucleus and surrounding structures [173].

Co^{2+} has toxic effects on macrophages at lower concentrations (8,000 µg/L) than Cr^{3+} (350,000 µg/L) [178]. Higher toxic thresholds, 30,000 µg/L (equivalent to 0.5mM) for Co^{2+} and 590,000 µg/L for Cr^{3+} (equivalent to 10mM), were observed for primary human lymphocytes [163]. Moreover, Cr^{6+} is highly toxic, as quite low concentrations (520 µg/L) significantly impair viability and proliferation of human lymphocytes [179]. An experiment with mouse macrophages showed induction of apoptosis at 24 h of incubation with Co^{2+} or Cr^{3+} and cellular necrosis at 48 h, but at very high concentrations (6,000-10,000 µg/L for Co^{2+} or 150,000 – 500,000 µg/L for Cr^{3+}) [180]. Necrosis has been reported on some ALVAL observations, but such high levels of Co^{2+} and Cr^{3+} were never observed in periprosthetic tissues. Metal type, concentration and time of exposure seem to be the major factors for macrophage mortality induced by metal ions [111]. Reduction of the cytotoxicity induced by CoCr particles after phagocytosis by monocytes and fibroblasts has been observed [118]. CoCr particles that underwent phagocytosis by monocytes have also presented a reduced genotoxicity, with the surface of the particle appearing to be a critical factor in this process [118].

Nevertheless, sub-lethal levels of Co and Cr ions seem to play a role in inflammation. In mouse macrophages, Co^{2+} and Cr^{3+} induced a concentration- and time-dependent increase in

tumor necrosis factor-α (TNF-α) secretion [178]. CoCrMo microparticles as well as sub-millimolar Co^{2+} levels (4,000-5,900 µg/L) induce primary human macrophages to produce proinflammatory cytokines, namely IL-1β, IL-6, and TNF-α, together with ROS and vascular endothelial growth factor (VEGF) [181; 182]. Macrophages are reported to sense CoCrMo particles via Toll-like receptor 4 (TLR4)-MyD88 signaling pathways, promoting nuclear translocation of nuclear factor kappa-light-chain-enhancer of activated B cells (NF-kB) by reducing its antagonist I-kB, which results in overexpression of IL-1β, IL-6, IL-8 and TNF-α [183; 184]. In addition, CoCrMo particles and Co^{2+}ions, at concentration from 0.01 mM (590 µg/L) to 0.3 mM (17,700 µg/L), lead to an increase in hypoxia-inducible factor (HIF-1α) protein expression what in turn augments NF-kB signaling [182]. Co^{2+} ions were demonstrated to directly activate TLR-4 promoting the secretion of IL-8 and (C-X-C motif) ligand 10 (CXCL10), chemokines that are involved in the recruitment of other immune cells [185]. This may also occur in ARMD, since the mRNA levels of both cytokines were reported to be 18-fold and 10-fold higher in peri-implant tissues of metallosis cases [186]. Furthermore, Co^{2+} may act at endothelial cells level easing the migration of immune cells to the periprosthetic environment. At 1 mM, Co^{2+} directly activates endothelial cells leading to increased secretion of IL-8 and monocyte chemoattractant protein-1 (MCP-1) and also intercellular adhesion molecule 1 (ICAM-1) overexpression, which may justify the augmented lymphocyte binding and transmigration [187]. Thus, chronic inflammatory response may be supported by the proinflammatory role of Co and Cr ions.

Delayed hypersensitivity reaction is likely to occur in presence of CoCrMo particles and ions released by implants. The Th lymphocyte population is thought to play a major role in this inflammatory response. T cell activation (up-regulated CD69 expression) has been reported after incubation of peripheral blood mononuclear cells (PBMCs) from patients with loosening artificial hip joint with Cr ions (36.8 µg/L) [188]. Exposure to CoCrMo alloys appears to lead to T cell sensitization, as primary lymphocytes isolated from patients with well-functioning hip prostheses present increased reactivity, both frequency and magnitude, to Cr^{3+} when compared to lymphocytes from healthy donors [163]. The same study showed that among the tested metallic ions, Co^{2+}, Cr^{3+}, Ni^{2+} and Ti^{4+}, only Cr^{3+} significantly promoted the production of IFN-γ, often secreted by the Th1 subpopulation. Other molecules involved in T cells stimulation (CD80, CD86 and ICAM-1) were up-regulated after incubation with Co^{2+} (4,000 µg/L) [181]. On the other hand, a single study has reported reduced CD3-induced cell proliferation after 48h incubation with CoCr nanoparticles at concentrations from 2,500 µg/L to 25,000 µg/L. Under the same testing conditions, DCs and B cells were not activated and no direct cytotoxicity to T or B cells has assigned to CoCr nanoparticles [189]. When exposed to CoCrMo particles, T cells showed overexpression of TNF-α, IL-1β, IL-13, GM-CSF and IL-10 [190]. Interestingly, up-regulation of the anti-inflammatory cytokine IL-10 is significantly higher in women than in

men [190]. Overall, the effects of metal prosthetic debris on immune cells seems to be highly influenced by the individual susceptibility [163; 190].

Pathological bone resorption is the major biological event underlining aseptic loosening and implant failure. The activity of bone-producer cells (osteoblasts) seems to be reduced at 48h of exposure to low doses of Co^{2+} (10 µg/L) whereas the production of proinflammatory molecules, such as prostaglandin E2 (PGE_2), cyclooxygenase-1 (COX-1), COX-2, IL-8 and MCP-1, is up-regulated [191].

As high systemic levels of metal ions have been reported in THA patients [192], their cytotoxicity towards vital organs has also been assessed. However, the concentrations of Co or Cr generally tested *in vitro* experiments tend to be higher than the ones found in clinical setting. Furthermore, short exposure time to metallic ions, undetermined local concentrations (oral administration) and incomplete protein and ions content of culture media may limit the relationship of these results with clinical findings.

Lung, intestine, liver and kidney cell lines and primary mouse dendritic cells (DCs) exposed to Co^{2+} ions or Co nanoparticles at concentrations higher than 12,000 µg/L for 48 and 72 h. Lung cells were the most Co^{2+} sensitive cell line, presenting signs of toxicity at lower concentration (< 3,000 µg/L) and after 72 h of incubation. On the other hand, DCs were the most resistant to ions, and one of the most resistant to nanoparticles [123]. The viability of macrophages and fibroblasts was reduced by more than 95% after 5 days of incubation with Co^{2+} and Cr^{3+} levels higher than 300 µg/L. At lower concentration of Co^{2+} and $Cr^{3'}$ (about 50 µg/L), fibroblast viability was more affected (-50%) than that of macrophages (-20%) [111].

The systemic effects underlying the dissemination of metallic particles and ions have been addressed in animal experiments [193-196]. Differential deposition of ions seems to depend on time of tissue exposure to ions/particles, element and tissue. Despite Co accumulating more than Cr, both ions levels showed an increase in liver, kidney, spleen, lung, heart, brain, testes and serum 48 hours after CoCr particles implantation in the air pouch model in mice [193]. Long-term exposure (9 months) to CoCrMo implant led to reduced animal growth and demonstrated the accumulation of Cr and Mo but not of Co in the liver, which was likely excreted in urine [194]. Moreover, differences on Co and Cr distribution and accumulation were associated to intramuscular or peritoneal implantation of a CoCrMo wire [194]. It has been reported that the accumulation of metal particles and ions leads to oxidative stress, namely in the liver, spleen and kidneys. In these tissues the expression of antioxidant enzymes was altered, which correlates with the increased ROS production and DNA damage [193; 195]. The toxic effects of Co and Cr seem to persist even after their concentration at systemic level decreases [194; 195]. In line with *in vitro* observations, the implantation of CoCr particles induce early immune response with increased production of IL-1β and macrophage infiltration [196].

3.2.1.2 Clinical Evidence

According to Hallab *et al*, more case reports of hypersensitivity reactions are associated with CoCrMo alloy implants than with Ti alloy components [197]. Levels of metallic ions in serum have been used for monitoring artificial MoM joints in terms of wear generation, risk of ARMD and implant functional outcome [129; 130; 149; 159; 198-201]. In summary, increased concentrations of metallic ions in body fluids are observed following implantation of MoM implants, specially Co^{2+}, even when compared to MoP THA [192].

Serum Co and Cr levels in healthy control subjects were usually bellow 0.29 µg/L and 0.34 µg/L, respectively. Nonetheless, levels below 2 µg/L are considered normal by several authors, for well-functioning MoM implants [136; 144; 149; 165; 199; 202; 203]. The concentrations of both ions usually vary from one to few dozens of µg per liter, in all tested human fluids (serum, blood, whole blood, urine) [132; 144; 192; 204]. Clinically, the average serum Co and Cr levels after MoM prostheses implantation are often reported to be within the range of 1-7 µg/L but failing MoM hip implants, some pseudotumors cases [144], and extensive corrosion on the modular MoP stem-neck interface [136] often present concentrations in the order of hundreds of µg/L [129-131; 144; 149; 159; 198-201; 203]. There is no international consensus on toxic threshold limits for metallic ions concentrations found in the blood and urine of patients with hip prostheses, namely with large head MoM bearing (≥36 mm). Moreover, it remains unclear the true meaning of these levels. US Food and Drug Administration (FDA) has not defined Co or Cr threshold values for MoM management, due to the lack of scientific evidence linking serum or whole blood metal ions levels to excessive wear or failing of MoM hip implants. Nonetheless, in Europe is recommended that MoM patients presenting serum concentration of Co from 2 to 7 µg/L should be followed-up by imaging techniques to evaluate ARMD [202]. Serum Co or Cr levels above 7 µg/L may be a sign of ARMD and should be considered in discriminating well-functioning from failed MoM hip prostheses [205]. Revision surgery should be performed if abnormal radiological findings are observed, metal ions levels are steadily rising or serum concentration of Co surpasses 20 µg/L [202; 206]. The levels of Co ions in serum were demonstrated to reduce to normal levels (10.96 µg/L vs 1.61 µg/L) after removal of their source [203].

Despite the fact that metallic ions reach the circulatory system, the majority of the particles remain entrapped in nearby tissues. Joint capsule is the tissue where higher Co, Cr and Ti concentrations have been found, ranging in the thousands of µg/L, what constitutes a 100 to 1000-fold increase after hip replacement [136; 165]. This is an expectable finding since synovial fluid and membrane, capsule and bone constitute the closest biological environment to the origin of the metallic debris. Thus, local toxicity may occur, inducing a local biological response that provokes swelling in the hip region and impairs the functioning of the implant.

The mechanisms underlying the accumulation of metallic particles and ions in the tissues and their potential role in regeneration remains vastly unknown.

The adverse effects of metallic particles and ions at systemic level are a major concern, namely in the long-term. Numerous small blood and lymphatic vessels are present in synovial membranes [207], allowing particles and metallic ions to travel to distant parts of the body. Lymphatic vessels transport molecules and ions from the synovial fluid and allow the trafficking of immune cells such as macrophages between the synovial membrane and the lymph nodes or other secondary lymphoid tissues, such as spleen. The capacity of macrophages, also present in synovial fluid, to phagocyte small particles may be responsible for particle deposition in lymph nodes, bone marrow, liver, lungs and spleen [208-210]. Lymph nodes and spleen are involved in the filtering of lymphatic fluid and blood, respectively. Thus, it is expectable that higher levels of metallic particles are found in those tissues in a free form, inside macrophages or in organometallic complexes [208; 210; 211]. Para-aortic lymph nodes are the most affected by metallic particles deposition and in severe cases tissue necrosis has been reported [208; 209]. The fate of wear particles in other organs such as liver, spleen or heart is unknown. Probably, they remain trapped and continue to be corroded intracellularly, due to the corrosive environment of the phago-lysossome, potentially inducing higher local levels of metal ions, even after implant removal [165; 212]. However, environmental sources can also be responsible for increased levels of Co, Cr and Ti species in the body [208].

One of the most worrying aspects of long-term exposure to increased levels of metallic particles and metallic ions is cancer risk. Overall, the incidence of prostate cancer and melanoma seems to be higher among THA patients [213; 214], while lung cancer incidence is decreased compared to general population [213]. The period of ten years following THA appears to register an increased risk of cancer, namely kidney, likely related to the run-in wear period, where the amount of metallic debris is often very high, challenging renal clearance capacity. Augmented risk of chronic renal disease was observed in a 9-year follow-up of MoM patients [215]. In the period between 10 and 20 postoperative years, the general cancer incidence seems not to be increased in MoM or MoP THA patients [213]. Nonetheless, there is not enough evidence associating metallic debris and increased cancer incidence, so there is a need for longer follow-up periods (more than 20 years) and further epidemiological studies.

Significant increases in mortality due to cardiovascular diseases were verified in patients with MoP or MoM bearings, 20 years after implantation [216]. A case report of fatal cardiomyopathy secondary to severe wear of CoCr alloy femoral head was previously described [217]. The patient presented very high Co levels in the blood (6521 µg/L) and in the heart (3.85 µg/L), when compared to Co concentration in heart tissue of healthy individuals, which ranges from 0.1 to 0.4 µg/L. Cobalt toxicity at mitochondrial level with subsequent fibrosis of cardiac tissue is the most plausible cause of death.

Since artificial hip joints such as MoM bearings are being applied in younger patients, new problems may arise. For example, the possibility of transplacental transfer of metal ions during pregnancy was evaluated. Increased levels of Co^{2+} and Cr^{3+} have been detected in the umbilical cord of pregnant women with MoM bearings, when compared to controls [200]. However, these metal ion concentrations have been lower than 1 µg/L, with the placenta appearing to play a modulatory role.

3.2.2 Titanium and titanium alloys

3.2.2.1 Research evidence – in vitro and other pre-clinical data

Titanium particles and ions are considered less toxic than those derived from cobalt [218]. However, Ti ions are prone to bind and induce damage to phosphorus-rich molecules (e.g. RNA, DNA and phospholipids) [219; 220], leading to aneuploidy events *in vitro* and *in vivo* [139]. Although other elements present in titanium alloys are highly toxic (vanadium) or known allergen (aluminum), few studies addressing them in the context of implant/prostheses are available.

Particulate and ionic Ti debris are reported to influence the immune system. In macrophages, Ti ions appear to increase the production of proinflammatory cytokines (IL-1β, IL-6 and TNF-α) with concomitant downregulation of TGF-β expression [221]. Ti ions activate T cells, leading to increased expression of CD69, CCR4 and RANKL in a concentration-dependent manner [219; 220]. Moreover, the ability of Ti ions to promote T cell proliferation seems to be affected by pre-existing inflammatory conditions, since rheumatoid arthritis patients present augmented reactivity against Ti ions [222]. Recent *in vitro* evidence indicates that Ti^{4+} ions promote adaptive immune responses, the authors show that human dendritic cells (DCs) exposed to Ti^{4+} are able to select T cells specific for Ti^{4+}, that are not reactive against Ti^{3+} ions [172]. Moreover, Ti^{4+} ions influence cytokine and surface receptors prolife on DCs, towards a Th1 mediated-inflammatory response [219]. Ti-induced delayed hypersensitivity may occur due to chronic exposure to Ti ions or TiO_2 particles, but it seems that Ti allergy is confined to a reduced number of patients [222; 223] even considering that TiO_2 particles are widely used in food, cosmetics and medicines. Moreover, a proteomic evaluation of draining lymph nodes of skin challenged with TiO_2 nanoparticles found that the expression of proteins related to mRNA processing, immune response and antimicrobial activity, and lipid metabolism was significantly decreased [224]. Many details related to metal sensitivity are still unclear, since the individual contribution of each element that constitutes metal alloys is not fully known and the role of the host susceptibility to allergic response is only partially understood [154].

Similarly to other types of particles, Ti microparticles may be phagocytosed by macrophages. This process is reported to involve scavenger receptors [225], it affects enzymes that manage intracellular ROS level [226] and leads to changes on the surface chemistry of Ti particles, inactivating them [227]. In a study comparing human primary macrophage response to different types of prosthetic debris, Ti_6Al_4V, CoCr, alumina and PE microparticles, Ti was found to elicit higher expression of proinflammatory cytokines [228]. While CoCr particles induced increased secretion of TNF-α, IL-6 and IL-8, exposure to Ti_6Al_4V led to higher concentration of those cytokines and also IL-1β, IL-1a, MCP-1, granulocyte macrophage colony-stimulating factor (GM-CSF), but also IL-10 [228]. Concentration of Ti particles is critical as IL-1β production was found to be concentration-dependent, in both human and mouse macrophages [229]. Moreover, the interaction between Ti microparticles and macrophages involves the cellular receptors TLR-2,3,4 and 9, and the intracellular adaptors MyD88, TIR-domain-containing adapter-inducing interferon-β (TRIF) and NF-kB, whose involvement in particle-induced inflammation has been reported [230]. It is known that activation of NF-kB increases secretion of proinflammatory cytokines, such as TNF-α, IL1-β and IL-6 [230-232].

Some *in vitro* studies have addressed the effect of Ti microparticles on bone remodeling. Osteoblasts incubated with very high concentrations of Ti microparticles (30,000 μg/L) for 48 h led to increased production of osteoclastogenesis factors, such as receptor activator of nuclear factor kappa-B ligand (RANKL) and CSF-1 [233]. Additionally, bone marrow stromal/stem cells (MSCs) exposed to Ti microparticles presented impaired osteogenic differentiation and increased production of IL-8 [234], a chemokine that is involved in the recruitment of neutrophils and is overexpressed in periprosthetic tissues of aseptic loosening patients [235].

Although Ti ions may diffuse systemically, most of the studies evaluate the local biological response to Ti particles. This fact may be related with Ti alloys susceptibility to degradation by wear, generating particles, accompanied by a high resistance to corrosion [236]. Distinct patterns of distribution and accumulation were found *in vivo* for TiO_2 microparticles, TiO_2 nanoparticles and Ti^{4+} ions. Ti microparticles accumulated mostly in the lungs, while TiO_2 nanoparticles and Ti^{4+} ions diffused systemically and are found in several different organs, namely spleen, kidneys, lungs, liver, heart, blood and brain [237; 238]. TiO_2 nanoparticles are small enough to overcome the blood–brain barrier (BBB) but further studies are required to clarify the neurotoxicity reported by some *in vitro* and *in vivo* studies [238]. Although Ti exhibits thrombogenic properties [239] cases of orthopedic patients reporting altered clothing due to exposure to Ti were not found. This feature seems to be more concerning for the performance of other medical devices, such as Ti-based heart valves [240].

Animal experiments have recapitulated the Ti particle-induced immune response and associated osteolysis. Intraperitoneal injection of Ti microparticles in mouse caused at short-term acute inflammation with signs of neutrophil recruitment, IL-1β production and activation of NALP3 inflammasome [196; 229]. Fibrous tissue formation and bone resorption were also observed one week after Ti microparticles having been injected [241; 242]. Osteolysis was also found using the murine calvaria bone defect model [230; 243]. In this context, decreased bone density and volume with increased RANKL/osteopontegrin (OPG) ratio, number of osteoclasts, and also augmented TNF-α and IL-1β were locally found, in presence of Ti microparticles [242; 243]. Interestingly, epithelial cells upon recognizing bacteria via TLR4 receptor in the presence of Ti ions, were reported to increase the RANKL/OPG ratio and (C-C motif) ligand 2 (CCL2) production, which highlights the potential modulatory effect of Ti ions during host-pathogen interactions and provides an explanation for increased osteolysis in the case of bacterial infection [244]. Another study has found increased serum IFN-γ levels in rats two weeks after implantation of Ti plates in muscle tissue, which is positively correlated with peri-implant macrophages [245].

3.2.2.2 Clinical Evidence

Uncemented acetabular and femoral stem components are often made of Ti alloys. Although these components do not suffer much wear as materials applied on head-cup interface, Ti alloys at particular micromovements, like the interface with bone or other metallic prosthetic parts, suffer corrosion releasing metallic ions to surrounding tissues [246]. Soft tissues surrounding failed Ti_6Al_4V femoral stem presented high concentrations of Ti and Al ions, when compared to the levels of Co and Cr ions found in patients with both cemented and uncemented CoCrMo alloy femoral stems [246]. Locally, the accumulation of Ti debris may also occur in the synovial capsule (39400 µg/g) as well as in synovial fluid (556 µg/L) together with Al (654 µg/L) and V (62 µg/L) [165]. Ti is more soluble than V but less than Al, so its concentrations in serum and synovial fluid are intermediate [247; 248]. Serum Ti ions concentrations are from the same order of magnitude as those of Co and Cr ions and may achieve less than 4 µg/L for well-functioning hip prostheses and 8 µg/L for failed implants [130; 208]. Moreover, the concentration of Ti in urine seems to significantly increase after MoM and MoP hip replacement [249]. Nevertheless, in the clinical setting, hip implants management is not based on Ti levels.

4 New therapies for bone repair and regeneration

In response to the adverse biological and impaired healing responses, new bio-inspired approaches have been developed in Orthopedics, specially exploring the immunomodulatory and pro-regenerative properties of materials and drugs. While immunomodulatory therapies for orthopedic applications are still in research phase [250-252], the application of bioactive molecules and cells to foster bone, cartilage and soft tissue regeneration is in the clinical arena [49; 253; 254]. In the next sections, the new orthobiologic therapies under investigation and development will be discussed, focusing on 1) metal ions, 2) protein therapeutics, 3) biomimetic biomaterials and 4) immunomodulatory strategies.

4.1 Metal ions

The prevalent idea that ions released from metal-based implants induce negative effects on biological systems is changing. Depending on the element, duration of exposure and tissue microenvironment, ions can modulate tissue response promoting regeneration or, conversely, leading to cell toxicity, oxidative stress and death. New strategies using metal ions are being developed focusing on different medical fields. The toxicity of some metal ions at low concentrations has been explored for application in Oncology. A bioglass incorporating vanadium was engineered to release this metal ion in a controlled fashion, to induce apoptosis of cancer cells [255]. Additionally, metal corrosion processes may be tuned to control tumor growth or infection, using systems such as galvanically coupled Mg-Ti particles [256]. Metal ions can be applied to improve the bioselectivity of surfaces used in medical devices, promoting tissue repair in bacterial-challenged environments [257; 258]. The interaction between metal ions and proteins may generate metalloproteins such as organic vanadium compounds. In this form, the toxicity of inorganic vanadium is diminished, allowing the vanadium insulin-mimetic effect to improve bone fracture healing, by accelerating angiogenesis and chondrogenesis [259]. Besides vanadium, aluminum (Al) is another metal element present in Ti_6Al_4V alloy that has been applied in vaccine development. Al is currently applied as a vaccine adjuvant, due to its capacity to induce a humoral response involving Th2 lymphocytes, boosting the production of antibodies (mainly IgG1) [260]. Alternatively, and as described above, the metal hypersensitivity response to CoCrMo alloys is closer to a Th1 profile, which has prompted the application of cobalt nanoparticles as alternative adjuvants, when IgG2c antibodies (Th1) are also required [261].

Amongst the wide potential applications of metallic ions, tissue engineering is certainly a promising field, where metals ions may be generated by the biomaterial used or added as a

supplement. There is an increasing number of studies reporting successful therapies based on metallic ions, highlighting the role of these ionic agents as new tools for tissue engineering [262]. Depending on the application, the template/biomaterial may be designed to be durable or biodegradable. In the context of joints, application of complete biodegradable biomaterials is not yet feasible as the current technologies are not able to promote regeneration of extensive defects of bone and cartilage tissues. However, it is tempting to speculate that the pro-regenerative effects of some metal ions may be used at the interface of metal implants and surrounding tissues [263]. The trend in tissue engineering seems to be towards biodegradable materials that may incorporate growth factors, drugs or cells. On the other hand, the fabrication of biodegradable biomaterials is still a hot topic since there is no effective solution to avoid the foreign body response against implants often registered at long-term. The development of "smart" biomaterials that are able to degrade at controlled rates for *synchronized* tissue regeneration is at an early stage. Similarly, in Cardiology, the durable metallic stents are being substituted by biodegradable drug-eluting stents, aiming to reduce the risk of stent thrombosis and to restore vascular physiology [264].

The application of metal ions in the development of orthopedic biomaterials is related to their positive effect in angiogenesis and osteogenesis. A new generation of biomaterials aiming at controlled release of metal ions to induce bone healing has been developed [106; 107; 265; 266], as summarized in Figure 8. Embedding ions (e.g. magnesium, strontium, cobalt, calcium, among others) into ceramic or metallic matrices has been a concept underlying new regenerative strategies. In the next section, the application of magnesium and cobalt-based strategies for cartilage and bone repair will be discussed as both ions are released by orthopedic implants already available in clinical practice. Moreover, the evidence for magnesium and cobalt clearly corroborates the importance of the balance between the elicited immune response and the effect of a biomaterial on tissue regeneration/repair. While magnesium is safe, may have a regulatory effect on immune cells and promote bone tissue healing, cobalt is still perceived as a toxic agent and its angiogenic potential trough hypoxia-mimetic effect is thus far limited by the immune system.

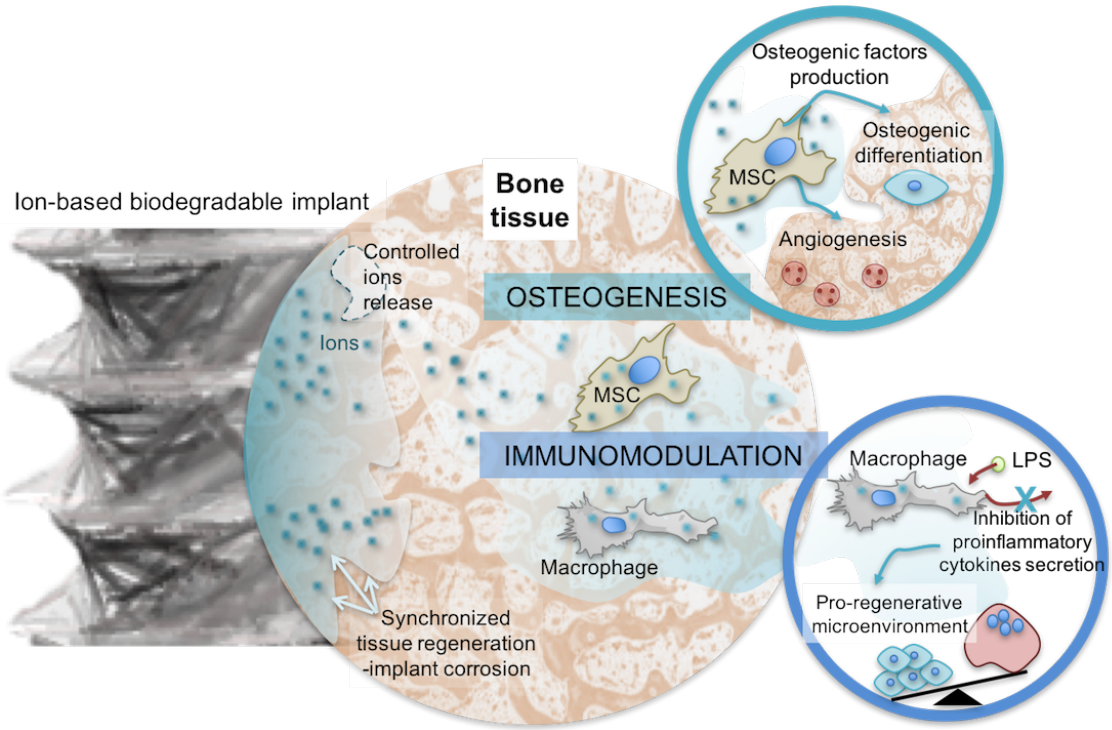

Figure 8 - Application of biodegradable materials for controlled release of metal ions in regenerative medicine. In bone tissue context, ions are able to promote osteogenesis coupled with a pro-regenerative immune response. The ion-enriched environment may induce osteogenic differentiation of mesenchymal stem/stromal cells (MSCs) as well as improve angiogenesis. Moreover, metal ions may modulate the response of immune cells to proinflammatory stimuli such as lipopolysaccharide (LPS), modifying the expression of cytokines such as TNF-α, IL-1β, IL-6 and PEG_2, which ultimately affect the regenerative capacity of the tissues. From [70].

4.1.1 Magnesium

Magnesium and magnesium alloys have been tested for biomedical applications, namely in Cardiology, as biodegradable cardiovascular stents [267], or in Orthopedics as screws, fixation devices and bone filler materials [268; 269]. Biodegradable magnesium-based metal implants are groundbreaking, providing a temporary solution that can fill the gap between the corrosion-resistant metallic devices with long-term problems (e.g. infections or hypersensitivity response) and the polymeric biodegradable materials with poor biomechanical performance. The biodegradability of magnesium and magnesium alloys resides on their corrosion in physiological environment, releasing mostly Mg^{2+} and H_2. However, controlling the degradation rate of magnesium alloys has been challenging, with implants degrading faster than tissue is able to repair, or releasing high amounts of H_2 that remains entrapped in periprosthetic tissues destabilizing bone-implant interface [269]. Thus, several magnesium alloys have been developed, to overcome the described drawbacks, these can be grouped in three families [270]: 1-pure magnesium with traces of other elements, 2-Al-containing alloys (e.g. AZ91, AZ31 or LAE442) and 3-Al-free alloys (e.g. WE43, WZ21 and Mg-Ca alloy) [268; 269; 271-

273]. Combining magnesium with other elements such as aluminum (A), zinc (Z), manganese (M), yttrium (W), calcium (Ca), strontium (Sr) and rare earth elements (E), leads to improved mechanical properties and corrosion behavior. Nonetheless, envisaging orthopedic applications further optimization is still required [274]. Moreover, research has been improving the biological response to pure Mg and Mg alloys creating hybrid biomaterials combining this metal with polymers [275], ceramics [107], ECM proteins and cells [273].

Once implanted in animal models, pure Mg and Mg alloys promoted higher bone formation and complete fracture healing, overcoming the limited mechanical properties of polymeric biodegradable models (e.g. polylactic acid) [268; 269; 273; 276-281]. Moreover, Mg-based screws supported improved reconstruction of rabbit anterior cruciate ligament, with fibrocartilaginous tissue regeneration, when compared to Ti screws [281]. These findings prompted a controlled clinical pilot study where MAGNEZIX® screws, a Mg alloy similar to WE43, were successfully implanted in 26 patients that underwent orthopedic surgery [271]. Mg alloys biodegradability and mechanical properties similar to bone are believed to be the major factors underlying their success [282]. However, the ionic magnesium (Mg^{2+}), released upon corrosion of magnesium-based implants, may have a critical role in the induced biological response. Indeed, Mg^{2+} is crucial for health and life and is involved in stabilizing key biological molecules (e.g. ATP, DNA), acting as a co-factor of enzymes, in cell signaling, and cell migration, among other processes that guarantee the proper function of tissues such as muscles, heart or nervous system [283-285]. Although not in Orthopedics, Mg^{2+} is already applied in clinics through administration of magnesium sulfate ($MgSO_4$) for neuroprotection [286], muscle relaxing and treatment of pre-eclampsia [287].

Therapeutic concentrations of Mg^{2+} have been tested in bone and cartilage tissue engineering [288; 289]. Exposing human BMSCs to millimolar levels of Mg^{2+}, from Mg-containing salts, pure Mg or Mg alloys extracts, increased cell proliferation and osteogenic-guided differentiation [106; 281; 289; 290]. After 3 days in Mg^{2+}-enriched environment, molecules involved in osteogenesis such as TGFβ-1, BMP-2, SMAD4, VEGF and collagen I were found increased, while condrogenesis (SOX9) and pluripotency (SOX2) markers were downregulated [106]. Interestingly, after 14 days, another study has also reported the overexpression of VEGF, BMP-2 and COL2A1 but accompanied by an up-regulation of SOX9, which was likely related to the regeneration of fibrocartilaginous tissue observed *in vivo* [281]. In this context, the most described cellular pathways affected by Mg^{2+} are TGF-β1/SMAD4, HIF-2a and PGC-1a but the effect of Mg^{2+} on osteogenesis depends on the differentiation status of human MSCs [106; 289]. In fact, the cellular demand for Mg^{2+} increases during osteogenesis, as reported for rat MSCs overexpressing Mg^{2+} selective transporter (MagT1), whose knockdown led to decreased osteogenic differentiation [291]. Additionally, the deposition of bone matrix elements, calcium and collagen type X, were augmented in human

MSCs exposed to Mg^{2+} concentrations of 5 and 10 mM [289]. Despite concentrations of Mg^{2+} up to 15 mM improving osteoclast function [292], animal studies testing Mg alloys for bone repair indicate that Mg balances bone remodeling towards repair instead of osteolysis. Moreover, Mg^{2+} accelerate the regeneration of cartilage [288]. The underlying mechanism is thought to be linked to integrins, ion-sensitive proteins that mediate the cellular adhesion to extracellular matrix [288; 293]. However, Mg^{2+} concentrations above 20 mM negatively affect cartilage mechanical properties by reducing the production of collagen and glycosaminoglycans [294].

In addition to the pro-regenerative stimuli on MSCs, Mg-based strategies can modulate the immune response to support tissue healing (Figure 8). Thus, it is vital to understand the role of Mg^{2+} on cells, namely immune cells, where most of the knowledge stems from studies involving Mg-deficient models [295-297]. In hypomagnesemia conditions, cells suffer oxidative stress and the ability of the immune system to respond to challenges (e.g. infection) is reduced, leading to ineffective or uncontrolled responses [105; 295; 297]. On the other hand, Mg^{2+} supplementation was demonstrated to have an immunomodulatory role [105; 298; 299]. The production of proinflammatory cytokines such as TNF-α, IL-1β, IL-6 and PEG_2 after immune cells stimulation with lipopolysaccharide (LPS) was demonstrated to be reduced in the presence of increased concentrations of Mg^{2+} [298-300]. In an osteoarthritis rat model, injections of $MgSO_4$ reduced cartilage degeneration, nociception and synovial inflammation, while increasing chondrocyte survival [301]. The action of Mg^{2+} is believed to be NF-kB-dependent, a central regulator underlying proinflammatory cytokine production [299].

4.1.2 Cobalt

Most of the studies so far address Co as a toxic agent. Environmental sources (e.g. mining activity) or failed Co-containing biomaterials provide cases of massive human exposure to this element, which may lead to allergic reactions, tissue destruction and ultimately death [302; 303]. Nevertheless, sub-toxic concentrations of Co may promote angiogenesis, which may contribute for tissue regeneration.

Novel strategies for bone tissue engineering have been investigated, taking advantage of the hypoxic-mimicking conditions generated by Co [304-306]. Biologically, Co signals cells for low O_2 pressure by stabilizing HIF-1α, which induces the secretion of factors that support cell survival in hypoxia environment and promote the formation of new blood vessels.

A possible strategy consists in pre-conditioning cells, namely stem cells using high doses of Co [307; 308]. Enhanced vascularized bone formation was achieved through implantation of constructs with human BMSCs pre-treated with media containing 5900 μg/L of Co (equivalent to 0.1 mM Co) in rat bone defects [307]. Alternatively, Co-containing ceramics and

bioglasses have been developed aiming to mimic hypoxia through Co action [309-312]. Cobalt was shown to promote angiogenesis by increasing the production of VEGF and enhancing the osteogenic differentiation of human MSCs [309; 311-313], which is in line with the, tube-like structures formed *in vitro* by endothelial cells (HUVECs) when treated with Co [309; 311]. A recent work presented a polymeric core-shell scaffold with sustain release of Co^{2+} and BMP-2 that successfully promoted early angiogenesis and improved bone formation in rat calvaria defect model [306].

Notwithstanding, cobalt may be a double-edge sword. The history of Co as pro-regenerative agent may be spoiled by the immune system response. Immune cells are sensitive to Co exposure, macrophage activation and ROS production was found to take place at Co concentration used for cell pre-conditioning (0.1 mM) [185]. Exposing human MSCs to conditioned media from macrophages treated with extracts from Co-containing ceramic led to decreased osteogenesis while osteogenic differentiation was observed when these cells were directly treated with the extracts [313]. Of note, the most part of the promising results using cobalt-inspired strategies have been obtained *in vitro* or using the immunocompromised animal model SCID mice [307], which could imply an immune system-related impairment of the regenerative potential of Co. However, a very recent study reports pro-regenerative results obtained using imunocompetent animals and implanting core-shell scaffolds that release small amounts of Co^{2+} (maximum of 14 μM at 6 days) [306].

In summary, the success of Co^{2+} for regenerative purposes seems to be highly dependent on the doses used. The current solutions using Co may lead to high concentrations of Co at the periphery of implants, such as levels of 20,000 μg/L that were reported *in vitro* at 7 days, decreasing then to 1,000 μg/L [311]. The frontiers for therapeutic, immunological and toxic Co concentrations are still unclear. The role of Co in the immune response associated to bone repair/regeneration, the identification of pro-healing Co levels and the development of biomaterials that ensure desirable Co levels and timing should be further investigated.

4.2 Protein therapeutics

In Orthopedics, the use of BMPs as a protein therapeutic to induce the formation of bone and cartilage has been a topic of intense discussion [314; 315]. Due to the osteoinductive effects of BMPs, intensive research has been carried out to enlarge the knowledge on this family of morphogenic proteins, with commercial products based on BMP-2 and BMP-7 reaching the market for spine-fusion surgery and bone non-union [78]. Although BMPs have been originally discovered in bone, further studies have shown the contribute of BMP signaling on the architecture of different tissues [314]. Moreover, the balance between BMP-like signals and other growth factors, specially TGF-β, have been demonstrated to affect tissue homeostasis [314]. The safety and efficacy of BMP-based strategies have been under surveillance due to the risk of adverse effects (e.g. ectopic bone formation and cancer) and cost-effectiveness [315]. Data currently available supports improved efficacy of BMP use in the treatment of severe and acute fractures (tibial) but not in non-union cases [78]. BMP-based strategies are promising but refined delivery strategies are required to avoid uncontrolled protein diffusion and unbalanced tissues response.

Simultaneously, PRP, blood plasma enriched in platelets has been tested *in vivo* [316] and in clinical trials [317] to promote bone, cartilage and soft tissue repair. The pro-healing properties of PRP seem to be related to its supra-physiological levels of autologous cytokines and growth factors such as PDGF, TGF, IL-1, VEGF, IGF, osteocalcin, osteonectin, fibrinogen (Fg), among others [318]. However, the use of PRP is still limited to experimental works. The main drawback pointed by the experts is related with the impact of variable PRP preparation methods have on the composition of the cocktail [317; 319].

4.3 Biomimetic material-based approaches

Biomimetic approaches also constitute promising solutions to the drawbacks presented by the conventional inert materials. Cells live in an organic and dynamic environment, relying on biological clues provided, not only by soluble factors, but also from the ECM. In fact, ECM offers both structural and biochemical support to cells. Therefore, ECM components may be used in regenerative medicine and tissue engineering.

Collagen, mostly type I, is one of the most explored ECM components in biomaterials field due to the fact of being biodegradable, biocompatible and suitable for different types of applications [320]. Although type I collagen is the major organic component of bone ECM, other proteins and new preparation methods have been studied with the aim to recapitulate several tissues properties. In a recent study, the authors have synthetized elastic-like collagen

scaffolds using a new crosslinking method, as alternative to the addition of elastin, to support the development of dynamic tissues such as blood vessels and lung tissue [321]. Scaffolds based on collagen and glycosaminoglycan or calcium phosphate have also been widely explored for applications in cartilage and bone [322]. Alternatively, small bioactive fragments of the proteins can be used to improve the biological response of synthetic biomaterials [77]. Another strategy that has been considered in the field of protein-based materials is the use of decellularized matrices [323; 324]. These 3D structures are prepared by removing the cellular component from tissues but maintaining the biochemical composition of ECM, establishing an interesting pro-healing microenvironment with interesting results upon re-cellularization and *in vivo* implantation [323; 324].

Fibrinogen-based materials have been addressed by numerous studies and clinical investigations, especially as fibrin sealants [325]. The rational underlying this type of material is inspired in the blood clot formation, where a fibrin mesh is formed by fibrinogen cleaved by thrombin to stop bleeding and form a provisional ECM. Thus, most applications of fibrin sealants are related to their hemostatic properties [326]. However, fibrin hydrogels and constructs have been explored in research for tissue engineering and drug delivery purposes [252; 254; 327; 328]. Due to their viscoelastic properties and their biological composition that resembles the primordial and temporary matrix formed upon blood cloth, fibrin hydrogels have been tested as carrier for cell therapies [252; 327]. A study showed that when implanted in plate-stabilized rat femoral defects, fibrin hydrogels with MSCs lead to the overexpression of VEGF at day 3 as well as the recruitment of higher ratio of M1 macrophages (CD68+CCR7+) over M2 macrophages (CD68+CD163+) at the periphery of the implant, when compared with the fibrin hydrogels alone [252]. The application of fibrin materials in Orthopedics and Dental Medicine has been tested combining fibrin with constructs with mechanical properties similar to bone such as demineralized bone [329], calcium phosphate granules [330] and metallic implants [331]. Additional strategies to tune the biological response induced by fibrin-based materials have also been explored and involved the adsorption of other proteins [327] and the use of fibrin materials as delivery systems of soluble factors such as BMPs [254; 331].

Previous work from our group has shown that modifying chitosan materials by fibrinogen adsorption led to their interaction with monocytes through TLR4, leading to the production of BMP-2 [332], enhanced macrophage secretion of pro-osteogenic and angiogenic factors [333], NK cell capacity of recruiting MSC [334]. Also, *in vivo* fibrinogen improved the bone regenerative response to chitosan biomaterials, which was related to changes in the systemic immune response [251]. Although many promising results have been achieved applying fibrin-based materials *in vitro* and in small animal models, further studies involving larger animal models and humans are still required previously to their translation to clinics.

4.4 Immunomodulatory strategies

Recent works have been reflecting a paradigm shift, from “fighting” to “modulating” the immune response to biomaterials [251; 335; 336]. The key role of the immune system on the establishment and progression of musculoskeletal pathologies such as OA, aseptic loosening and bone defects have prompted the study of immunomodulatory biomaterials [336].

As previously discussed, macrophages are an important immune cell population in clinical scenarios such as aseptic loosening. Upon implantation, conventional biomaterials and their degradation products lead to pro-inflammatory microenvironments characterized by macrophage-driven chronic inflammation. In this context, pro-regenerative pathways are dampened while scar formation occurs as part of FBR. Therefore, macrophage polarization has been a hot topic in the biomaterials field [337].

The use of resolvins, lipid mediators that induce resolution of inflammation, for immunomodulation purposes has been successfully tested in our group [338]. The incorporation of resolvin D1 in chitosan scaffolds led to decreased recruitment of immune cells to the implant while promoted increased local ratio of M2/M1 macrophages in comparison to the control [338]. Moreover, lower levels of pro-inflammatory cytokines such as IL-1α, IL-1β, MIP-1α, MIP-1β, MIP-2, IL-6 and IL-16 were found 4 days post-implantation in the local exudates of animals with resolving D1-chitosan scaffolds [338]. Other strategy to polarize non activated (M0), and even classically activated (M1) macrophage towards pro-regenerative M2 phenotypes is through IL-4 stimuli, which anti-inflammatory effects are well known [339]. A recent report has shown improved implant integration by applying a layer-by-layer coating, designed for gradually elute IL-4, on Gynemesh®, a non-absorbable polypropylene mesh used for vaginal wall prolapse surgical treatment [340]. This diminished formation of fibrotic tissue around the medical device observed using mouse subcutaneous implantation model was also correlated with a local increase of the proportion of M2 with concomitant decrease of M1 macrophages [340].

As an alternative approach, therapies based on cells such as MSCs, reported to have pro-regenerative and immunomodulatory effects, are explored to improve the host response to biomaterials [83; 250]. Although undifferentiated MSCs reduce the production of pro-inflammatory cytokines TNF-α and IL-6, attenuating *in vivo* fibrosis associated to FBR, the modulatory role of MSCs is lost as the cells undergo osteogenic differentiation [250]. However, the role of MSCs on the immune response and tissue healing is not completely understood. In a study focused on the tissue engineering approach, the seeding and culture of MSCs in two types of constructs during 28 days previous to cranial implantation in rats, led to decreased bone repair when compared to the controls without cells. Moreover, increased M1 macrophages were found at the periphery of the scaffolds seeded with MSCs [322]. Cell

therapies based on MSCs are promising, but the mixed results from clinical trials assessing their immunomodulatory effect highlight the need to understand the mechanisms involved in the crosstalk between MSC and immune cell populations. Additionally, the translation of MSC therapies to clinical practice is still facing challenges regarding the cell quality, dose and origin, both in terms of donor and tissue differences [341].

5 Aims of the Thesis

Orthopedic biomaterials have been designed to simultaneously restore skeletal integrity and motion to patients and to be “stealth” to the host immune response. Inflammation is natural to occur upon injury or biomaterials implantation, being a crucial part of the tissue healing process. Upon implantation, orthopedic devices degrade, releasing prosthetic debris that elicit adverse immune responses, lead to tissue destruction and, ultimately, to implant failure. These clinical findings stress the need of a new generation of biomaterials that are able to actively interact with the host, namely with the immune system.

The main objective of this PhD thesis is to understand and challenge the role of inflammation in the response to biomaterials, providing new tools to modulate the immune response towards regenerative microenvironments.

Thereby, the following specific objectives were defined:

1) *Dissect the local players at tissue, cellular and molecular levels with potential systemic translation, in the context of hip osteoarthritis and aseptic implant loosening.*

   In order to achieve this objective, peri-articular soft tissues and blood were collected from patients during total hip replacement and hip revision surgeries. Histopathological evaluation, gene expression and serological analyses combined with clinical data assessment were carried out to provide an integrated perspective of the local and systemic immune response underlying osteoarthritis and aseptic implant loosening. These results are presented within *Chapter II*, highlighting the role of macrophages as a key immune cell population in the particle-induced inflammation and consequent medical device failure.

2) *Development of a new biomaterial to modulate the immune response in orthopedics applications*

   A biomimetic approach was chosen, and scaffolds made exclusively of fibrinogen ere (Fg-3D). Fg-3D were firstly characterized *in vitro* in terms of morphology and porosity (SEM), protein structure (FTIR and NMR), endotoxin levels, degradability and cytotoxicity. A critical-size bone defect rat model was used to evaluate the biological response to Fg-3D at two time-points: at 6 days post-injury, to assess the transition between the acute and chronic stage of inflammation, and at 8 weeks, to investigate the effect of Fg-3D on bone repair. Histological evaluation revealed that improved bone tissue healing and changes in systemic immune response at 6 days in presence of Fg-

3D, which correlated with extensive bone repair at 8 weeks. These results are described within *Chapter III.*

3) *Use of magnesium ions to modulate macrophage behavior in pro-inflammatory scenarios*

The clinical application of biodegradable magnesium alloys, in orthopedics, and the administration of $MgSO_4$ in Obstetrics to damp placental and fetal immune responses have inspired the use of magnesium ions to modulate macrophage response. Primary human macrophages were exposed to three concentrations of Mg^{2+} and their morphology, survival rate, macrophage polarization surface markers and cytokine production were evaluated. The role of the factors secreted by macrophages on the osteogenic differentiation of mesenchymal stem/stromal cells was also assessed. The obtained results showed that magnesium ions have an anti-inflammatory effect, particularly in presence of M1 polarizing stimuli, such as LPS. These findings are integrated in *Chapter IV*.

References

[1] - Taichman, R. S. (2005), Blood and bone: two tissues whose fates are intertwined to create the hematopoietic stem-cell niche, Blood, 105(7), 2631-2639.

[2] - Sophia Fox, A. J., A. Bedi, and S. A. Rodeo (2009), The basic science of articular cartilage: structure, composition, and function, Sports Health, 1(6), 461-468.

[3] - Clarke, B. (2008), Normal bone anatomy and physiology, Clin J Am Soc Nephrol, 3 Suppl 3, S131-139.

[4] - Humanbodyanatomy.us (2016). *Human Anatomy Diagram - Lower Limb Muscles Anatomy*. Retrieved from http://humanbodyanatomy.us/lower-limb-muscles-anatomy/. 16th December 2016

[5] - Li, Y., Q. Qiu, S. S. Watson, R. Schweitzer, and R. L. Johnson (2010), Uncoupling skeletal and connective tissue patterning: conditional deletion in cartilage progenitors reveals cell-autonomous requirements for Lmx1b in dorsal-ventral limb patterning, Development, 137(7), 1181-1188.

[6] - Boskey, A. L. (2013), Bone composition: relationship to bone fragility and antiosteoporotic drug effects, Bonekey Rep, 2, 447.

[7] - Nakahama, K. (2010), Cellular communications in bone homeostasis and repair, Cell Mol Life Sci, 67(23), 4001-4009.

[8] - Bianco, P. (2014), "Mesenchymal" stem cells, Annu Rev Cell Dev Biol, 30, 677-704.

[9] - Beederman, M., et al. (2013), BMP signaling in mesenchymal stem cell differentiation and bone formation, J Biomed Sci Eng, 6(8A), 32-52.

[10] - Veeriah, V., A. Zanniti, R. Paone, S. Chatterjee, N. Rucci, A. Teti, and M. Capulli (2016), Interleukin-1beta, lipocalin 2 and nitric oxide synthase 2 are mechano-responsive mediators of mouse and human endothelial cell-osteoblast crosstalk, Sci Rep, 6, 29880.

[11] - Hattori, T., et al. (2010), SOX9 is a major negative regulator of cartilage vascularization, bone marrow formation and endochondral ossification, Development, 137(6), 901-911.

[12] - Loebel, C., E. M. Czekanska, M. Bruderer, G. Salzmann, M. Alini, and M. J. Stoddart (2015), In vitro osteogenic potential of human mesenchymal stem cells is predicted by Runx2/Sox9 ratio, Tissue Eng Part A, 21(1-2), 115-123.

[13] - Cheng, A., and P. G. Genever (2010), SOX9 determines RUNX2 transactivity by directing intracellular degradation, J Bone Miner Res, 25(12), 2680-2689.

[14] - Hughes, F. J., W. Turner, G. Belibasakis, and G. Martuscelli (2006), Effects of growth factors and cytokines on osteoblast differentiation, Periodontol 2000, 41, 48-72.

[15] - Schaffler, M. B., W. Y. Cheung, R. Majeska, and O. Kennedy (2014), Osteocytes: master orchestrators of bone, Calcif Tissue Int, 94(1), 5-24.

[16] - Ikeda, K., and S. Takeshita (2016), The role of osteoclast differentiation and function in skeletal homeostasis, J Biochem, 159(1), 1-8.

[17] - Roshandel, D., et al. (2010), Genetic variation in the RANKL/RANK/OPG signaling pathway is associated with bone turnover and bone mineral density in men, J Bone Miner Res, 25(8), 1830-1838.

[18] - Anatomy & Physiology Connexions website (2016). *Bone Structure*. Retrieved from http://cnx.org/contents/FPtK1zmh@6.27:kwbeYj9S@3/Bone-Structure. 28th December 2016

[19] - Roschger, P., E. P. Paschalis, P. Fratzl, and K. Klaushofer (2008), Bone mineralization density distribution in health and disease, Bone, 42(3), 456-466.

[20] - Torres, A. M., J. B. Matheny, T. M. Keaveny, D. Taylor, C. M. Rimnac, and C. J. Hernandez (2016), Material heterogeneity in cancellous bone promotes deformation recovery after mechanical failure, Proc Natl Acad Sci U S A, 113(11), 2892-2897.

[21] - Einhorn, T. A., and L. C. Gerstenfeld (2015), Fracture healing: mechanisms and interventions, Nat Rev Rheumatol, 11(1), 45-54.

[22] - Claes, L., S. Recknagel, and A. Ignatius (2012), Fracture healing under healthy and inflammatory conditions, Nat Rev Rheumatol, 8(3), 133-143.

[23] - Marsell, R., and T. A. Einhorn (2011), The biology of fracture healing, Injury, 42(6), 551-555.

[24] - Chan, J. K., et al. (2015), Low-dose TNF augments fracture healing in normal and osteoporotic bone by up-regulating the innate immune response, EMBO Mol Med, 7(5), 547-561.

[25] - Wu, A. C., L. J. Raggatt, K. A. Alexander, and A. R. Pettit (2013), Unraveling macrophage contributions to bone repair, Bonekey Rep, 2, 373.

[26] - Konnecke, I., et al. (2014), T and B cells participate in bone repair by infiltrating the fracture callus in a two-wave fashion, Bone, 64(0), 155-165.

[27] - Schmidt-Bleek, K., et al. (2014), Initial immune reaction and angiogenesis in bone healing, J Tissue Eng Regen Med, 8(2), 120-130.

[28] - Lafage-Proust, M. H., B. Roche, M. Langer, D. Cleret, A. Vanden Bossche, T. Olivier, and L. Vico (2015), Assessment of bone vascularization and its role in bone remodeling, Bonekey Rep, 4, 662.

[29] - Sfeir, C., L. Ho, B. A. Doll, K. Azari, and J. O. Hollinger (2005), “Fracture Repair” in *Bone Regeneration and Repair: Biology and Clinical Applications*, edited by J. R. L. a. G. E. Friedlaender. Totowa. Humana Press Inc., pp. 21-44.

[30] - Claes, L., M. Reusch, M. Gockelmann, M. Ohnmacht, T. Wehner, M. Amling, F. T. Beil, and A. Ignatius (2011), Metaphyseal fracture healing follows similar biomechanical rules as diaphyseal healing, J Orthop Res, 29(3), 425-432.

[31] - Boonrungsiman, S., E. Gentleman, R. Carzaniga, N. D. Evans, D. W. McComb, A. E. Porter, and M. M. Stevens (2012), The role of intracellular calcium phosphate in osteoblast-mediated bone apatite formation, Proc Natl Acad Sci U S A, 109(35), 14170-14175.

[32] - Martin, R. B., and D. L. Boardman (1993), The effects of collagen fiber orientation, porosity, density, and mineralization on bovine cortical bone bending properties., J. Biomech, 26(9), 1047-1054.

[33] - Grässel, S. (2014), The role of peripheral nerve fibers and their neurotransmitters in cartilage and bone physiology and pathophysiology, Arthritis Research & Therapy, 16(6).

[34] - Ralphs, J. R., and M. Benjamin (1994), The joint capsule: structure, composition, ageing and disease, J Anat, 184 (Pt 3), 503-509.

[35] - Egloff, C., A. Sawatsky, T. Leonard, D. A. Hart, V. Valderrabano, and W. Herzog (2014), Effect of muscle weakness and joint inflammation on the onset and progression of osteoarthritis in the rabbit knee, Osteoarthritis Cartilage, 22(11), 1886-1893.

[36] - Benjamin, M., H. Toumi, J. R. Ralphs, G. Bydder, T. M. Best, and S. Milz (2006), Where tendons and ligaments meet bone: attachment sites ('entheses') in relation to exercise and/or mechanical load, J Anat, 208(4), 471-490.

[37] - Iwanaga, T., M. Shikichi, H. Kitamura, H. Yanase, and K. Nozawa-Inoue (2000), Morphology and functional roles of synoviocytes in the joint, Arch Histol Cytol, 63(1), 17-31.

[38] - Mateos, J., L. Lourido, P. Fernandez-Puente, V. Calamia, C. Fernandez-Lopez, N. Oreiro, C. Ruiz-Romero, and F. J. Blanco (2012), Differential protein profiling of synovial fluid from rheumatoid arthritis and osteoarthritis patients using LC-MALDI TOF/TOF, J Proteomics, 75(10), 2869-2878.

[39] - Jay, G. D., and K. A. Waller (2014), The biology of lubricin: near frictionless joint motion, Matrix Biol, 39, 17-24.

[40] - Philschtaz.com website (2016). *Anatomy & Physiology - Synovial Joints*. Retrieved from http://philschatz.com/anatomy-book/contents/m46394.html. 29th December 2016

[41] - Cross, M., et al. (2014), The global burden of hip and knee osteoarthritis: estimates from the global burden of disease 2010 study, Ann Rheum Dis, 73(7), 1323-1330.

[42] - Barr, A. E., M. F. Barbe, and B. D. Clark (2004), Work-related musculoskeletal disorders of the hand and wrist: epidemiology, pathophysiology, and sensorimotor changes, J Orthop Sports Phys Ther, 34(10), 610-627.

[43] - Palazzo, C., C. Nguyen, M. M. Lefevre-Colau, F. Rannou, and S. Poiraudeau (2016), Risk factors and burden of osteoarthritis, Ann Phys Rehabil Med, 59(3), 134-138.

[44] - Steiman, A. J., et al. (2013), Non-biologic disease-modifying antirheumatic drugs (DMARDs) improve pain in inflammatory arthritis (IA): a systematic literature review of randomized controlled trials, Rheumatol Int, 33(5), 1105-1120.

[45] - Ruderman, E. M. (2012), Overview of safety of non-biologic and biologic DMARDs, Rheumatology (Oxford), 51 Suppl 6, vi37-43.

[46] - Hossain, N., and M. Barry (2011), Management of traumatic bone loss, The Journal of Bone & Joint Surgery

[47] - Giannoudis (2007), Management of tong-bone non-unions, Injury, 38(10), 1224.

[48] - Burge, R., B. Dawson-Hughes, D. H. Solomon, J. B. Wong, A. King, and A. Tosteson (2007), Incidence and economic burden of osteoporosis-related fractures in the United States, 2005-2025, J Bone Miner Res, 22(3), 465-475.

[49] - Liebergall, M., J. Schroeder, R. Mosheiff, Z. Gazit, Z. Yoram, L. Rasooly, A. Daskal, A. Khoury, Y. Weil, and S. Beyth (2013), Stem cell-based therapy for prevention of delayed fracture union: a randomized and prospective preliminary study, Mol Ther, 21(8), 1631-1638.

[50] - Antonova, E., T. K. Le, R. Burge, and J. Mershon (2013), Tibia shaft fractures: costly burden of nonunions, Bmc Musculoskel Dis, 14, 42.

[51] - Mills, L. A., and A. H. Simpson (2013), The relative incidence of fracture non-union in the Scottish population (5.17 million): a 5-year epidemiological study, BMJ Open, 3(2)

[52] - Bastian, O. W., A. Kuijer, L. Koenderman, R. K. Stellato, W. W. van Solinge, L. P. Leenen, and T. J. Blokhuis (2016), Impaired bone healing in multitrauma patients is associated with altered leukocyte kinetics after major trauma, J Inflamm Res, 9, 69-78.

[53] - Claes, L., K. Eckert-Hübner, and P. Augat (2002), The effect of mechanical stability on local vascularization and tissue differentiation in callus healing, Journal of Orthopaedic Research, 20(5), 1099-1105.

[54] - Utvag, S. E., O. Grundnes, D. B. Rindal, and O. Reikeras (2003), Influence of extensive muscle injury on fracture healing in rat tibia, J Orthop Trauma, 17(6), 430-435.

[55] - Mehta, M., G. N. Duda, C. Perka, and P. Strube (2011), Influence of gender and fixation stability on bone defect healing in middle-aged rats: a pilot study, Clin Orthop Relat Res, 469(11), 3102-3110.

[56] - Lu, C., E. Hansen, A. Sapozhnikova, D. Hu, T. Miclau, and R. S. Marcucio (2008), Effect of age on vascularization during fracture repair, J Orthop Res, 26(10), 1384-1389.

[57] - El-Zawawy, H. B., C. S. Gill, R. W. Wright, and L. J. Sandell (2006), Smoking delays chondrogenesis in a mouse model of closed tibial fracture healing, J Orthop Res, 24(12), 2150-2158.

[58] - Daftari, T. K., T. E. Whitesides, Jr., J. G. Heller, A. C. Goodrich, B. E. McCarey, and W. C. Hutton (1994), Nicotine on the revascularization of bone graft. An experimental study in rabbits, Spine (Phila Pa 1976), 19(8), 904-911.

[59] - O'Connor, J. P., J. T. Capo, V. Tan, J. A. Cottrell, M. B. Manigrasso, N. Bontempo, and J. R. Parsons (2009), A comparison of the effects of ibuprofen and rofecoxib on rabbit fibula osteotomy healing, Acta orthopaedica, 80(5), 597-605.

[60] - Jiao, H., E. Xiao, and D. T. Graves (2015), Diabetes and Its Effect on Bone and Fracture Healing, Curr Osteoporos Rep, 13(5), 327-335.

[61] - Trevisiol, C. H., R. T. Turner, J. E. Pfaff, J. C. Hunter, P. J. Menagh, K. Hardin, E. Ho, and U. T. Iwaniec (2007), Impaired osteoinduction in a rat model for chronic alcohol abuse, Bone, 41(2), 175-180.

[62] - Zhang, X., E. M. Schwarz, D. A. Young, J. E. Puzas, R. N. Rosier, and R. J. O'Keefe (2002), Cyclooxygenase-2 regulates mesenchymal cell differentiation into the osteoblast lineage and is critically involved in bone repair, J Clin Invest, 109(11), 1405-1415.

[63] - Timmen, M., H. Hidding, B. Wieskotter, W. Baum, T. Pap, M. J. Raschke, G. Schett, J. Zwerina, and R. Stange (2014), Influence of antiTNF-alpha antibody treatment on fracture healing under chronic inflammation, Bmc Musculoskel Dis, 15, 184.

[64] - Takagi, M., S. Kasayama, T. Yamamoto, T. Motomura, K. Hashimoto, H. Yamamoto, B. Sato, S. Okada, and T. Kishimoto (1997), Advanced glycation endproducts stimulate interleukin-6 production by human bone-derived cells, J Bone Miner Res, 12(3), 439-446.

[65] - Lee, J. H., et al. (2016), The frequency of and risk factors for osteoporosis in Korean patients with rheumatoid arthritis, Bmc Musculoskel Dis, 17, 98.

[66] - Rauner, M., W. Sipos, and P. Pietschmann (2007), Osteoimmunology, Int Arch Allergy Immunol, 143(1), 31-48.

[67] - Recknagel, S., R. Bindl, J. Kurz, T. Wehner, C. Ehrnthaller, M. W. Knoferl, F. Gebhard, M. Huber-Lang, L. Claes, and A. Ignatius (2011), Experimental blunt chest trauma impairs fracture healing in rats, J Orthop Res, 29(5), 734-739.

[68] - Reikeras, O., H. Shegarfi, J. E. Wang, and S. E. Utvag (2005), Lipopolysaccharide impairs fracture healing: an experimental study in rats, Acta orthopaedica, 76(6), 749-753.

[69] - Rochford, E. T., M. Sabate Bresco, S. Zeiter, K. Kluge, A. Poulsson, M. Ziegler, R. G. Richards, L. O'Mahony, and T. F. Moriarty (2016), Monitoring immune responses in a mouse model of fracture fixation with and without Staphylococcus aureus osteomyelitis, Bone, 83, 82-92.

[70] - Glyn-Jones, S., A. J. Palmer, R. Agricola, A. J. Price, T. L. Vincent, H. Weinans, and A. J. Carr (2015), Osteoarthritis, Lancet, 386(9991), 376-387.

[71] - Kinge, J. M., A. K. Knudsen, V. Skirbekk, and S. E. Vollset (2015), Musculoskeletal disorders in Norway: prevalence of chronicity and use of primary and specialist health care services, Bmc Musculoskel Dis, 16, 75.

[72] - Zhang, Y., and J. M. Jordan (2010), Epidemiology of osteoarthritis, Clin Geriatr Med, 26(3), 355-369.

[73] - Berenbaum, F. (2013), Osteoarthritis as an inflammatory disease (osteoarthritis is not osteoarthrosis!), Osteoarthritis Cartilage, 21(1), 16-21.

[74] - Hwang, H. S., S. J. Park, E. J. Cheon, M. H. Lee, and H. A. Kim (2015), Fibronectin fragment-induced expression of matrix metalloproteinases is mediated by MyD88-dependent TLR-2 signaling pathway in human chondrocytes, Arthritis Res Ther, 17, 320.

[75] - Nefla, M., D. Holzinger, F. Berenbaum, and C. Jacques (2016), The danger from within: alarmins in arthritis, Nat Rev Rheumatol, 12(11), 669-683.

[76] - Lohmann, H., G. Grass, C. Rangger, and G. Mathiak (2007), Economic impact of cancellous bone grafting in trauma surgery, Arch Orthop Trauma Surg, 127(5), 345-348.

[77] - Wojtowicz, A. M., A. Shekaran, M. E. Oest, K. M. Dupont, K. L. Templeman, D. W. Hutmacher, R. E. Guldberg, and A. J. Garcia (2010), Coating of biomaterial scaffolds with the collagen-mimetic peptide GFOGER for bone defect repair, Biomaterials, 31(9), 2574-2582.

[78] - Garrison, K. R., I. Shemilt, S. Donell, J. J. Ryder, M. Mugford, I. Harvey, F. Song, and V. Alt (2010), Bone morphogenetic protein (BMP) for fracture healing in adults, Cochrane Database Syst Rev(6), CD006950.

[79] - Blokhuis, T. J., and T. Lindner (2008), Allograft and bone morphogenetic proteins: an overview, Injury, 39, S33-S36.

[80] - Anderson, J. M., A. Rodriguez, and D. T. Chang (2008), Foreign body reaction to biomaterials, Seminars in immunology, 20(2), 86-100.

[81] - Sica, A., and A. Mantovani (2012), Macrophage plasticity and polarization: in vivo veritas, J Clin Invest, 122(3), 787-795.

[82] - Murray, P. J., et al. (2014), Macrophage activation and polarization: nomenclature and experimental guidelines, Immunity, 41(1), 14-20.

[83] - Cho, D. I., M. R. Kim, H. Y. Jeong, H. C. Jeong, M. H. Jeong, S. H. Yoon, Y. S. Kim, and Y. Ahn (2014), Mesenchymal stem cells reciprocally regulate the M1/M2 balance in mouse bone marrow-derived macrophages, Exp Mol Med, 46, e70.

[84] - Mantovani, A., A. Sica, S. Sozzani, P. Allavena, A. Vecchi, and M. Locati (2004), The chemokine system in diverse forms of macrophage activation and polarization, Trends Immunol, 25(12), 677-686.

[85] - Kim, D., and J. Y. Kim (2014), Anti-CD14 antibody reduces LPS responsiveness via TLR4 internalization in human monocytes, Mol Immunol, 57(2), 210-215.

[86] - Ziegler-Heitbrock, L., et al. (2010), Nomenclature of monocytes and dendritic cells in blood, Blood, 116(16), e74-80.

[87] - Oliveira, M. I., S. G. Santos, M. J. Oliveira, A. Torres, and M. A. Barbosa (2012), Chitosan drives anti-inflammatory macrophage polarization and pro-inflammatory dendritic cell stimulation, e Cells and Materials Journal, 24, 136-153.

[88] - Ma, J., L. Liu, G. Che, N. Yu, F. Dai, and Z. You (2010), The M1 form of tumor-associated macrophages in non-small cell lung cancer is positively associated with survival time, BMC Cancer, 10, 112.

[89] - Allaire, M. A., B. Tanne, S. C. Cote, and N. Dumais (2013), Prostaglandin E 2 Does Not Modulate CCR7 Expression and Functionality after Differentiation of Blood Monocytes into Macrophages, Int J Inflam, 2013, 918016.

[90] - Raes, G., R. Van den Bergh, P. De Baetselier, G. H. Ghassabeh, C. Scotton, M. Locati, A. Mantovani, and S. Sozzani (2005), Arginase-1 and Ym1 Are Markers for Murine, but Not Human, Alternatively Activated Myeloid Cells, The Journal of Immunology, 174(11), 6561-6562.

[91] - Schneemann, M., and G. Schoeden (2007), Macrophage biology and immunology: man is not a mouse, J Leukoc Biol, 81(3), 579; discussion 580.

[92] - Antonios, J. K., Z. Yao, C. Li, A. J. Rao, and S. B. Goodman (2013), Macrophage polarization in response to wear particles in vitro, Cell Mol Immunol, 10(6), 471-482.

[93] - David, S., and A. Kroner (2011), Repertoire of microglial and macrophage responses after spinal cord injury, Nat Rev Neurosci, 12(7), 388-399.

[94] - Asai, A., K. Nakamura, M. Kobayashi, D. N. Herndon, and F. Suzuki (2012), CCL1 released from M2b macrophages is essentially required for the maintenance of their properties, J Leukoc Biol, 92(4), 859-867.

[95] - Smith, A. J., P. Dieppe, K. Vernon, M. Porter, A. W. Blom, E. National Joint Registry of, and Wales (2012), Failure rates of stemmed metal-on-metal hip replacements: analysis of data from the National Joint Registry of England and Wales, Lancet, 379(9822), 1199-1204.

[96] - Caicedo, M. S., R. Desai, K. McAllister, A. Reddy, J. J. Jacobs, and N. J. Hallab (2009), Soluble and particulate Co-Cr-Mo alloy implant metals activate the inflammasome danger signaling pathway in human macrophages: a novel mechanism for implant debris reactivity, J Orthop Res, 27(7), 847-854.

[97] - Korovessis, P., G. Petsinis, M. Repanti, and T. Repantis (2006), Metallosis after contemporary metal-on-metal total hip arthroplasty. Five to nine-year follow-up, J Bone Joint Surg Am, 88(6), 1183-1191.

[98] - Campbell, P., E. Ebramzadeh, S. Nelson, K. Takamura, K. De Smet, and H. C. Amstutz (2010), Histological features of pseudotumor-like tissues from metal-on-metal hips, Clin Orthop Relat Res, 468(9), 2321-2327.

[99] - Willert, H. G., G. H. Buchhorn, A. Fayyazi, R. Flury, M. Windler, G. Koster, and C. H. Lohmann (2005), Metal-on-metal bearings and hypersensitivity in patients with artificial hip joints. A clinical and histomorphological study, J Bone Joint Surg Am, 87(1), 28-36.

[100] - Konttinen, Y. T., and J. Pajarinen (2013), Adverse reactions to metal-on-metal implants, Nat Rev Rheumatol, 9(1), 5-6.

[101] - Revell, P. A. (2008), The combined role of wear particles, macrophages and lymphocytes in the loosening of total joint prostheses, J R Soc Interface, 5(28), 1263-1278.

[102] - Coleman, R. F., J. Herrington, and J. T. Scales (1973), Concentration of wear products in hair, blood, and urine after total hip replacement, British medical journal, 1(5852), 527-529.

[103] - Clarke, M. T., P. T. Lee, A. Arora, and R. N. Villar (2003), Levels of metal ions after small- and large-diameter metal-on-metal hip arthroplasty, J. Bone Joint Surg.-Br. Vol., 85(6), 913-917.

[104] - Smith, A. J., P. Dieppe, M. Porter, A. W. Blom, E. National Joint Registry of, and Wales (2012), Risk of cancer in first seven years after metal-on-metal hip replacement compared with other bearings and general population: linkage study between the National Joint Registry of England and Wales and hospital episode statistics, Brit Med J, 344(apr03 1), e2383.

[105] - Chaigne-Delalande, B., et al. (2013), Mg2+ regulates cytotoxic functions of NK and CD8 T cells in chronic EBV infection through NKG2D, Science, 341(6142), 186-191.

[106] - Li, R. W., N. T. Kirkland, J. Truong, J. Wang, P. N. Smith, N. Birbilis, and D. R. Nisbet (2014), The influence of biodegradable magnesium alloys on the osteogenic differentiation of human mesenchymal stem cells, J Biomed Mater Res A, 102(12), 4346-4357.

[107] - Chen, Z., X. Mao, L. Tan, T. Friis, C. Wu, R. Crawford, and Y. Xiao (2014), Osteoimmunomodulatory properties of magnesium scaffolds coated with beta-tricalcium phosphate, Biomaterials, 35(30), 8553-8565.

[108] - Graves, S. (2011), National Joint Replacement Registry Annual Report 2011*Rep.*, Australian Orthopaedic Association.

[109] - Mathew, M. T., M. J. Runa, M. Laurent, J. J. Jacobs, L. A. Rocha, and M. A. Wimmer (2011), Tribocorrosion behavior of CoCrMo alloy for hip prosthesis as a function of loads: a comparison between two testing systems, Wear, 271(9-10), 1210-1219.

[110] - Doorn, P. F., P. A. Campbell, J. Worrall, P. D. Benya, H. A. McKellop, and H. C. Amstutz (1998), Metal wear particle characterization from metal on metal total hip replacements: transmission electron microscopy study of periprosthetic tissues and isolated particles, J Biomed Mater Res, 42(1), 103-111.

[111] - Germain, M. A., A. Hatton, S. Williams, J. B. Matthews, M. H. Stone, J. Fisher, and E. Ingham (2003), Comparison of the cytotoxicity of clinically relevant cobalt-chromium and alumina ceramic wear particles in vitro, Biomaterials, 24(3), 469-479.

[112] - Brown, C., S. Williams, J. L. Tipper, J. Fisher, and E. Ingham (2007), Characterisation of wear particles produced by metal on metal and ceramic on metal hip prostheses under standard and microseparation simulation, J Mater Sci Mater Med, 18(5), 819-827.

[113] - Catelas, I., J. D. Bobyn, J. B. Medley, J. J. Krygier, D. J. Zukor, and O. L. Huk (2003), Size, shape, and composition of wear particles from metal-metal hip simulator testing: effects of alloy and number of loading cycles, J Biomed Mater Res A, 67(1), 312-327.

[114] - Billi, F., P. Benya, A. Kavanaugh, J. Adams, H. McKellop, and E. Ebramzadeh (2012), The John Charnley Award: an accurate and extremely sensitive method to separate, display, and characterize wear debris: part 2: metal and ceramic particles, Clin Orthop Relat Res, 470(2), 339-350.

[115] - Pourzal, R., I. Catelas, R. Theissmann, C. Kaddick, and A. Fischer (2011), Characterization of Wear Particles Generated from CoCrMo Alloy under Sliding Wear Conditions, Wear, 271(9-10), 1658-1666.

[116] - Tipper, J. L., A. L. Galvin, S. Williams, H. M. McEwen, M. H. Stone, E. Ingham, and J. Fisher (2006), Isolation and characterization of UHMWPE wear particles down to ten nanometers in size from in vitro hip and knee joint simulators, J Biomed Mater Res A, 78(3), 473-480.

[117] - Milosev, I., and M. Remskar (2009), In vivo production of nanosized metal wear debris formed by tribochemical reaction as confirmed by high-resolution TEM and XPS analyses, J Biomed Mater Res A, 91(4), 1100-1110.

[118] - Papageorgiou, I., V. Shadrick, S. Davis, L. Hails, R. Schins, R. Newson, J. Fisher, E. Ingham, and C. P. Case (2008), Macrophages detoxify the genotoxic and cytotoxic effects of surgical cobalt chrome alloy particles but not quartz particles on human cells in vitro, Mutat Res, 643(1-2), 11-19.

[119] - Gallo, J., M. Slouf, and S. B. Goodman (2010), The relationship of polyethylene wear to particle size, distribution, and number: A possible factor explaining the risk of osteolysis after hip arthroplasty, J Biomed Mater Res B Appl Biomater, 94(1), 171-177.

[120] - Champion, J. A., A. Walker, and S. Mitragotri (2008), Role of particle size in phagocytosis of polymeric microspheres, Pharm Res, 25(8), 1815-1821.

[121] - Gallo, J., M. Raska, F. Mrázek, and M. Petrek (2008), Bone remodeling, particle disease and individual susceptibility to periprosthetic osteolysis, Physiol Res., 57(3), 339-349.

[122] - Landgraeber, S., M. Jager, J. J. Jacobs, and N. J. Hallab (2014), The pathology of orthopedic implant failure is mediated by innate immune system cytokines, Mediators Inflamm, 2014, 185150.

[123] - Horev-Azaria, L., et al. (2011), Predictive toxicology of cobalt nanoparticles and ions: comparative in vitro study of different cellular models using methods of knowledge discovery from data, Toxicol Sci, 122(2), 489-501.

[124] - Hallab, N. J., J. J. Jacobs, A. Skipor, J. Black, K. Mikecz, and J. O. Galante (2000), Systemic metal-protein binding associated with total joint replacement arthroplasty, J Biomed Mater Res, 49(3), 353-361.

[125] - Nuevo-Ordonez, Y., M. Montes-Bayon, E. Blanco Gonzalez, and A. Sanz-Medel (2011), Titanium preferential binding sites in human serum transferrin at physiological concentrations, Metallomics : integrated biometal science, 3(12), 1297-1303.

[126] - Ren, P. G., A. Irani, Z. Huang, T. Ma, S. Biswal, and S. B. Goodman (2011), Continuous infusion of UHMWPE particles induces increased bone macrophages and osteolysis, Clin Orthop Relat Res, 469(1), 113-122.

[127] - Green, T. R., J. Fisher, M. Stone, B. M. Wroblewski, and E. Ingham (1998), Polyethylene particles of a 'critical size' are necessary for the induction of cytokines by macrophages in vitro, Biomaterials, 19(24), 2297-2302.

[128] - Ingham, E., and J. Fisher (2005), The role of macrophages in osteolysis of total joint replacement, Biomaterials, 26(11), 1271-1286.

[129] - Langton, D. J., S. S. Jameson, T. J. Joyce, J. N. Gandhi, R. Sidaginamale, P. Mereddy, J. Lord, and A. V. Nargol (2011), Accelerating failure rate of the ASR total hip replacement, J. Bone Joint Surg.-Br. Vol., 93(8), 1011-1016.

[130] - Vendittoli, P. A., A. Roy, S. Mottard, J. Girard, D. Lusignan, and M. Lavigne (2010), Metal ion release from bearing wear and corrosion with 28 mm and large-diameter metal-on-metal bearing articulations: a follow-up study, J. Bone Joint Surg.-Br. Vol., 92(1), 12-19.

[131] - Williams, D. H., N. V. Greidanus, B. A. Masri, C. P. Duncan, and D. S. Garbuz (2011), Prevalence of pseudotumor in asymptomatic patients after metal-on-metal hip arthroplasty, J Bone Joint Surg Am, 93(23), 2164-2171.

[132] - Langton, D. J., T. J. Joyce, S. S. Jameson, J. Lord, M. Van Orsouw, J. P. Holland, A. V. Nargol, and K. A. De Smet (2011), Adverse reaction to metal debris following hip resurfacing: the influence of component type, orientation and volumetric wear, J. Bone Joint Surg.-Br. Vol., 93(2), 164-171.

[133] - Langton, D. J., S. S. Jameson, T. J. Joyce, N. J. Hallab, S. Natu, and A. V. Nargol (2010), Early failure of metal-on-metal bearings in hip resurfacing and large-diameter total hip replacement: A consequence of excess wear, J. Bone Joint Surg.-Br. Vol., 92(1), 38-46.

[134] - Engh, C. A., H. Ho, C. A. Engh, W. G. Hamilton, and K. B. Fricka (2010), Metal-on-Metal Total Hip Arthroplasty Adverse Local Tissue Reaction, Seminars in Arthroplasty, 21(1), 19-23.

[135] - von Domarus, C., J. P. Rosenberg, W. Ruther, and J. Zustin (2011), Necrobiosis and T-lymphocyte infiltration in retrieved aseptically loosened metal-on-polyethylene arthroplasties, Acta orthopaedica, 82(5), 596-601.

[136] - Gill, I. P., J. Webb, K. Sloan, and R. J. Beaver (2012), Corrosion at the neck-stem junction as a cause of metal ion release and pseudotumour formation, J. Bone Joint Surg.-Br. Vol., 94(7), 895-900.

[137] - Walsh, A. J., V. S. Nikolaou, and J. Antoniou (2012), Inflammatory pseudotumor complicating metal-on-highly cross-linked polyethylene total hip arthroplasty, J Arthroplasty, 27(2), 324 e325-328.

[138] - Yan, Y., A. Neville, D. Dowson, S. Williams, and J. Fisher (2009), Effect of metallic nanoparticles on the biotribocorrosion behaviour of Metal-on-Metal hip prostheses, Wear, 267(5-8), 683-688.

[139] - Daley, B., A. T. Doherty, B. Fairman, and C. P. Case (2004), Wear debris from hip or knee replacements causes chromosomal damage in human cells in tissue culture, J. Bone Joint Surg.-Br. Vol., 86(4), 598-606.

[140] - Hart, A. J., K. Satchithananda, A. D. Liddle, S. A. Sabah, D. McRobbie, J. Henckel, J. P. Cobb, J. A. Skinner, and A. W. Mitchell (2012), Pseudotumors in association with well-functioning metal-on-metal hip prostheses: a case-control study using three-dimensional computed tomography and magnetic resonance imaging, J Bone Joint Surg Am, 94(4), 317-325.

[141] - Hwang, K. T., Y. H. Kim, Y. S. Kim, and J. A. Ryu (2014), Prevalence of a soft-tissue lesion after small head metal-on-metal total hip replacement: 13- to 19-year follow-up study, Bone Joint J, 96-B(12), 1594-1599.

[142] - Harvie, P., H. Giele, C. Fang, O. Ansorge, S. Ostlere, M. Gibbons, and D. Whitwell (2008), The treatment of femoral neuropathy due to pseudotumour caused by metal-on-metal resurfacing arthroplasty, Hip Int, 18(4), 313-320.

[143] - Mahendra, G., H. Pandit, K. Kliskey, D. Murray, H. S. Gill, and N. Athanasou (2009), Necrotic and inflammatory changes in metal-on-metal resurfacing hip arthroplasties, Acta orthopaedica, 80(6), 653-659.

[144] - Kwon, Y. M., S. J. Ostlere, P. McLardy-Smith, N. A. Athanasou, H. S. Gill, and D. W. Murray (2011), "Asymptomatic" pseudotumors after metal-on-metal hip resurfacing arthroplasty: prevalence and metal ion study, J Arthroplasty, 26(4), 511-518.

[145] - Pandit, H., S. Glyn-Jones, P. McLardy-Smith, R. Gundle, D. Whitwell, C. L. Gibbons, S. Ostlere, N. Athanasou, H. S. Gill, and D. W. Murray (2008), Pseudotumours associated with metal-on-metal hip resurfacings, J. Bone Joint Surg.-Br. Vol., 90(7), 847-851.

[146] - Aroukatos, P., M. Repanti, T. Repantis, V. Bravou, and P. Korovessis (2010), Immunologic adverse reaction associated with low-carbide metal-on-metal bearings in total hip arthroplasty, Clin Orthop Relat Res, 468(8), 2135-2142.

[147] - Watters, T. S., D. M. Cardona, K. S. Menon, E. N. Vinson, M. P. Bolognesi, and L. G. Dodd (2010), Aseptic lymphocyte-dominated vasculitis-associated lesion: a clinicopathologic review of an underrecognized cause of prosthetic failure, Am J Clin Pathol, 134(6), 886-893.

[148] - Kosukegawa, I., S. Nagoya, M. Kaya, K. Sasaki, M. Sasaki, and T. Yamashita (2011), Revision total hip arthroplasty due to pain from hypersensitivity to cobalt-chromium in total hip arthroplasty, J Arthroplasty, 26(6), 978 e971-973.

[149] - Hasegawa, M., K. Yoshida, H. Wakabayashi, and A. Sudo (2012), Pseudotumor with dominant B-lymphocyte infiltration after metal-on-metal total hip arthroplasty with a modular cup, J Arthroplasty, 27(3), 493 e495-497.

[150] - Witzleb, W. C., U. Hanisch, N. Kolar, F. Krummenauer, and K. P. Guenther (2007), Neo-capsule tissue reactions in metal-on-metal hip arthroplasty, Acta orthopaedica, 78(2), 211-220.

[151] - Kwon, Y. M., S. Glyn-Jones, D. J. Simpson, A. Kamali, P. McLardy-Smith, H. S. Gill, and D. W. Murray (2010), Analysis of wear of retrieved metal-on-metal hip resurfacing implants revised due to pseudotumours, J. Bone Joint Surg.-Br. Vol., 92(3), 356-361.

[152] - Evans, E. M., M. A. R. Freeman, A. J. Miller, and Vernonro.B (1974), Metal Sensitivity as a Cause of Bone Necrosis and Loosening of Prosthesis in Total Joint Replacement, Journal of Bone and Joint Surgery-British Volume, B 56(4), 626-642.

[153] - Brown, G. C., M. D. Lockshin, E. A. Salvati, and P. G. Bullough (1977), Sensitivity to Metal as a Possible Cause of Sterile Loosening After Cobalt-Chromuym Total Hip-Replacement Arthroplasty, J. Bone Joint Surg.-Am. Vol., 59(2), 164-168.

[154] - Wood, M. M., and E. M. Warshaw (2015), Hypersensitivity reactions to titanium: diagnosis and management, Dermatitis, 26(1), 7-25.

[155] - Thyssen, J. P., S. S. Jakobsen, K. Engkilde, J. D. Johansen, K. Soballe, and T. Menne (2009), The association between metal allergy, total hip arthroplasty, and revision, Acta orthopaedica, 80(6), 646-652.

[156] - Hallab, N., K. Merritt, and J. J. Jacobs (2001), Metal sensitivity in patients with orthopaedic implants, J Bone Joint Surg Am, 83-A(3), 428-436.

[157] - Granchi, D., E. Cenni, D. Tigani, G. Trisolino, N. Baldini, and A. Giunti (2008), Sensitivity to implant materials in patients with total knee arthroplasties, Biomaterials, 29(10), 1494-1500.

[158] - Goodman, S. B. (2007), Wear particles, periprosthetic osteolysis and the immune system, Biomaterials, 28(34), 5044-5048.

[159] - Hailer, N. P., R. A. Blaheta, H. Dahlstrand, and A. Stark (2011), Elevation of circulating HLA DR(+) CD8(+) T-cells and correlation with chromium and cobalt concentrations 6 years after metal-on-metal hip arthroplasty, Acta orthopaedica, 82(1), 6-12.

[160] - Hercus, B., S. Saeed, and P. A. Revell (2002), Expression profile of T cell associated molecules in the interfacial tissue of aseptically loosened prosthetic joints, J Mater Sci Mater Med, 13(12), 1153-1156.

[161] - Whittingham-Jones, P. M., E. Dunstan, H. Altaf, S. R. Cannon, P. A. Revell, and T. W. Briggs (2008), Immune responses in patients with metal-on-metal hip articulations: a long-term follow-up, J Arthroplasty, 23(8), 1212-1218.

[162] - Chen, Z., Z. Wang, Q. Wang, W. Cui, F. Liu, and W. Fan (2014), Changes in early serum metal ion levels and impact on liver, kidney, and immune markers following metal-on-metal total hip arthroplasty, J Arthroplasty, 29(3), 612-616.

[163] - Hallab, N. J., M. Caicedo, A. Finnegan, and J. J. Jacobs (2008), Th1 type lymphocyte reactivity to metals in patients with total hip arthroplasty, Journal of orthopaedic surgery and research, 3(6), 6.

[164] - Hart, A. J., J. A. Skinner, P. Winship, N. Faria, E. Kulinskaya, D. Webster, S. Muirhead-Allwood, C. H. Aldam, H. Anwar, and J. J. Powell (2009), Circulating levels of cobalt and chromium from metal-on-metal hip replacement are associated with CD8+ T-cell lymphopenia, J. Bone Joint Surg.-Br. Vol., 91(6), 835-842.

[165] - Hallab, N. J., K. Mikecz, C. Vermes, A. Skipor, and J. J. Jacobs (2001), Orthopaedic implant related metal toxicity in terms of human lymphocyte reactivity to metal-protein complexes produced from cobalt-base and titanium-base implant alloy degradation, Molecular and cellular biochemistry, 222(1-2), 127-136.

[166] - Zhang, Y., and D. Wilcox (2002), Thermodynamic and spectroscopic study of Cu(II) and Ni(II) binding to bovine serum albumin, Journal of Biological Inorganic Chemistry, 7(3), 327-337.

[167] - Gamerdinger, K., C. Moulon, D. R. Karp, J. Van Bergen, F. Koning, D. Wild, U. Pflugfelder, and H. U. Weltzien (2003), A new type of metal recognition by human T cells: contact residues for peptide-independent bridging of T cell receptor and major histocompatibility complex by nickel, J Exp Med, 197(10), 1345-1353.

[168] - Van Den, B., Heffler, L. Tengvall, Nilsson, Karlberg, and Scheynius (1999), Direct Ni2+ antigen formation on cultured human dendritic cells, Immunology, 96(4), 578-585.

[169] - Sargeant, A., and T. Goswami (2007), Hip implants - Paper VI - Ion concentrations, Mater Design, 28(1), 155-171.

[170] - Liang, H., J. Huang, C. Q. Tu, M. Zhang, Y. Q. Zhou, and P. W. Shen (2001), The subsequent effect of interaction between Co2+ and human serum albumin or bovine serum albumin, J Inorg Biochem, 85(2-3), 167-171.

[171] - Tinoco, A. D., E. V. Eames, and A. M. Valentine (2008), Reconsideration of serum Ti(IV) transport: albumin and transferrin trafficking of Ti(IV) and its complexes, J Am Chem Soc, 130(7), 2262-2270.

[172] - Chan, E., D. Cadosch, O. P. Gautschi, K. Sprengel, and L. Filgueira (2011), Influence of metal ions on human lymphocytes and the generation of titanium-specific T-lymphocytes, J Appl Biomater Biomech, 9(2), 137-143.

[173] - Ortega, R., et al. (2009), Cobalt distribution in keratinocyte cells indicates nuclear and perinuclear accumulation and interaction with magnesium and zinc homeostasis, Toxicol Lett, 188(1), 26-32.

[174] - Jomova, K., and M. Valko (2011), Advances in metal-induced oxidative stress and human disease, Toxicology, 283(2-3), 65-87.

[175] - Bagchi, D., S. J. Stohs, B. W. Downs, M. Bagchi, and H. G. Preuss (2002), Cytotoxicity and oxidative mechanisms of different forms of chromium, Toxicology, 180(1), 5-22.

[176] - Merritt, K., and S. A. Brown (1995), Release of hexavalent chromium from corrosion of stainless steel and cobalt-chromium alloys, J Biomed Mater Res, 29(5), 627-633.

[177] - Salnikow, K., S. P. Donald, R. K. Bruick, A. Zhitkovich, J. M. Phang, and K. S. Kasprzak (2004), Depletion of intracellular ascorbate by the carcinogenic metals nickel and cobalt results in the induction of hypoxic stress, J Biol Chem, 279(39), 40337-40344.

[178] - Catelas, I., A. Petit, D. J. Zukor, J. Antoniou, and O. L. Huk (2003), TNF-α secretion and macrophage mortality induced by cobalt and chromium ions in vitro-Qualitative analysis of apoptosis, Biomaterials, 24(3), 383-391.

[179] - Akbar, M., J. M. Brewer, and M. H. Grant (2011), Effect of chromium and cobalt ions on primary human lymphocytes in vitro, J Immunotoxicol, 8(2), 140-149.

[180] - Catelas, I., A. Petit, H. Vali, C. Fragiskatos, R. Meilleur, D. J. Zukor, J. Antoniou, and O. L. Huk (2005), Quantitative analysis of macrophage apoptosis vs. necrosis induced by cobalt and chromium ions in vitro, Biomaterials, 26(15), 2441-2453.

[181] - Caicedo, M. S., P. H. Pennekamp, K. McAllister, J. J. Jacobs, and N. J. Hallab (2010), Soluble ions more than particulate cobalt-alloy implant debris induce monocyte costimulatory molecule expression and release of proinflammatory cytokines critical to metal-induced lymphocyte reactivity, J Biomed Mater Res A, 93(4), 1312-1321.

[182] - Samelko, L., M. S. Caicedo, S. J. Lim, C. Della-Valle, J. Jacobs, and N. J. Hallab (2013), Cobalt-alloy implant debris induce HIF-1alpha hypoxia associated responses: a mechanism for metal-specific orthopedic implant failure, PLoS One, 8(6), e67127.

[183] - Potnis, P. A., D. K. Dutta, and S. C. Wood (2013), Toll-like receptor 4 signaling pathway mediates proinflammatory immune response to cobalt-alloy particles, Cell Immunol, 282(1), 53-65.

[184] - Shweta, K. P. Mishra, S. Chanda, S. B. Singh, and L. Ganju (2015), A comparative immunological analysis of CoCl2 treated cells with in vitro hypoxic exposure, Biometals, 28(1), 175-185.

[185] - Lawrence, H., D. Deehan, J. Holland, J. Kirby, and A. Tyson-Capper (2014), The immunobiology of cobalt: demonstration of a potential aetiology for inflammatory pseudotumours after metal-on-metal replacement of the hip, Bone Joint J, 96-B(9), 1172-1177.

[186] - Dapunt, U., T. Giese, F. Lasitschka, J. Reinders, B. Lehner, J. P. Kretzer, V. Ewerbeck, and G. M. Hansch (2014), On the inflammatory response in metal-on-metal implants, J Transl Med, 12, 74.

[187] - Ninomiya, J. T., S. A. Kuzma, T. J. Schnettler, J. G. Krolikowski, J. A. Struve, and D. Weihrauch (2013), Metal ions activate vascular endothelial cells and increase lymphocyte chemotaxis and binding, J Orthop Res, 31(9), 1484-1491.

[188] - Granchi, D., G. Ciapetti, L. Savarino, S. Stea, F. Filippini, A. Sudanese, R. Rotini, and A. Giunti (2000), Expression of the CD69 activation antigen on lymphocytes of patients with hip prosthesis, Biomaterials, 21(20), 2059-2065.

[189] - Ogunwale, B., A. Schmidt-Ott, R. M. Meek, and J. M. Brewer (2009), Investigating the immunologic effects of CoCr nanoparticles, Clin Orthop Relat Res, 467(11), 3010-3016.

[190] - Pearson, M. J., R. L. Williams, H. Floyd, D. Bodansky, L. M. Grover, E. T. Davis, and J. M. Lord (2015), The effects of cobalt-chromium-molybdenum wear debris in vitro on serum cytokine profiles and T cell repertoire, Biomaterials, 67, 232-239.

[191] - Queally, J. M., B. M. Devitt, J. S. Butler, A. P. Malizia, D. Murray, P. P. Doran, and J. M. O'Byrne (2009), Cobalt ions induce chemokine secretion in primary human osteoblasts, J Orthop Res, 27(7), 855-864.

[192] - Hartmann, A., F. Hannemann, J. Lutzner, A. Seidler, H. Drexler, K. P. Gunther, and J. Schmitt (2013), Metal ion concentrations in body fluids after implantation of hip replacements with metal-on-metal bearing--systematic review of clinical and epidemiological studies, PLoS One, 8(8), e70359.

[193] - Afolaranmi, G. A., M. Akbar, J. Brewer, and M. H. Grant (2012), Distribution of metal released from cobalt-chromium alloy orthopaedic wear particles implanted into air pouches in mice, J Biomed Mater Res A, 100(6), 1529-1538.

[194] - Jakobsen, S. S., G. Danscher, M. Stoltenberg, A. Larsen, J. M. Bruun, T. Mygind, K. Kemp, and K. Soballe (2007), Cobalt-Chromium-Molybdenum Alloy Causes Metal Accumulation and Metallothionein Up-Regulation in Rat Liver and Kidney, Basic & Clinical Pharmacology & Toxicology, 101(6), 441-446.

[195] - Madejczyk, M. S., C. E. Baer, W. E. Dennis, V. C. Minarchick, S. S. Leonard, D. A. Jackson, J. D. Stallings, and J. A. Lewis (2015), Temporal changes in rat liver gene expression after acute cadmium and chromium exposure, PLoS One, 10(5), e0127327.

[196] - Wooley, P. H., R. Morren, J. Andary, S. Sud, S.-Y. Yang, L. Mayton, D. Markel, A. Sieving, and S. Nasser (2002), Inflammatory responses to orthopaedic biomaterials in the murine air pouch, Biomaterials, 23(2), 517-526.

[197] - Hallab, N. J., and J. J. Jacobs (2009), Biologic effects of implant debris, Bull NYU Hosp Jt Dis., 67(2), 182-188.

[198] - Kim, P. R., P. E. Beaule, M. Dunbar, J. K. Lee, N. Birkett, M. C. Turner, N. Yenugadhati, V. Armstrong, and D. Krewski (2011), Cobalt and chromium levels in blood and urine following hip resurfacing arthroplasty with the Conserve Plus implant, J Bone Joint Surg Am, 93 Suppl 2, 107-117.

[199] - Hallows, R. K., C. E. Pelt, J. A. Erickson, and C. L. Peters (2011), Serum metal ion concentration: comparison between small and large head metal-on-metal total hip arthroplasty, J Arthroplasty, 26(8), 1176-1181.

[200] - Ziaee, H., J. Daniel, A. K. Datta, S. Blunt, and D. J. McMinn (2007), Transplacental transfer of cobalt and chromium in patients with metal-on-metal hip arthroplasty: a controlled study, J. Bone Joint Surg.-Br. Vol., 89(3), 301-305.

[201] - Afolaranmi, G. A., J. Tettey, R. M. Meek, and M. H. Grant (2008), Release of chromium from orthopaedic arthroplasties, Open Orthop J, 2, 10-18.

[202] - Gunther, K. P., et al. (2013), Consensus statement "Current evidence on the management of metal-on-metal bearings"--April 16, 2012, Hip Int, 23(1), 2-5.

[203] - Cooper, H. J., C. J. Della Valle, R. A. Berger, M. Tetreault, W. G. Paprosky, S. M. Sporer, and J. J. Jacobs (2012), Corrosion at the Head-Neck Taper as a Cause for Adverse Local Tissue Reactions After Total Hip Arthroplasty, J. Bone Joint Surg.-Am. Vol., 94a(18), 1655-1661.

[204] - Dunstan, E., A. P. Sanghrajka, S. Tilley, P. Unwin, G. Blunn, S. R. Cannon, and T. W. Briggs (2005), Metal ion levels after metal-on-metal proximal femoral replacements: a 30-year follow-up, J. Bone Joint Surg.-Br. Vol., 87(5), 628-631.

[205] - Hart, A. J., S. A. Sabah, A. S. Bandi, P. Maggiore, P. Tarassoli, B. Sampson, and A. S. J (2011), Sensitivity and specificity of blood cobalt and chromium metal ions for predicting failure of metal-on-metal hip replacement, J. Bone Joint Surg.-Br. Vol., 93(10), 1308-1313.

[206] – Medicines and Healthcare Products Regulatory Agency (2010), Medical Device Alert MDA/2010/033: all metal-on-metal (MOM) hip replacements.

[207] - Xu, H., J. Edwards, S. Banerji, R. Prevo, D. G. Jackson, and N. A. Athanasou (2003), Distribution of lymphatic vessels in normal and arthritic human synovial tissues, Ann Rheum Dis, 62(12), 1227-1229.

[208] - Urban, R. M., J. J. Jacobs, M. J. Tomlinson, J. Gavrilovic, J. Black, and M. Peoc'h (2000), Dissemination of wear particles to the liver, spleen, and abdominal lymph nodes of patients with hip or knee replacement, J Bone Joint Surg Am, 82(4), 457-476.

[209] - Case, C. P., V. G. Langkamer, C. James, M. R. Palmer, A. J. Kemp, P. F. Heap, and L. Solomon (1994), Widespread dissemination of metal debris from implants, J. Bone Joint Surg.-Br. Vol., 76(5), 701-712.

[210] - Anderson, C. E., Jr. , A. K. D. Moore, T. N. Vinh, D. C. Washington, G. A. Engh, and V. Alexandria (1997), Titanium Prosthetic Wear Debris in Remote Bone Marrow. A Report of Two Cases, The Journal of Bone & Joint Surgery, 79(11), 1721-1725.

[211] - Campbell, P., R. M. Urban, I. Catelas, A. K. Skipor, and T. P. Schmalzried (2003), Autopsy analysis thirty years after metal-on-metal total hip replacement. A case report, J Bone Joint Surg Am, 85-A(11), 2218-2222.

[212] - Lundborg, M., R. Falk, A. Johansson, W. Kreyling, and P. Camner (1992), Phagolysosomal pH and dissolution of cobalt oxide particles by alveolar macrophages, Environ. Health Perspect., 97, 153-157.

[213] - Visuri, T., P. Pulkkinen, P. Paavolainen, and E. Pukkala (2010), Cancer risk is not increased after conventional hip arthroplasty, Acta orthopaedica, 81(1), 77-81.

[214] - Wagner, P., H. Olsson, L. Lidgren, O. Robertsson, and J. Ranstam (2011), Increased cancer risks among arthroplasty patients: 30 year follow-up of the Swedish Knee Arthroplasty Register, Eur. J. Cancer, 47(7), 1061-1071.

[215] - Chandran, S. E., and N. J. Giori (2011), Nine-year incidence of kidney disease in patients who have had total hip arthroplasty, J Arthroplasty, 26(6 Suppl), 24-27.

[216] - Visuri, T., H. Borg, P. Pulkkinen, P. Paavolainen, and E. Pukkala (2010), A retrospective comparative study of mortality and causes of death among patients with metal-on-metal and metal-on-polyethylene total hip prostheses in primary osteoarthritis after a long-term follow-up, Bmc Musculoskel Dis, 11(1), 78.

[217] - Zywiel, M. G., J. M. Brandt, C. B. Overgaard, A. C. Cheung, T. R. Turgeon, and K. A. Syed (2013), Fatal cardiomyopathy after revision total hip replacement for fracture of a ceramic liner, Bone Joint J, 95-B(1), 31-37.

[218] - Kwon, Y. M., Z. Xia, S. Glyn-Jones, D. Beard, H. S. Gill, and D. W. Murray (2009), Dose-dependent cytotoxicity of clinically relevant cobalt nanoparticles and ions on macrophages in vitro, Biomed Mater, 4(2), 025018.

[219] - Chan, E. P., A. Mhawi, P. Clode, M. Saunders, and L. Filgueira (2009), Effects of titanium(iv) ions on human monocyte-derived dendritic cells, Metallomics : integrated biometal science, 1(2), 166-174.

[220] - Cadosch, D., M. Sutanto, E. Chan, A. Mhawi, O. P. Gautschi, B. von Katterfeld, H. P. Simmen, and L. Filgueira (2010), Titanium uptake, induction of RANK-L expression, and enhanced proliferation of human T-lymphocytes, J Orthop Res, 28(3), 341-347.

[221] - Wang, J. Y., B. H. Wicklund, R. B. Gustilo, and D. T. Tsukayama (1996), Titanium, chromium and cobalt ions modulate the release of bone-associated cytokines by human monocytes/macrophages in vitro, Biomaterials, 17(23), 2233-2240.

[222] - Stejskal, V., T. Reynolds, and G. Bjorklund (2015), Increased frequency of delayed type hypersensitivity to metals in patients with connective tissue disease, J Trace Elem Med Biol, 31, 230-236.

[223] - Muller, K., and E. Valentine-Thon (2006), Hypersensitivity to titanium: clinical and laboratory evidence, Neuro Endocrinol Lett, 27 Suppl 1, 31-35.

[224] - Gao, Y., N. V. Gopee, P. C. Howard, and L. R. Yu (2011), Proteomic analysis of early response lymph node proteins in mice treated with titanium dioxide nanoparticles, J Proteomics, 74(12), 2745-2759.

[225] - Rakshit, D. S., J. T. Lim, K. Ly, L. B. Ivashkiv, B. J. Nestor, T. P. Sculco, and P. E. Purdue (2006), Involvement of complement receptor 3 (CR3) and scavenger receptor in macrophage responses to wear debris, J Orthop Res, 24(11), 2036-2044.

[226] - Chen, W., et al. (2015), Wear particles promote reactive oxygen species-mediated inflammation via the nicotinamide adenine dinucleotide phosphate oxidase pathway in macrophages surrounding loosened implants, Cell Physiol Biochem, 35(5), 1857-1867.

[227] - Xing, Z., L. P. Schwab, C. F. Alley, K. A. Hasty, and R. A. Smith (2008), Titanium particles that have undergone phagocytosis by macrophages lose the ability to activate other macrophages, J Biomed Mater Res B Appl Biomater, 85(1), 37-41.

[228] - Kaufman, A. M., C. I. Alabre, H. E. Rubash, and A. S. Shanbhag (2008), Human macrophage response to UHMWPE, TiAlV, CoCr, and alumina particles: analysis of multiple cytokines using protein arrays, J Biomed Mater Res A, 84(2), 464-474.

[229] - St Pierre, C. A., M. Chan, Y. Iwakura, D. C. Ayers, E. A. Kurt-Jones, and R. W. Finberg (2010), Periprosthetic osteolysis: characterizing the innate immune response to titanium wear-particles, J Orthop Res, 28(11), 1418-1424.

[230] - Obando-Pereda, G. A., L. Fischer, and D. R. Stach-Machado (2014), Titanium and zirconia particle-induced pro-inflammatory gene expression in cultured macrophages and osteolysis, inflammatory hyperalgesia and edema in vivo, Life Sci, 97(2), 96-106.

[231] - Cheng, T., G. Y. Zhang, C. J. Guo, and X. Zhang (2010), Effects of NF-kappaB inhibitor on titanium particulate-induced inflammation in a murine model, J Surg Res, 162(2), 225-230.

[232] - Baumann, B., J. Seufert, F. Jakob, U. Noth, O. Rolf, J. Eulert, and C. P. Rader (2005), Activation of NF-kappaB signalling and TNFalpha-expression in THP-1 macrophages by TiAlV- and polyethylene-wear particles, J Orthop Res, 23(6), 1241-1248.

[233] - Pioletti, D. P., and A. Kottelat (2004), The influence of wear particles in the expression of osteoclastogenesis factors by osteoblasts, Biomaterials, 25(27), 5803-5808.

[234] - Haleem-Smith, H., E. Argintar, C. Bush, D. Hampton, W. F. Postma, F. H. Chen, T. Rimington, J. Lamb, and R. S. Tuan (2012), Biological responses of human mesenchymal stem cells to titanium wear debris particles, J Orthop Res, 30(6), 853-863.

[235] - Jamsen, E., V. P. Kouri, J. Olkkonen, A. Cor, S. B. Goodman, Y. T. Konttinen, and J. Pajarinen (2014), Characterization of macrophage polarizing cytokines in the aseptic loosening of total hip replacements, J Orthop Res, 32(9), 1241-1246.

[236] - Geetha, M., A. K. Singh, R. Asokamani, and A. K. Gogia (2009), Ti based biomaterials, the ultimate choice for orthopaedic implants - A review, Prog. Mater. Sci., 54(3), 397-425.

[237] - Sarmiento-Gonzalez, A., J. R. Encinar, J. M. Marchante-Gayon, and A. Sanz-Medel (2009), Titanium levels in the organs and blood of rats with a titanium implant, in the absence of wear, as determined by double-focusing ICP-MS, Anal. Bioanal. Chem., 393(1), 335-343.

[238] - Song, B., J. Liu, X. Feng, L. Wei, and L. Shao (2015), A review on potential neurotoxicity of titanium dioxide nanoparticles, Nanoscale Res Lett, 10(1), 1042.

[239] - Hong, J., A. Azens, K. N. Ekdahl, C. G. Granqvist, and B. Nilsson (2005), Material-specific thrombin generation following contact between metal surfaces and whole blood, Biomaterials, 26(12), 1397-1403.

[240] - Phillips, S. J. (2001), Thrombogenic influence of biomaterials in patients with the Omni series heart valve: pyrolytic carbon versus titanium, ASAIO J, 47(5), 429-431.

[241] - Schwarz, E. M., A. P. Lu, J. J. Goater, E. B. Benz, G. Kollias, R. N. Rosier, J. E. Puzas, and R. J. O'Keefe (2000), Tumor necrosis factor-alpha/nuclear transcription factor-kappaB signaling in periprosthetic osteolysis, J Orthop Res, 18(3), 472-480.

[242] - Childs, L. M., J. J. Goater, R. J. O'Keefe, and E. M. Schwarz (2001), Efficacy of etanercept for wear debris-induced osteolysis, J Bone Miner Res, 16(2), 338-347.

[243] - Liu, X., S. Zhu, J. Cui, H. Shao, W. Zhang, H. Yang, Y. Xu, D. Geng, and L. Yu (2014), Strontium ranelate inhibits titanium-particle-induced osteolysis by restraining inflammatory osteoclastogenesis in vivo, Acta Biomater, 10(11), 4912-4918.

[244] - Wachi, T., T. Shuto, Y. Shinohara, Y. Matono, and S. Makihira (2015), Release of titanium ions from an implant surface and their effect on cytokine production related to alveolar bone resorption, Toxicology, 327, 1-9.

[245] - Hoene, A., M. Patrzyk, U. Walschus, B. Finke, S. Lucke, B. Nebe, K. Schroder, and M. Schlosser (2015), Systemic IFNgamma predicts local implant macrophage response, J Mater Sci Mater Med, 26(3), 131.

[246] - Kmiec, K., M. Synder, P. Kozlowski, M. Drobniewski, and M. Sibinski (2014), Metal debris concentrations in soft tissues adjacent to loosened femoral stems is higher in uncemented than cemented implants, Bmc Musculoskel Dis, 15, 267.

[247] - Shahgaldi, B. F., F. W. Heatley, A. Dewar, and B. Corrin (1995), In vivo corrosion of cobalt-chromium and titanium wear particles, J. Bone Joint Surg.-Br. Vol., 77(6), 962-966.

[248] - Lalor, P. A., P. A. Revell, A. B. Gray, S. Wright, G. T. Railton, and M. A. Freeman (1991), Sensitivity to titanium. A cause of implant failure?, J. Bone Joint Surg.-Br. Vol., 73(1), 25-28.

[249] - Qu, X., X. Huang, and K. Dai (2011), Metal-on-metal or metal-on-polyethylene for total hip arthroplasty: a meta-analysis of prospective randomized studies, Arch Orthop Trauma Surg, 131(11), 1573-1583.

[250] - Swartzlander, M. D., A. K. Blakney, L. D. Amer, K. D. Hankenson, T. R. Kyriakides, and S. J. Bryant (2015), Immunomodulation by mesenchymal stem cells combats the foreign body response to cell-laden synthetic hydrogels, Biomaterials, 41, 79-88.

[251] - Santos, S. G., et al. (2013), Adsorbed fibrinogen leads to improved bone regeneration and correlates with differences in the systemic immune response, Acta Biomater, 9(7), 7209-7217.

[252] - Seebach, E., H. Freischmidt, J. Holschbach, J. Fellenberg, and W. Richter (2014), Mesenchymal stroma cells trigger early attraction of M1 macrophages and endothelial cells into fibrin hydrogels, stimulating long bone healing without long-term engraftment, Acta Biomater, 10(11), 4730-4741.

[253] - Lin, S. S., N. J. Montemurro, and E. S. Krell (2016), Orthobiologics in Foot and Ankle Surgery, J Am Acad Orthop Surg, 24(2), 113-122.

[254] - Fujioka-Kobayashi, M., M. Mottini, E. Kobayashi, Y. Zhang, B. Schaller, and R. J. Miron (2017), An in vitro study of fibrin sealant as a carrier system for recombinant human bone morphogenetic protein (rhBMP)-9 for bone tissue engineering, J Craniomaxillofac Surg, 45(1), 27-32.

[255] - Kilcup, N., S. Gaynard, U. Werner-Zwanziger, E. Tonkopi, J. Hayes, and D. Boyd (2016), Stimulation of apoptotic pathways in liver cancer cells: An alternative perspective on the biocompatibility and the utility of biomedical glasses, J Biomater Appl, 30(10), 1445-1459.

[256] - Kim, J., and J. L. Gilbert (2016), Cytotoxic effect of galvanically coupled magnesium-titanium particles, Acta Biomater, 30, 368-377.

[257] - Burghardt, I., F. Luthen, C. Prinz, B. Kreikemeyer, C. Zietz, H. G. Neumann, and J. Rychly (2015), A dual function of copper in designing regenerative implants, Biomaterials, 44, 36-44.

[258] - Jin, G., H. Qin, H. Cao, Y. Qiao, Y. Zhao, X. Peng, X. Zhang, X. Liu, and P. K. Chu (2015), Zn/Ag micro-galvanic couples formed on titanium and osseointegration effects in the presence of S. aureus, Biomaterials, 65, 22-31.

[259] - Paglia, D. N., A. Wey, A. G. Park, E. A. Breitbart, S. K. Mehta, J. D. Bogden, F. W. Kemp, J. Benevenia, J. P. O'Connor, and S. S. Lin (2012), The effects of local vanadium treatment on angiogenesis and chondrogenesis during fracture healing, J Orthop Res, 30(12), 1971-1978.

[260] - Aimanianda, V., J. Haensler, S. Lacroix-Desmazes, S. V. Kaveri, and J. Bayry (2009), Novel cellular and molecular mechanisms of induction of immune responses by aluminum adjuvants, Trends Pharmacol Sci, 30(6), 287-295.

[261] - Cho, W. S., K. Dart, D. J. Nowakowska, X. Zheng, K. Donaldson, and S. E. Howie (2012), Adjuvanticity and toxicity of cobalt oxide nanoparticles as an alternative vaccine adjuvant, Nanomedicine (Lond), 7(10), 1495-1505.

[262] - Mourino, V., J. P. Cattalini, and A. R. Boccaccini (2012), Metallic ions as therapeutic agents in tissue engineering scaffolds: an overview of their biological applications and strategies for new developments, J R Soc Interface, 9(68), 401-419.

[263] - Zhang, J., X. Ma, D. Lin, H. Shi, Y. Yuan, W. Tang, H. Zhou, H. Guo, J. Qian, and C. Liu (2015), Magnesium modification of a calcium phosphate cement alters bone marrow stromal cell behavior via an integrin-mediated mechanism, Biomaterials, 53, 251-264.

[264] - Kitabata, H., R. Waksman, and B. Warnack (2014), Bioresorbable metal scaffold for cardiovascular application: current knowledge and future perspectives, Cardiovasc Revasc Med, 15(2), 109-116.

[265] - Schumacher, M., A. Lode, A. Helth, and M. Gelinsky (2013), A novel strontium(II)-modified calcium phosphate bone cement stimulates human-bone-marrow-derived mesenchymal stem cell proliferation and osteogenic differentiation in vitro, Acta Biomater, 9(12), 9547-9557.

[266] - Cattalini, J. P., A. Hoppe, F. Pishbin, J. Roether, A. R. Boccaccini, S. Lucangioli, and V. Mourino (2015), Novel nanocomposite biomaterials with controlled copper/calcium release capability for bone tissue engineering multifunctional scaffolds, J R Soc Interface, 12(110), 0509.

[267] - Moravej, M., and D. Mantovani (2011), Biodegradable metals for cardiovascular stent application: interests and new opportunities, Int J Mol Sci, 12(7), 4250-4270.

[268] - Chaya, A., S. Yoshizawa, K. Verdelis, N. Myers, B. J. Costello, D. T. Chou, S. Pal, S. Maiti, P. N. Kumta, and C. Sfeir (2015), In vivo study of magnesium plate and screw degradation and bone fracture healing, Acta Biomater, 18, 262-269.

[269] - Bondarenko, A., N. Angrisani, A. Meyer-Lindenberg, J. M. Seitz, H. Waizy, and J. Reifenrath (2014), Magnesium-based bone implants: immunohistochemical analysis of peri-implant osteogenesis by evaluation of osteopontin and osteocalcin expression, J Biomed Mater Res A, 102(5), 1449-1457.

[270] - Witte, F., N. Hort, C. Vogt, S. Cohen, K. U. Kainer, R. Willumeit, and F. Feyerabend (2008), Degradable biomaterials based on magnesium corrosion, Curr Opin Solid St M, 12(5-6), 63-72.

[271] - Windhagen, H., K. Radtke, A. Weizbauer, J. Diekmann, Y. Noll, U. Kreimeyer, R. Schavan, C. Stukenborg-Colsman, and H. Waizy (2013), Biodegradable magnesium-based screw clinically equivalent to titanium screw in hallux valgus surgery: short term results of the first prospective, randomized, controlled clinical pilot study, Biomed Eng Online, 12, 62.

[272] - Pichler, K., T. Kraus, E. Martinelli, P. Sadoghi, G. Musumeci, P. J. Uggowitzer, and A. M. Weinberg (2014), Cellular reactions to biodegradable magnesium alloys on human growth plate chondrocytes and osteoblasts, Int Orthop, 38(4), 881-889.

[273] - Yoshizawa, S., A. Chaya, K. Verdelis, E. A. Bilodeau, and C. Sfeir (2015), An in vivo model to assess magnesium alloys and their biological effect on human bone marrow stromal cells, Acta Biomater, 28, 234-239.

[274] - Martinez Sanchez, A. H., B. J. Luthringer, F. Feyerabend, and R. Willumeit (2015), Mg and Mg alloys: how comparable are in vitro and in vivo corrosion rates? A review, Acta Biomater, 13, 16-31.

[275] - Brown, A., S. Zaky, H. Ray, Jr., and C. Sfeir (2015), Porous magnesium/PLGA composite scaffolds for enhanced bone regeneration following tooth extraction, Acta Biomater, 11, 543-553.

[276] - Witte, F., H. Ulrich, C. Palm, and E. Willbold (2007), Biodegradable magnesium scaffolds: Part II: peri-implant bone remodeling, J Biomed Mater Res A, 81(3), 757-765.

[277] - Witte, F., V. Kaese, H. Haferkamp, E. Switzer, A. Meyer-Lindenberg, C. J. Wirth, and H. Windhagen (2005), In vivo corrosion of four magnesium alloys and the associated bone response, Biomaterials, 26(17), 3557-3563.

[278] - Cha, P. R., et al. (2013), Biodegradability engineering of biodegradable Mg alloys: tailoring the electrochemical properties and microstructure of constituent phases, Sci Rep, 3, 2367.

[279] - Marukawa, E., et al. (2016), Comparison of magnesium alloys and poly-l-lactide screws as degradable implants in a canine fracture model, J Biomed Mater Res B Appl Biomater, 104(7), 1282-1289.

[280] - Charyeva, O., et al. (2015), Histological Comparison of New Biodegradable Magnesium-Based Implants for Maxillofacial Applications, J Maxillofac Oral Surg, 14(3), 637-645.

[281] - Cheng, P., et al. (2015), High-purity magnesium interference screws promote fibrocartilaginous entheses regeneration in the anterior cruciate ligament reconstruction rabbit model via accumulation of BMP-2 and VEGF, Biomaterials, 81, 14-26.

[282] - Staiger, M. P., A. M. Pietak, J. Huadmai, and G. Dias (2006), Magnesium and its alloys as orthopedic biomaterials: a review, Biomaterials, 27(9), 1728-1734.

[283] - Chaigne-Delalande, B., and M. J. Lenardo (2014), Divalent cation signaling in immune cells, Trends Immunol, 35(7), 332-344.

[284] - de Baaij, J. H., J. G. Hoenderop, and R. J. Bindels (2015), Magnesium in man: implications for health and disease, Physiol Rev, 95(1), 1-46.

[285] - Grzesiak, J. J., and M. D. Pierschbacher (1995), Shifts in the concentrations of magnesium and calcium in early porcine and rat wound fluids activate the cell migratory response, J Clin Invest, 95(1), 227-233.

[286] - Doyle, L. W., C. A. Crowther, P. Middleton, and S. Marret (2007), Magnesium sulphate for women at risk of preterm birth for neuroprotection of the fetus, Cochrane Database Syst Rev(3), CD004661.

[287] - Duley, L., A. M. Gulmezoglu, D. J. Henderson-Smart, and D. Chou (2010), Magnesium sulphate and other anticonvulsants for women with pre-eclampsia, Cochrane Database Syst Rev(11), CD000025.

[288] - Shimaya, M., T. Muneta, S. Ichinose, K. Tsuji, and I. Sekiya (2010), Magnesium enhances adherence and cartilage formation of synovial mesenchymal stem cells through integrins, Osteoarthritis Cartilage, 18(10), 1300-1309.

[289] - Yoshizawa, S., A. Brown, A. Barchowsky, and C. Sfeir (2014), Magnesium ion stimulation of bone marrow stromal cells enhances osteogenic activity, simulating the effect of magnesium alloy degradation, Acta Biomater, 10(6), 2834-2842.

[290] - Han, P., et al. (2015), In vitro and in vivo studies on the degradation of high-purity Mg (99.99wt.%) screw with femoral intracondylar fractured rabbit model, Biomaterials, 64, 57-69.

[291] - Zheng, J., X. Mao, J. Ling, C. Chen, and W. Zhang (2015), Role of Magnesium Transporter Subtype 1 (MagT1) in the Osteogenic Differentiation of Rat Bone Marrow Stem Cells, Biol Trace Elem Res, 171(1), 131-137.

[292] - Wu, L., B. J. Luthringer, F. Feyerabend, A. F. Schilling, and R. Willumeit (2014), Effects of extracellular magnesium on the differentiation and function of human osteoclasts, Acta Biomater, 10(6), 2843-2854.

[293] - Grzesiak, J. J., and M. Bouvet (2008), Divalent cations modulate the integrin-mediated malignant phenotype in pancreatic cancer cells, Cancer science, 99(8), 1553-1563.

[294] - Hagandora, C. K., M. A. Tudares, and A. J. Almarza (2012), The effect of magnesium ion concentration on the fibrocartilage regeneration potential of goat costal chondrocytes, Ann Biomed Eng, 40(3), 688-696.

[295] - Mazur, A., J. A. Maier, E. Rock, E. Gueux, W. Nowacki, and Y. Rayssiguier (2007), Magnesium and the inflammatory response: potential physiopathological implications, Archives of biochemistry and biophysics, 458(1), 48-56.

[296] - Ferre, S., E. Baldoli, M. Leidi, and J. A. Maier (2010), Magnesium deficiency promotes a pro-atherogenic phenotype in cultured human endothelial cells via activation of NFkB, Biochimica et biophysica acta, 1802(11), 952-958.

[297] - Li, F. Y., B. Chaigne-Delalande, C. Kanellopoulou, J. C. Davis, H. F. Matthews, D. C. Douek, J. I. Cohen, G. Uzel, H. C. Su, and M. J. Lenardo (2011), Second messenger role for Mg2+ revealed by human T-cell immunodeficiency, Nature, 475(7357), 471-476.

[298] - Lin, C. Y., P. S. Tsai, Y. C. Hung, and C. J. Huang (2010), L-type calcium channels are involved in mediating the anti-inflammatory effects of magnesium sulphate, British journal of anaesthesia, 104(1), 44-51.

[299] - Sugimoto, J., A. M. Romani, A. M. Valentin-Torres, A. A. Luciano, C. M. Ramirez Kitchen, N. Funderburg, S. Mesiano, and H. B. Bernstein (2012), Magnesium decreases inflammatory cytokine production: a novel innate immunomodulatory mechanism, Journal of immunology, 188(12), 6338-6346.

[300] - Son, E. W., S. R. Lee, H. S. Choi, H. J. Koo, J. E. Huh, M. H. Kim, and S. Pyo (2007), Effects of supplementation with higher levels of manganese and magnesium on immune function, Archives of pharmacal research, 30(6), 743-749.

[301] - Lee, C. H., Z. H. Wen, Y. C. Chang, S. Y. Huang, C. C. Tang, W. F. Chen, S. P. Hsieh, C. S. Hsieh, and Y. H. Jean (2009), Intra-articular magnesium sulfate (MgSO4) reduces experimental osteoarthritis and nociception: association with attenuation of N-methyl-D-aspartate (NMDA) receptor subunit 1 phosphorylation and apoptosis in rat chondrocytes, Osteoarthritis Cartilage, 17(11), 1485-1493.

[302] - Kim, J. H., H. J. Gibb, and P. D. Howe (2006), Cobalt and Inorganic Cobalt Compounds*Rep.*, World Health Organization.

[303] - Tower, S. S. (2010), Arthroprosthetic Cobaltism: Neurological and Cardiac Manifestations in Two Patients with Metal-on-Metal Arthroplasty, The Journal of Bone & Joint Surgery, 92(2), 2847-2851.

[304] - Kim, H. K., H. Bian, J. Aya-ay, A. Garces, E. F. Morgan, and S. R. Gilbert (2009), Hypoxia and HIF-1alpha expression in the epiphyseal cartilage following ischemic injury to the immature femoral head, Bone, 45(2), 280-288.

[305] - Huang, Y., et al. (2003), Cobalt chloride and low oxygen tension trigger differentiation of acute myeloid leukemic cells: possible mediation of hypoxia-inducible factor-1alpha, Leukemia, 17(11), 2065-2073.

[306] - Perez, R. A., J. H. Kim, J. O. Buitrago, I. B. Wall, and H. W. Kim (2015), Novel therapeutic core-shell hydrogel scaffolds with sequential delivery of cobalt and bone morphogenetic protein-2 for synergistic bone regeneration, Acta Biomater, 23, 295-308.

[307] - Fan, W., R. Crawford, and Y. Xiao (2010), Enhancing in vivo vascularized bone formation by cobalt chloride-treated bone marrow stromal cells in a tissue engineered periosteum model, Biomaterials, 31(13), 3580-3589.

[308] - Ng, K. M., Y. C. Chan, Y. K. Lee, W. H. Lai, K. W. Au, M. L. Fung, C. W. Siu, R. A. Li, and H. F. Tse (2011), Cobalt chloride pretreatment promotes cardiac differentiation of human embryonic stem cells under atmospheric oxygen level, Cellular reprogramming, 13(6), 527-537.

[309] - Quinlan, E., S. Partap, M. M. Azevedo, G. Jell, M. M. Stevens, and F. J. O'Brien (2015), Hypoxia-mimicking bioactive glass/collagen glycosaminoglycan composite scaffolds to enhance angiogenesis and bone repair, Biomaterials, 52, 358-366.

[310] - Ignjatovic, N., Z. Ajdukovic, V. Savic, S. Najman, D. Mihailovic, P. Vasiljevic, Z. Stojanovic, V. Uskokovic, and D. Uskokovic (2013), Nanoparticles of cobalt-substituted hydroxyapatite in regeneration of mandibular osteoporotic bones, J Mater Sci Mater Med, 24(2), 343-354.

[311] - Zhang, M., C. Wu, H. Li, J. Yuen, J. Chang, and Y. Xiao (2012), Preparation, characterization and in vitro angiogenic capacity of cobalt substituted beta-tricalcium phosphate ceramics, Journal of Materials Chemistry, 22(40), 21686-21694.

[312] - Wu, C., Y. Zhou, W. Fan, P. Han, J. Chang, J. Yuen, M. Zhang, and Y. Xiao (2012), Hypoxia-mimicking mesoporous bioactive glass scaffolds with controllable cobalt ion release for bone tissue engineering, Biomaterials, 33(7), 2076-2085.

[313] - Chen, Z., J. Yuen, R. Crawford, J. Chang, C. Wu, and Y. Xiao (2015), The effect of osteoimmunomodulation on the osteogenic effects of cobalt incorporated beta-tricalcium phosphate, Biomaterials, 61, 126-138.

[314] - Salazar, V. S., L. W. Gamer, and V. Rosen (2016), BMP signalling in skeletal development, disease and repair, Nat Rev Endocrinol, 12(4), 203-221.

[315] - Carragee, E. J., E. L. Hurwitz, and B. K. Weiner (2011), A critical review of recombinant human bone morphogenetic protein-2 trials in spinal surgery: emerging safety concerns and lessons learned, Spine J, 11(6), 471-491.

[316] - Shiga, Y., et al. (2016), Freeze-Dried Platelet-Rich Plasma Accelerates Bone Union with Adequate Rigidity in Posterolateral Lumbar Fusion Surgery Model in Rats, Sci Rep, 6, 36715.

[317] - Grambart, S. T. (2015), Sports medicine and platelet-rich plasma: nonsurgical therapy, Clin Podiatr Med Surg, 32(1), 99-107.

[318] - Eppley, B. L., J. E. Woodell, and J. Higgins (2004), Platelet quantification and growth factor analysis from platelet-rich plasma: implications for wound healing, Plast Reconstr Surg, 114(6), 1502-1508.

[319] - Malhotra, A., M. H. Pelletier, Y. Yu, and W. R. Walsh (2013), Can platelet-rich plasma (PRP) improve bone healing? A comparison between the theory and experimental outcomes, Arch Orthop Trauma Surg, 133(2), 153-165.

[320] - Parenteau-Bareil, R., R. Gauvin, and F. Berthod (2010), Collagen-Based Biomaterials for Tissue Engineering Applications, Materials, 3(3), 1863-1887.

[321] - Versteegden, L. R., et al. (2016), Design of an elasticized collagen scaffold: A method to induce elasticity in a rigid protein, Acta Biomater, 44, 277-285.

[322] - Lyons, F. G., A. A. Al-Munajjed, S. M. Kieran, M. E. Toner, C. M. Murphy, G. P. Duffy, and F. J. O'Brien (2010), The healing of bony defects by cell-free collagen-based scaffolds compared to stem cell-seeded tissue engineered constructs, Biomaterials, 31(35), 9232-9243.

[323] - Hashimoto, Y., S. Funamoto, T. Kimura, K. Nam, T. Fujisato, and A. Kishida (2011), The effect of decellularized bone/bone marrow produced by high-hydrostatic pressurization on the osteogenic differentiation of mesenchymal stem cells, Biomaterials, 32(29), 7060-7067.

[324] - Silva, A. C., et al. (2016), Three-dimensional scaffolds of fetal decellularized hearts exhibit enhanced potential to support cardiac cells in comparison to the adult, Biomaterials, 104, 52-64.

[325] - Spotnitz, W. D. (2014), Fibrin Sealant: The Only Approved Hemostat, Sealant, and Adhesive-a Laboratory and Clinical Perspective, ISRN Surg, 2014, 203943.

[326] - Wang, H., L. Shan, H. Zeng, M. Sun, Y. Hua, and Z. Cai (2014), Is fibrin sealant effective and safe in total knee arthroplasty? A meta-analysis of randomized trials, Journal of orthopaedic surgery and research, 9, 36.

[327] - Linsley, C. S., B. M. Wu, and B. Tawil (2016), Mesenchymal stem cell growth on and mechanical properties of fibrin-based biomimetic bone scaffolds, J Biomed Mater Res A, 104(12), 2945-2953.

[328] - Linnes, M. P., B. D. Ratner, and C. M. Giachelli (2007), A fibrinogen-based precision microporous scaffold for tissue engineering, Biomaterials, 28(35), 5298-5306.

[329] - Kim, B. S., H. M. Sung, H. K. You, and J. Lee (2014), Effects of fibrinogen concentration on fibrin glue and bone powder scaffolds in bone regeneration, Journal of bioscience and bioengineering, 118(4), 469-475.

[330] - Kim, B. S., and J. Lee (2015), Enhanced bone healing by improved fibrin-clot formation via fibrinogen adsorption on biphasic calcium phosphate granules, Clin Oral Implants Res, 26(10), 1203-1210.

[331] - van der Stok, J., et al. (2015), Full regeneration of segmental bone defects using porous titanium implants loaded with BMP-2 containing fibrin gels, e Cells and Materials Journal, 4(29), 153-154.

[332] - Oliveira, M. I., M. L. Pinto, R. M. Goncalves, M. C. Martins, S. G. Santos, and M. A. Barbosa (2017), Adsorbed Fibrinogen stimulates TLR-4 on monocytes and induces BMP-2 expression, Acta Biomater, 49, 296-305.

[333] - Maciel, J., M. I. Oliveira, E. Colton, A. K. McNally, C. Oliveira, J. M. Anderson, and M. A. Barbosa (2014), Adsorbed fibrinogen enhances production of bone- and angiogenic-related factors by monocytes/macrophages, Tissue Eng Part A, 20(1-2), 250-263.

[334] - Almeida, C. R., D. P. Vasconcelos, R. M. Goncalves, and M. A. Barbosa (2012), Enhanced mesenchymal stromal cell recruitment via natural killer cells by incorporation of inflammatory signals in biomaterials, J R Soc Interface, 9(67), 261-271.

[335] - Mountziaris, P. M., P. P. Spicer, F. K. Kasper, and A. G. Mikos (2011), Harnessing and modulating inflammation in strategies for bone regeneration, Tissue engineering. Part B, Reviews, 17(6), 393-402.

[336] - Hotaling, N. A., L. Tang, D. J. Irvine, and J. E. Babensee (2015), Biomaterial Strategies for Immunomodulation, Annu Rev Biomed Eng, 17, 317-349.

[337] - Sadtler, K., et al. (2016), Developing a pro-regenerative biomaterial scaffold microenvironment requires T helper 2 cells, Science, 352(6283), 366-370.

[338] - Vasconcelos, D. P., M. Costa, I. F. Amaral, M. A. Barbosa, A. P. Aguas, and J. N. Barbosa (2015), Modulation of the inflammatory response to chitosan through M2 macrophage polarization using pro-resolution mediators, Biomaterials, 37, 116-123.

[339] - Hart, P. H., G. F. Vitti, D. R. Burgess, G. A. Whitty, D. S. Piccoli, and J. A. Hamilton (1989), Potential antiinflammatory effects of interleukin 4: suppression of human monocyte tumor necrosis factor alpha, interleukin 1, and prostaglandin E2, Proc Natl Acad Sci U S A, 86(10), 3803-3807.

[340] - Hachim, D., S. T. LoPresti, C. C. Yates, and B. N. Brown (2016), Shifts in macrophage phenotype at the biomaterial interface via IL-4 eluting coatings are associated with improved implant integration, Biomaterials, 112, 95-107.

[341] - Gao, F., S. M. Chiu, D. A. Motan, Z. Zhang, L. Chen, H. L. Ji, H. F. Tse, Q. L. Fu, and Q. Lian (2016), Mesenchymal stem cells and immunomodulation: current status and future prospects, Cell Death Dis, 7, e2062.

CHAPTER II

Immune response and innervation signatures in aseptic hip implant loosening

Article 2

Published in Journal of Translational Medicine 14:205, 2016

doi: 10.1186/s12967-016-0950-5

Immune response and innervation signatures in aseptic hip implant loosening

Daniel M. Vasconcelos[1,2,3,*], Manuel Ribeiro-da-Silva[1,2,4,5,*], António Mateus[4,5], Cecília Juliana Alves[1,2], Gil Costa Machado[1,2], Joana Machado-Santos[1,2], Diogo Paramos-de-Carvalho[1,2], Inês S. Alencastre[1,2], Rui Henrique[3,6], Gilberto Costa[4,5], Mário A. Barbosa[1,2,3,#] and Meriem Lamghari[1,2,3,#]

(*), (#) These authors contributed equally to this work

[1] i3S- Instituto de Investigação e Inovação em Saúde, Universidade do Porto, Rua Alfredo Allen, 208, 4200-135 Porto, Portugal

[2] INEB- Instituto de Engenharia Biomédica, Universidade do Porto, Rua Alfredo Allen, 208, 4200-135 Porto, Portugal

[3] ICBAS- Instituto Ciências Biomédicas Abel Salazar, Rua de Jorge Viterbo Ferreira 228, 4050-313 Porto, Portugal

[4] Serviço de Ortopedia e Traumatologia, Centro Hospitalar São João, Alameda Prof. Hernâni Monteiro, 4200-319 Porto, Portugal

[5] FMUP-Faculdade de Medicina da Universidade do Porto, Departamento de Cirurgia, Serviço de Ortopedia, Alameda Prof. Hernâni Monteiro, 4200-319 Porto, Portugal

[6] Department of Pathology, Portuguese Oncology Institute of Porto (IPO Porto), Rua Dr. António Bernardino de Almeida, Porto 4200-072, Portugal

Abstract

Aseptic loosening (AL) of hip prosthesis presents inflammation and pain as sign and symptom similarly to arthritis pathologies. Still, the immune and innervation profiles in hip AL remain unclear and their interplay is poorly explored. Herein, local tissue inflammatory response, sensory and sympathetic innervation as well as associated local mediators were assessed in hip joint microenvironment underlying AL and compared to osteoarthritis (OA).

The profile of immune cells (macrophages, T, B cells and PMNs) and sensory and sympathetic nerve fibers (Substance P+, CGRP+, TH+) were analyzed on tissues retrieved from patients with failed hip prostheses due to AL (n=20) and hip OA (n=15) by immunohistochemistry. Additionally, transcriptional levels of pro-inflammatory cytokines (TNF-α, IL-1β, IL-6, IL-12a, iNOS), anti-inflammatory cytokine (IL-10), osteoclastic factor (RANKL) and bone remodeling factor (TGF-β1) were locally evaluated by qRT-PCR. Serum TGF-β1 levels were assessed preoperatively by ELISA.

Histopathological analysis revealed that aseptic interface membranes of AL patients had distinct tissue architecture and immune cells profile when compared to OA synovial tissues. Macrophages, T cells and B cells showed significant differences in tissue distribution. In OA, inflammation is mostly confined to the vicinity of synovial membrane while in AL macrophages infiltrated throughout the tissue. This differential immune profile was also accompanied with a distinct pattern of sensory and sympathetic innervation. Importantly, in AL patients, a lack of sympathetic innervation aseptic interface membranes without compensation mechanisms at cellular levels was observed with simultaneous reorganization of sensorial innervation. Despite the different histopathological portrait, AL and OA patients exhibited similar transcriptional levels of genes encoding key proteins in local immune response. Nevertheless, in both pathologies, TGF-β1 expression was prominent in sites where the inflammation is occurring. However, at systemic level no differences were found.

These findings indicate that AL patients exhibit different local inflammatory response and innervation signatures from OA patients in hip joint. These insights shed the light on neuro-immune interplay in AL and highlight the need to better understand this crosstalk to unravel potential mechanisms for targeted-therapies to improve hip joint lifetime and treatment.

Keywords: osteoarthritis, aseptic loosening, prosthetic debris, immune response, hip innervation

Introduction

Osteoarthritis (OA) has long been considered a cartilage driven “wear and tear” disease that may lead to hip joint failure [1; 2]. The pain and diminished hip joint motion induced by OA may be effectively treated through primary hip replacement [3; 4]. Unfortunately, hip replacement is not a permanent solution as prostheses often fail 15-25 years after primary surgery, mostly due to aseptic loosening (AL), infection and dislocation [5; 6]. Other therapeutic solutions are then urgently required to expand implants’ lifetime.

Inflammation is common to AL and OA [1; 7; 8]. Immune cells and cytokines have been previously reported in both clinical scenarios [8-11]. Synovial inflammation is often observed in OA patients and is frequently characterized by the infiltration of specific immune cell populations, such as macrophages, T cells and mast cells, as well as by the expression of pro-inflammatory cytokines, as Tumor necrosis factor-α (TNF-α) and interleukin-1β (IL-1β) [7]. Nevertheless, these findings were mostly described in studies focusing on the knee or in studies combining data from both knee and hip, without anatomical discrimination [7]. On the other hand, periprosthetic joint inflammation is commonly known as a complex local biological response that takes place on synovial membrane-like interface tissues, triggered by implant released by-products (particles and ions) [12-15]. Of note, the nature, size and amount of released particles are recognized to define the inflammatory profile [13-16]. While polymeric particles such as polyethylene (PE) and polymethylmethacrylate (PMMA) are often associated with macrophage mediated foreign body reaction and tissue fibrosis, high levels of metallic particles and ions have been demonstrated to promote tissue necrosis and lymphocyte-driven responses [17].

Pain is one of the clinical features observed in both AL and OA conditions [18; 19]. Innervation profile is mostly studied in the context of arthritic diseases but not in the presence of implantable biomaterials. Patients and animal studies highlighted innervation of synovial tissues as a possible player in the pain process and, based on anatomical mapping, suggested a coupling of innervation and inflammation in osteoarthritic synovial tissues [20; 21]. It is well documented that both sympathetic, tyrosine-hydroxylase $(TH)^+$ or neuropeptide Y $(NPY)^+$, and sensory nerve fibers, substance P^+ and calcitonin gene related peptide $(CGRP)^+$, are present in OA synovial tissue and grow towards cartilage along blood vessels [21]. On the other hand, so far, two studies addressed the innervation of the interface membranes surrounding AL hip prostheses [19; 22]. Unfortunately, the data is still unclear. Niissalo *et al* reported that the synovial membrane-like interface did not contain C-sensory peptidergic or sympathetic neural structures while Ahmed *et al* identified sympathetic nerve fibers in these interface membranes [19; 22]. Thus, innervation profile and its possible association with periprosthetic joint inflammation, triggered by prosthetic debris in AL scenario, should be revised. Furthermore,

the comparison of the inflammatory versus innervation profiles of AL and OA has never been examined and requires further investigation. In this study, the immune and innervation profiles of AL and OA were addressed dissecting local players at tissue, cellular and molecular levels with potential systemic translation.

Materials and methods

Patients and Samples

Centro Hospitalar São João ethics committee approved this study and all patients consented to the use of their tissue and blood for research purposes. The followed procedures were in accordance with the Helsinki Declaration of 1975, as revised in 2000. Samples from synovial membrane-like interface tissue/aseptic interface membrane were collected from twenty patients during hip revision surgeries due to AL of hip prostheses. All revised hips had a metal-on-polyethylene (MoP) coupling, eleven out twenty cemented and bone defects were classified according to the Paprosky classification [23]. Relevant clinical information is summarized in Table 1. Infection, recurrent dislocation and periprosthetic fracture were considered exclusion criteria in the aseptic loosening group. Osteoarthritic synovial tissues were collected from fifteen patients undergoing primary hip replacement surgeries for primary OA. OA patients were classified for OA severity according Tönnis OA grade [24] and presented scores from moderate (2) to severe (3). The clinical information of these patients is summarized in Table 2. For both OA and AL groups, the same orthopedic team performed the collection of tissue samples. Previously to surgery, blood was collected and leukograms and plain radiographies were registered.

Immediately after excision, both OA synovial tissues and aseptic interface tissues were split. Half of the tissue was immersed in formalin for further histological analysis, while dry ice was used to freeze the remaining tissue until storage at -80ºC. No more than 4 hours elapsed between tissue collection and storage.

Table 1 - Clinical data from aseptic loosening patients

Aseptic Loosening Case Number	Age	Gender	Hip prostheses type	Implant Fixation	Time to Revision (months)	Component Revised	Type of bone defect	Metallosis
1	79	M	MoP	Cemented	13	Acetabular	2B	No
2	61	F	MoP	Cemented	24	Acetabular	2A	No
3	74	F	MoP	Cemented	23	Acetabular	2B	No
4	86	F	MoP	Cemented	46	Acetabular	2B	No
5	50	F	MoP	Uncemented	56	Acetabular	3A	Yes
6	79	F	MoP	Cemented	96	Acetabular	3A	No
7	73	M	MoP	Cemented	108	Acetabular	3A	No
8	69	F	MoP	Cemented	117	Acetabular	2C	No
9	74	M	MoP	Cemented	120	Acetabular	2A	No
10	77	M	MoP	Uncemented	120	Acetabular	2B	No
11	45	F	MoP	Uncemented	129	Acetabular	3A	No
12	73	F	MoP	Uncemented	130	Acetabular	1	Yes
13	63	F	MoP	Cemented	138	Acetabular	3A	No
14	75	M	MoP	Cemented	144	Acetabular	3A	No
15	62	F	MoP	Uncemented	153	Acetabular	2C	No
16	53	F	MoP	Uncemented	156	Acetabular	2A	No
17	86	F	MoP	Cemented	168	Acetabular	2A	No
18	71	F	MoP	Uncemented	204	Acetabular	1	No
19	82	F	MoP	Uncemented	216	Acetabular	1	Yes
20	75	M	MoP	Uncemented	240	Acetabular	1	Yes

Table 2 - Clinical data from osteoarthritis patients.

Osteoarthritis Case Number	Age	Gender	OA severity (Tonnis Classification)
1	79	F	2
2	45	F	3
3	54	F	3
4	80	F	3
5	55	M	3
6	49	F	2
7	76	M	3
8	51	F	2
9	56	F	3
10	71	M	3
11	74	F	3
12	83	M	3
13	37	F	3
14	74	M	3
15	66	M	2

Histochemistry and immunostaining

Half of collected tissues were formaldehyde-fixed paraffin embedded and cross-sections of 3 µm thickness were cut. Contiguous sections were stained with hematoxylin & eosin (H&E) and Masson's trichrome (MT). For immunohistochemistry, tissue sections were deparaffinized and rehydrated before heat induced antigen retrieval (98ºC, 10 mM citrate buffer, pH 6.0). Endogenous peroxidases were blocked using 3% H_2O_2 and non-specific binding sites were blocked using Background Block (Cell Marque, USA), previously to the incubation with antibody diluent 1% BSA (negative control) or with primary antibodies: anti-CD3 (clone PS1, dilution 1:100, Biocare Medical, USA), anti-CD20 (clone L26, dilution 1:100, Cell Marque, USA), anti-CD68 (clone 514H12, dilution 1:100, Novocastra, UK), anti-CD163 (clone MRQ-26, dilution 1:150, Cell Marque, USA), anti-HLA-DR (clone TAL1B5, dilution 1:5000, Abcam, USA) and anti-TGF-β1 (clone TB21, dilution 1:2000, Abcam, USA). After primary antibody incubation, tissue sections were incubated with BrightVision Poly-HRP-Anti Mouse/Rabbit/Rat IgG (Immunologic, the Netherlands) and then revealed using DAB Plus Substrate System (Thermo Scientific, USA), before hematoxylin counterstaining. The specificity of immunostainings of CD20, CD163, CD68, HLA-DR and CD3 was confirmed using human spleen as positive control.

For immunofluorescence studies, tissue sections were deparaffinized and antigen retrieval of rehydrated sections was performed using Proteinase K (0.2 mg/mL in PBS) for NF200 immunostaining and incubated for 20 min at 98ºC in Citrate buffer (pH 6.0), or TE Buffer

(pH 9.0) for Substance P and CGRP staining, respectively. After quenching endogenous fluorescence with 0.1 % sodium borohydride and 100 mM NH_4Cl, sections were incubated with blocking buffer (10 % FBS, 1 % BSA, 0.2 % Triton X-100). Primary antibody rabbit anti-human neurofilament heavy subunit (NF200) (dilution 1:1000, Abcam, USA), anti-Substance P (dilution 1: 1000, Millipore, USA), anti-TH (dilution 1:100, Millipore, USA), anti-CGRP (dilution 1:4000, Sigma-Aldrich, USA) or blocking buffer (negative control) was applied overnight at 4 ºC. For signal detection, tissue sections were incubated with anti-rabbit Alexa Fluor 568 antibody (dilution 1:1000, Life Technologies, USA), incubated with DAPI and then mounted with Fluoroshield Mounting Medium (Abcam, USA). The specificity of immunostainings for NF200, Substance P, TH and CGRP was confirmed using a specimen of human Morton's neuroma as positive control.

Semi-quantitative histopathological evaluation

In order to characterize synovial microenvironment, tissues were semi-quantified considering the total immunoreactive area and scored into four categories: absent (0), present (1), frequent (2) or abundant (3), according to the histological grading system illustrated in the supplementary figures Figure S1 (tissue reaction), Figure S2 (prosthetic debris accumulation) and Figure S3 (immune cells distribution), similarly to the methodology followed by others [25; 26].

Structural changes, fibrosis and necrosis in OA synovial tissues and aseptic interface tissues were evaluated after H&E and MT staining. The thickening/hyperplasia and increased villi of synovial membrane were assessed in OA patients. The accumulation of polymeric, ceramic and metallic particles was assessed in synovial membrane-like interface tissues. A polarized filter was used to detect polymeric particles. Ceramic and metallic particles were studied through Scanning Electron Microscopy (SEM) and their elemental composition assessed by Energy Dispersive Spectroscopy (EDS). Additionally, a phase contrast filter (Ph3) was used with an optical microscope to ease the detection of clusters of ceramic or metallic particles in histological slices, allowing a deep study of the interaction between particles and cells. The infiltration of target immune cell populations, identified by immunohistochemistry, was determined regarding the presence of macrophages ($CD68^+$ cells), T cells ($CD3^+$ cells) and B cells ($CD20^+$ cells). The semi-quantification of polymorphonucleated cells (PMNs) was performed after PMNs identification as these cells have a lobed nucleus while multinucleated giant cells (GC) were detected due to their bigger size, multiples nucleus and $CD68^+$ labeling.

Tissue samples retrieved from five out thirty-five patients (4/15 OA and 1/20 AL) were excluded from histopathological evaluation because they do not correspond to OA synovial tissue or aseptic interface tissue. H&E, MT and immunohistochemistry slices were analyzed

using a light microscope Olympus CX31 while immunofluorescence, polarized light and phase contrast Ph3 images were captured on Carls Zeiss Axiovert 200 inverted microscope.

Gene expression analysis

Synovial tissues were homogenized in liquid nitrogen using a mortar and pestle to preserve RNA integrity. RNA was extracted and purified using TRIzol (Invitrogen, UK) and Direct-zol™ RNA MiniPrep (ZYMO Research, USA), according to the manufacturers' instructions. The amount and quality of extracted RNA were evaluated by Nanodrop ND-1000 (Thermo Fisher Scientific, USA) and running RNA samples in a 2% agarose gel. The transcriptional levels of pro-inflammatory cytokines (TNF-α, IL-1β, IL-6, IL-12a and iNOS), anti-inflammatory cytokine (IL-10), osteoclastic factor (RANKL) and bone remodeling factor (TGF-β1) were evaluated by quantitative real time PCR (qRT-PCR) in PCR iQ™5 system (Bio-rad, USA). All used primers, listed in Table 3, were optimized and melting curves of PCR products were evaluated to guarantee primers specificity. β2 microglobulin (B2M) and β-actin were used as reference genes. Experiments were performed in triplicated. Relative gene expression levels were calculated using the quantification cycle (C_q) method, according to MIQE guidelines [27]. Fourteen out thirty-six cases (5/15 OA and 9/20 aseptic loosening) were excluded from gene expression analysis when average Cq for reference genes was above 26, to avoid bias in the evaluation of genes with later expression.

Table 3 - List of primers used for quantitative qRT-PCR analysis

Gene	GenBank number	Forward primer sequence (5'-3')	Reverse primer sequence (5'-3')
B2M	[NM_004048]	CCAGCGTACTCCAAAGATTCAG	AGTCAACTTCAATGTCGGATGG
β-actin	[NM_001101]	TACCTCATGAAGATCCTCA	TTCGTGGATGCCACAGGAC
IL-1β	[NM_000576]	CTTCAGCCAATCTTCATT	CACTGTAATAAGCCATCAT
IL-6	[NM_000600]	CAATCTGGATTCAATGAGGAGACT	CTGTTCTGGAGGTACTCTAGGTAT
IL-10	[NM_000572]	GGAGAACCTGAAGACCCTCA	TATAGAGTCGCCACCCTGAT
IL-12a	[NM_000882]	TACCAGGTGGAGTTCAAG	GTTCTTCAAGGGAGGATTT
iNOS	[NM_000625]	AATTGAATGAGGAGCAGGTC	TCCTTCTTCGCCTCGTAA
TNF-α	[NM_000594]	TCTCTCTAATCAGCCCTCTG	TGCTACAACATGGGCTACAG
RANKL	[NM_003701]	GGATGGCTCATGGTTAGA	CAAGAGGACAGACTCACTT
TGF-β1	[NM_000660]	CCTGGACACCAACTATTG	CTTGCGGAAGTCAATGTA
Y1R	[NM_000909]	AAGAGGATTGTTCAGTTCA	GATTGGTTTGGTTGTTATAGA
Y2R	[NM_000910]	ACTCTTACCTATACCTTAATG	GTGATTGTGGATACTTGT
Y5R	[NM_006174]	AAGGAAGGGAAAGGGTGTTAC	CGAGTGGCAGCAGTATTATTCT
VMAT2	[NM_003054]	TGCGGGATTCTGCATCATGT	CATCCAAGAGTACCAGGGCG

ELISA

Serum transforming growth factor β1 (TGF-β1) concentrations were measured using Quantikine® ELISA Kit for human TGF-β1 (R&D Systems, USA), according to the manufacturer's protocol. Cytokine concentration was calculated against a standard curve.

Statistical analysis

Statistical analysis was performed using SPSS 21.0 (SPSS Inc. Chicago, IL, USA). The level of significance was set at $p < 0.05$ (*). Visual histogram analysis and Kolmogorov-Smirnov test were used to evaluate the normal distribution of continuous variables (gene expression data, TGF-β1 plasma concentration and percentage of immune cells in blood). Accordingly, these variables were analyzed using Student's t-test or its non-parametric counterpart, Mann-Whitney test. Tissue immune response and innervation was histologically classified in different grading categories and comparisons between aseptic interface tissues and OA synovial were done using Chi-square test. All graphs were prepared using Prism software (GraphPad software, San Diego, CA, USA).

Results

Local immune responses in OA synovial tissues and synovial membrane-like interface tissue

In this study, fifteen patients underwent primary hip replacement due to OA (Figure 1A) and twenty hip implants were revised and their acetabular defects classified by X-ray imaging (Figure 1B). Macroscopically, the collected synovial tissues at primary and revision surgeries were morphologically distinct. Synovial surface was white and with diffuse papillary architecture (dashed black line, Figure 1C and D) whereas synovial membrane-like interface tissues were highly fibrotic (Figure 1E) or with greyish appearance (Figure 1F), in case of metallosis.

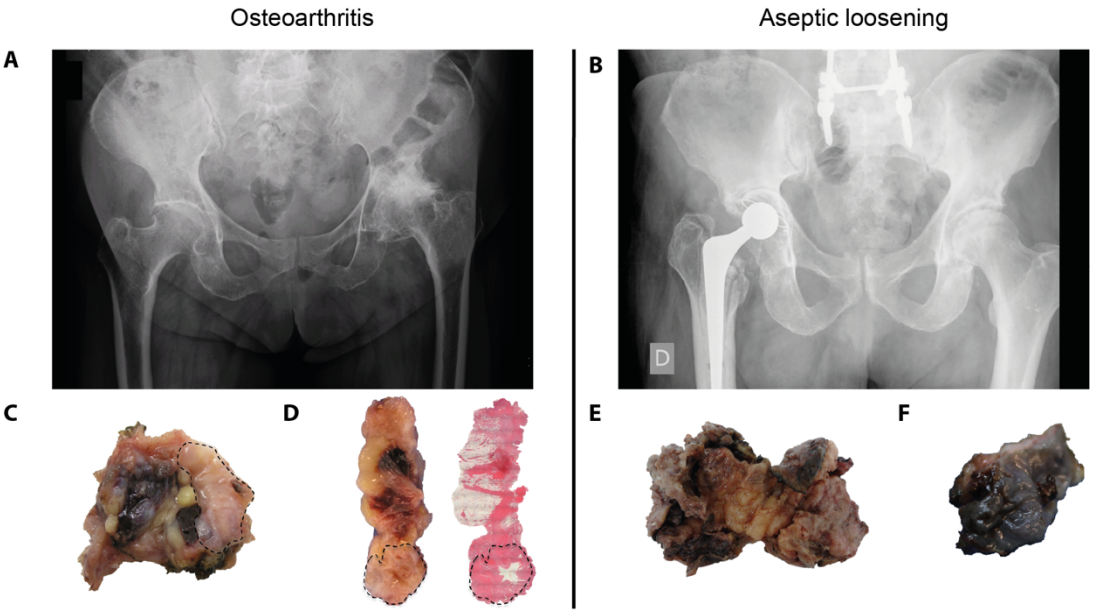

Figure 1 - Radiological and macroscopic tissue features of OA, AL and metallosis. (A) Anteroposterior X-rays showing OA of the hip. **(B)** Failed metal-on-polyethylene total hip joint due to AL. **(C,D)** Macroscopic images of OA synovial tissue collected at primary hip replacement. **(E)** Synovial membrane-like interface tissue retrieved at hip revision surgery due to AL. **(F)** Metallic debris accumulation in synovial membrane-like tissue from AL patient with metallosis.

Semi-quantitative analysis of tissue organization and immune cell distribution in OA synovial tissue and aseptic interface tissues showed distinct local profiles. OA synovial membranes displayed a bicellular lining layer (LL) and a sublining layer (SLL) (Figure 2A) enriched in blood vessels (black arrows) and collagen (Figure 2B), as well as structural changes induced by synovial inflammation, such as synovial hyperplasia (Figure 2C and D) and increased number of villi (Figure 2E and F). OA patients presented at least one sign of synovial inflammation (thickening or villi) but their magnitude was variable among patients

(Figure 2C and E). Synovial membrane-like interface tissues presented fibrotic stroma with increased collagen deposition (Figure 2G and H) than OA synovial tissues (p=0.001) and with some necrotic regions (Figure 2I).

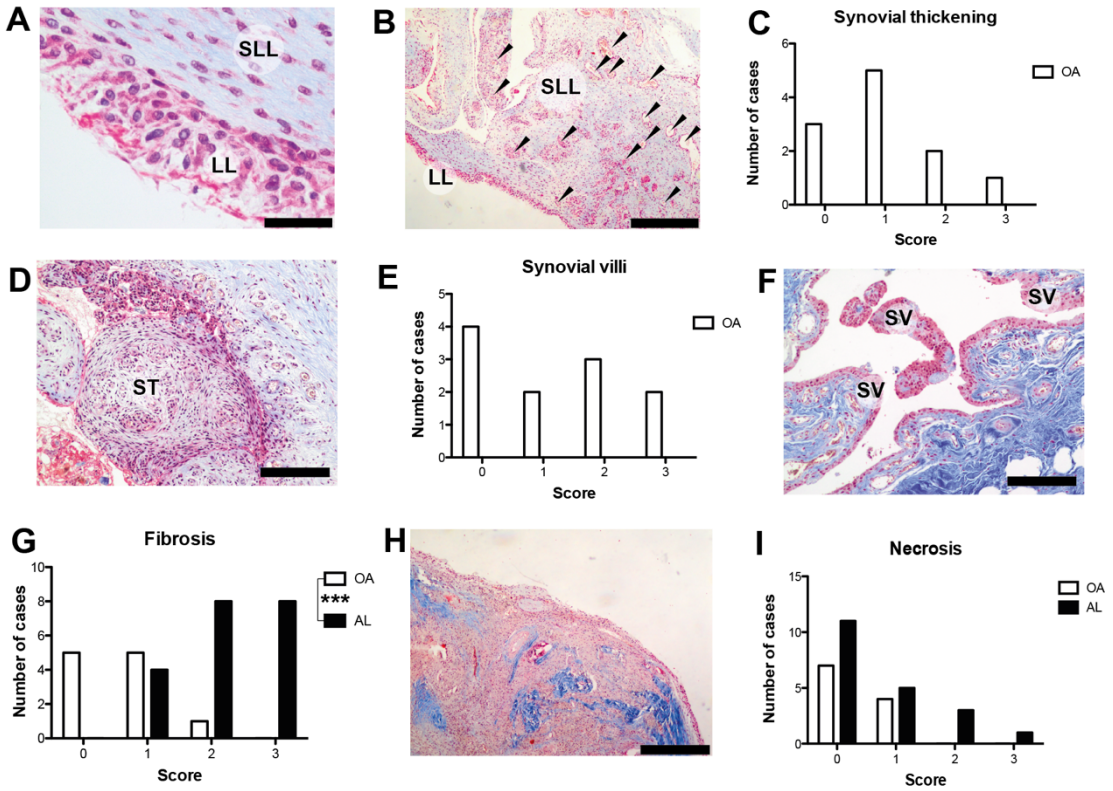

Figure 2 - Histological evaluation of tissues organization. (A) OA synovial tissue is composed by different cell types and matrixes organized in synovial lining layer (LL) and sublining layer (SLL). **(B)** Dense net of blood vessels (black arrows) was found in SLL together with loose connective tissue (blue stain). **(C)** Histological grading for synovial membrane thickening in OA. **(D)** Synovial membrane thickening (ST) with reactive neo vascularization. **(E)** Histological grading for synovial villous expansion in OA. **(F)** OA synovial membrane presenting villous hypertrophy (SV). **(G)** Histological grading for tissue fibrosis. **(H)** Synovial membrane-like interface tissue showing fibrosis characterized by intense deposition of collagen fibers (blue stain). **(I)** Histological grading for tissue necrosis. Masson's trichrome (A,B,D,F,H) staining. Scale bars correspond to 500 µm (B,F,H), 200 µm (D) and 50 µm (A). Semi-quantitative histological evaluation of tissue architecture was performed in specimens retrieved from 11/15 OA and 19/20 AL patients. *** p<0.001. Chi-square test was used to compare OA and AL groups.

The accumulation of prosthetic debris in synovial membrane-like interface tissues was semi-quantified. Polymeric particles were just detected in 11/20 analyzed aseptic interface tissues (Figure 3A) after tissue analysis under polarized light (Figure 3B and C). No significant difference was found between AL patients with cemented and uncemented MoP bearings regarding the amount of polymeric particles entrapped in synovial membrane-like tissues. Zirconia particles (ZrO_2) were observed in almost all synovial membrane-like interface tissues retrieved from patients with loose cemented prostheses (Figure 3D-F) and mainly phagocytized by macrophages or multinucleated giant cells (Figure 3G). Ph3 contrast filter eased the detection of ZrO_2 particles (Figure 3E and F). White color particles under Ph3 filter were confirmed to be ZrO_2 and to be organized in clusters of nanoparticles by SEM/EDS

(Figure 3H and I). Intense deposition of metallic particles was just found in the four cases of metallosis that were patients with uncemented metal-back acetabular cups (Figure 3J). Aseptic interface membranes with metallosis presented high deposition of metallic particles with concomitant macrophage infiltration (Figure 3K), tissue fibrosis (Figure 3L) and necrosis (Figure 3M). Under Ph3 filter, metallic nanoparticles and haemoglobin presented violet and red color respectively, which allow distinguishing them from ZrO_2 particles (Figure 3N and O).

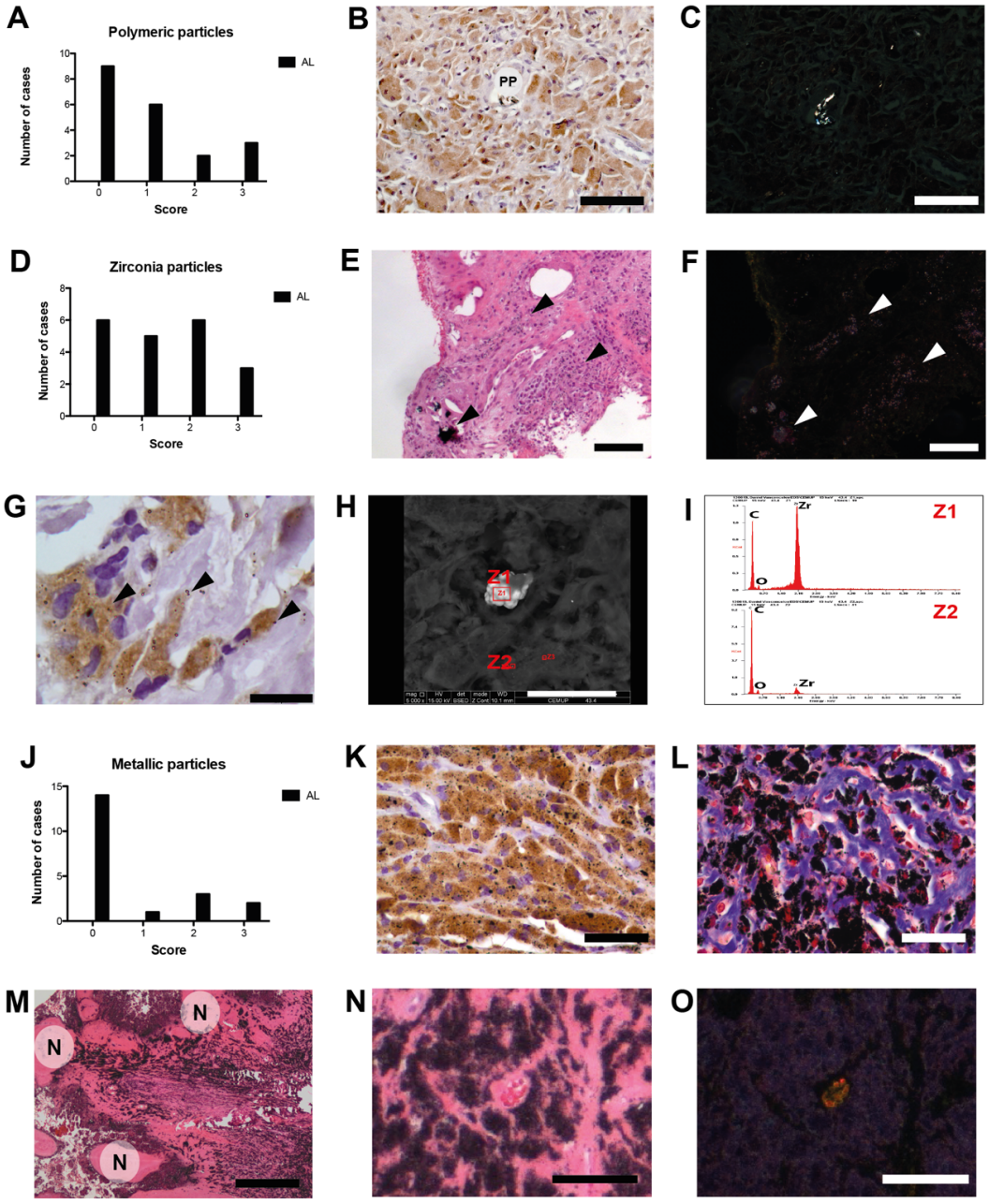

Figure 3 - Prosthetic debris accumulation in synovial membrane-like tissues. (A) Histological grading for accumulation of polymeric particles (PP) in aseptic interface membranes. **(B)** PP surrounded by macrophages (brown cells). **(C)** Same section of (H) under polarized light showing birefringent PP. **(D)** Histological grading for deposition of ZrO_2 particles in synovial membrane-like interface tissues. **(E)** H&E image of aseptic interface membrane with intense deposition of ZrO_2 particles (black arrows) using conventional light microscopy. **(F)** Same tissue region observed using Ph3 filter with white and bright particles corresponding to ZrO_2 debris (white arrows). **(G)** Macrophages (brown cells) phagocytizing ZrO_2 debris (black arrows). **(H)** SEM image of synovial membrane-like interface tissues containing clusters (Z1) and sole (Z2) ZrO_2 nanoparticles. **(I)** EDS analysis confirming the elemental composition of ZrO_2 nanoparticles. **(J)** Histological grading for entrapment of metallic particles in tissues. **(K)** Macrophages (brown cells, CD68+ cells) with phagocytized metallic particles. **(L)** Metallic particles co-localized with macrophages and high deposition of collagen (blue stain). **(M)** Necrosis (N) in regions of aseptic interface membranes with massive accumulation of metallic particles. **(N)** Tissue from an AL patient with metallosis showing metallic particles and erythrocytes. **(O)** Same tissue section shwoing bright metallic particles and erythrocytes but exhibited under Ph3 filter violet and red colors, respectively. H&E staining (E,M,N), polarized light (C), Ph3 filter (F,O), Masson's trichrome (L) immunohistochemistry (B,G,K), SEM imaging (H) and EDS spectra (I). Scale bars correspond to 500 µm (E,M), 50 µm (B,K,L) and 20 µm (G,N,O). Semi-quantitative histological evaluation was performed in tissues retrieved from 19/20 AL patients.

Immune cell distribution was studied in tissues from AL and OA patients. In AL, macrophages ($CD68^+$ cells) were more abundant than in AL ($p=0.007$; Figure 4A), often confined to lining layer in OA patients (Figure 4B), while significant macrophage infiltration was found in synovial membrane-like interface tissues (Figure 4C). In these tissues, co-localization between polymeric particles and macrophages was often found (Figure 4D) and a similar pattern was observed in AL patients with cemented and uncemented MoP bearings. In AL patients, macrophages were the most prevalent immune cell population, even in metallosis cases, and in overall highly express M1 (HLA-DR; Figure 4E) and M2 (CD163; Figure 4F) markers. Multinucleated giant cells in foreign body reaction setting were mostly found in synovial membrane-like interface tissues ($p=0.037$, Figure 4G) surrounding big polymeric particles, likely PMMA, with ZrO_2 particles entrapped inside (Figure 4H). T cells ($CD3^+$ cells) (Figure 4J), and B cells ($CD20^+$ cells; Figure 4L) in lower number, could be detected in the majority of tissues collected from AL and OA patients (Figure 4I and K), including AL patients with uncemented implants or signs of metallosis. Moreover, the number of PMNs was also low in both aseptic interface membranes and OA synovial tissues (Figure 4M and N). Overall, the immune cell populations addressed, namely macrophages, T cells, B cells and PMNs, in this study were most located in the vicinity of synovial membrane in OA patients, while in AL patients these cells were identified throughout the aseptic interface membranes.

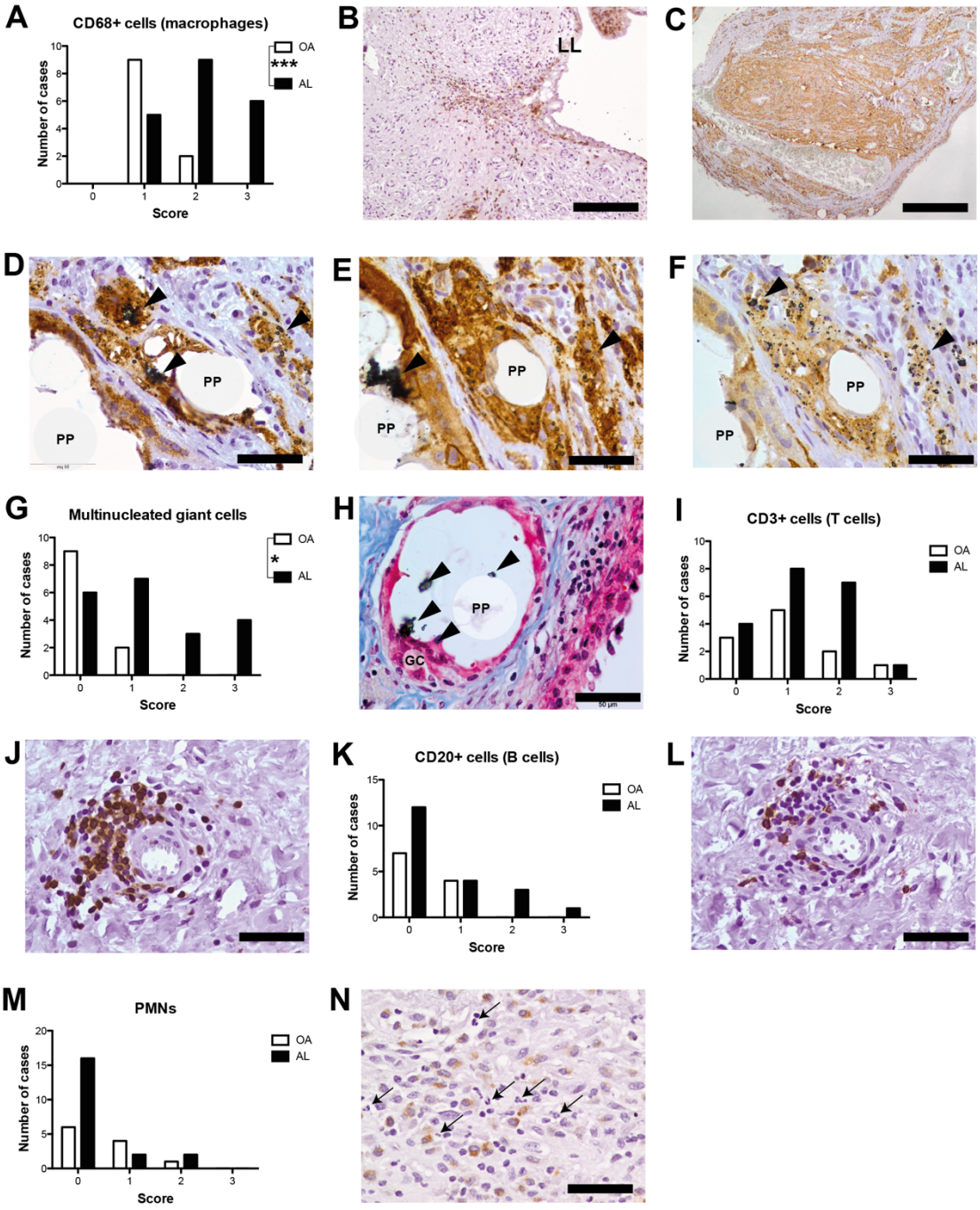

Figure 4 - Immune cells distribution in OA synovial tissues and aseptic interface membranes. (A) Histological grading for macrophage (CD68+ cells) infiltration in tissues. **(B)** In OA, macrophages (brown cells) were almost found at LL. **(C)** Intense macrophage (brown cells) infiltration was detected in synovial membrane-like interface tissues. **(D)** In aseptic interface tissues, macrophages (brown cells) were often found surrounding or phagocytizing prosthetic debris such as polymeric particles (PP) and ZrO_2 particles (black arrows). **(E)** HLA-DR+ cells – an M1 macrophage marker. **(F)** CD163+ cells – an M2 macrophage marker. **(G)** Histological grading for multinucleated giant cells in tissues **(H)** Multinucleated giant cells (GC) phagocyting a big PP particle with ZrO_2 particles (black arrows) entrapped inside. **(I)** Histological grading for T cells (CD3+ cells). **(J)** Perivascular T cells (brown cells) clusters in OA synovial tissue. **(K)** Histological grading for B cells (CD20+ cells). **(L)** B cells (brown cells) in lymphocyte aggregates around blood vessels but in lower number than T cells. **(M)** Histological grading for polymorphonucleated cells (PMNs). **(N)** Increased number of PMNs (black arrows) in synovial membrane-like tissue with macrophages (brown cells, CD68+ cells). Masson's trichrome staining (H) and immunohistochemistry (B,C,D,E,F,J,L,N). Scale bars correspond to 500 µm (B,C) and 50 µm (D,E,F,H,J,L,N). Semi-quantitative histological evaluation was performed in synovial tissues retrieved from 11/15 OA and 19/20 AL patients. * $p<0.05$, *** $p<0.001$. Chi-square test was used to compare OA and AL groups.

Local innervation in AL and OA patients

Myelinated nerve fibers identified by NF200 immunoreactivity were detected in both synovial membrane-like interface tissues and OA synovial tissues. They were presented as single fibers (Figure 5A and C) and were preferentially arranged around blood vessels (Figure 5C) particularly in tissue regions of reactive vascularization induced by immune responses underlying AL and OA. Alternatively, nerve fibers were also found in neurome-like structures (Figure 5B and D) in both AL and OA patients. Sensory and sympathetic innervation, as seen by immunohistochemical markers of sensory nerve-associated peptides (Substance P and CGRP) and catecholaminergic marker of sympathetic neurons (TH), showed different pattern between OA patients and AL patients. TH immunoreactive nerve fibers were observed in OA synovial tissues (Figure 5F) but not in synovial membrane-like interface tissues (Figure 5G and H). Substance P and CGRP were found both in OA synovial tissues and synovial membrane-like interface tissues but showed different pattern. In OA synovial tissues, nerve fibers immunoreactive to Substance P and SGRP were observed mainly around blood vessels in the vicinity of synovial membrane (Figure 5J and N). In addition, a high number of cells in the OA synovial membrane also stained for TH, Substance P and CGRP (Figure 5E, I and M). In synovial membrane-like interface tissues, the expression of Substance P and CGRP was also found in both nerve fibers and cells but with a broad distribution throughout the tissue (Figure 5K, L, O and P).

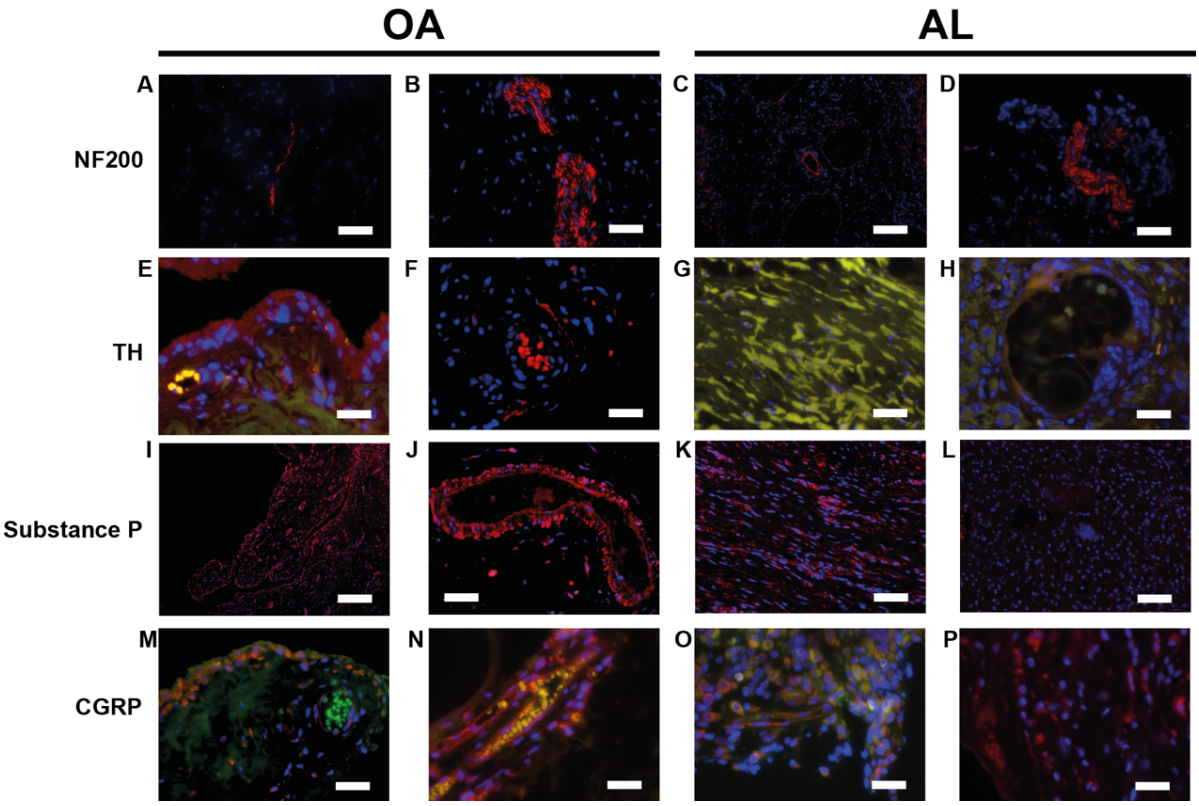

Figure 5 - Local tissue innervation in OA and AL patients. (A-D) NF200+ fibers (red) as sole fiber or organized in neurome-like structures in OA synovial tissues as well as in aseptic interface membranes. **(E)** Synovial cells expressing TH (red). **(F)** TH+ fiber surround a blood vessel. **(G,H)** Nor fibrotic nor reactive tisue with giant cells presented positive labelling for TH. **(I)** Substance P+ cells in OA synovium membrane. **(J)** Substance P+ fibers and cells surrounding a blood vessel located at subintimia of OA synovial tissue. **(K,L)** In AL patients, Substance P+ fibers were just found in fibrotic regions. **(M)** CGRP+ cells in synovial membrane. **(N)** CGRP+ fibers along a blood vessel in OA synovial tissue. **(O,P)** Some cells expressing CGRP in aspetic interface tissue. red=NF200+ or TH+ or Substance P+ or CGRP+, blue=cell nuclei, green=autofluorescence) Scale bars correspond to 50 µm (A,B,D,F,G,H,I,J,K,L,M,N,O,P) and 200 µm (E). 100 µm (C).

Local gene expression profile

The expression levels of pro-inflammatory cytokines tumor necrosis factor-α (TNF-α), interleukin-1β (IL-1β) and IL-6 were similar in aseptic interface tissues and OA synovial tissues (Figure 6A-C). Inducible nitric oxide synthase (iNOS) and IL-12a expression levels were found to be low when compared with the TNF-α, IL-1β and IL-6 mRNA levels detected in AL and OA groups (Figure 6D and E). Interestingly, the anti-inflammatory cytokine IL-10 presented a tendency (p=0.084) to be higher expressed in synovial membrane-like tissues than in OA synovial tissues (Figure 6F). Two genes involved in bone remodeling were evaluated: TGF-β1 and receptor activator of nuclear factor kappa-B ligand (RANKL). The mRNA levels of TGF-β1 were significantly reduced (p=0.038) in aseptic interface tissues when compared to OA synovial tissues (Figure 6G). However, no differences between AL and OA patients were verified for RANKL (Figure 6H) and no correlation was found between mRNA levels of RANKL and the bone defect type.

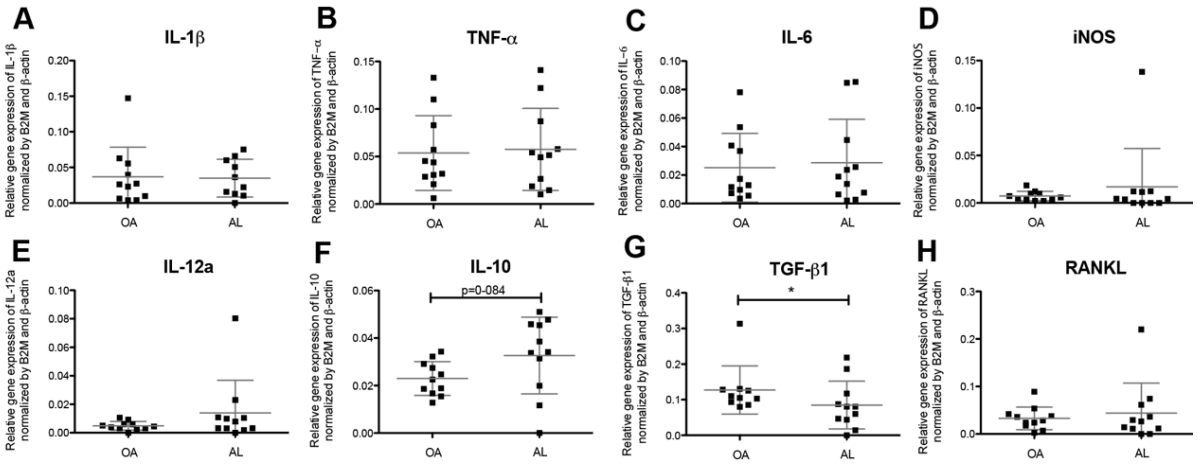

Figure 6 - Gene expression profiles of cytokines in aseptic interface membrane and OA synovial tissues. Relative expression levels of genes of interest determined through qRT-PCR and normalized by two reference genes, β-actin and B2M: **(A)** IL-1β, **(B)** TNF-α, **(C)** IL-6, **(D)** iNOS, **(E)** IL-12a, **(F)** IL-10, **(G)** TGF-β1 and **(H)** RANKL. Data of 10/15 OA patients and 11/20 AL patients are shown. Significant difference of TGF-β1 expression between AL and OA groups (*p < 0.05). Mann-Whitney test was utilized to compare and analyze the obtainded data.

Local production of TGF-β1

In both AL and OA patients, TGF-β1 was detected in blood vessels endothelium cells (Figure 7A), macrophages (Figure 7B) and fibroblasts (Figure 7C). Interestingly, differences in the pattern of TGF-β1 expression were found between AL patients and OA. Aseptic interface tissues presented a trend (p=0.1672) toward increased number of regions expressing TGF-β1 (Figure 7D). In OA synovial tissues, TGF-β1 was present in the sublining layer of synovial membrane (Figure 7E), in aggregates of lymphocytes (Figure 7F) and blood vessels. In synovial membrane-like interface tissues, the distribution of TGF-β1-positive regions was heterogeneous (Figure 7G and H).

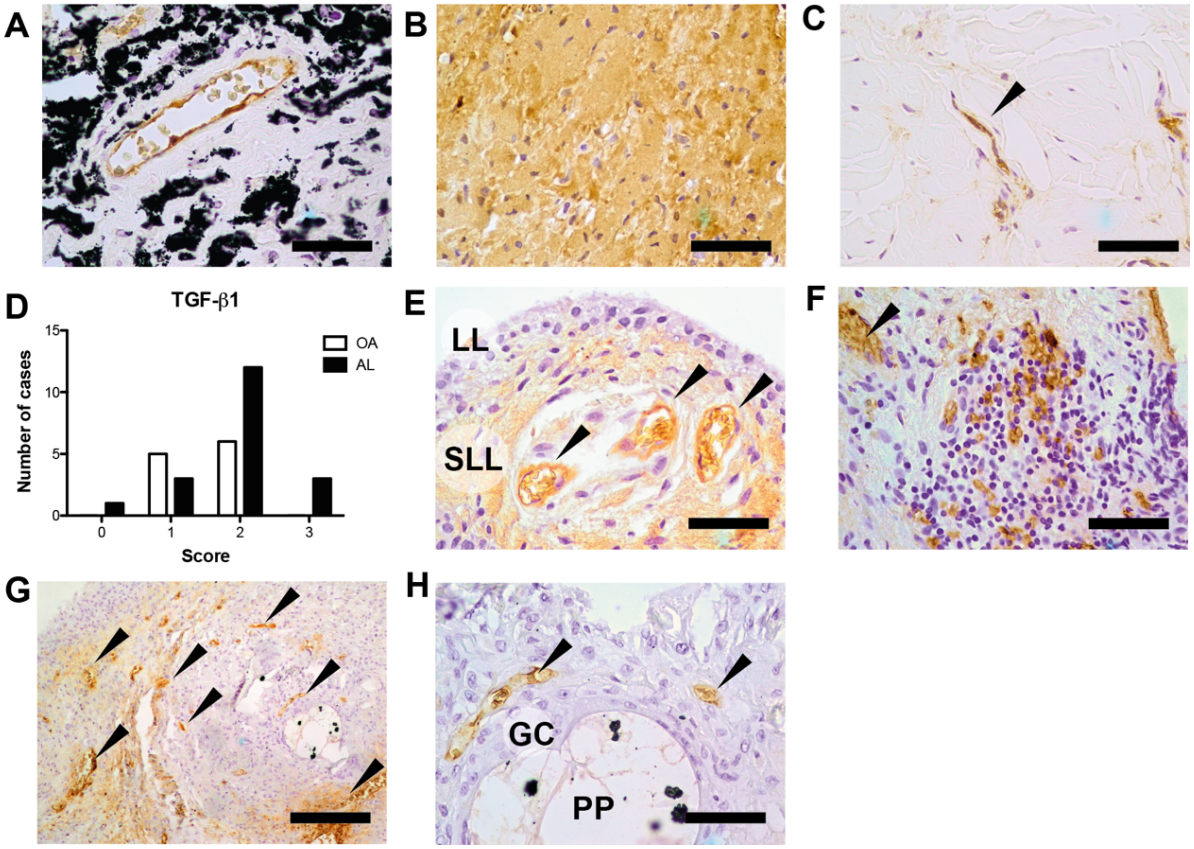

Figure 7 - TGF-β1 expression in synovial membrane-like interface tissues and OA synovial tissues. (A) TGF-β1+ endothelial cells in aseptic interface tissue with metallosis. **(B)** TGF-β1+ macrophages in synovial membrane-like interface tissue. **(C)** TGF-β1+ fibroblast in aseptic interface membrane. **(D)** Number of OA and AL patients classified with score from 0 to 3 regarding the presence of TGF-β1 in tissue. **(E)** OA synovial membrane with positive labelling at sublining layer and endotethelium (black arrows). **(F)** Lymphocyte aggregate in OA synovial tissue with positive cells for TGF-β1. **(G)** Aseptic interface membrane presenting heterogenous TGF-β1 labelling. **(H)** Multinucleated giant cell (GC) phagocyting a polymeric particle (PP) with ZrO_2 particles inside (black clusters) with TGF-β1+ endothelial cells in the vicinity. Scale bars correspond to 500 µm (G) and 50 µm (A,B,C,E,F,H). Data was collected for 11/15 OA patients and for 19/20 AL patients. Chi-square test was used to compare OA and AL groups.

Immune cells proportions and TGF-β1 concentration in blood

The preoperative leukograms were analyzed and the concentration of TGF-β1 determined in plasma of both AL and OA patients. The percentage of circulating monocytes in both groups tended to be similar (Figure 8A). Interestingly, the percentage of lymphocytes seemed to be low in AL patients but within the reference interval in OA group (Figure 8B). Neutrophils did not present significant alterations compared with the reference values (Figure 8C). Remarkably, the levels of TGF-β1 in serum were similar in both groups (Figure 8D).

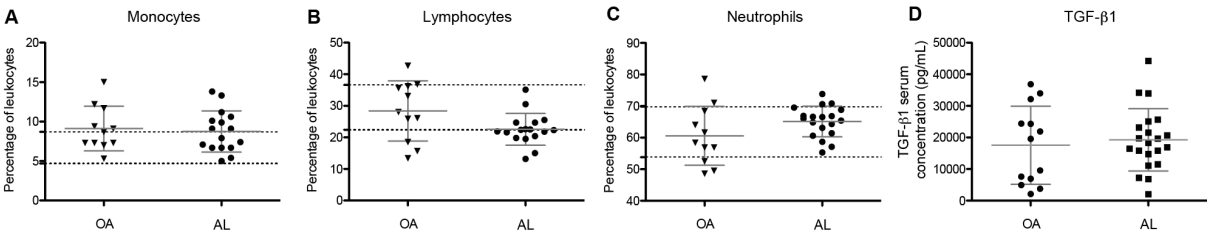

Figure 8 - Pre-operative evaluation of immune populations and TGF-β1 in blood. Data regarding the percentage of the following immune population in leukocytes count. **(A)** Monocytes. **(B)** Lymphocytes. **(C)** Neutrophils. Data was collected for 14/15 OA patients and for 17/20 AL patients. Dashed lines represent minimum and maximum reference values. **(D)** TGF-β1 serum concentration was determined for 13/15 OA patients and for all 20 AL patients.

Discussion

AL and OA differences rely on tissue architecture, immune cell distribution, local TGF-β1 expression as well as sensory and sympathetic synovial innervation. On the other hand, both pathologies share identical mRNA profiles of inflammatory mediators and similar TGF-β1 concentrations in serum, as summarized in Figure 9.

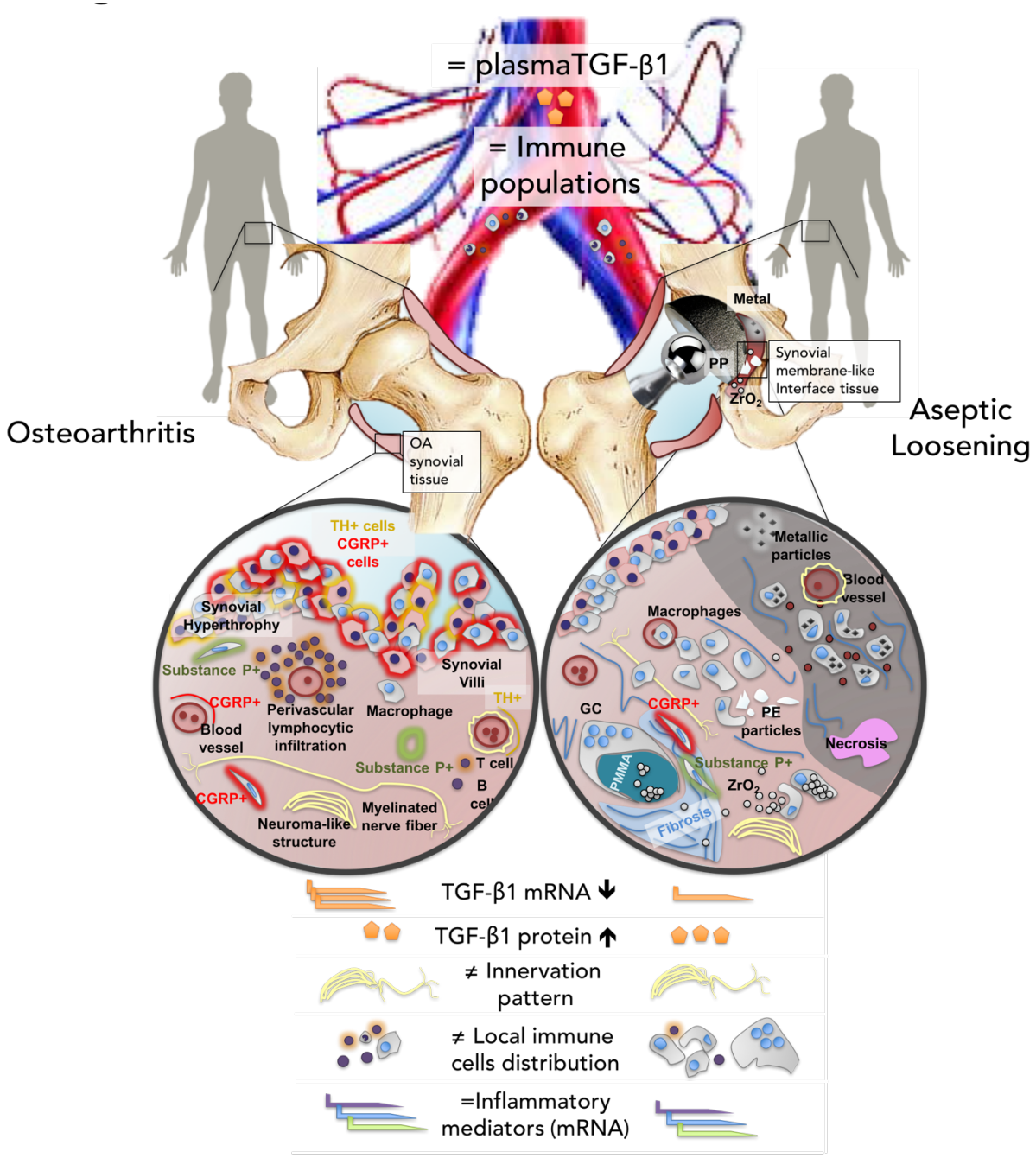

Figure 9 - Overview of hip microenvironment in OA and AL.

Synovial membrane-like interface tissues, present in the vicinity of loose prostheses, showed a macrophage-driven chronic inflammation. This immune response is likely influenced by both OA inflammatory background and the presence of prosthetic debris, leading to significant changes of local TGF-β1 expression but not systemically.

Distinct tissue organization and immune cell distribution were found in the tissues retrieved from the hip joint of AL and OA patients. OA synovial tissues presented signs of synovial inflammation (synovitis), such as synovial hyperplasia and villous hypertrophy, while aseptic interface membranes, formed after primary hip replacement, exhibited a particle-driven chronic inflammation. Intense infiltration of macrophages ($CD68^+$ cells) was observed in AL patients in comparison to OA synovial tissues. In synovial membrane-like interface tissues retrieved from AL patients, macrophages were the predominant immune cell type and were involved in the phagocytosis of small particles (< 10μm) or encapsulating bigger polymeric particles as multinucleated giant cells, in line with previous works about the role of macrophages on AL [28]. Although PE particles, released by MoP prostheses, have been pointed out as AL catalyzers [29; 30], other types of particles may play a role on the pro-inflammatory microenvironment underlying osteolysis. Large amounts of metallic particles were observed in four out nine AL patients due to impingement of metallic components of uncemented MoP bearings.

Ceramic ZrO_2 particles, incorporated in bone cements for implants fixation as radiopacifier agent, were found in synovial membrane-like interface tissues from all the patients with cemented prostheses. Light microscopy with Ph3 contrast filter and SEM/EDS analysis revealed that ZrO_2 gradually migrate from cement particles (PMMA) to other regions of aseptic interface tissues in high number, namely after being phagocytized by macrophages. ZrO_2 particles were shown to be moderately toxic, activate macrophages, promote the expression of pro-inflammatory cytokines (TNF-α) and induce osteolysis *in vivo* [31; 32]. Despite reported not toxic as metallic particles or studied as polymeric debris [12; 33; 34], ZrO_2 particles should not be neglected, as they are numerous, common and nano-sized with potential to unbalance inflammation towards osteolysis. It has been reported that particle-induced response is prone to drive macrophages towards M1 phenotype and that M1:M2 ratio was higher in synovial membrane-like interface tissue than in OA synovial tissues [35; 36]. However, macrophage polarization in joint tissues remains controversial. In this study, the density of polymeric, metallic or ZrO_2 particles on aseptic interface tissues did not lead to local preferential macrophage polarization in M1 pro-inflammatory ($HLA\text{-}DR^+$) or M2 pro-regenerative phenotypes ($CD163^+$) as both receptors were similarly expressed on macrophages. In addition to the involvement of macrophages and lymphocytes in local inflammatory response, preoperative leukograms suggested monocyte expansion and contraction of lymphoid population in AL group.

Cytokines expression profile was found similar in synovial membrane-like interface tissues and OA synovial tissues, despite their distinct tissue architecture and immune cell distribution. The response of macrophages to prosthetic debris is believed to induce the production of the pro-inflammatory markers such as TNF-α, IL-1β, IL-6, IL-12a, and iNOS [28; 34; 37]. However those genes revealed similar mRNA levels in AL and OA patients, which is in line with comparable studies [26; 30; 38]. The changes in cytokine expression induced by AL seem to be controversial [25]. Reduced mRNA levels of IL-6 have also been described in aseptic interface membranes [26] while IL-6 was found significantly increase in synovial fluid of AL patients [25; 30]. A trend for higher mRNA levels of the anti-inflammatory cytokine IL-10 was observed in synovial membrane-like interface tissues in comparison to OA synovial tissues ($p=0.084$). This result corroborates with other findings showing significant increase of IL10 protein levels in synovial fluid and interface tissues of AL patients [25; 26; 30]. The up-regulation of IL-10 in aseptic interface tissues may constitute an attempt to balance the pro-inflammatory microenvironment induced by prosthetic debris [39; 40].

Although RANKL is involved in osteoclastogenesis and osteolysis, similar mRNA levels were found in AL and OA patients, in agreement with other authors [26; 30; 38; 41]. In overall, identical pattern regarding the expression of cytokines was found in AL and OA patients. In the context of AL, no significant differences were registered between polyethylene-drive and metallosis cases as previously shown [42]. The expression of TGF-β1 mRNA in synovial membrane-like interface tissues was found significantly lower than in OA synovial tissues but local TGF-β1 immunostaining suggested increased expression of this protein in AL patients in comparison to OA patients. These findings corroborate the results presented by other authors that have also found increased TGF-β1 mRNA levels in OA cartilage [9; 43; 44] and augmented TGF-β1 expression in synovial membrane-like interface tissues [45]. In both AL and OA, TGF-$\beta1^+$ labeling was prominent in sites where the inflammation is occurring and mostly expressed in macrophages, fibroblasts and endothelium cells. However, while in OA the TGF-$\beta1^+$ cells were found in the region of synovial membrane, in AL, the distribution was more heterogeneous and throughout different tissue regions. These results suggest a possible association between TGF-β1 and the immune responses that underlie AL and OA. Despite a previous report indicates that in OA pathogenesis, TGF-β1 might have a pro-inflammatory effect by inducing fibroblasts to express TNF-α and IL-1β [46], its involvement in inflammatory response is not fully understood. Although the involvement of TGF-β1 in fibrosis is widely described, this growth factor may have dual effects on arthritic diseases [47]. Both immune cells and fibroblasts are part of the complex microenvironments that underlie AL and OA and in which TGF-β1 may have different effects depending on levels of other inflammatory mediators. Additionally, in the context of particle-induced immune response, TGF-β1 has a conjoint role with other factors on bone remodeling [12].

Moreover, previous studies demonstrated that serum TGF-β1 has not predictive value to assess OA incidence and progression [48; 49]. In our study, despite the difference in tissues regarding TGF-β1, AL and OA patients presented similar concentrations of TGF-β1 in serum.

The crosstalk between inflammation and innervation has been widely investigated in several joint-related disorders but not in presence of prostheses [50; 51]. Previous studies have reported sensory and sympathetic innervation in joints diseases namely OA and rheumatoid arthritis (RA), where an inflammatory response is taken place within synovial tissues or in the vicinity of the articulation. Our study demonstrated for the first time distinct pattern of sensory and sympathetic innervation in AL patients characterized by a loss of sympathetic nerve fibers when compared to OA patients. This differential profile has been also described in a comparative study showing lack of sympathetic innervation in RA patients while in OA patients this does not occur [52]. The authors suggested that the reduction or absence of sympathetic innervation might be a consequence of the initial synovial inflammation, probably involving nerve repellent molecules [53], and a key factor to its maintenance in RA. In AL, a sustained chronic inflammatory response is maintained by the presence of prosthetic debris, primarily generated at the bearing surface of hip prostheses. Therefore, our findings, supported by those described in RA, strongly indicate a close correlation between sympathetic innervation pattern and the degree of the inflammatory response. A previous study described the appearance of TH^+ cells in the collagen-induced arthritis in mice and hypothesized that the presence of those cells might be a compensatory mechanism to the deprivation of sympathetic neurotransmitters in the joint [54]. In AL patients, TH^+ catecholamine-producing cells were not detected in the synovial membrane-like interface, suggesting total uncoupling of local joint inflammation from the sympathetic activity (nerve fibers and cells).

Several animal and human studies have addressed the pattern of the sensory innervation in arthritis, namely in OA, and reported a significant re-organization of the sensory nerve fibers characterized by an alteration in the morphology, density and sprouting into areas of the joint that are normally poorly innervated [21]. In this study, we showed that there is also alteration in the sensorial innervation of synovial membrane-like interface tissues in AL patients with a notable distinct tissue distribution when compared to OA. Substance P and CGRP immunoreactive nerve fibers were observed in subintima regions (outer layer) mainly around blood vessels while in AL they were distributed throughout synovial membrane-like interface tissues. Of note, Substance P^+ and $CGRP^+$ cells were also found in these tissues as an additional source of these neuropeptides. Although, Substance P and CGRP are recognized as neuro-inflammatory modulators in arthritic joints, their functional role in the inflammatory response associated to prosthetic debris as well as in the reorganization of sensory and sympathetic nerve fibers in inflamed joint need to be clarified.

We acknowledge certain limitations in this study. To study the differences between AL and OA, thirty-five patients were included in our study, an average number in the field [40]. OA synovial tissues and synovial membrane-like interface tissues were retrieved by the same surgeon to minimize location bias. The histological semi-quantification of accumulation of prosthetic debris in aseptic interface tissues was limited to micro-sized particles, or clusters of nanoparticles, although tissues have been previously evaluated by SEM. Gene expression analysis was successfully performed in eleven out of twenty AL patients due to low RNA quality. Patients' stratification concerning implant fixation and metallosis (AL group) or disease severity (OA group) was performed but no significant effect was identified. On the other hand, the interpretation of the variability between patients may not be just influenced by a specific biological response in joint region but by other factors such as patient's comorbidities (e.g. diabetes mellitus and dyslipidemia), geriatric condition, or genetic susceptibility to AL [16; 55].

Conclusions

Overall this study showed that AL and OA are two joint pathologies characterized by local immune response however with distinct tissue organization and immune cell distribution. This differential immune profile is also accompanied with changes of sensory and sympathetic innervation in hip joint. These findings highlight that the interplay between inflammation and innervation may be joint pathology-specific. Therefore, a deeper and conjoint understanding of these processes will constitute a solid base for targeted-therapies to improve hip joint lifetime and treatment.

Acknowledgments

We thank orthopedic surgeons Dr. Rui Pinto, Dr. Manuel Seara, Dr. Silva Pereira, Dr. Nuno Neves, Dr. Carlos Dopico, Dr. Artur Antunes, Dr. João Duarte Silva and Dra. Mariana Cunha Ferreira and nurses from Serviço de Ortopedia e Traumatologia from Centro Hospitalar de S. João and Dr. Francisco Costa Almeida from Serviço de Ortopedia e Traumatologia from Centro Hospitalar V.N.Gaia/Espinho, for the collaboration in samples retrieve and clinical data analysis. Special thanks to Dra. Daniela Linhares for the help with statistical analysis. We also thank pathology technicians Paula Lopes and Isa Carneiro from IPO-Porto for their support with immunohistochemistry technique. The authors acknowledge to Marta Laranjeiro Pinto and Maria José Oliveira for providing the anti-human HLA-DR antibody used in this study. This work was supported by Portuguese funds through FCT – Fundação para a Ciência e a Tecnologia in the framework of project PTDC/BIM-MED/1047/2012. DP was supported by research grant from project PTDC/BIM-MED/1047/2012. DMV, CJA and ISA were supported by PhD and post-doc fellowships SFRH/BD/87516/2012, SFRH/BPD/63618/2009 and SFRH/BPD/75285/2010, respectively.

Supplementary Information

Published in Journal of Translational Medicine 14:205, 2016

Supplementary information

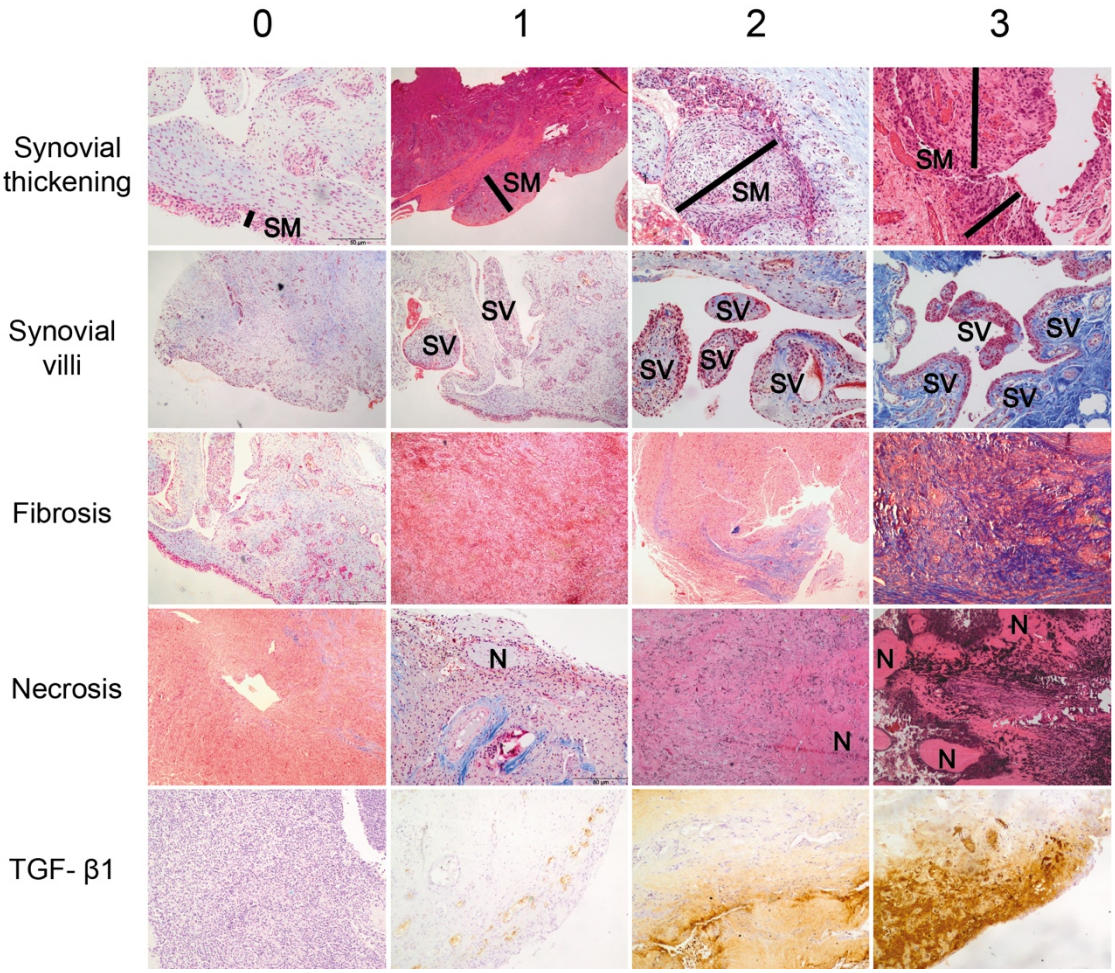

Figure S1 - Histological grading applied in semi-quantification of OA synovial tissues inflammation and tissue fibrosis, necrosis, innervation (NF200) and TGF-β1 in tissues collected from OA and AL patients.

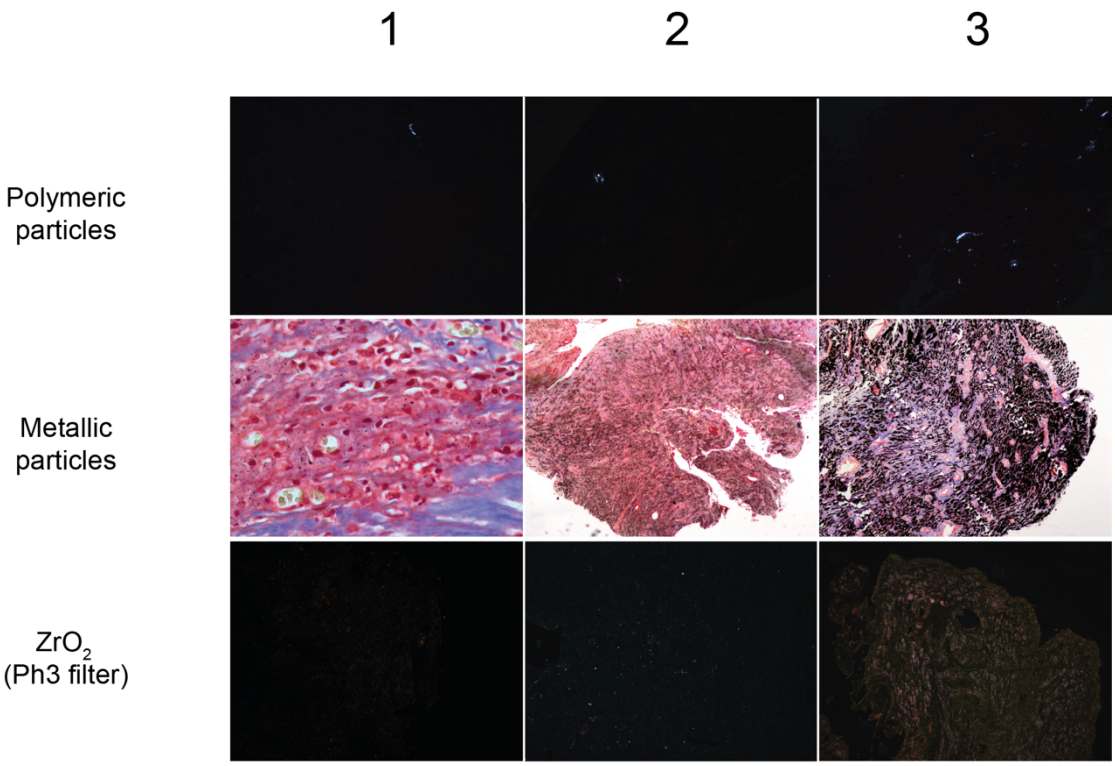

Figure S2 - Histological grading applied in semi-quantification regarding the accumulation of prosthetic debris in synovial membrane-like interface tissues.

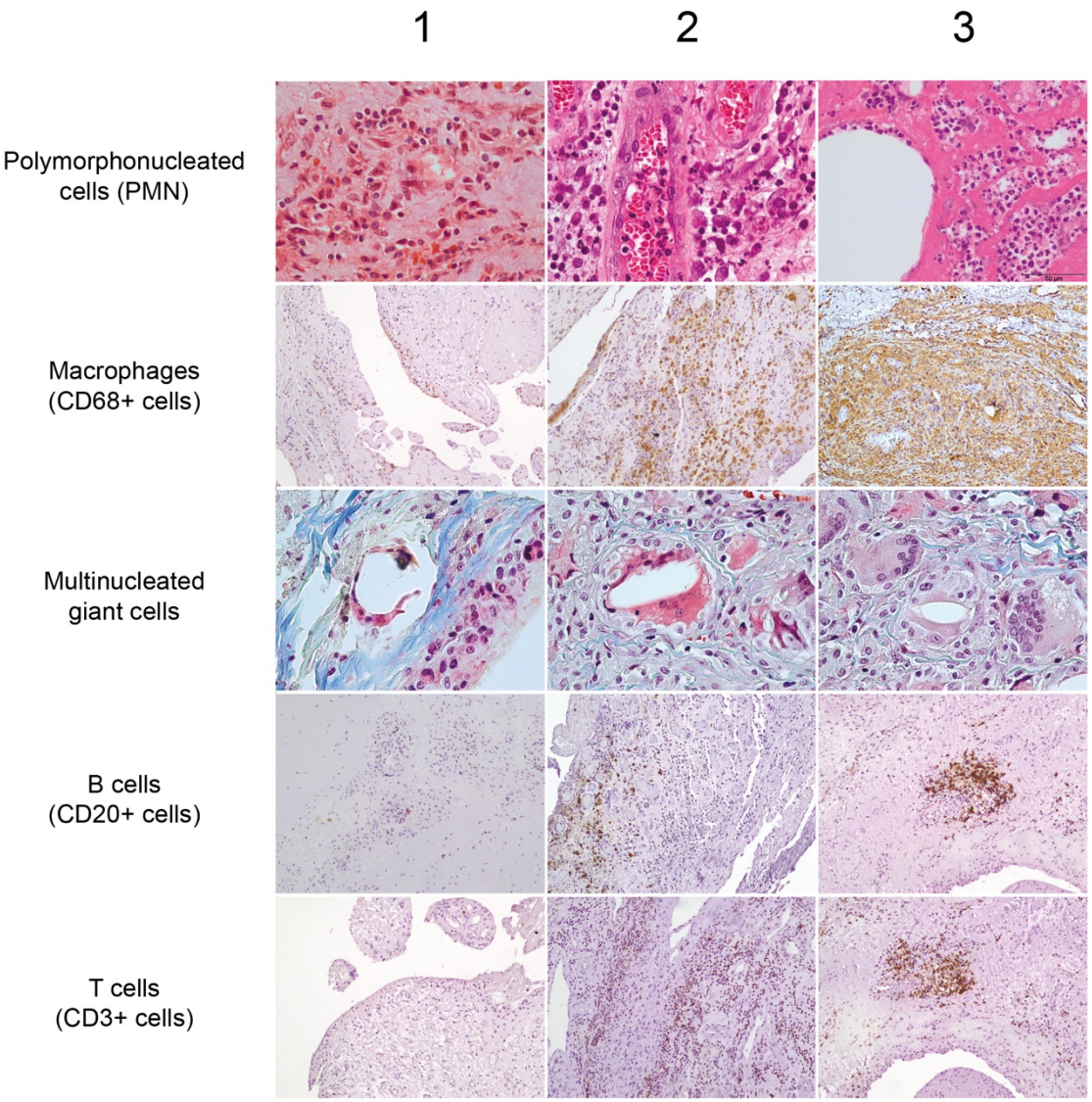

Figure S3 - Histological grading applied in semi-quantification of immune cells prevalence and distribution in tissues retrieved from OA and AL patients

References

[1] - Berenbaum, F. (2013), Osteoarthritis as an inflammatory disease (osteoarthritis is not osteoarthrosis!), Osteoarthritis Cartilage, 21(1), 16-21.

[2] - Glyn-Jones, S., A. J. Palmer, R. Agricola, A. J. Price, T. L. Vincent, H. Weinans, and A. J. Carr (2015), Osteoarthritis, Lancet, 386(9991), 376-387.

[3] - Jourdan, C., S. Poiraudeau, S. Descamps, R. Nizard, M. Hamadouche, P. Anract, S. Boisgard, M. Galvin, and P. Ravaud (2012), Comparison of patient and surgeon expectations of total hip arthroplasty, PLoS One, 7(1), e30195.

[4] - Smith, G. H., S. Johnson, J. A. Ballantyne, E. Dunstan, and I. J. Brenkel (2012), Predictors of excellent early outcome after total hip arthroplasty, J Orthop Surg Res, 7(1), 13.

[5] - Ulrich, S. D., et al. (2008), Total hip arthroplasties: what are the reasons for revision?, Int Orthop, 32(5), 597-604.

[6] - Kurtz, S., K. Ong, E. Lau, F. Mowat, and M. Halpern (2007), Projections of primary and revision hip and knee arthroplasty in the United States from 2005 to 2030, J Bone Joint Surg Am, 89(4), 780-785.

[7] - de Lange-Brokaar, B. J., A. Ioan-Facsinay, G. J. van Osch, A. M. Zuurmond, J. Schoones, R. E. Toes, T. W. Huizinga, and M. Kloppenburg (2012), Synovial inflammation, immune cells and their cytokines in osteoarthritis: a review, Osteoarthritis Cartilage, 20(12), 1484-1499.

[8] - Gallo, J., S. B. Goodman, Y. T. Konttinen, M. A. Wimmer, and M. Holinka (2013), Osteolysis around total knee arthroplasty: a review of pathogenetic mechanisms, Acta Biomater, 9(9), 8046-8058.

[9] - Shen, J., S. Li, and D. Chen (2014), TGF-beta signaling and the development of osteoarthritis, Bone Res, 2

[10] - Loria, M. P., et al. (2004), Role of cytokines in gonarthrosis and knee prosthesis aseptic loosening, J Orthop Sci, 9(3), 274-279.

[11] - Martinez-Calatrava, M. J., I. Prieto-Potin, J. A. Roman-Blas, L. Tardio, R. Largo, and G. Herrero-Beaumont (2012), RANKL synthesized by articular chondrocytes contributes to juxta-articular bone loss in chronic arthritis, Arthritis Res Ther, 14(3), R149.

[12] - Gallo, J., S. B. Goodman, Y. T. Konttinen, and M. Raska (2013), Particle disease: biologic mechanisms of periprosthetic osteolysis in total hip arthroplasty, Innate Immun, 19(2), 213-224.

[13] - Papageorgiou, I., V. Shadrick, S. Davis, L. Hails, R. Schins, R. Newson, J. Fisher, E. Ingham, and C. P. Case (2008), Macrophages detoxify the genotoxic and cytotoxic effects of surgical cobalt chrome alloy particles but not quartz particles on human cells in vitro, Mutat Res, 643(1-2), 11-19.

[14] - Germain, M. A., A. Hatton, S. Williams, J. B. Matthews, M. H. Stone, J. Fisher, and E. Ingham (2003), Comparison of the cytotoxicity of clinically relevant cobalt–chromium and alumina ceramic wear particles in vitro, Biomaterials, 24(3), 469-479.

[15] - Gallo, J., M. Slouf, and S. B. Goodman (2010), The relationship of polyethylene wear to particle size, distribution, and number: A possible factor explaining the risk of osteolysis after hip arthroplasty, J Biomed Mater Res B Appl Biomater, 94(1), 171-177.

[16] - Del Buono, A., V. Denaro, and N. Maffulli (2012), Genetic susceptibility to aseptic loosening following total hip arthroplasty: a systematic review, Br Med Bull, 101, 39-55.

[17] - Watters, T. S., D. M. Cardona, K. S. Menon, E. N. Vinson, M. P. Bolognesi, and L. G. Dodd (2010), Aseptic lymphocyte-dominated vasculitis-associated lesion: a clinicopathologic review of an underrecognized cause of prosthetic failure, Am J Clin Pathol, 134(6), 886-893.

[18] - Bijlsma, J. W. J., F. Berenbaum, and F. P. J. G. Lafeber (2011), Osteoarthritis: an update with relevance for clinical practice, Lancet, 377(9783), 2115-2226.

[19] - Niissalo, S., T. F. Li, S. Santavirta, M. Takagi, J. Hietanen, and Y. T. Konttinen (2002), Dense innervation in pseudocapsular tissue compared to aneural interface tissue in loose totally replaced hips, J Rheumatol, 29(4), 796-803.

[20] - Pearle, A. D., C. R. Scanzello, S. George, L. A. Mandl, E. F. DiCarlo, M. Peterson, T. P. Sculco, and M. K. Crow (2007), Elevated high-sensitivity C-reactive protein levels are associated with local inflammatory findings in patients with osteoarthritis, Osteoarthritis Cartilage, 15(5), 516-523.

[21] - Grässel, S. (2014), The role of peripheral nerve fibers and their neurotransmitters in cartilage and bone physiology and pathophysiology, Arthritis Research & Therapy, 16(6).

[22] - Ahmed, M., J. Bergstrom, H. Lundblad, W. J. Gillespie, and A. Kreicbergs (1998), Sensory nerves in the interface membrane of aseptic loose hip prostheses, Journal of Bone and Joint Surgery-British Volume, 80B(1), 151-155.

[23] - Paprosky, W. G., P. G. Perona, and J. M. Lawrence (1994), Acetabular defect classification and surgical reconstruction in revision arthroplasty. A 6-year follow-up evaluation, J Arthroplasty, 9(1), 33-44.

[24] - Tönnis, D. (1987), Dysplasia and Dislocation of the Hip in Children and Adults., Springer, New York.

[25] - Clarke, S. A., R. A. Brooks, J. L. Hobby, J. A. Wimhurst, B. J. Myer, and N. Rushton (2001), Correlation of synovial fluid cytokine levels with histological and clinical parameters of primary and revision total hip and total knee replacements, Acta Orthop Scand, 72(5), 491-498.

[26] - Jamsen, E., V. P. Kouri, J. Olkkonen, A. Cor, S. B. Goodman, Y. T. Konttinen, and J. Pajarinen (2014), Characterization of macrophage polarizing cytokines in the aseptic loosening of total hip replacements, J Orthop Res, 32(9), 1241-1246.

[27] - Bustin, S. A., et al. (2009), The MIQE guidelines: minimum information for publication of quantitative real-time PCR experiments, Clin Chem, 55(4), 611-622.

[28] - Nich, C., et al. (2013), Macrophages-Key cells in the response to wear debris from joint replacements, J Biomed Mater Res A, 101(10), 3033-3045.

[29] - Kobayashi, A., M. A. Freeman, W. Bonfield, Y. Kadoya, T. Yamac, N. Al-Saffar, G. Scott, and P. A. Revell (1997), Number of polyethylene particles and osteolysis in total joint replacements. A quantitative study using a tissue-digestion method, J Bone Joint Surg Br, 79(5), 844-848.

[30] - Wang, C. T., Y. T. Lin, B. L. Chiang, S. S. Lee, and S. M. Hou (2010), Over-expression of receptor activator of nuclear factor-kappaB ligand (RANKL), inflammatory cytokines, and chemokines in periprosthetic osteolysis of loosened total hip arthroplasty, Biomaterials, 31(1), 77-82.

[31] - Obando-Pereda, G. A., L. Fischer, and D. R. Stach-Machado (2014), Titanium and zirconia particle-induced pro-inflammatory gene expression in cultured macrophages and osteolysis, inflammatory hyperalgesia and edema in vivo, Life Sci, 97(2), 96-106.

[32] - Lanone, S., F. Rogerieux, J. Geys, A. Dupont, E. Maillot-Marechal, J. Boczkowski, G. Lacroix, and P. Hoet (2009), Comparative toxicity of 24 manufactured nanoparticles in human alveolar epithelial and macrophage cell lines, Part Fibre Toxicol, 6, 14.

[33] - Lin, T. H., Z. Yao, T. Sato, M. Keeney, C. Li, J. Pajarinen, F. Yang, K. Egashira, and S. B. Goodman (2014), Suppression of wear-particle-induced pro-inflammatory cytokine and chemokine production in macrophages via NF-kappaB decoy oligodeoxynucleotide: a preliminary report, Acta Biomater, 10(8), 3747-3755.

[34] - Hallab, N. J., M. Caicedo, A. Finnegan, and J. J. Jacobs (2008), Th1 type lymphocyte reactivity to metals in patients with total hip arthroplasty, J Orthop Surg Res, 3, 6.

[35] - Goodman, S. B., et al. (2014), Novel biological strategies for treatment of wear particle-induced periprosthetic osteolysis of orthopaedic implants for joint replacement, J R Soc Interface, 11(93), 20130962.

[36] - Lin, T. H., S. Kao, T. Sato, J. Pajarinen, R. Zhang, F. Loi, S. B. Goodman, and Z. Yao (2015), Exposure of polyethylene particles induces interferon-gamma expression in a natural killer T lymphocyte and dendritic cell coculture system in vitro: A preliminary study, J Biomed Mater Res A, 103(1), 71-75.

[37] - Hukkanen, M., S. A. Corbett, J. Batten, Y. T. Konttinen, I. D. McCarthy, J. Maclouf, S. Santavirta, S. P. F. Hughes, and J. M. Polak (1997), Aseptic loosening of total hip replacement: macrophage expression of inducible nitric oxide synthase and cyclo-oxygenase-2, together with peroxynitrite formation, as a possible mechanism for early prosthesis failure, Journal of Bone & Joint Surgery, British Volume, 79-B(3), 467-474.

[38] - Koulouvaris, P., K. Ly, L. B. Ivashkiv, M. P. Bostrom, B. J. Nestor, T. P. Sculco, and P. E. Purdue (2008), Expression profiling reveals alternative macrophage activation and impaired osteogenesis in periprosthetic osteolysis, J Orthop Res, 26(1), 106-116.

[39] - Baer, M., A. Dillner, R. C. Schwartz, C. Sedon, S. Nedospasov, and P. F. Johnson (1998), Tumor necrosis factor alpha transcription in macrophages is attenuated by an autocrine factor that preferentially induces NF-kappaB p50, Mol Cell Biol, 18(10), 5678-5689.

[40] - Gallo, J., J. Vaculova, S. B. Goodman, Y. T. Konttinen, and J. P. Thyssen (2014), Contributions of human tissue analysis to understanding the mechanisms of loosening and osteolysis in total hip replacement, Acta Biomater, 10(6), 2354-2366.

[41] - Koivu, H., Z. Mackiewicz, Y. Takakubo, N. Trokovic, J. Pajarinen, and Y. T. Konttinen (2012), RANKL in the osteolysis of AES total ankle replacement implants, Bone, 51(3), 546-552.

[42] - Dapunt, U., T. Giese, F. Lasitschka, J. Reinders, B. Lehner, J. P. Kretzer, V. Ewerbeck, and G. M. Hansch (2014), On the inflammatory response in metal-on-metal implants, J Transl Med, 12, 74.

[43] - van der Kraan, P. M., E. N. Blaney Davidson, and W. B. van den Berg (2010), A role for age-related changes in TGFbeta signaling in aberrant chondrocyte differentiation and osteoarthritis, Arthritis Res Ther, 12(1), 201.

[44] - Pombo-Suarez, M., M. T. Castano-Oreja, M. Calaza, J. Gomez-Reino, and A. Gonzalez (2009), Differential upregulation of the three transforming growth factor beta isoforms in human osteoarthritic cartilage, Ann Rheum Dis, 68(4), 568-571.

[45] - Konttinen, Y. T., V. Waris, J. W. Xu, W. A. Jiranek, T. Sorsa, I. Virtanen, and S. Santavirta (1997), Transforming growth factor-beta 1 and 2 in the synovial-like interface membrane between implant and bone in loosening of total hip arthroplasty, Journal of Rheumatology, 24(4), 694-701.

[46] - Cheon, H., S. J. Yu, D. H. Yoo, I. J. Chae, G. G. Song, and J. Sohn (2002), Increased expression of pro-inflammatory cytokines and metalloproteinase-1 by TGF-beta1 in synovial fibroblasts from rheumatoid arthritis and normal individuals, Clin Exp Immunol, 127(3), 547-552.

[47] - Pohlers, D., J. Brenmoehl, I. Loffler, C. K. Muller, C. Leipner, S. Schultze-Mosgau, A. Stallmach, R. W. Kinne, and G. Wolf (2009), TGF-beta and fibrosis in different organs - molecular pathway imprints, Biochim Biophys Acta, 1792(8), 746-756.

[48] - Nelson, A. E., F. Fang, X. A. Shi, V. B. Kraus, T. Stabler, J. B. Renner, T. A. Schwartz, C. G. Helmick, and J. M. Jordan (2009), Failure of serum transforming growth factor-beta (TGF-beta1) as a biomarker of radiographic osteoarthritis at the knee and hip: a cross-sectional analysis in the Johnston County Osteoarthritis Project, Osteoarthritis Cartilage, 17(6), 772-776.

[49] - Nelson, A. E., Y. M. Golightly, V. B. Kraus, T. Stabler, J. B. Renner, C. G. Helmick, and J. M. Jordan (2010), Serum transforming growth factor-beta 1 is not a robust biomarker of incident and progressive radiographic osteoarthritis at the hip and knee: the Johnston County Osteoarthritis Project, Osteoarthritis Cartilage, 18(6), 825-829.

[50] - Pongratz, G., and R. H. Straub (2014), The sympathetic nervous response in inflammation, Arthritis Research & Therapy, 16(6), 504.

[51] - Prod'homme, T., M. S. Weber, L. Steinman, and S. S. Zamvil (2006), A neuropeptide in immune-mediated inflammation, Y?, Trends Immunol, 27(4), 164-167.

[52] - Miller, L. E., H. P. Justen, J. Scholmerich, and R. H. Straub (2000), The loss of sympathetic nerve fibers in the synovial tissue of patients with rheumatoid arthritis is accompanied by increased norepinephrine release from synovial macrophages, FASEB J, 14(13), 2097-2107.

[53] - Fassold, A., W. Falk, S. Anders, T. Hirsch, V. M. Mirsky, and R. H. Straub (2009), Soluble neuropilin-2, a nerve repellent receptor, is increased in rheumatoid arthritis synovium and aggravates sympathetic fiber repulsion and arthritis, Arthritis Rheum, 60(10), 2892-2901.

[54] - Capellino, S., K. Weber, M. Gelder, P. Harle, and R. H. Straub (2012), First appearance and location of catecholaminergic cells during experimental arthritis and elimination by chemical sympathectomy, Arthritis Rheum, 64(4), 1110-1118.

[55] - Blaney Davidson, E. N., P. M. van der Kraan, and W. B. van den Berg (2007), TGF-beta and osteoarthritis, Osteoarthritis Cartilage, 15(6), 597-604.

CHAPTER III

Fibrinogen scaffolds with immunomodulatory properties promote *in vivo* bone regeneration

Article 3
Published in Biomaterials 111: 163-178, 2016
doi: 10.1016/j.biomaterials.2016.10.004

Fibrinogen scaffolds with immunomodulatory properties promote *in vivo* bone regeneration

Daniel M. Vasconcelos[1,2,3], Raquel M. Gonçalves[1,2,#], Catarina R. Almeida[1,2,9,#], Inês O. Pereira[2], Marta I.Oliveira[2,4], Nuno Neves[1,2,5], Andreia M. Silva[1,2,3], António C. Ribeiro[2], Carla Cunha[1,2], Ana R. Almeida[1,2,3], Cristina C. Ribeiro[1,2,7], Ana M. Gil[8], Elisabeth Seebach[6], Katharina L. Kynast[6], Wiltrud Richter[6], Meriem Lamghari[1,2], Susana G. Santos[1,2,*] and Mário A. Barbosa[1,2,3,*]

(#)(*) These authors contributed equally to this work

[1] i3S - Instituto de Investigação e Inovação em Saúde, Universidade do Porto, Rua Alfredo Allen, 208, 4200-135 Porto, Portugal

[2] INEB - Instituto de Engenharia Biomédica, Universidade do Porto, Rua Alfredo Allen, 208, 4200-135 Porto, Portugal

[3] ICBAS-Instituto de Ciências Biomédicas Abel Salazar, Universidade do Porto, Rua de Jorge Viterbo Ferreira 228, 4050-313 Porto, Portugal

[4] INL- International Iberian Nanotechnology Laboratory, Braga 4715-330, Portugal.

[5] FMUP-Faculdade de Medicina da Universidade do Porto, Departamento de Cirurgia, Serviço de Ortopedia, Alameda Prof. Hernâni Monteiro, 4200-319 Porto, Portugal

[6] Research Center for Experimental Orthopaedics, Department of Orthopaedics, Trauma Surgery and Paraplegiology, Heidelberg University Hospital, Schlierbacher Landstraße 200a. 69118 Heidelberg, Germany

[7] Instituto Superior de Engenharia do Porto, Instituto Politécnico do Porto, Rua Dr. António Bernardino de Almeida 431, 4249-015 Porto, Portugal

[8] CICECO-Aveiro Institute of Materials, Department of Chemistry, Universidade de Aveiro, Campus Universitário de Santiago, 3810-193 Aveiro, Portugal

[9] Department of Medical Sciences and Institute for Biomedicine – iBiMED, University of Aveiro, 3810-193 Aveiro, Portugal

Abstract

The hypothesis behind this work is that fibrinogen (Fg), classically considered a pro-inflammatory protein, can promote bone repair/regeneration. Injury and biomaterial implantation naturally lead to an inflammatory response, which should be under control, but not necessarily minimized. Herein, porous scaffolds entirely constituted of Fg (Fg-3D) were implanted in a femoral rat bone defect and investigated at two important time points, addressing the bone regenerative process and the local and systemic immune responses, both crucial to elucidate the mechanisms of tissue remodelling. Fg-3D led to early infiltration of granulation tissue (6 days post-implantation), followed by bone defect closure, including periosteum repair (8 weeks post-injury). In the acute inflammatory phase (6 days) local gene expression analysis revealed significant increases of pro-inflammatory cytokines IL-6 and IL-8, when compared with non-operated animals. This correlated with modified proportions of systemic immune cell populations, namely increased T cells and decreased B, NK and NKT lymphocytes and myeloid cell, including the Mac-1+ (CD18+/CD11b+) subpopulation. At 8 weeks, Fg-3D led to decreased plasma levels of IL-1β and increased TGF-β1. Thus, our data supports the hypothesis, establishing a link between bone repair induced by Fg-3D and the immune response. In this sense, Fg-3D scaffolds may be considered immunomodulatory biomaterials.

Keywords: fibrinogen, *in vivo*, bone repair/regeneration, inflammation, biomaterial

Introduction

Upon injury and/or biomaterial implantation there is an inflammatory response, which is required for the regenerative process to begin. This inflammatory response to implantable, and particularly non-degradable biomaterials, can culminate in a foreign body reaction, which is related with the failure to establish a pro-regenerative environment [1]. First generations of materials applied in clinics aimed at restoration of the physical properties of the damaged tissues, while minimizing or even avoiding the immune response. Most of the currently used dental and orthopaedic implants are examples of biomaterials that still follow that strategy [2]. However, in terms of biomedical research the paradigm is shifting from “fighting inflammation” to “modulating inflammation” [3].

Inflammation, repair and remodelling are the three stages that compose bone healing [4]. First, a blood clot forms after bone injury, which provides a temporary matrix for immune cell recruitment to the injury site. Polymorphonuclear leukocytes (PMN) quickly migrate to bone injury and interact with damaged tissue during the first 24 hours. Monocytes/Macrophages and lymphocytes (NK, T and B cells) are attracted to the injury in the next days [5]. Although acute inflammation is described as lasting 4 days and the chronic inflammation to be over in about 2 weeks, immune cells have an active role throughout bone repair and remodelling [4; 5]. In fact, the balance between cytokines, chemokines and immune cell populations in the injury microenvironment is essential for tissue regeneration. This can be impaired by infection or chronic inflammatory conditions, such as autoimmune diseases and the foreign body response against a biomaterial, and when inflammation does not resolve and tissue healing is impaired [4; 6]. In agreement, previous work has shown that successful osteointegration of implants correlates with systemic changes in immune cells [7].

Fibrinogen (Fg) is a blood protein involved in blood clotting. During haemorrhage, a fibrin clot is formed from Fg cleaved by thrombin, which prevents extensive blood loss. The Fg-derived clot is the primordial extracellular matrix (ECM) that supports tissue regeneration, thus providing Fg with pro-healing properties [8; 9]. Two arginine-glycine-aspartate (RGD) motifs were identified in Fg structure [10], which are related with improved cell adhesion to Fg-modified materials [11]. Additionally, Mac-1, an important receptor of activated immune cells, finds numerous binding sites on the Fg molecule [12]. Also, vascular endothelial growth factor (VEGF), an important factor for neovascularization, binds Fg with high affinity [13], what may explain the improved angiogenesis induced by Fg [7; 14].

Clinically, fibrinogen is applied together with thrombin as fibrin hydrogels that are used as biological adhesives [15]. Beyond their well-known haemostatic and sealant properties, alternative applications in tissue engineering have been tested, combining fibrin with ceramics,

cells or other proteins [16-20]. Although the use of thrombin is a standard in fibrin sealants, it increases the risk of thrombosis and life-threatening complications.

The strategy of Fg delivery appears to be of paramount importance to the host response. Soluble Fg does not enhance wound healing [11], instead elicits autoimmunity and nervous tissue damage [21]. The pro-regenerative potential of Fg-incorporating biomaterials has been previously reported by us [7] and others [22]. We have explored the potential of adsorbed Fg to modulate immune cell responses and induce regeneration. Materials modified with Fg led to increased recruitment of mesenchymal stem/stromal cells (MSC) mediated by different immune cells [23], downregulation of pro-inflammatory molecules and up-regulation of bone and angiogenic factors secreted by macrophages [24]. The degradation of chitosan films by osteoclasts was also accelerated by Fg adsorption [25]. Most importantly, our previous work showed that implantation of Fg-modified chitosan scaffolds in a femoral critical bone defect led to increased angiogenesis and new bone formation at the defect periphery, together with significant changes in myeloid and B cell populations in the draining lymph nodes [7].

Due to the potential revealed by Fg-modified materials [7; 23; 24], whole-Fg scaffolds (Fg-3D) were here produced to assess the hypothesis that, when stabilized in a 3D porous structure, Fg can promote a pro-regenerative microenvironment, mimicking the blood clot. Fg-3D scaffolds were produced by freeze drying, without addition of any exogenous enzymatic compound, and their capacity to stimulate bone repair was addressed. For that, Fg-3D were extensively characterized by SEM, ATR-FTIR and NMR, their degradation profile, cytotoxicity and endotoxin levels were assessed, following the international standard ISO 10993-5:2009. Fg-3D scaffolds were then implanted in a load-bearing bone defect in the rat femur. Local and systemic immune responses were analysed at two critical time points post-implantation, 6 days and 8 weeks. A combination of flow cytometry and ELISA was used to investigate the systemic response, while qRT-PCR complemented the histological analysis of the local response. Bone repair was also more closely evaluated by micro-CT. By assessing the early and long-term biological response we aim at understanding the impact of Fg-3D on the inflammatory response and subsequent influence on bone tissue repair (Figure 1).

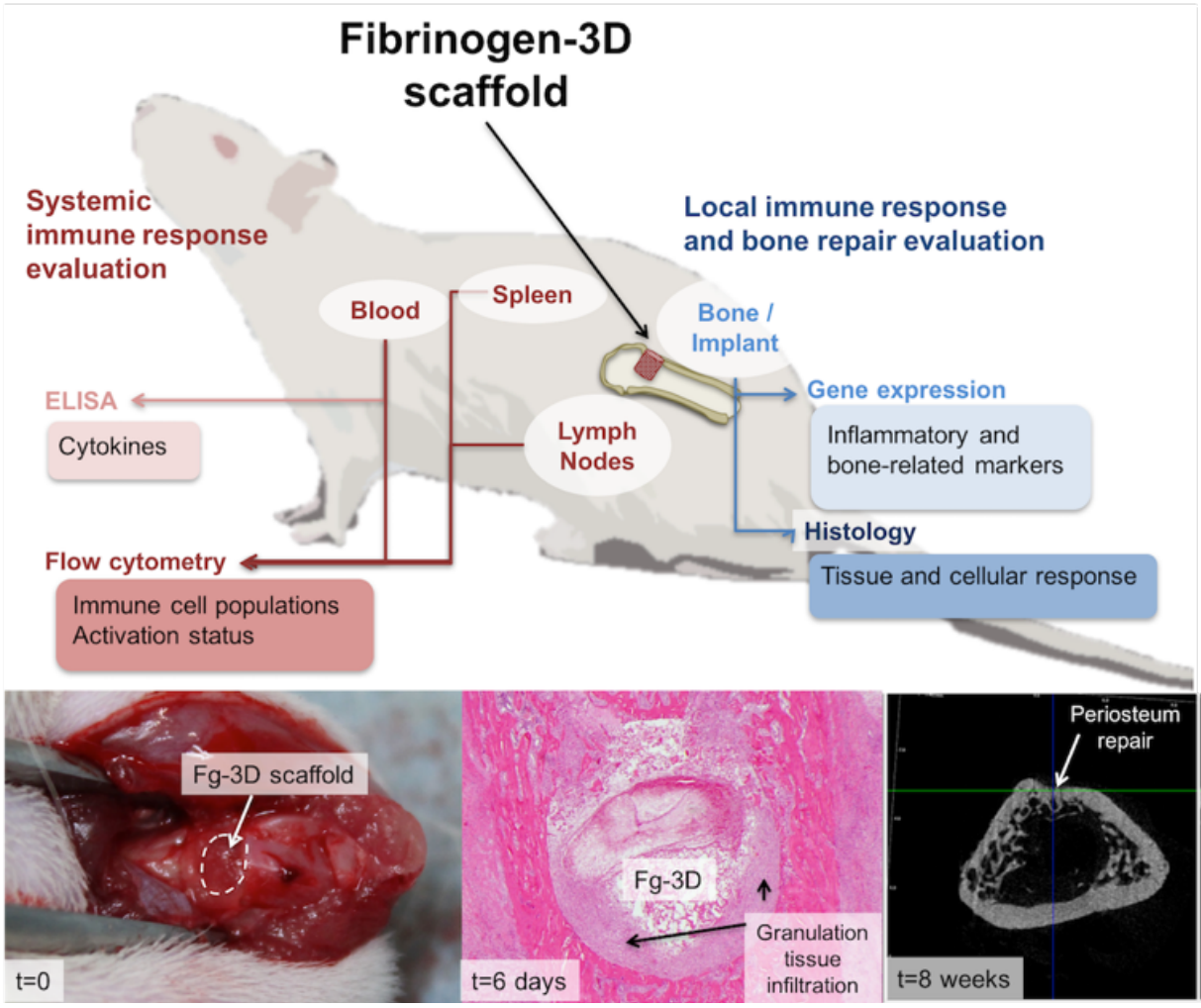

Figure 1. Biomimetic Fg scaffolds (Fg-3D) for immunomodulation and bone repair. Fg-3D were produced by freeze-drying without the use of thrombin and implanted in a femoral bone defect. The biological response induced by Fg-3D scaffolds was evaluated at local and systemic levels. At 6 days post-implantation, the biomaterial promoted a pro-regenerative microenvironment with granulation tissue infiltration and changes in the proportions of immune cell populations in spleen, draining lymph nodes and blood. Interestingly, bone defect, including periosteum, was repaired in the animals with Fg-3D, 8 weeks upon injury.

Materials and methods

Preparation of Fg-3D Scaffolds

Fibrinogen 3D scaffolds (Fg-3D) were prepared by freeze-drying, similarly to chitosan scaffolds previously prepared by our group [7]. A solution of human Fg (fraction I, type III from human plasma; cat. F4129, Sigma), 70 mg/mL, was prepared in Phosphate Buffered Saline Solution (PBS) at neutral pH (7.4). The solution was then casted into 48-well plate (800 µl/well), frozen overnight at -20ºC in a horizontal surface and freeze-dried at -80°C for 48 h to produce scaffolds. These were removed from the plate and cut in the shape of cylinders with 4 mm diameter and 5 mm height. Scaffolds were neutralized and disinfected through impregnation under vacuum in a gradient of ethanol solutions (99.9%, for 10 min, 70% for 30 min, 50% and 25% for 10 min each), followed by three 10 min washes in sterile PBS. Fg-3D scaffolds were maintained overnight in sterile PBS at 4°C protected from light, before further analysis or implantation.

Scanning Electron Microscopy Characterization

Cross-sections of 1 mm thickness were cut and mounted with carbon tape, for scanning electron microscopy (SEM) analysis. Samples were sputter-coated with gold and observed with a JEOL JSM-6301F SEM, at 15 kV and magnifications of 30x or 250x. Twenty-five pores and interconnecting pores were measured in a representative scaffold to determine the range of pore sizes.

ATR-FTIR Spectroscopy

Previously to FTIR analysis, all samples were dried in a vacuum chamber overnight at room temperature. ATR-FTIR spectra of Fg powder, lyophilized Fg scaffolds and after ethanol neutralization (Fg-3D) were obtained using a FTIR spectrophotometer (SpectrumTwo, Perkin Elmer). All samples were submitted to the same pressure and 16 scans were collected with 4 cm^{-1} resolution. Peak analysis was performed through spectra analysis and evaluation of first and second derivatives.

NMR Analysis

The ^{13}C NMR spectra were recorded using a Bruker Avance III (9.4 T) spectrometer operating at 400 MHz for proton and a 4-mm double-bearing magic-angle spinning (MAS) probe. For the ^{13}C cross-polarization and MAS (CP-MAS) NMR experiments, we used 90° pulse lengths of 3–5 μs, a 2 ms contact time, a 5 s recycle delay and a spinning rate of 12 kHz. For the ^{13}C Single Pulse Excitation (SPE) spectra, 90º pulse lengths of 4-5 μs, a 20s recycle delay and a spinning rate of 12 kHz were employed.

Measuring Endotoxin Levels

Extracts were prepared from 35mg of Fg-3D scaffolds in 1.4 ml of endotoxin-free water (40 mL per g of material) by continuous shaking (250 rpm) at 50 ºC for 24 h. Endotoxin levels were assessed using the Food and Drug Administration (FDA, USA) approved Endosafe™-PTS system (Charles River, USA). The analysis was performed and certified by an external entity (Analytical Services Unit, IBET/ITQB, Oeiras, Portugal). Extracts from Fg-3D scaffolds revealed endotoxin levels of 0.132 EU/mL (EU: unit of measurement for endotoxin activity), which are far below the recommended FDA limit (0.500 EU/mL).

Degradation assay

Fg-3D were incubated at 37ºC with distilled water or heat-inactivated fetal bovine serum (FBS) to evaluate hydrolysis and proteolysis at 0.1 mg of scaffold to 1 mL of fluid according to ISO 10993-5:2009 standard. Supernatants were discarded after 6, 24, 48 and 100 h of incubation and remaining scaffolds were freeze-dried and weighted.

Evaluation of cytotoxicity

The cytotoxicity of Fg-3D was assessed using the MC3T3 cell line according to the guidelines presented in ISO 10993-5:2009 standard. In detail, MC3T3 cells were seeded in a 96-well plate at a final density of 10,000 cells per well in supplemented minimum essential medium eagle-alpha modification (α-MEM, with 10% v/v FBS and 1% v/v penicillin/streptomycin) and allowed to adhere for 24 h at 37ºC. Afterwards, the medium was removed and the experimental conditions were set: control (only basal medium), direct contact (in presence of Fg-3D) and four conditions using 100, 75, 50 and 25% of Fg extract complemented with α-MEM without FBS. Extracts were produced by incubating Fg-3D in α-

MEM at 100 mg/mL under agitation (100 rpm), for 24 h at 37 ºC. After 24 h the medium and the scaffolds were removed and 300 µL of 10% resazurin solution in basal medium was added. Supernatants were transferred to a black 96-well plate 3 hours after incubation at 37 ºC and fluorescence was read (excitation λ=530 nm, emission λ=590 nm). Experiments were done in triplicate and data were normalized by the control. Conditions that lead to a percentage of metabolic activity bellow 70% of the control were considered cytotoxic.

Animal Model

All animal experiments were conducted following protocols approved by the Ethics Committee of the Portuguese Official Authority on Animal Welfare and Experimentation (DGV). We have used a critical size bone defect model, adapted from the study of Le Guehennec L *et al* [26], and previously used by our team [7]. Briefly, three months old male Wistar rats (n=17 per group, 12 for analysis after 6 days, and 5 after 8 weeks) were operated under general anaesthesia performed by inhalation of isoflurane. The knees were shaved and disinfected. An incision was made in the skin, and both skin and muscle were retracted. After lateral knee arthrotomy, a cylindrical defect with 3 mm diameter and depth of approximately 4 mm was created using a surgical drill in the anterior wall of the lateral condyle of the right femur. Animal care and analgesics (subcutaneous injection of Buprex-buprenorphine, 0.05mg/kg) were provided during post-surgery. Surgery was performed in only one femur per animal and defects either received Fg-3D or remained empty. Non-operated animals were used as control.

Blood, Spleen and Lymph Nodes Collection

The number and type of biological samples collected at 6 days and 8 weeks post-implantation as well as the methods applied in their analysis are summarized in Figure S1. Twelve animals per group were sacrificed 6 days post-injury while five were euthanized at 8 weeks. Unfortunately, three animals from the empty group at 6 days were excluded from the analysis, two due to infection and one due to non-standard defect size. For tissue collection and euthanasia, animals were anesthetized and kept under general anaesthesia by inhalation of isoflurane. Blood was collected by intracardiac puncture and placed in a tube containing heparin solution (B.Braun) at a 1:10 dilution, to avoid blood coagulation. Animals were then dissected and the spleen, as well as the inguinal and popliteal lymph nodes on the side of injury, were collected into a tube with 2mL of RPMI supplemented with 10% FBS to maintain cell viability until processing.

Bone Collection

Immediately after organs collection, the muscle tissue around the defect region was carefully removed and femurs were retrieved. At 6 days, 7 out of 12 femurs per group were prepared for gene expression analysis. Briefly, the femur to be analysed was placed in a Teflon holder and a cylindrical sample including the bone defect with or without Fg-3D and peripheral bone tissue was cut using a 5 mm diameter driller. Bone cylinders were transferred to 1.5 mL tubes and gently swirled in liquid nitrogen until completely frozen. Samples were maintained at -80ºC until RNA extraction. The remaining five femurs were collected for histological analysis at day 6 and 8 weeks upon injury.

Bone Histological Analysis

Femurs were retrieved, fixed, decalcified, dehydrated and defatted before embedding in paraffin, as previously described [7; 27; 28], in five animals per group. Sagittal tissue sections, 3 µm thick, were mounted on pre-coated poly-L-lysine glass slides and dried overnight at 37ºC. Prior to the different staining procedures, the sections were first deparaffinized in xylol (3 x 5 min) and rehydrated through a decreasing ethanol series (2 x 100% ethanol, 96% ethanol, 70% ethanol, 50% ethanol, distilled water, 3 min each). Contiguous sections were stained with haematoxylin & eosin (H&E) and Masson's trichrome (MT) at three depths, and analysed using a light microscope Olympus CX31 for both studied time-points. Images were acquired with Olympus DP 25 camera, using the Cell B software.

The inflammatory response was evaluated at day 6, namely the presence of PMN and the infiltration of granulation tissue in the vicinity of the bone defect. Tartrate resistant acid phosphatase (TRAP) assay (Sigma–Aldrich) was performed according to the manufacturer's instructions. After rehydration, slices were immersed in a staining solution containing water, acetate, naphthol and one capsule of fast garnet GBC salt for 1 h at 37 °C in the dark, and counterstained with acid haematoxylin solution. For alkaline phosphatase (ALP) staining slices were incubated in a Naphtol AS-MX phosphate solution containing the Fast Violet B salt (both from Sigma) for 30 min at 37 ºC.

Micro-Computed Tomography (micro-CT)

New bone formation was evaluated 8 weeks post-injury using a high-resolution micro-CT Sky-Scan 1072 (Skyscan, Belgium) at 3B's Services and Consulting (Caldas das Taipas, Portugal). Images were acquired using a pixel size of 17.58 µm and an exposure time of 8550 ms. The X-ray source was set at 80 kV and 104 µA. Approximately 400 projections were acquired over a rotation range of 180°, with a rotation step of 0.45°. Datasets were reconstructed using standardized cone-beam reconstruction software NRecon® and CTvox® software (SkyScan, Belgium). The amount of calcified tissue was quantified in cylindrical volume of interest (VOI) with 3 mm in diameter and 114 slices in deepness (2 mm). The VOI was centred with the defect region (Figure S2), and bone parameters were quantified using CTan® software (Skyscan, Belgium). Threshold was set at 70 to define calcified tissue. The mean grayscale within the VOI was determined to evaluate bone density. Changes in bone architecture were assessed in the VOI by 3D analysis of bone volume/tissue volume (BV/TV), trabecular number (Tb.N), trabecular thickness (Tb.Th) and trabecular separation (Tb.Sp). Parameters are shown following ASBMR nomenclature [29].

Local qRT-PCR Analysis

Local gene expression of pro-inflammatory cytokines and growth factors at the defect/implant site was analysed in 7 animals for each condition 6 days upon injury. N_2 shock-frozen bone cylinders were pulverized using a micro-dismembrator (B Braun Biotech, Germany) at 3000 rpm for 2 min and total RNA was extracted using Mirvana RNA extraction kit (Invitrogen) immediately after. RNA was quantified by Nanodrop ND-1000 (Thermo Fisher Scientific). cDNA was obtained from 1 µg of total RNA with oligo(dT) primers (Qiagen) using Superscript II kit (Invitrogen) according to manufacturer instructions. All used primers, listed in Supplementary Table 1, were designed using Primer 3 software to be inter-exonic and were obtained from Eurofins Genomics (Ebersberg, Germany). Primer pairs for IL-1β, IL-2, IL-6, IL-8 (MIP-2), IL-10, OC, TNF-α and VEGF evaluation were designed and used previously [18]. Quantitative real time PCR (qRT-PCR) reactions containing 12.5 µL of SYBR Green PCR Mastermix (Thermo), 2 µL of 5 times diluted cDNA template, 0.5 µL of forward and reverse primers (100 pmol/µL) and 9.5 µL of RNAse free water were carried out on a LightCycler 96 (Roche). The reactions were pre-incubated for 10 min at 95 ºC, followed by 40 thermal cycles of amplification (95 ºC for 15 s; 58 ºC for 10 s; 72 ºC for 30 s), ending with a melting cycle 95 ºC for 30 s; 58 ºC for 60 s; 95 ºC for 1 s. Relative gene expression was calculated using the $2^{-\Delta Ct}$ method and normalized using GAPDH as reference gene.

Tissue Processing and Flow Cytometry

Peripheral blood mononuclear cells were isolated from blood by density centrifugation over Lymphoprep (Axis-Shield) at 800g, for 30 min without brake, at room temperature. Plasma was collected, spun to remove cell debris and kept at -80ºC until further analysis. Cells were collected from the interface between plasma and Lymphoprep and washed twice with PBS. Lymph node cells were obtained by placing lymph nodes on top of a 100 μm pore cell strainer and gently crushing with the end of a syringe piston. The strainer was then washed with PBS. To collect cells from the spleen, half of this organ was injected with 100 U/ml Collagenase I (Sigma) and gently crushed with the top of a syringe piston on the top of a 100 μm pore cell strainer. The strainer was then washed with PBS and red blood cells (RBC) were lysed with RBC lysis buffer (10 mM Tris, 150 mM NH_4Cl, pH 7.4) for 8 min at 37ºC. The cells obtained from each tissue were washed with PBS and transferred to 96-well U-bottom plates. Cells were incubated for 5 min on ice with 1 μl per sample of Mouse Anti-Rat CD32 (FcγII Receptor) Monoclonal Antibody (BD), diluted in PBS, 0.5% BSA, 0.01% sodium azide, to prevent unspecific binding to Fc receptors. Cell surface staining for flow cytometry was then performed by incubating for 30 min on ice with the following antibodies diluted in PBS, 0.5% BSA, 0.01% sodium azide: anti-rat CD45R-PE (clone HIS24, 4 μg/mL), anti-rat TCR-PerCP (clone R73, 2 μg/mL), anti-rat CD4-APC (clone OX35, 2μg/mL), anti-rat CD4-V450 (clone OX-35, 4 μg/mL), anti-rat CD8-V450 (clone OX-8, 4 μg/mL), anti-rat CD18-FITC (clone WT.3, 2 μg/mL), anti-rat CD161a-FITC (clone 10/78, 2 μg/mL), anti-rat MHC class II-AlexaFluor 647 (clone OX-6, 2 μg/mL) and anti-rat CD11b/c-PE-Cy7 (clone OX-42, 4 μg/mL), all from BD. Cells were also stained with the corresponding isotype controls. Samples were then washed 4 times in PBS, followed by fixation in paraformaldehyde 4%, 20 min on ice, and washed twice with PBS. Samples were acquired on a Flow Cytometer (FACSCanto, Becton Dickinson) and data was analysed with FlowJo software. Only samples resulting in more than 10,000 gated events were considered for further analysis.

Cytokine Production

For cytokine evaluation, plasma from each animal was assayed by ELISA specific for TNF-α, IL-6, IL-17A and TGF-β1 (Legend Max Rat ELISA kits, BioLegend, CA, USA) and IL-1β (Rat IL-1β Mini ABTS ELISA Development Kit, Peprotech, NJ, USA) according to the manufacturer's protocol. Cytokine concentration was calculated against a standard curve.

Statistical Analysis

Statistical analysis was performed using Prism software. Visual histogram analysis and Kolmogorov-Smirnov test were used to evaluate the normal distribution of the studied variables (all continuous). To compare data from two different groups, Mann-Whitney U test (or its parametric counterpart Student's t-test) were used. When comparing three different groups, Kruskal-Wallis followed by Dunn's Multiple Comparison test (or their parametric counterpart ANOVA) were used. Statistical significance was considered for $p<0.05$ (*) (**: $p<0.01$, ***: $p<0.001$).

Results

To test our hypothesis that fibrinogen (Fg) can promote bone repair/regeneration when stabilized as a 3D structure, Fg-3D scaffolds were produced, characterized and implanted in a rat femoral defect. Bone regeneration/repair was evaluated at 6 days (acute phase of inflammation) and 8 weeks (repair of bone defect) post-injury, together with the local and systemic immune responses.

Production and characterization of Fg-3D scaffolds

Fg scaffolds were produced using freeze-drying methodologies, as previously described for other materials [7]. The influence of the major steps involved in the preparation of Fg-3D (lyophilization and ethanol neutralization) on the protein structure was characterized by ATR-FTIR spectroscopy and solid state ^{13}C NMR spectroscopy (Figure 2).

Fg secondary structures are known to comprise segments in α-helix, β-sheet, β-turn and random coils, which can be evaluated through the IR spectra fingerprint region (1800-1000 cm^{-1}), namely the Amide I (1700-1600 cm^{-1}) and Amide II (1600-1500 cm^{-1}) band regions [30; 31]. ATR-FTIR analysis of Fg powder showed bands at 1644 cm^{-1} (random coil), 1548 cm^{-1} (α-helix), 1532 cm^{-1} (β-sheet), 1516 cm^{-1} (tyrosine side chains), 1398 cm^{-1} (COO^- symmetric stretching band and/or the deformation of CH_2 and CH_3) and 1078 cm^{-1} (C-O stretching modes of glycoprotein in the Fg structure) (Figure 2A*)*. Lyophilized Fg scaffold presented a relative increase of the peak at 1591 cm^{-1} (compression carboxylate side chains of amino acids) and at 1610 cm^{-1} (β-sheet aggregates structure) together with changes in 1235-1270 band region, which are related with the C-N stretching in Amide III region. The spectrum obtained for the neutralized Fg scaffold (Fg-3D) was broadly similar to that obtained for Fg powder. Moreover, the hydration water of Fg was not modified by the production of Fg-3D, as no significant changes of the ratios between Amides and hydrogen bonds (Amide I/3280 cm^{-1} and Amide II/3280 cm^{-1} ratios) were observed. Remarkably, a relevant decrease of intensity of peaks at 1398 cm^{-1} and 1591 cm^{-1} were registered in Fg-3D.

Human Fg is a dimeric glycoprotein composed of three pairs of peptide chains, where all 20 amino acids are present, and the corresponding ^{13}C CP-MAS spectrum showed a typical protein profile (Figure 2B). Some spectral changes were noted between lyophilized Fg scaffolds and Fg-3D. Upon scaffold neutralization, the ^{13}C CP-MAS spectrum revealed a profile with increased resolution, indicating that there is increased molecular organization in the rigid domains of the protein for Fg-3D. Concomitantly, the ^{13}C SPE spectrum also showed better resolved resonances in the neutralized Fg samples, which points towards increased molecular

mobility of the more mobile protein domains. Moreover, a peak clearly observed at 76 ppm in the CP-MAS spectrum of the lyophilized Fg scaffolds, was no longer observed upon neutralization.

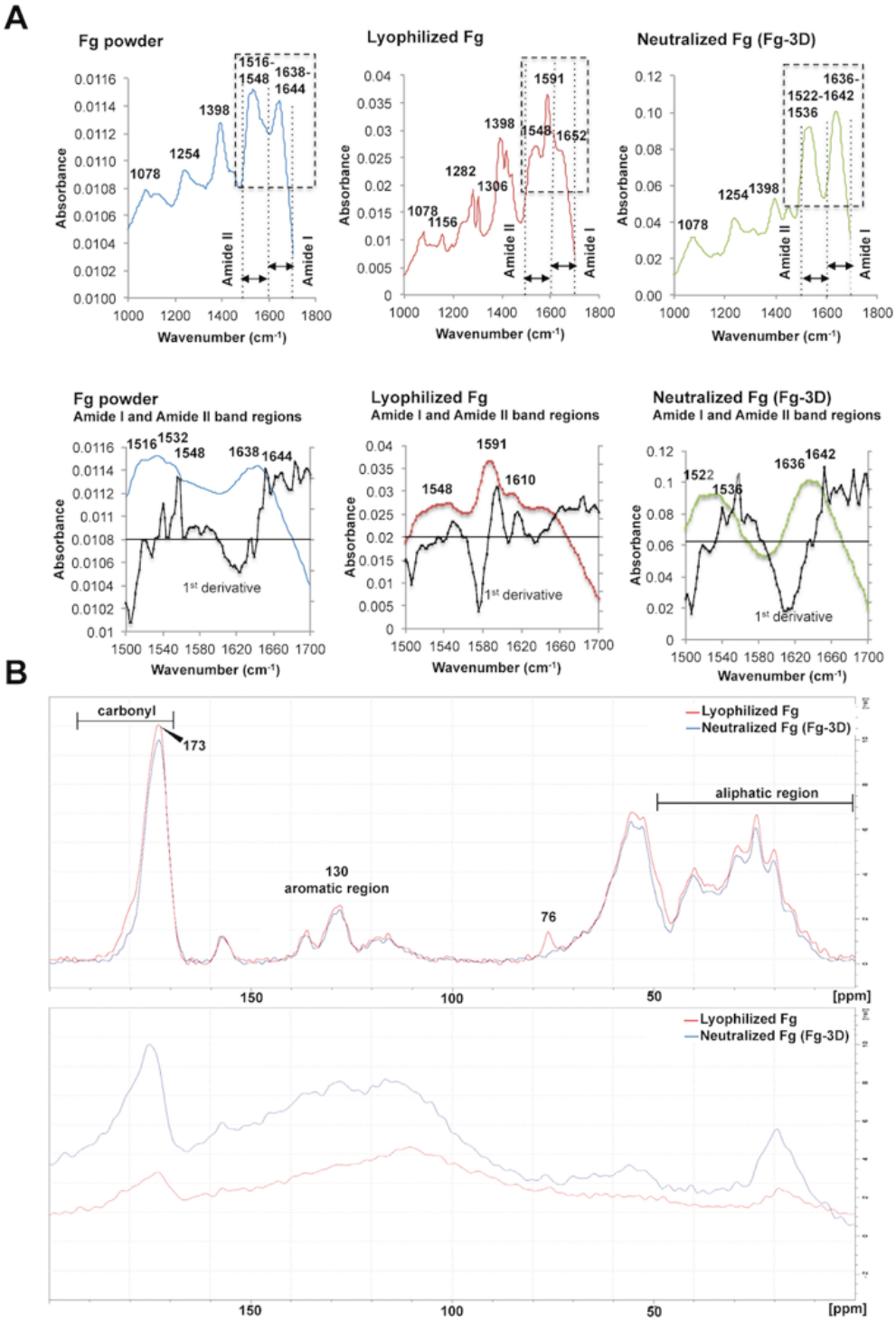

Figure 2. ATR-FTIR and solid-state ^{13}C NMR spectra of Fg at critical stages of scaffolds preparation. (A) Representative ATR-FTIR spectra of Fg powder (blue), lyophilized Fg (red) and ethanol-neutralized Fg (Fg-3D; green) with the most relevant peaks identified and the Amide I and II band regions details presenting first derivate of IR spectra to clarify the determination of the wavenumbers of the peaks. **(B)** ^{13}C solid-state NMR analysis of Fg scaffolds: ^{13}C CP-MAS (top) and SPE (bottom) spectra.

Fg-3D scaffolds have interconnected porosity, are degradable and non-cytotoxic

To determine their structure and porosity, Fg-3D scaffolds were observed using scanning electron microscopy (SEM), and after haematoxylin-eosin (H&E) staining by light microscopy (Figure S3). Overall, Fg scaffolds presented a uniform porous network with macroporosity ranging from 104 to 165 μm in diameter and interconnecting micropores varying in diameter between 17 and 57 μm (Figure 3 A and B).

Then, the susceptibility of Fg-3D to hydrolysis and proteolysis was evaluated through incubation at 37ºC for up to 4 days in water and in serum (FBS) (Figure 3C). Fg-3D showed a fast degradation rate in water (82% of mass loss at 100 h), most of it during the first 6 h (54% of mass loss). In FBS, Fg-3D degraded less (42% of mass loss at 100 h) but exhibited a similar degradation rate during the first 6 h (40% of mass loss) to the one observed in water.

The cytotoxicity of Fg-3D was evaluated following the recommendations in the ISO10993-5 standard. It was estimated by quantifying the metabolic activity of MC3T3 (murine pre-osteoblasts) cells after 24 h in culture with scaffolds (direct contact) or with extracts of Fg-3D, and expressing the results as a percentage relative to tissue culture plastic control conditions. Higher concentrations of Fg-3D extracts (75% and 100%) seemed to cause stress to the cells, but the loss of metabolic activity was less than 30% (Figure 3D). Moreover, cells in direct contact with a scaffold or in media containing 25% or 50% extracts presented a small increase (up to 18%) in their metabolic activity after 24 h of incubation.

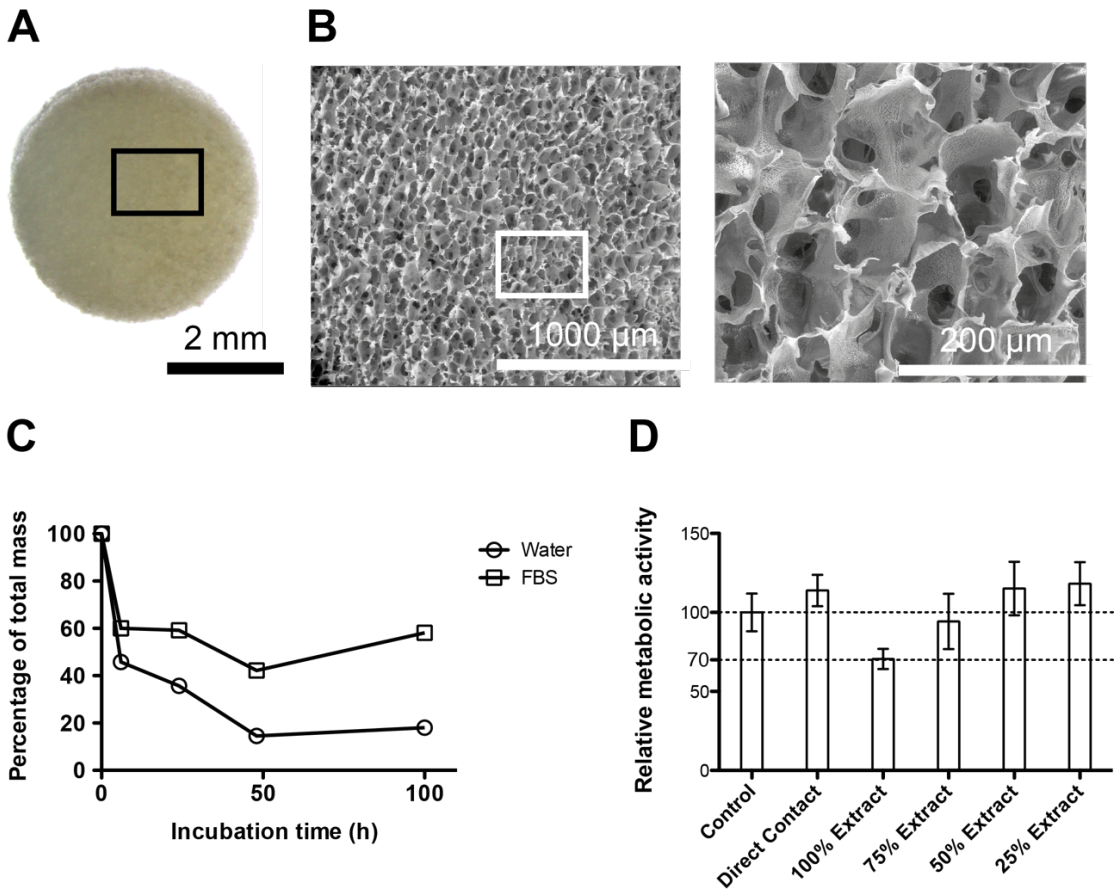

Figure 3. Structure, degradability and cytotoxicity of Fg 3D scaffolds. (A) Macroscopic view of Fg 3D scaffolds (Fg-3D) **(B)** Evaluation of the porous structure of Fg-3D by SEM analysis: general view of Fg-3D showing their porous interconnected structure (left) and high magnification image where large pores (104-165 µm in diameter) and interconnecting pores (17-57 µm in diameter) were visible (right). **(C)** Degradation profiles of Fg-3D during 100 h of incubation in water or serum (FBS). Results presented in percentage of remaining weight according to original weight. **(D)** Metabolic activity of the cell line MC3T3 incubated with Fg scaffolds (Fg-3D) or extracts. Error bars represent the standard deviation (n=3/condition). Kruskal-Wallis test was used to compare the data.

Fg-3D stimulated bone repair/regeneration

The osteogenic potential of Fg-3D was tested *in vivo* using a critical bone defect model in the rat (Figure 4A). The follow up, was performed 6 days and 8 weeks post-implantation. A favourable evolution of the repair process was observed in presence of Fg-3D (Figure 4B). At 6 days post-injury Fg-3D led to an increased number of cells related with granulation tissue (GT) infiltration in the centre of the defect, while few cells and no granulation tissue were detected in the animals where no biomaterial was implanted (empty). The images reveal that acute immune response had already subsided, as PMN were hardly detected in either group. Furthermore, Fg-3D appear well-preserved and in intimate contact with surrounding bone, without visible fibrous capsule. After 8 weeks of implantation new bone tissue had formed filling in the defects and Fg-3D were no longer observable. Moreover, no chronic immune reaction was detectable. Residual granulation tissue was still identifiable in four out of five animals implanted with Fg-3D, particularly closer to the surface of the defect, and surrounded by newly formed bone tissue and bone marrow. The newly formed bone was mostly woven bone, presenting a disorganized structure and enriched in collagen (blue stained fibres). Mature bone was also observed, with a distinctive trabecular organization, oriented along the lines of stress. The new trabecular bone formed in the defect region was functional, since bone mineralization regions, with ALP activity, and bone resorption pits with osteoclasts (TRAP positive cells; Figure 4C) were observed, indicating that bone was going through remodelling. Bone remodelling is a dynamic process, requiring coupling between bone apposition and resorption processes, and Fg-3D seems to control the initial immune response to injury, while supporting bone repair/regeneration.

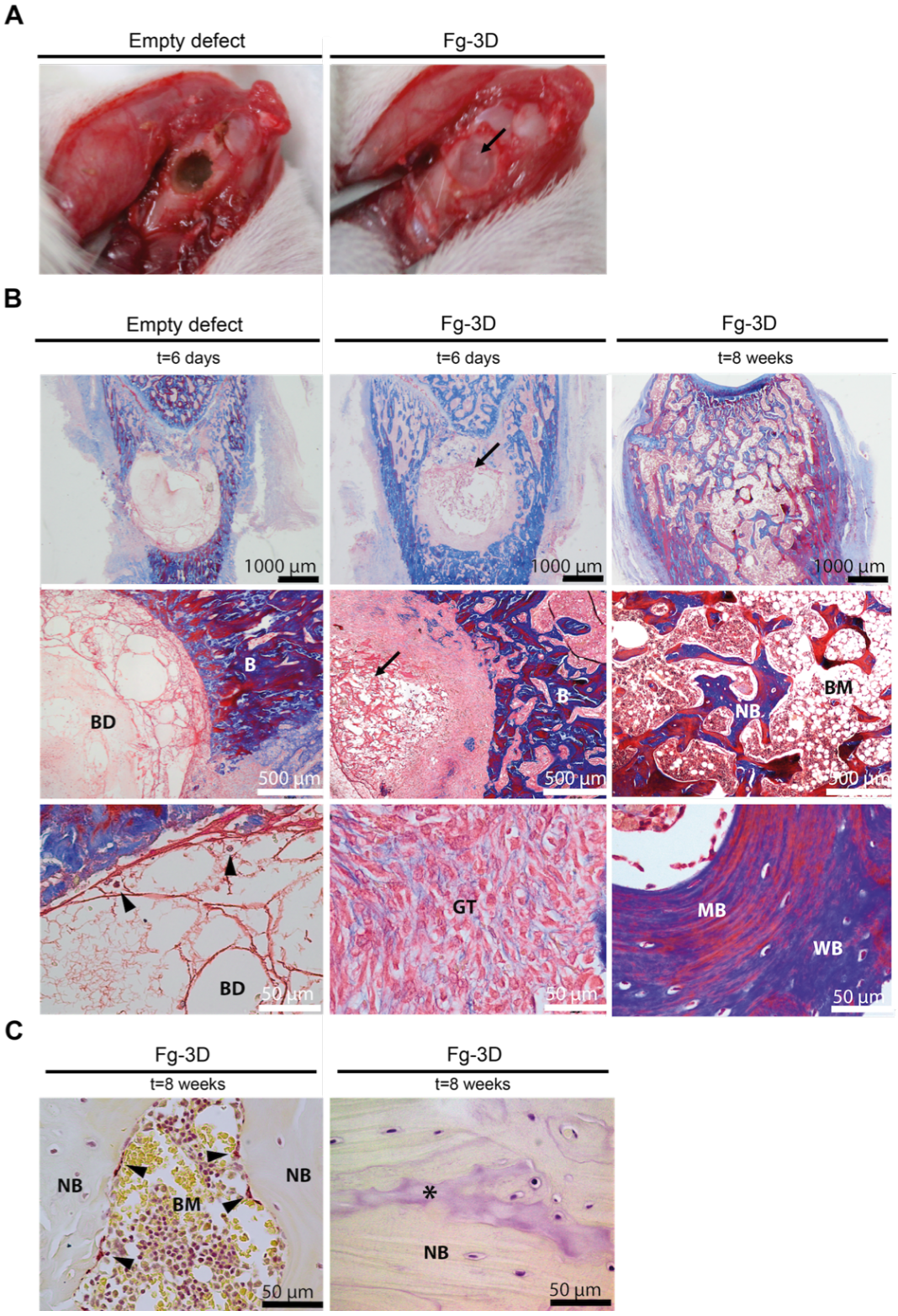

Figure 4. Histological evaluation of bone repair upon Fg-3D scaffolds implantation. (A) Photographs of a bone defect left empty and implanted with Fg-3D (black arrow). **(B)** Histological images of Masson's trichrome stained slices of 6 days empty (left column) and Fg-3D filled (middle column) defects; and 8 weeks Fg-3D implanted (right column) defects. Arrowheads point to PMN. **(C)** Histological view of bone remodelling in progress at 8 weeks with tartrate resistant acid phosphatase (TRAP) positive cells (arrowheads, left image) and alkaline phosphatase (ALP) positive regions (asterisk, right image). B indicates the bone tissue, BD the bone defect area, GT the infiltrating granulation tissue, BM is the bone marrow, NB notes new bone, while WB corresponds to woven and MB to mature bone.

In order to further confirm the new bone formation observed by histological analysis, we performed micro-CT analysis. This corroborated the induction of new bone formation and additionally revealed periosteal repair in femurs implanted with Fg-3D, at 8 weeks post-injury (Figure 5A). In detail, the quantification of calcified tissue in the original defect region (dashed line) revealed that two out of three animals of the Fg group showed higher bone density and bone volume than animals with empty defects (Figure 5B and C). Moreover, all injured animals showed higher trabecular bone separation (Tb.Sp) and trabecular number (Tb.N), when compared to the non-operated animal (Figure 5D and E). Importantly, Fg-3D-treated animals showed a tendency to present a higher trabecular bone thickness (Tb.Th) compared to empty animals ($p=0.1$, Figure 5F), which is likely related to the bone remodelling that is still occurring 8 weeks post-injury. Together, histological analysis and micro-CT evaluation showed that Fg-3D supported bone repair with formation of new and thicker bone trabeculae, which contributed to the closure of the bone defects.

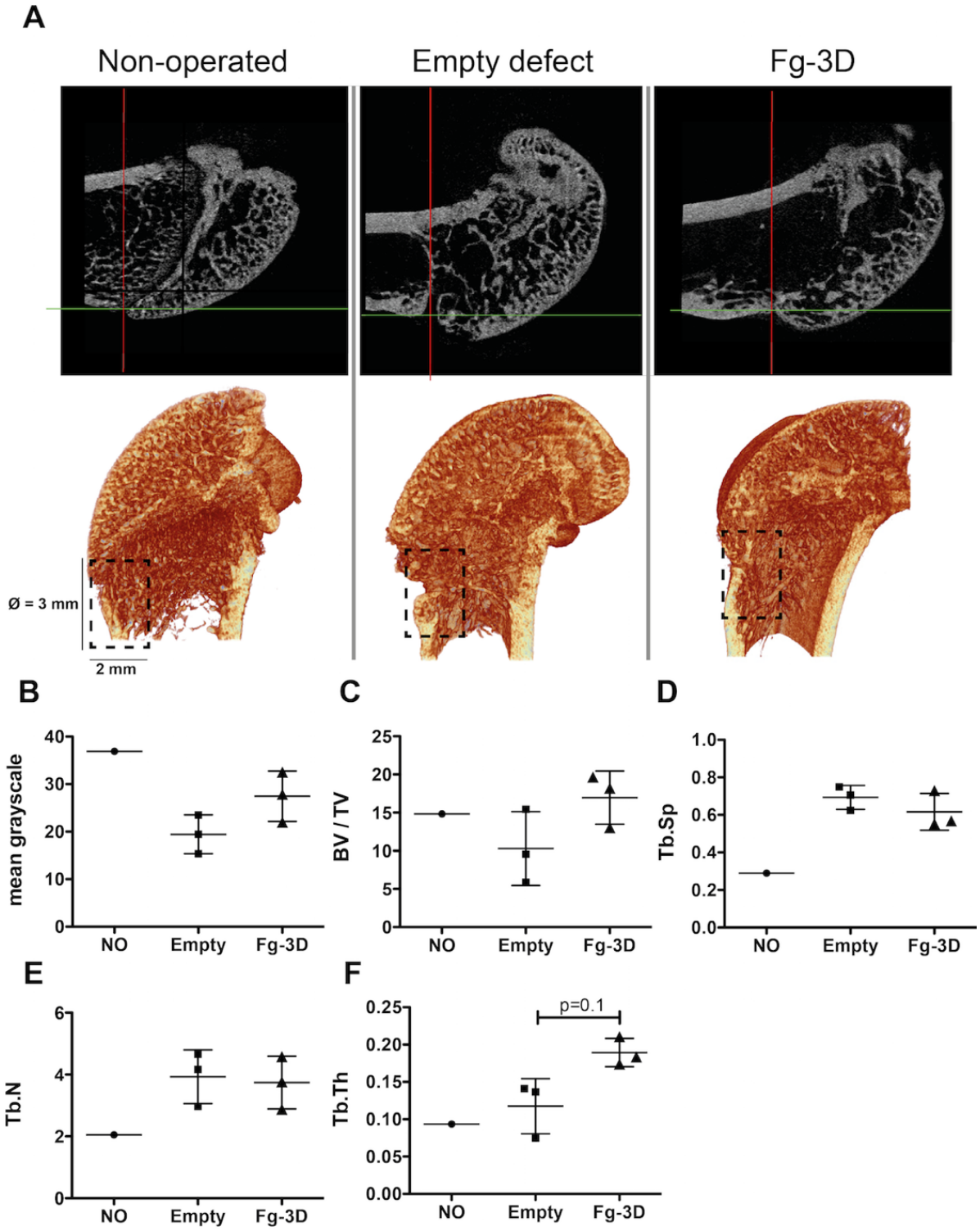

Figure 5. Evaluation of bone regeneration at defect region 8 weeks post-implantation. **(A)** X-ray images and 3D reconstruction of non-operated (n=1), versus injured femurs, left empty (n=3) or implanted with Fg-3D (n=3): sagittal plane X-ray images indicating the centre of the original defect that is pointed at the intersection of green and red lines (top row) and 3D reconstruction of femurs indicating the cylindrical volume of interest (dashed line) with 3 mm in diameter (Ø) and 2 mm in deepness (bottom row), where the following parameters related to bone architecture were quantified. **(B)** mean grayscale in a pixel intensity scale from 0 to 255. **(C)** percentage of bone volume (BV) relative to total tissue volume (TV). **(D)** trabecular bone separation (Tb.Sp) in mm. (*E*) trabecular bone number (Tb.N). (*F*) trabecular bone thickness (Tb.Th) in mm. Data is presented as dot plots, with the mean as a horizontal line and standard deviation as whiskers. Mann Whitney test was used to compare the data.

Fg-3D modulates cytokine production

In order to understand the mechanisms involved in stimulation of bone repair/regeneration induced by Fg-3D, the expression levels of inflammatory and pro-regenerative related genes at the bone defect site were evaluated 6 days after injury. Bone/implant cylinders were cut to include the bone defect with the implant and some of the surrounding tissue and then analysed for gene expression. Regarding inflammatory cytokines, a significant up-regulation of both IL-6 and IL-8 ($p<0.05$), but not of IL-1β, was observed for both empty defects and Fg-3D, in comparison with non-operated animals (NO; Figure 6 A-C). Other cytokines that could be involved in regulation of an immune response, IL-2, IL-4, IL-10, TNF-α and IFN-γ, were not detected. Gene expression of growth factors involved in angiogenesis and bone remodelling was also analysed. Similar levels of osteocalcin (OC) were observed for all tested groups (Figure 6D). A tendency for transforming growth factor beta 1 (TGF-β1) up-regulation in operated animals was registered, though not statistically significant (Figure 6E). On the other hand, VEGF was up-regulated in operated rats whose defect remained empty comparatively to NO animals ($p<0.01$; Figure 6F), but there were no statistically significant differences to the Fg-3D group. This difference in the extent of reactive angiogenesis, that is part of the response to injury, may be explained by the stronger inflammatory response in empty animals, that is dampened in Fg-3D implanted animals.

The systemic concentration of TNF-α, IL-1β, IL-17a, IL-6 and TGF-β1 was evaluated in the plasma, since they are crucial mediators of immune responses and regenerative processes. No detectable levels of TNF-α, IL-17a and IL-6 were found in plasma for any of the animals. Systemic levels of IL-1β (Figure 6G) were significantly decreased for the Fg-3D group at 8 weeks post-implantation, when compared to Fg-3D at 6 days and with a strong tendency to be decreased, when compared to the Empty at 8 weeks ($p=0,0521$) and the NO ($p=0,0600$) groups. Also, systemic levels of TGF-β1 (Figure 6H) were significantly higher for empty-defect animals at 6 days post-injury and for Fg-3D animals at 8 weeks post-implantation, both when compared with NO animals. The time-dependent modulation of TGF- β1 production is likely involved in the wound healing processes, and its sustained increase up to 8 weeks in the animals implanted with Fg-3D may contribute to the regenerative response observed.

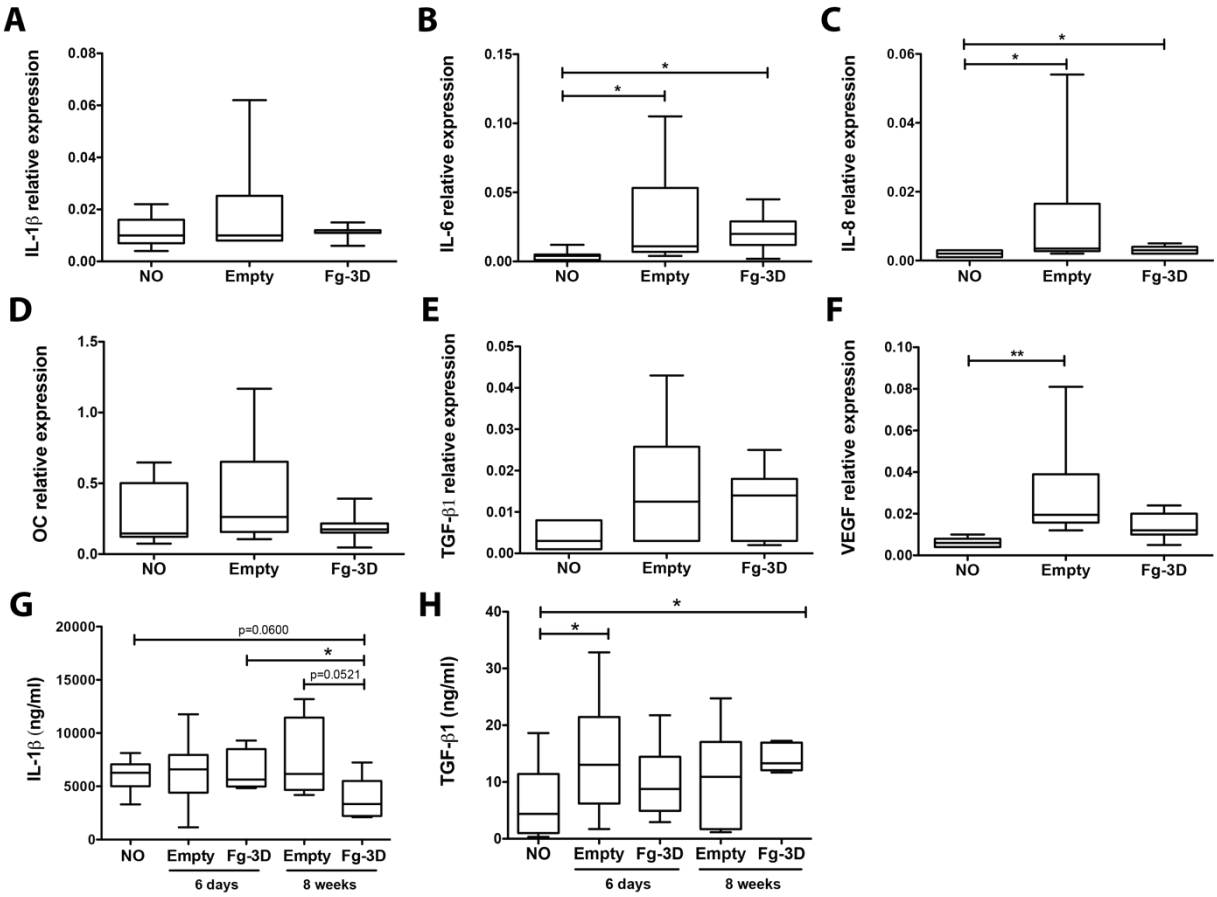

Figure 6. Cytokine levels upon Fg-3D implantation. Local relative mRNA expression levels, normalized by GAPDH expression, were determined for non-operated (NO) animals (n=7), animals with empty defects (Empty; n=6) and Fg-3D implanted animals (n=7) for the following targets: **(A)** IL-1β, **(B)** IL-6, **(C)** IL-8, **(D)** osteocalcin (OC), **(E)** transforming growth factor beta 1 (TGF-β1) and **(F)** vascular endothelial growth factor (VEGF). Systemic concentrations of **(G)** IL-1β and **(H)** TGF-β1 were determined in the plasma of NO, empty and Fg-3D animals at 6 days (n=11/group) and 8 weeks (n=7 empty group, n=5 Fg-3D) post-injury by ELISA. Results are presented as box and whiskers graphs (box represents median and quartiles while whiskers represent min to maximum values); *p < 0.05 and **p < 0.01. Mann Whitney test was used to compare the data.

Implantation of Fg-3D leads to sustained alterations in systemic immune responses

In order to evaluate the impact of Fg-3D on the systemic immune response, blood, spleen and draining lymph nodes were recovered to study the proportions of the different immune cell populations. Representative plots of the flow cytometry analysis illustrating the gates and surface markers used to evaluate the different immune populations are presented in supplementary data (Figure S4).

The proportions of the different immune cell populations were analysed at 6 days post-implantation, in blood (BL), spleen (SP) and lymph nodes (LN) (Figure 7). The response induced by the bone injury itself (empty group), when compared with NO animals was mild, and by comparison, the Fg-3D implanted group showed some significant differences to NO and in some cases also to empty animals. In BL and SP, empty and Fg-3D groups followed the same tendency for the most abundant subsets, increased T cells and decreased B cells (Figure 7A). While in BL the reduction is also significant for NK, NKT and myeloid cells, particularly for Fg-3D implanted animals, in SP these populations do not show significant differences (Figure 7A and B). On the other hand, in draining LN the response of empty and Fg-3D groups was in opposite directions, at least for the most abundant T and B cell populations. Empty defects led to increased B cells and decreased T cells, while the Fg-3D implanted group remained closer to NO and significantly different from empty in the B cells. Additionally, the percentage of T cells with downregulated TCR (TCR^{dim}), which can be correlated with T cell activation, was lower in the SP of animals with Fg-3D, when compared with NO animals. The proportions of CD4+ T cells and CD8+ T cells were similar between different groups in BL, LN and SP.

We then examined the cells expressing Mac-1 ($CD11b/c^{+}/CD18^{+}$), the receptor for Fg [12; 32], and found that Mac-1 expression was significantly decreased in the BL, LN and SP of animals implanted with Fg-3D, in comparison with animals with an empty defect (Figure 7C). CD4 and CD8 co-receptors are reported to enhance FcR responses in myeloid cells [33], so we analysed if myeloid cell decrease preferentially occurred within CD4 or CD8 positive populations. The results obtained indicate that implantation of Fg-3D led to a reduction in the percentages of $CD4^{+}$ cells amongst $CD11b/c^{+}$ cells in all assessed tissues from animals with Fg-3D when compared with animals with empty defect (Figure 7B). A significant decrease of the percentage of $CD8^{+}$ cells, within the $CD11b/c^{+}$ population, in animals of the Fg-group, was also found, but only in SP.

Furthermore, the percentage of positive cells for MHC class II (MHC-II), a molecule expressed mainly on the surface of antigen presenting cells, was also analysed (Figure 7C). Fg-implanted animals presented lower percentages of $MHC\text{-}II^{+}CD11b/c^{+}$ cells, in BL, LN and

SP in comparison with NO group. In addition, the percentage of MHC-II$^+$ cells within CD11b/c$^+$ cells showed also a tendency to decrease in empty and Fg-3D groups when compared to NO animals, but differences were only statistically significant in the BL, when comparing Fg-3D with NO groups. Overall, these results clearly show that implantation of Fg-3D impacts the host response at systemic level, involving different immune cell populations and their activation status.

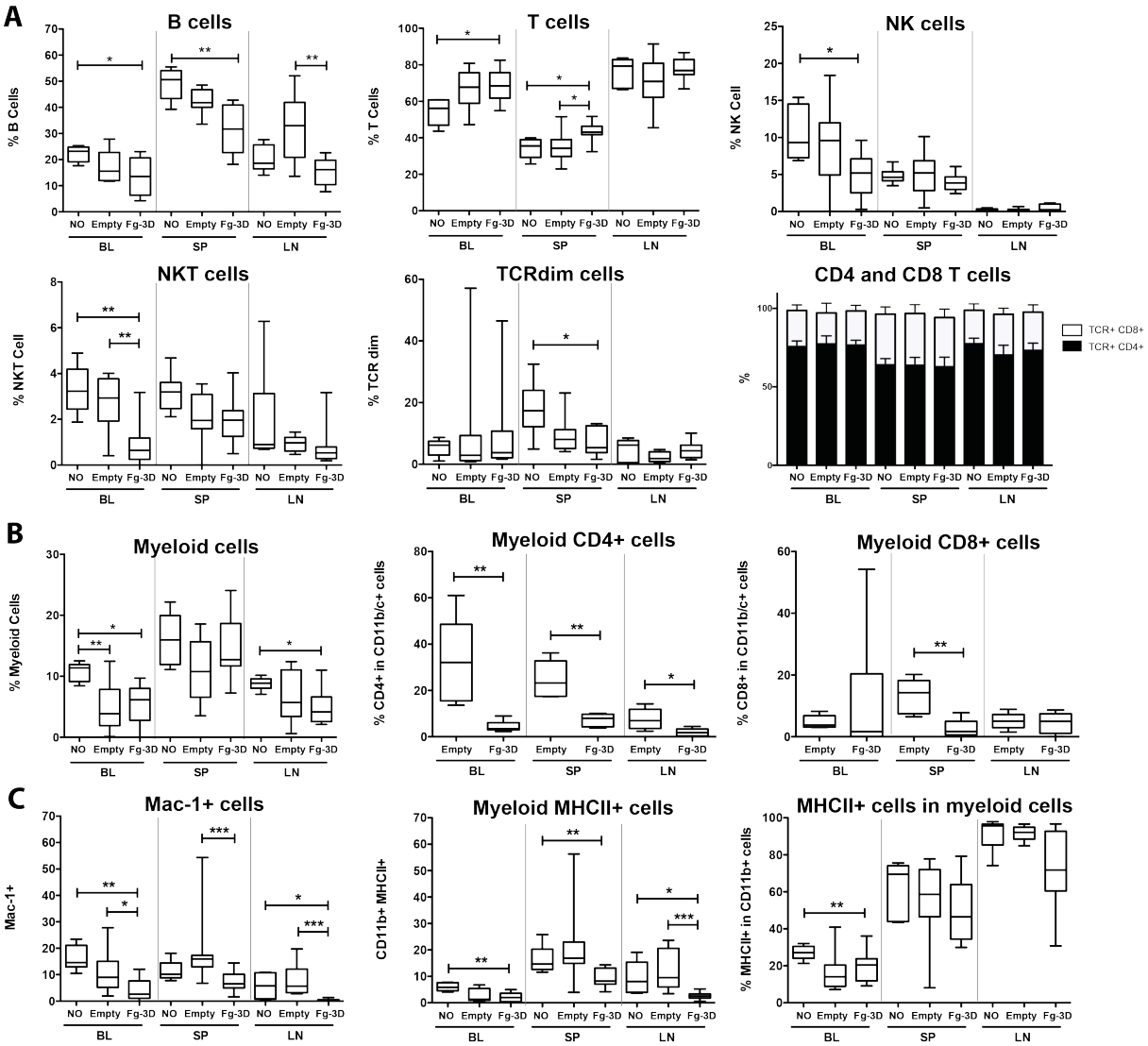

Figure 7. Characterization of systemic immune cell populations. At 6 days post-implantation immune cells in blood (BL), draining lymph nodes (LN) and spleen (SP) were analysed by FACS. **(A)** Main lymphoid populations: percentage of B cells (CD45R+TCR-), T cells (TCR+CD161a-), NK cells (CD161a+TCR-), NKT cells (CD161a+TCR+), TCR^{dim} T cells and CD4+ and CD8+ T cells. **(B)** Myeloid populations and subpopulations: percentage of myeloid cells (CD11b/c+CD161a-TCR-), CD4+ in CD11b/c+ cells, and CD8+ in CD11b/c+ cells. **(C)** Percentage of Mac-1+ cells (CD18+/CD11b/c+), MHC-II+CD11b/c+ cells and MHC-II+ within CD11b/c+ cells. NO - non-operated (n=6), empty (n=10) and Fg-3D (n=12). Results are presented as box and whiskers graphs (box represents median and quartiles while whiskers represent min to maximum values); *p < 0.05, **p < 0.01 and ***p < 0.001. Kruskal-Wallis test (or ANOVA when data distributions were normal) were used to analyse the data.

The systemic immune cell populations were also analysed at 8 weeks post-implantation, by looking at the percentages of B cells, T cells and myeloid cells (Figure 8). These cell populations had been found to be altered in the BL and LN in response to Fg-modified implants in this late time point [7]. In this study, it was interesting to observe that the decreased frequencies of B cells and myeloid cells in the BL at 6 days were still observed 8 weeks after injury in the Fg-3D group. In the LN of animals with Fg-3D, the percentage of B cells was still decreased 8 weeks post-injury, while the percentage of T cells is increased (79.28% in NO vs. 85.50% in Fg-3D). In parallel to the ongoing process of bone repair observed at 8 weeks in the Fg-3D group, the changes induced by Fg-3D in immune cells populations in BL and LN are still detectable, suggesting a relation between the two biological events.

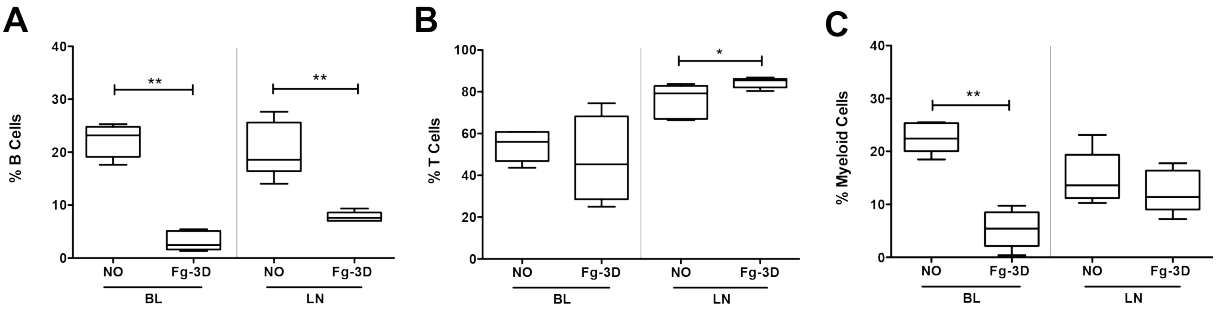

Figure 8. Evaluation of long-term effect of Fg-3D implantation on immune cell populations at a systemic level. (A) Percentage of B cells (CD45R+TCR-), **(B)** T cells (TCR+CD161a-) and **(C)** myeloid cells (CD163+) in blood (BL) and draining lymph nodes (LN) of non-operated (NO, n=6), and implanted with Fg-3D injured femurs (Fg-3D, n=5) at 8 weeks post-implantation. Results are presented as box and whiskers graphs (box represents median and quartiles while whiskers represent min to maximum values); *$p < 0.05$ and **$p < 0.01$. Mann Whitney test was used to compare the data.

Discussion

In this study, we have found that scaffolds made of fibrinogen (Fg-3D) promote bone repair and impact the inflammatory and immune responses both at local and systemic levels. We have observed a pro-regenerative local environment, with a resolving inflammatory response and granulation tissue formation at 6 days after implantation of Fg-3D. This translated to extensive bone repair at 8 weeks post injury. Importantly, bone tissue healing observed in the presence of Fg-3D was correlated with significant changes in the systemic immune cell balance. We believe that this is a crucial aspect of the response to biomaterials, that has been generally overlooked in other studies.

To the best of our knowledge, the current study is the first one describing the preparation of pure Fg scaffolds by freeze-drying, without using exogenous enzymes. Here, we present a biomimetic approach where Fg lyophilized scaffolds are neutralized using ethanol in order to reduce their solubility, easing their manipulation and implantation. Neutralization using ethanol resembles the application of methanol in the development of 3D matrices of fibroin [34]. Previously, other groups [18; 19; 35; 36] have prepared solutions of Fg and exogenous thrombin, leading to polymerization into fibrin networks, carried out outside the animal. Ethanol precipitated porous Fg scaffolds, further crosslinked with genipin have also been produced by microsphere templating, and compared to thrombin polymerized ones [37]. However, the authors proceeded to more extensive *in vitro* and *in vivo* characterization only with the thrombin polymerized materials [38].

Our rationale for not using thrombin was to develop a new, simpler and cheaper biomaterial, without the problems associated with the use of exogenous thrombin. As reviewed by Lew WK *et al*, thrombin delivery may elicit adverse immune reactions and the co-injection of thrombin increases the risk of thrombosis [39]. However, as thrombin is present at injury settings, we investigated if it could further stabilize Fg-3D structure. FTIR analysis of Fg-3D performed before and after incubation with thrombin, revealed similar spectral profiles (Figure S5), indicating that added thrombin does not lead to significant changes in the molecular conformation of Fg. Although we cannot completely rule out that host endogenous thrombin can contribute to further stabilize the Fg-3D structure, we believe that any contribution of endogenous thrombin would be advantageous for the biomaterial and its integration with the surrounding tissue.

The spectrum obtained here for Fg powder was in agreement with previous studies [30]. The findings obtained for lyophilized Fg scaffolds are in line with the reversible changes in secondary structure of proteins induced by lyophilization, namely increasing β-sheet content and decreasing α-helix content, previously reported by others [40]. Upon neutralization, Fg-3D presented an IR spectrum similar to Fg powder but the detailed Amide I and Amide II band

structure of neutralized Fg scaffolds suggested a slight increase of β-sheet content, consistent with the transition from α-helix to β-sheet described for fibrin formation [31]. In fact, similar peaks, albeit less intense, were observed when our Fg solution was polymerized using thrombin (Figure S5).

On the other hand, the reduction observed in the intensity peak in carboxylate side chains in Fg-3D may explain their lower solubility in comparison to the lyophilized Fg scaffolds or Fg powder. Fg carboxyl groups participate in fibrin formation (polymerization pocket "a" is located at carboxyl region), and may affect cell adhesion (cellular integrins interacts with carboxyl-terminal RGD) [41; 42]. Moreover, NMR spectroscopy revealed that the peak at 76 ppm in the CP-MAS spectrum is no longer visible after Fg scaffolds neutralization. This peak at 76 ppm in the CP-MAS spectrum may arise from the small amounts of carbohydrate moieties that bind to Fg, that is, N-acetylglucosamine, mannose, galactose, N-acetylneuraminic acid. The fact that this peak is no longer visible after neutralization suggests that the sugars moieties in neutralized Fg scaffolds become significantly more mobile, while the rigid glycoprotein domains become more organized or crystalline. Notably, no significant conformational changes are observed in the rigid protein environment, since the conformation-dependent carbonyl region in the CP-MAS spectra remains unchanged (peak at 173 ppm with shoulders at 175, 177 and 180 ppm), probably due to the large bandwidth noted.

Fg-3D scaffolds presented an interconnected porous network, similar to the one observed for chitosan scaffolds produced using similar methodology [7]. The macro pores observed in Fg scaffolds likely support cell migration, bone ingrowth and capillaries formation while micro pores favour a suitable hypoxic microenvironment for the cartilage formation that occurs during osteogenesis, as described for other biomaterials [43]. The *in vitro* degradation of Fg-3D mostly occurred during the first six hours and was faster in water than in presence of FBS. This behaviour was most likely due to a protective role of calcium ions and residual thrombin present in FBS towards the Fg-3D [44]. The results obtained when culturing pre-osteoblastic cells with Fg-3D extracts indicate that the material was not cytotoxic, according to the ISO10993-5 standard.

When Fg-3D scaffolds were implanted in a femoral bone defect, the histological evaluation performed 6 days post-injury revealed that the scaffold structure was still present. It is possible that a fraction of the fibrinogen in Fg-3D could be polymerized by the host thrombin present at defect region. However, any potential polymerization was not extensive, as the porous scaffold structure is still similar to non-implanted materials (Figures 3B and S1), and different from the endogenously formed fibrin mesh identified in the empty defects. Moreover, the histological findings support that Fg-3D eased cell migration and induced granulation tissue infiltration, correlating with a decrease in the size of the defect area. Importantly, in the context of bone healing, granulation tissue replaces hematoma during the

early stage of bone repair [45; 46]. Previous reports showed that Fg cell-binding domains can promote migration [11] and proliferation [47] of human fibroblasts, a key cell population involved in granulation tissue formation and wound healing [48].

Eight weeks upon implantation, newly formed bone was detected, presenting bone marrow cavity-like morphology. In some animals residual highly vascularized soft tissue could still be observed in the centre of the defect, which may be related with the fact that bone repair occurs from the periphery to the central region of the defect [49]. No trace of the Fg-3D was observed 8 weeks post-implantation, suggesting scaffold biodegradation by fibrinolysis without impairing tissue regeneration. When compared to our previous results, using chitosan-based materials modified or not by Fg adsorption, in the same animal model and at the same time post-implantation [7], the outcome here reveals a much more advanced stage of bone formation and repair, with complete degradation of Fg-3D material and its replacement with new bone, in the vast majority of the defect area.

Bone repair was further characterized by micro-CT, revealing that animals implanted with Fg-3D were at an early stage of bone healing, having formed compact bone tissue in the defect region. This compact bone is expected to be gradually remodelled to trabecular bone. Mature bone is structurally more porous and presents lower percentages of calcified tissue, as observed in the micro-CT of the non-operated animal, whose bone parameters were in agreement with the literature [50; 51]. Importantly, Fg-3D implanted, but not empty defect, animals presented periosteal repair, which is reported to have a positive effect on biomechanics and bone healing, as it constitutes an important reservoir of bone cell precursors [52; 53]. The bone repair process described here is in line with what has been found *in vivo* after implanting fibrin glue combined with cells or calcium phosphate particles in a critical rabbit calvarial bone defect model [35; 54]. Conversely, a previous study in the mouse calvarial defect reported that fibrin porous scaffolds, produced by sphere templating and thrombin polymerization, only promoted new bone formation when modified to incorporate calcium phosphate [38]. Interestingly, although their evaluation was at 45 days post-implantation, by that point the fibrin material was already undetectable at implant site. In the current study Fg-3D scaffolds were implanted alone, relying on the host cells to promote self-regeneration of bone tissue.

The local gene expression results indicate a mild inflammatory response in empty animals that is not augmented when Fg-3D are present. Our findings on the local immune response indicate that the bone injury seems to be the driving force underlying the increase of IL-8, IL-6 and IL-1β. Cytokines such as IL-4 and IL-10, which have anti-inflammatory roles were not detected 6 days post-injury at the mRNA level. This is in line with a previous report on bone injury in a sheep model, where the highest mRNA IL-10 levels were found 24 hours post-osteotomy followed by decreasing levels of this cytokine until the end of the experiment

(60 h) [6]. The slight increase of IL-8 levels locally detected may be related to the chemoattraction of PMN, which were histologically identified. A significant increase of IL-6 mRNA levels was observed in the bone defect of both operated groups, while plasma IL-6 levels were bellow detection in all groups (data not shown). IL-6 is a pleiotropic cytokine and its role in bone healing, namely in the early stage, is believed to be related with angiogenesis and osteoclastogenesis, whose malfunction delays bone maturation [55]. Interestingly, augmented levels of local and systemic IL-6 and IL-8 concentrations have been found in patients with bone trauma [56]. Other pro-inflammatory cytokines such as IL-17a, associated with graft rejection and autoimmunity, or TNF-α, highly related with exacerbated inflammation and infection, were not detected in the plasma of these animals (data not shown). Of note, the presence of Fg-3D significantly homogenized the host response, dampening the immune reaction. This can be confirmed by a lower coefficient of variation of the Fg-3D implanted group, for the majority of the different molecules evaluated by gene expression analysis, FACS and ELISA (Supplementary Table 2).

Although at 6 days no significant differences in local IL-1β mRNA levels or systemic protein levels, a significant reduction of IL-1β in plasma was found at 8 weeks post-implantation for Fg-3D group. These findings are in line with the literature as the first peak of IL-1β, induced by the initial immune response, is expected to occur 24h after the injury and a second peak at 3 weeks later [57]. At later stage, IL-1β is reported to be mainly produced by osteoblasts during bone remodelling [57]. In this sense, the lower concentration of IL-1β in the plasma of the animals implanted with Fg-3D should be likely related to the stage of bone repair observed at 8 weeks post-implantation.

TGF-β1 has been reported as an instrumental player in a balanced bone remodelling [58]. The results obtained showed a tendency for TGF-β1 increase at early time-points locally at mRNA level, and systemically at the protein level. Interestingly, its protein levels in plasma remained high for Fg-3D implanted animals at 8 weeks post-implantation, when compared with NO animals. This is in line with our previous results showing an increase in plasma levels of TGF-β1 at 8 weeks post-implantation, when bone regeneration was promoted using Fg-modified chitosan implants [7]. Additionally, TGF-β1 is considered an immunoregulatory factor due to its effects on immune cell populations. Regulatory T cells produce TGF-β1 and IL-10 to inhibit other T cell population [59], and TGF-β1 signaling in T cell affects bone metabolism [60]. The function of B cells may also be modulated by TGF-β1 [61]. Moreover, TGF-β1 induces and regulates the recruitment of myeloid cells, namely monocytes [62; 63], and is produced by the pro-healing M2 macrophages.

Angiogenesis is expected to occur during bone repair involving the angiogenic factor VEGF, whose production is reported to be stimulated in presence of Fg [14]. The mRNA levels

of VEGF were significantly higher in the empty group than in NO animals, while Fg-3D animals showed intermediate expression levels. The peak of local up-regulation of VEGF expression has been seen to occur between 24 and 36 h after bone defect surgery followed by a decrease [6], and high VEGF production may be linked to inflammation.

Overall, the data obtained suggests that the bone defect induced a mild inflammatory response, which was not potentiated by Fg-3D implantation. The short-term evaluation at 6 days post-injury is a snapshot that allows evaluating the transition from acute inflammation to chronic inflammation. Thus, it cannot be excluded that some early biological events might have been missed, namely infiltration of neutrophils, T cells and B cells and occurrence of a peak in the local levels of cytokines (e.g. IL-1β and TNF-α) [5; 6; 64].

How key immune cell populations present in blood (BL), spleen (SP) and draining lymph nodes (LN) react to the critical bone injury and to the implantation of Fg-3D was of paramount importance to understand the host response to Fg-3D. In our previous work Fg-adsorbed chitosan scaffolds prepared by freeze-drying were evaluated using the same animal model. Fg-adsorbed scaffolds led to a different systemic response with heighten percentage of B cells and myeloid cells (defined as $CD163^{+}$ cells) with a decrease in the percentage of T cells in the draining LN [7] at 8 weeks. Interestingly, here the systemic immune response in Fg-3D implanted animals showed a decrease in the percentage of myeloid cells, B cells, NK and NKT cells and higher T cell proportional representation, may be related to bone tissue response to injury. The increased percentages of circulating and SP T cells in Fg-3D group and the concomitant decrease in the proportion of B cells in BL, LN and SP could be part of the new equilibrium within lymphoid populations to support bone debris scavenging, needed in these initial stages of bone repair. Previous reports have noted a local increase in T cells starting 24h after fracture which is maintained until 21 days, as part of dynamics of immune cell infiltration in to the lesion site as elegantly described by [5]. Scaglione *et al* reported an increase in circulating lymphocytes and platelets 4 days after subcutaneous biomaterial implantation, while circulating monocytes decrease [65]. In agreement with these findings we also observed an increase in T cells and decrease in myeloid cells 6 days after implantation. Other studies showed that augmented CD8+ T cells correlated with a poorer bone healing, which can be reverted upon depletion of CD8+ T cells [66; 67]. Importantly, we did not find significant differences in CD8+ T cells, being the CD4+ T cells the predominant subset identified as expected. Moreover, Elisseeff's group recently proposed a pro-regenerative biomaterial through the modulation of the adaptive immune response. In this study, hypertrophic draining lymph nodes, accompanied by IL-4 expression, were observed in the animals with functional muscle tissue restore. Additionally, CD4+ Th2 T cells were identified as the main subset involved in this systemic response while B cells and CD8+ T cells were suggested to be potentially involved [68].

In terms of immune cell activation markers, a decrease of TCR^{dim} T cells with an increased proportion of splenic T cells of animals with Fg-3D may be correlated with reduced activation of T cells in this secondary lymphoid organ. This change in splenic T cell population was accompanied by a decrease in the proportion of CD45R expressing B cells, which could also be related with the loss of CD45R expression during differentiation to plasma cells, in response to the human Fg, upon a T-cell dependent immune response, as previously described in mice [69]. As we are implanting human Fg in rat we cannot exclude the possibility of an immune response from the rat against the human protein, especially when considering that the homology percentages between human and rat fibrinogen varies from 52% to 66% [70]. However, the perfect integration of Fg-3D scaffolds in bone, the reduced immune cell infiltration at 6 days, and the absence of fibrous capsule at 8 weeks, all argue against a strong immune response in this sense. The decreased percentage of MHC-II^+ cells within the CD11b/c^+ population may reflect reduced levels of expression, which by becoming lower than the detectable minimum appear as negative. An increase of the percentage of $CD8^+$, $CD161^+$ and MHC-II^+ cells was observed in other studies, namely in graft rejection [71; 72]. Therefore, the systemic decrease of the percentage of blood cells expressing MHC-II and CD11b/c in animals with Fg-3D scaffold might be related with a good integration of the implant in the bone.

Together, our findings support the pro-regenerative potential of Fg-3D and the systemic impact of injury and biomaterials implantation. Upon Fg-3D implantation, bone defect closure was faster and with periosteal repair, and promoted a more controlled biological response in comparison to the empty group. In future, new studies are required to acquire a comprehensive understanding how Fg-3D support bone healing and impact the immune system. This study is the first identifying the key immune cell populations and mediators, calling for further studies on the mechanisms and the role of these cell populations on establishing the pro-regenerative microenvironment.

Conclusions

The results discussed above show that Fg-3D scaffolds provided a temporary support and promoted a pro-regenerative microenvironment, which led to periosteal bone repair after 8 weeks of implantation. The significant changes observed draw attention to the systemic nature of response to injury and the potential for immunomodulation upon biomaterial implantation. The current study constitutes a basis for the development of Fg-based biomaterials, exploring Fg immunomodulatory properties for regenerative medicine.

Acknowledgments

This work was financed by FEDER - Fundo Europeu de Desenvolvimento Regional funds through the COMPETE 2020 - Operacional Programme for Competitiveness and Internationalisation (POCI), Portugal 2020, and by Portuguese funds through FCT - Fundação para a Ciência e a Tecnologia/ Ministério da Ciência, Tecnologia e Inovação in the framework of the project "Institute for Research and Innovation in Health Sciences" (POCI-01-0145-FEDER-007274). AS, DV, MIO, CC were supported by PhD and Post-Doc fellowships SFRH/BD/85968/2012, SFRH/BD/87516/2012, SFRH/BPD/37090/2007, SFRH/BDP/87071/2012, respectively. The NMR work was developed within the scope of the project CICECO-Aveiro Institute of Materials, POCI-01-0145-FEDER-007679 (FCT Ref. UID /CTM /50011/2013), financed by national funds through the FCT/MEC and when appropriate co-financed by FEDER under the PT2020 Partnership Agreement. AMG also thanks Portuguese National Nuclear Magnetic Resonance Network, supported with FCT funds. The authors thank Griffons, S.A. for supplying thrombin.

Supplementary Information

Published in Biomaterials 111: 163-178, 2016

Supplementary information

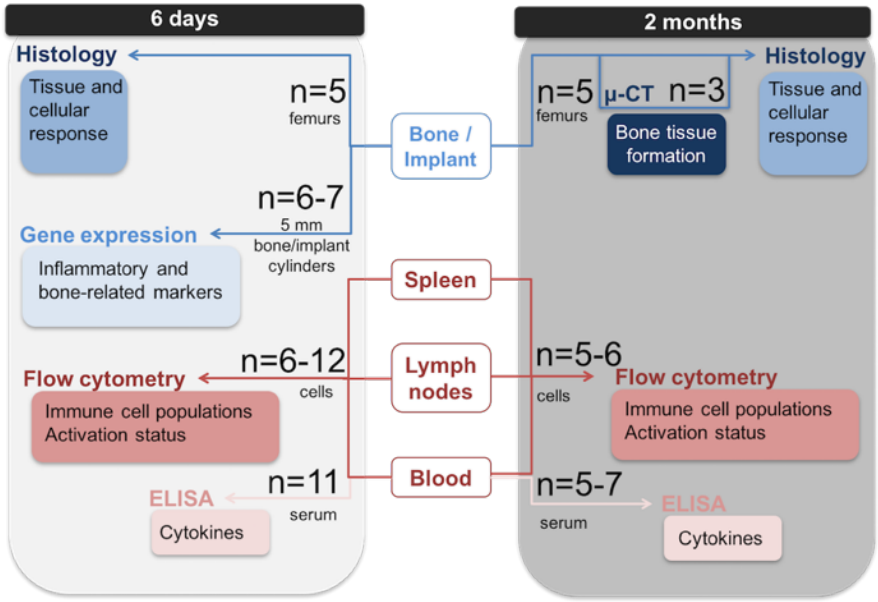

Figure S1. Experimental design diagram: bone defects were performed in Wistar rats and immune response and bone remodelling were evaluated at 6 days and 8 weeks post-injury. The methods applied in the evaluation of each sample type are indicated as well as the number of animals studied per condition (non-operated, empty defect and with Fg-3D scaffold).

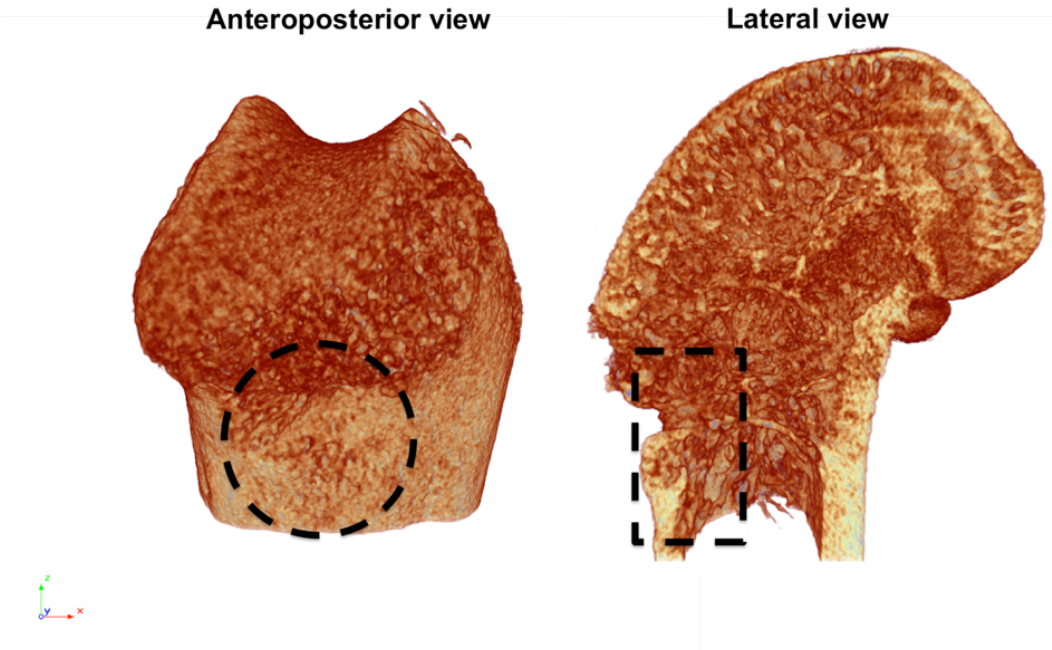

Figure S2. Cylindrical VOI with 3 mm in diameter and 2 mm in deepness used for microCT analysis of bone defect region at 8 weeks post-implantation.

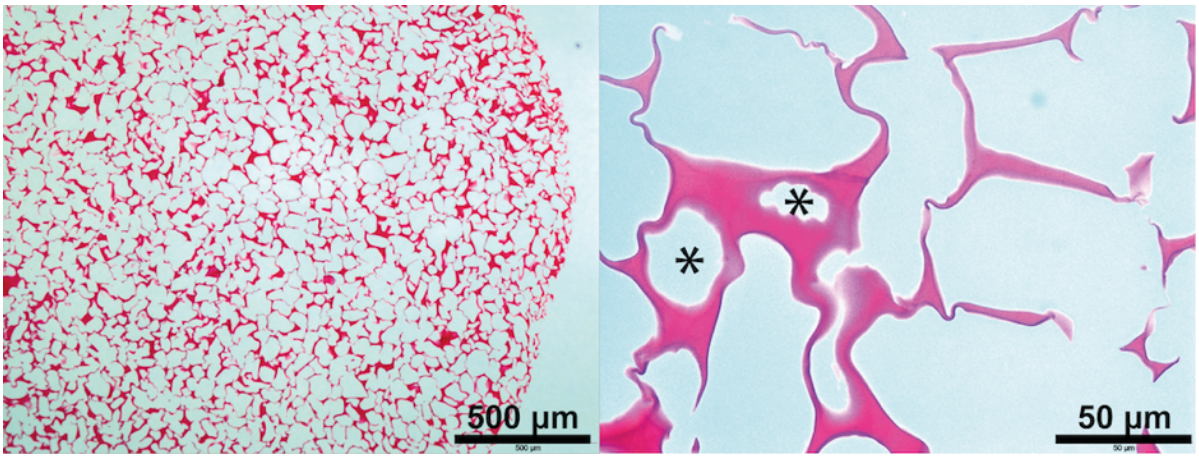

Figure S3 Light microscopy images of Fg-3D scaffolds after H&E staining. Interconnecting pores are indicated with asterisks.

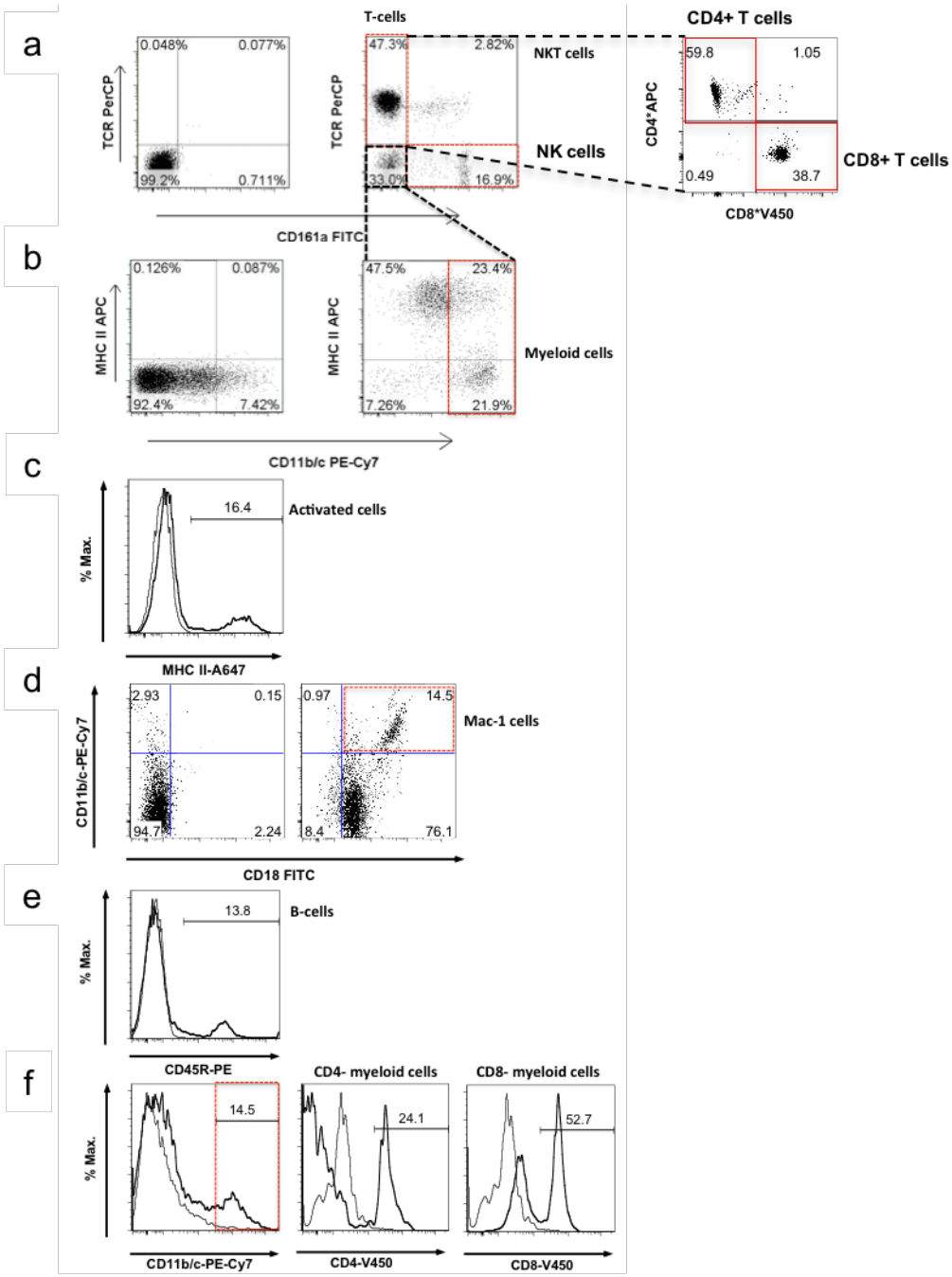

Figure S4. Representative plots of the flow cytometry analysis illustrating the gates and surface markers used to evaluate the different immune populations: T cells, NK cells, NKT cells and the subsets CD4+ T cells and CD8+ T cells (a), myeloid cells (b), activated cells (c), Mac-1+ cells (d), B cells (e) and CD4+ and CD8+ myeloid cells (f).

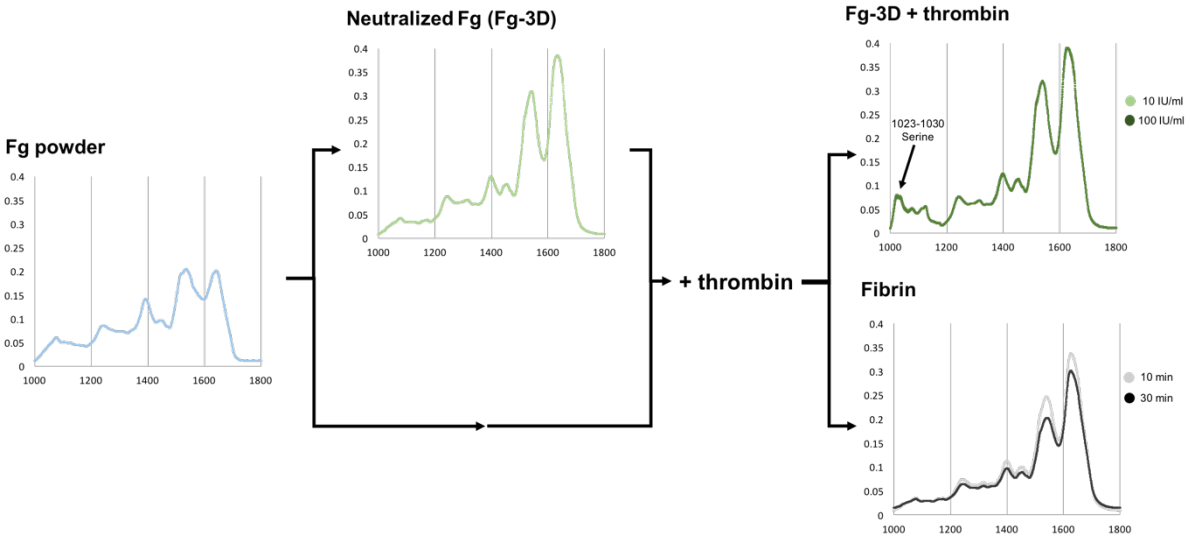

Figure S5. ATR-FTIR spectra of Fg powder, Fg-3D before and after incubation with thrombin solution at 10 or 100 IU/ml, 40 mM $CaCl_2$ and 37ºC.

Supplementary Table 1. List of primers used for quantitative RT-PCR analysis

Gene	Accession	Forward primer sequence (5'-3')	Reverse primer sequence (5'-3')
GAPDH	[NM_017008.4]	CTGGAGAAACCTGCCAAGTA	TACTCCTTGGAGGCCATGTA
IFN-Ɣ	[NM_138880.2]	GGCCATCAGCAACAACATA	GACAGCTTTGTGCTGGATCT
IL-1β	[NM_031512.2]	GACAAGCAACGACAAAATCC	ACCGCTTTTCCATCTTCTTC
IL-2	[NM_053836.1]	AGCGTGTGTTGGATTTGACT	TCTCCTCAGAAATTCCACCA
IL-4	[NM_201270.1]	TCCGTGCTTGAAGAACAAGT	CCAGGAAGTCTTTCAGTGTTGT
IL-6	[NM_012589.2]	AGCCAGAGTCATTCAGAGCA	AGTTGGATGGTCTTGGTCCT
IL-8 (MIP-2)	[NM_053647.1]	TGAAGTTTGTCTCAACCCTGA	GGTGCAGTTCGTTTCTTTTCT
IL-10	[NM_012854.2]	GACGCTGTCATCGATTTCTC	TTCATGGCCTTGTAGACACC
Osteocalcin	[NM_013414.1]	AGGGCAGTAAGGTGGTGAAT	CTAAACGGTGGTGCCATAGA
TNF-α	[NM_012675.3]	TCTACTGAACTTCGGGGTGA	CCACCAGTTGGTTGTCTTTG
TGF-β1	[NM_021578.2]	CGGACTACTACGCCAAAGAA	CCCGAATGTCTGACGTATTG
VEGFa	[NM_031836.3]	CAATGATGAAGCCCTGGA	CTATGCTGCAGGAAGCTCAT

Supplementary Table 2. Coefficients of variation for the most important biological parameters assessed in this study

Methodology	Molecule analyzed	Animal group		
		NO	Empty	Fg-3D
Gene expression	OC	79,4	96,4	54,3
	VEGF	35,7	89,1	47,8
	TGF-β1	81,7	95,0	75,5
	IL-1β	53,4	115,6	24,1
	IL-6	87,0	133,3	65,9
	IL-8	45,4	177,8	34,0
Flow Cytometry	Myeloid cells - blood	14,4	81,0	61,3
	Myeloid cells – spleen	26,2	46,6	34,6
	Myeloid cells – lymph nodes	12,2	66,6	58,0
	B cells – blood	13,5	34,8	51,7
	B cells – spleen	12,2	11,4	30,7
	B cells – lymph nodes	25,3	38,3	33,4
	T cells – blood	13,6	7,5	13,2
	T cells – spleen	15,7	26,0	11,4
	T cells – lymph nodes	10,0	19,6	8,0
ELISA	TGF-β1	98,1	65,5	58,6
	IL-1β	26,4	43,6	28,9

References

[1] - Anderson, J. M., A. Rodriguez, and D. T. Chang (2008), Foreign body reaction to biomaterials, Seminars in immunology, 20(2), 86-100.

[2] - Kweon, H., S. G. Kim, and J. Y. Choi (2014), Inhibition of foreign body giant cell formation by 4- hexylresorcinol through suppression of diacylglycerol kinase delta gene expression, Biomaterials, 35(30), 8576-8584.

[3] - Mountziaris, P. M., P. P. Spicer, F. K. Kasper, and A. G. Mikos (2011), Harnessing and modulating inflammation in strategies for bone regeneration, Tissue engineering. Part B, Reviews, 17(6), 393-402.

[4] - Claes, L., S. Recknagel, and A. Ignatius (2012), Fracture healing under healthy and inflammatory conditions, Nat Rev Rheumatol, 8(3), 133-143.

[5] - Konnecke, I., et al. (2014), T and B cells participate in bone repair by infiltrating the fracture callus in a two-wave fashion, Bone, 64(0), 155-165.

[6] - Schmidt-Bleek, K., et al. (2014), Initial immune reaction and angiogenesis in bone healing, J Tissue Eng Regen Med, 8(2), 120-130.

[7] - Santos, S. G., et al. (2013), Adsorbed fibrinogen leads to improved bone regeneration and correlates with differences in the systemic immune response, Acta Biomater, 9(7), 7209-7217.

[8] - Drew, A. F., H. Liu, J. M. Davidson, C. C. Daugherty, and J. L. Degen (2001), Wound-healing defects in mice lacking fibrinogen, Blood, 97(12), 3691-3698.

[9] - Rodrigues, S. N., I. C. Goncalves, M. C. Martins, M. A. Barbosa, and B. D. Ratner (2006), Fibrinogen adsorption, platelet adhesion and activation on mixed hydroxyl-/methyl-terminated self-assembled monolayers, Biomaterials, 27(31), 5357-5367.

[10] - Doolittle, R. F., K. W. K. Watt, B. A. Cottrell, D. D. Strong, and M. Riley (1979), The amino acid sequence of the α-chain of human fibrinogen, Nature, 280(5722), 464-468.

[11] - Rybarczyk, B. J., S. O. Lawrence, and P. J. Simpson-Haidaris (2003), Matrix-fibrinogen enhances wound closure by increasing both cell proliferation and migration, Blood, 102(12), 4035-4043.

[12] - Lishko, V. K., N. P. Podolnikova, V. P. Yakubenko, S. Yakovlev, L. Medved, S. P. Yadav, and T. P. Ugarova (2004), Multiple binding sites in fibrinogen for integrin alphaMbeta2 (Mac-1), J Biol Chem, 279(43), 44897-44906.

[13] - Sahni, A., and C. W. Francis (2000), Vascular endothelial growth factor binds to fibrinogen and fibrin and stimulates endothelial cell proliferation, Blood, 96(12), 3772-3778.

[14] - Shiose, S., Y. Hata, Y. Noda, Y. Sassa, A. Takeda, H. Yoshikawa, K. Fujisawa, T. Kubota, and T. Ishibashi (2004), Fibrinogen stimulates in vitro angiogenesis by choroidal endothelial cells via autocrine VEGF, Graefes Arch Clin Exp Ophthalmol, 242(9), 777-783.

[15] - Wang, H., L. Shan, H. Zeng, M. Sun, Y. Hua, and Z. Cai (2014), Is fibrin sealant effective and safe in total knee arthroplasty? A meta-analysis of randomized trials, Journal of orthopaedic surgery and research, 9, 36.

[16] - Kim, B. S., and J. Lee (2015), Enhanced bone healing by improved fibrin-clot formation via fibrinogen adsorption on biphasic calcium phosphate granules, Clin Oral Implants Res, 26(10), 1203-1210.

[17] - Yamada, Y., J. S. Boo, R. Ozawa, T. Nagasaka, Y. Okazaki, K. Hata, and M. Ueda (2003), Bone regeneration following injection of mesenchymal stem cells and fibrin glue with a biodegradable scaffold, J Craniomaxillofac Surg, 31(1), 27-33.

[18] - Seebach, E., H. Freischmidt, J. Holschbach, J. Fellenberg, and W. Richter (2014), Mesenchymal stroma cells trigger early attraction of M1 macrophages and endothelial cells into fibrin hydrogels, stimulating long bone healing without long-term engraftment, Acta Biomater, 10(11), 4730-4741.

[19] - Ikeda, T., Y. Miyata, Y. Tsutani, K. Misumi, K. Arihiro, and M. Okada (2012), Fibrinogen/thrombin-based collagen fleece (TachoComb(R)) promotes regeneration in pulmonary arterial injury, Eur J Cardiothorac Surg, 41(4), 926-932.

[20] - Singh, K., H. Moyer, J. K. Williams, Z. Schwartz, and B. D. Boyan (2011), Fibrin glue: a scaffold for cellular-based therapy in a critical-sized defect, Ann Plast Surg, 66(3), 301-305.

[21] - Ryu, J. K., et al. (2015), Blood coagulation protein fibrinogen promotes autoimmunity and demyelination via chemokine release and antigen presentation, Nat Commun, 6, 8164.

[22] - Peled, E., J. Boss, J. Bejar, C. Zinman, and D. Seliktar (2007), A novel poly(ethylene glycol)-fibrinogen hydrogel for tibial segmental defect repair in a rat model, J Biomed Mater Res A, 80(4), 874-884.

[23] - Almeida, C. R., D. P. Vasconcelos, R. M. Goncalves, and M. A. Barbosa (2012), Enhanced mesenchymal stromal cell recruitment via natural killer cells by incorporation of inflammatory signals in biomaterials, J R Soc Interface, 9(67), 261-271.

[24] - Maciel, J., M. I. Oliveira, E. Colton, A. K. McNally, C. Oliveira, J. M. Anderson, and M. A. Barbosa (2014), Adsorbed fibrinogen enhances production of bone- and angiogenic-related factors by monocytes/macrophages, Tissue Eng Part A, 20(1-2), 250-263.

[25] - Torres, A. L., S. G. Santos, M. I. Oliveira, and M. A. Barbosa (2013), Fibrinogen promotes resorption of chitosan by human osteoclasts, Acta Biomater, 9(5), 6553-6562.

[26] - Le Guehennec, L., E. Goyenvalle, E. Aguado, M. Houchmand-Cuny, B. Enkel, P. Pilet, G. Daculsi, and P. Layrolle (2005), Small-animal models for testing macroporous ceramic bone substitutes, J Biomed Mater Res B Appl Biomater, 72(1), 69-78.

[27] - Mori, S., T. Sawai, T. Teshima, and M. Kyogoku (1988), A new decalcifying technique for immunohistochemical studies of calcified tissue, especially applicable to cell surface marker demonstration, J Histochem Cytochem, 36(1), 111-114.

[28] - McLean, I. W., and P. K. Nakane (1974), Periodate-lysine-paraformaldehyde fixative. A new fixation for immunoelectron microscopy, J Histochem Cytochem, 22(12), 1077-1083.

[29] - Dempster, D. W., J. E. Compston, M. K. Drezner, F. H. Glorieux, J. A. Kanis, H. Malluche, P. J. Meunier, S. M. Ott, R. R. Recker, and A. M. Parfitt (2013), Standardized nomenclature, symbols, and units for bone histomorphometry: a 2012 update of the report of the ASBMR Histomorphometry Nomenclature Committee, J Bone Miner Res, 28(1), 2-17.

[30] - Lin, S. Y., Y. S. Wei, T. F. Hsieh, and M. J. Li (2004), Pressure dependence of human fibrinogen correlated to the conformational alpha-helix to beta-sheet transition: an Fourier transform infrared study microspectroscopic study, Biopolymers, 75(5), 393-402.

[31] - Litvinov, R. I., D. A. Faizullin, Y. F. Zuev, and J. W. Weisel (2012), The alpha-helix to beta-sheet transition in stretched and compressed hydrated fibrin clots, Biophys J, 103(5), 1020-1027.

[32] - Thacker, R. I., and G. S. Retzinger (2008), Adsorbed fibrinogen regulates the behavior of human dendritic cells in a CD18-dependent manner, Exp Mol Pathol, 84(2), 122-130.

[33] - Gibbings, D., and A. D. Befus (2009), CD4 and CD8: an inside-out coreceptor model for innate immune cells, J Leukoc Biol, 86(2), 251-259.

[34] - Lv, Q., and Q. Feng (2006), Preparation of 3-D regenerated fibroin scaffolds with freeze drying method and freeze drying/foaming technique, J Mater Sci Mater Med, 17(12), 1349-1356.

[35] - Kim, B. S., H. M. Sung, H. K. You, and J. Lee (2014), Effects of fibrinogen concentration on fibrin glue and bone powder scaffolds in bone regeneration, Journal of bioscience and bioengineering, 118(4), 469-475.

[36] - Johnson, P. J., S. R. Parker, and S. E. Sakiyama-Elbert (2010), Fibrin-based tissue engineering scaffolds enhance neural fiber sprouting and delay the accumulation of reactive astrocytes at the lesion in a subacute model of spinal cord injury, J Biomed Mater Res A, 92(1), 152-163.

[37] - Linnes, M. P., B. D. Ratner, and C. M. Giachelli (2007), A fibrinogen-based precision microporous scaffold for tissue engineering, Biomaterials, 28(35), 5298-5306.

[38] - Osathanon, T., M. L. Linnes, R. M. Rajachar, B. D. Ratner, M. J. Somerman, and C. M. Giachelli (2008), Microporous nanofibrous fibrin-based scaffolds for bone tissue engineering, Biomaterials, 29(30), 4091-4099.

[39] - Lew, W. K., and F. A. Weaver (2008), Clinical use of topical thrombin as a surgical hemostat., Biologics, 2(4), 593-599.

[40] - Griebenow, K., and A. M. Klibanov (1995), Lyophilization-induced reversible changes in the secondary structure of proteins, Proc Natl Acad Sci U S A, 92(24), 10969-10976.

[41] - Cote, H. C. F., K. P. Pratt, E. W. Davie, and D. W. Chung (1997), The polymerization pocket "a" within the carboxyl-terminal region of the gamma chain of human fibrinogen is adjacent to but independent from the calcium-binding site, Journal of Biological Chemistry, 272(38), 23792-23798.

[42] - Suehiro, K., J. Mizuguchi, K. Nishiyama, S. Iwanaga, D. H. Farrell, and S. Ohtaki (2000), Fibrinogen binds to integrin alpha(5)beta(1) via the carboxyl-terminal RGD site of the Aalpha-chain, J Biochem, 128(4), 705-710.

[43] - Karageorgiou, V., and D. Kaplan (2005), Porosity of 3D biomaterial scaffolds and osteogenesis, Biomaterials, 26(27), 5474-5491.

[44] - Haverkate, F., and G. Timan (1977), Protective effect of calcium in the plasmin degradation of fibrinogen and fibrin fragments D, Thrombosis Research, 10(6), 803-812.

[45] - Alexander, K. A., et al. (2011), Osteal macrophages promote in vivo intramembranous bone healing in a mouse tibial injury model, J Bone Miner Res, 26(7), 1517-1532.

[46] - Vieira, A. E., C. E. Repeke, B. Ferreira Junior Sde, P. M. Colavite, C. C. Biguetti, R. C. Oliveira, G. F. Assis, R. Taga, A. P. Trombone, and G. P. Garlet (2015), Intramembranous bone healing process subsequent to tooth extraction in mice: micro-computed tomography, histomorphometric and molecular characterization, PLoS One, 10(5), e0128021.

[47] - Gray, A. J., J. E. Bishop, J. T. Reeves, and G. J. Laurent (1993), A alpha and B beta chains of fibrinogen stimulate proliferation of human fibroblasts, J Cell Sci, 104 (Pt 2)(2), 409-413.

[48] - Micallef, L., N. Vedrenne, F. Billet, B. Coulomb, I. A. Darby, and A. Desmouliere (2012), The myofibroblast, multiple origins for major roles in normal and pathological tissue repair, Fibrogenesis Tissue Repair, 5(Suppl 1), S5.

[49] - Shapiro, F. (2008), Bone development and its relation to fracture repair. The role of mesenchymal osteoblasts and surface osteoblasts, Eur Cell Mater, 15, 53-76.

[50] - Lorenz, J., E. Seebach, G. Hackmayer, C. Greth, R. J. Bauer, K. Kleinschmidt, D. Bettenworth, M. Bohm, J. Grifka, and S. Grassel (2014), Melanocortin 1 receptor-signaling deficiency results in an articular cartilage phenotype and accelerates pathogenesis of surgically induced murine osteoarthritis, PLoS One, 9(9), e105858.

[51] - Frohbergh, M., Y. Ge, F. Meng, N. Karabul, A. Solyom, A. Lai, J. Iatridis, E. H. Schuchman, and C. M. Simonaro (2014), Dose responsive effects of subcutaneous pentosan polysulfate injection in mucopolysaccharidosis type VI rats and comparison to oral treatment, PLoS One, 9(6), e100882.

[52] - Roberts, S. J., N. van Gastel, G. Carmeliet, and F. P. Luyten (2015), Uncovering the periosteum for skeletal regeneration: the stem cell that lies beneath, Bone, 70, 10-18.

[53] - Bullens, P. H., H. W. Schreuder, M. C. de Waal Malefijt, N. Verdonschot, and P. Buma (2010), The presence of periosteum is essential for the healing of large diaphyseal segmental

bone defects reconstructed with trabecular metal: a study in the femur of goats, J Biomed Mater Res B Appl Biomater, 92(1), 24-31.

[54] - Kim, B. S., H. J. Kim, J. G. Choi, H. K. You, and J. Lee (2015), The effects of fibrinogen concentration on fibrin/atelocollagen composite gel: an in vitro and in vivo study in rabbit calvarial bone defect, Clin Oral Implants Res, 26(11), 1302-1308.

[55] - Yang, X., B. F. Ricciardi, A. Hernandez-Soria, Y. Shi, N. Pleshko Camacho, and M. P. Bostrom (2007), Callus mineralization and maturation are delayed during fracture healing in interleukin-6 knockout mice, Bone, 41(6), 928-936.

[56] - Perl, M., F. Gebhard, M. W. Knoferl, M. Bachem, H. J. Gross, L. Kinzl, and W. Strecker (2003), The pattern of preformed cytokines in tissues frequently affected by blunt trauma, Shock, 19(4), 299-304.

[57] - Mountziaris, P. M., and A. G. Mikos (2008), Modulation of the inflammatory response for enhanced bone tissue regeneration, Tissue Eng Part B Rev, 14(2), 179-186.

[58] - Tang, Y., et al. (2009), TGF-beta1-induced migration of bone mesenchymal stem cells couples bone resorption with formation, Nat Med, 15(7), 757-765.

[59] - Wan, Y. Y., and R. A. Flavell (2007), 'Yin-Yang' functions of transforming growth factor-beta and T regulatory cells in immune regulation, Immunol Rev, 220, 199-213.

[60] - Gao, Y., W. P. Qian, K. Dark, G. Toraldo, A. S. Lin, R. E. Guldberg, R. A. Flavell, M. N. Weitzmann, and R. Pacifici (2004), Estrogen prevents bone loss through transforming growth factor beta signaling in T cells, Proc Natl Acad Sci U S A, 101(47), 16618-16623.

[61] - Gros, M. J., P. Naquet, and R. R. Guinamard (2008), Cell intrinsic TGF-beta 1 regulation of B cells, J Immunol, 180(12), 8153-8158.

[62] - Wahl, S., D. Hunt, L. Wakefield, N. McCartney-Francis, L. Wahl, A. Roberts, and M. Sporn (1987), Transforming growth factor type beta induces monocyte chemotaxis and growth factor production., Proc Natl Acad Sci U S A, 84(16), 5788-5792.

[63] - Kim, J. S., et al. (2006), Transforming growth factor-beta1 regulates macrophage migration via RhoA, Blood, 108(6), 1821-1829.

[64] - Chung, R., J. C. Cool, M. A. Scherer, B. K. Foster, and C. J. Xian (2006), Roles of neutrophil-mediated inflammatory response in the bony repair of injured growth plate cartilage in young rats, J Leukoc Biol, 80(6), 1272-1280.

[65] - Scaglione, S., M. Cilli, M. Fiorini, R. Quarto, and G. Pennesi (2011), Differences in chemical composition and internal structure influence systemic host response to implants of biomaterials, Int J Artif Organs, 34(5), 422-431.

[66] - Schlundt, C., H. Schell, S. B. Goodman, G. Vunjak-Novakovic, G. N. Duda, and K. Schmidt-Bleek (2015), Immune modulation as a therapeutic strategy in bone regeneration, J Exp Orthop, 2(1), 1.

[67] - Reinke, S., et al. (2013), Terminally differentiated CD8(+) T cells negatively affect bone regeneration in humans, Sci Transl Med, 5(177), 177ra136.

[68] - Sadtler, K., et al. (2016), Developing a pro-regenerative biomaterial scaffold microenvironment requires T helper 2 cells, Science, 352(6283), 366-370.

[69] - Rubin, B., and C. Matron (2005), The mouse immune response to human fibrinogen reveals an autoimmune component against mouse fibrinogen, Cell Immunol, 233(1), 41-52.

[70] - Fowlkes, D. M., N. T. Mullis, C. M. Comeau, and G. R. Crabtree (1984), Potential basis for regulation of the coordinately expressed fibrinogen genes: homology in the 5' flanking regions, Proc Natl Acad Sci U S A, 81(8), 2313-2316.

[71] - Scriba, A., V. Grau, and B. Steiniger (1998), Phenotype of rat monocytes during acute kidney allograft rejection: increased expression of NKR-P1 and reduction of CD43, Scand J Immunol, 47(4), 332-342.

[72] - Grau, V., O. Stehling, H. Garn, and B. Steiniger (2001), Accumulating monocytes in the vasculature of rat renal allografts: phenotype, cytokine, inducible NO synthase, and tissue factor mRNA expression, Transplantation, 71(1), 37-46.

CHAPTER IV

The presence of magnesium ions impairs M1 macrophage polarization: impact on the crosstalk with MSCs

Manuscript

In preparation

The presence of magnesium ions impairs M1 macrophage polarization: impact on the crosstalk with MSCs

Daniel M. Vasconcelos[1,2,3], Ana R. Almeida[1,2,3], Susana G. Santos[1,2] and Mário A. Barbosa[1,2,3]

[1] i3S- Instituto de Investigação e Inovação em Saúde, Universidade do Porto, Rua Alfredo Allen, 208, 4200-135, Porto, Portugal

[2] INEB - Instituto de Engenharia Biomédica, Universidade do Porto, Rua Alfredo Allen, 208, 4200-135, Porto, Portugal

[3] ICBAS - Instituto Ciências Biomédicas Abel Salazar, Universidade do Porto, Rua de Jorge Viterbo Ferreira 228, 4050-313 Porto, Portugal

Abstract

With the advent of immunomodulatory biomaterials, many strategies have been explored to promote pro-regenerative responses. Among those new therapies, the use of metal ions constitutes a promising tool to interact and modulate immune cells. Magnesium ions have been applied in clinics and research for several purposes, but their role on macrophage behavior remains unclear.

Herein, primary human macrophages were differentiated to macrophages in presence of extracellular levels of Mg^{2+} up to 10 mM. In this range of concentrations, Mg^{2+} ions were not cytotoxic and did not induce macrophage apoptosis. Cell elongation was observed for doses of 2.5 mM and 10 mM Mg^{2+}, but it was not accompanied by major changes on the levels of cell surface molecules and cytokine secretion. Anti-inflammatory effects of Mg^{2+} were observed in LPS-induced M1 macrophages. Remarkably, the expression of CD86 and secretion of IL-8 was significantly decreased in M1 macrophages exposed to levels of 2.5 mM and 10 mM Mg^{2+}. Likewise, for 10 mM Mg^{2+}, IL-10 levels were found reduced with concomitant increase of TGF-β1 production. A slight increase in TGF-β1 secretion was observed in IL-10-induced M2 macrophages exposed to a concentration of 2.5 mM of Mg^{2+}.

The influence of the altered macrophages secretome on the osteogenic differentiation of primary MSC was also assessed. Our findings showed that conditioned media from Mg^{2+}-treated macrophages led to ALP up-regulation at day 7. However, no significant changes were detected for key transcription factors involved in chondrogenesis (SOX9) and osteogenesis (RUNX2), what points that Mg^{2+} is supporting both differentiation pathways.

The ability of Mg^{2+} to control the inflammatory response and enhance tissue healing may prove valuable in maximizing the longevity of implantable biomaterials. Therefore, magnesium-based implants constitute interesting delivery systems of Mg^{2+} that can have an immunomodulatory role on the host response.

Keywords: magnesium, human macrophage, inflammation, immunomodulation

Introduction

The central role of the immune response in tissue regeneration and in the long-term performance of medical devices has prompted many attempts to develop immunomodulatory biomaterials [1]. In this context, interesting results have been obtained by using metal ions to modulate inflammation and healing processes [2]. Among metal ions, magnesium (Mg^{2+}) has been gathering increasing interest due to its recognized immunomodulatory properties [3; 4]. The fact that Mg is already applied in clinical practice, as an ion [5; 6] and as the major component of metal alloys used to fabricate implants [7; 8], which then release Mg^{2+} ions.

The interactions of Mg^{2+} and the immune system have been explored, with Mg^{2+} reported as exerting both pro-inflammatory [3] and anti-inflammatory effects [5; 9; 10]. In detail, exposing human NK and CD8+ T cells to 10 mM Mg^{2+} restored their cytotoxic functions against EBV-infected cells, which were previously impaired due to a deficiency in the magnesium transporter MAGT1 [3]. Conversely, other studies showed that LPS-induced production of pro-inflammatory cytokines (TNF-α, IL-6 and CCL2) may be reduced by treating both immune cells [5] and organs *ex-vivo* [10] with Mg^{2+}. Moreover, animal studies addressing the effects of Mg^{2+} deficiency revealed unbalanced immune responses, with increased production of pro-inflammatory cytokines [10; 11], and also impaired cartilage [12] and bone formation [13].

In research, magnesium supplementation has also been tested towards improved tissue engineering strategies with optimal results in response to levels up to 10 mM [14-16]. The direct effect of high extracellular concentrations of Mg^{2+} on mesenchymal stem/stromal cells (MSCs) have been studied, showing improved cell adhesion and promotion of chondrogenesis [15] and osteogenesis [17]. MSCs exposed to Mg^{2+}-enriched media revealed higher production of ALP and up-regulation of the pro-regenerative molecules TGF-β1, BMP-2 and SMAD4 [17].

Although the crosstalk between macrophages and MSC is recognized as critical for tissue healing and repair [18], the influence of Mg^{2+}-enriched environments on human macrophage polarization remains unclear. Therefore, the effect of therapeutic doses of Mg^{2+} on pro-inflammatory M1 (LPS-activated) and anti-inflammatory M2 (IL-10-activated) macrophages was explored here. Moreover, as MSC differentiation is affected by soluble factors released the immune cells [19], the indirect effect of Mg^{2+} supplementation of macrophages on MSC osteogenic differentiation was also assessed.

Materials and methods

Ethics statement

All samples obtained and procedures performed were according to the principles of the Declaration of Helsinki. The monocytes used in this study were isolated from surplus buffy coats (BC) from healthy blood donors kindly donated by the Immunohemotherapy department of Centro Hospitalar de São João (CHSJ; Porto, Portugal). All experimental protocols were conducted following the approval and recommendations of the Ethics Committee for Health from CHSJ. All samples were analyzed anonymously since researchers were not informed about age, gender or any identifying element.

Primary Human Monocyte Isolation and Culture

Human monocytes were isolated from healthy blood donors by negative selection, as previously described in [20]. Briefly, BCs were centrifuged (35 min, 1200 g, room temperature, without brake) and peripheral blood mononuclear cells (PBMCs) were collected. PBMCs were then incubated for 20 min with RosetteSep® human monocyte enrichment cocktail (StemCell Technologies, Grenoble, France), following manufacturer's instructions. After 1:1 dilution in PBS supplemented with 2% FBS (heat inactivated, Biowest, Nuaillé, France), cells were carefully layered over Histopaque®-1077 (Sigma-Aldrich, Madrid, Spain) and centrifuged (35 min, 1200 g, room temperature, without brake). The monocyte-enriched layer was collected and washed three times with PBS through centrifugation (17 min, 700 rpm, room temperature). Population purity was evaluated by flow cytometry analysis (FACS) and over 70% of the cells were found to be CD14+, as previously reported by our team [20]. Monocytes were seeded at 10^6 cells/ml on glass coverslip in 6 well or 24 well plates and cultured for 13 days to allow cells differentiation into macrophages.

Cells were incubated in a humidified incubator at 37ºC and with 5%CO_2 in RPMI 1610 medium supplemented with 10% heat inactivated FBS (Biowest) and 1% penicillin G-streptomycin (P/S, Invitrogen, Paisley, UK), without supplementation with M-CSF. Three extracellular levels of magnesium were tested since cell seeding: 0.4 mM Mg^{2+}, the basal Mg^{2+} concentration in RPMI, or supplemented with $MgSO_4$ (pharma grade, Sigma) to a final concentration of 2.5 mM and 10 mM. At day 10, media were replaced keeping the same levels of Mg^{2+} and part of monocytes/macrophages were activated with 10 ng/ml of Escherichia coli derived lipopolysaccharide (LPS, Sigma) or 10 ng/ml of IL-10 (Immunotools, Germany), for additional 72h, to induce macrophage polarization into pro-inflammatory M1 and anti-

inflammatory M2 phenotypes, respectively. Supernatants were collected under sterile conditions at day 13, centrifuged (13 000 rpm, 5min, 4ºC) and stored at -20ºC until further analysis or use to prepare conditioned media for MSC cultures.

Macrophage morphology

Macrophage aspect ratio was quantified using ImageJ software on brightfield images of macrophages incubated in 0.4 mM, 2.5 mM and 10 mM Mg^{2+} RPMI during 13 days. Aspect ratio was calculated as the quotient between the length of each cell major and minor axes, as previously described [21].

Magnesium cytotoxic effects assessment

The potential cytotoxicity of Mg^{2+}-enriched media on monocytes/macrophages was evaluated after 13 days of culture by live/dead staining and apoptosis evaluation. Briefly, live/dead assay was performed to evaluate the integrity of cell membrane. After washing with PBS, cells were incubated in the dark at 37ºC with calcein solution at 2 μM for 20 min, propidium iodide solution at 2 μM for 1 min, and afterwards images were acquired in an inverted fluorescence microscope (Carl Zeiss Axiovert 200). Additionally, cell viability was assessed and quantified by flow cytometry. Macrophages were gently detached incubating with accutase™ (BD Biosciences) for 30 min at 37ºC and stained using the BD Pharmingen™ Annexin V FITC apoptosis detection kit (BD Biosciences). Cells were acquired in a BD FACSCanto II™ using FACSDiva™ software, both from BD Biosciences. The proportion of dead cells (PI+), apoptotic cells (AnnexinV+ / PI-) and viable cells were quantified using Flow Jo software.

Metabolic activity quantification of macrophages in Mg^{2+}-enriched media

The metabolic activity of macrophages exposed to supra-physiological concentrations of Mg^{2+} and polarization stimuli (LPS and IL-10) was assessed using a resazurin assay. Briefly, culture media were replaced by resazurin solutions at 0.1mg/mL (Sigma), prepared using 0.4 mM, 2.5 mM and 10 mM Mg^{2+} RPMI, and incubated for 2 h. After incubation time, the medium was collected, 100 μL was transferred to a well of a black 96-well plate (triplicates were made) and the intensity of fluorescence at 590 nm after excitation at 530 nm was read using a microplate reader (Biotek – Sinergy HT). Fluorescence values obtained for 0.4 mM, 2.5 mM

and 10 mM Mg^{2+} RPMI in absence of cells were used as background control, and subtracted in the final analysis.

Analysis of macrophage surface molecules

The potential changes induced by enriched-Mg^{2+} media on the expression of cell surface molecules were assessed by FACS. At day 13, macrophages were gently harvested, washed and resuspended in FACS buffer- (PBS/2%FBS/0.01%Azide). Cell surface staining for FACS analysis was then performed by incubating for 30 min on ice with the following antibodies diluted in FACS buffer: anti-human CD14-APC (clone MEM-18), anti-human CD86-FITC (clone BU63), anti-human HLA-DR-FITC (clone MEM-12), all from Immunotools, anti-human CD163-PE (clone GHI/61, BD Biosciences) and anti-human CD206 (clone 19.2, BD Biosciences). Macrophages were also stained with the corresponding isotype controls, all from ImmunoTools, used to define background staining. Samples were then washed three times with FACS buffer, followed by fixation in 1% paraformaldehyde on ice until sample analysis (máx 24h). Cells were acquired on a Flow Cytometer (FACSCanto™ II, BD Biosciences) and 10.000 events were collected per sample. Data was analyzed using FlowJo software and mean fluorescence intensity (MFI) values were calculated by subtracting the corresponding isotype control.

Analysis of IL-6, IL-8, IL-10, IL-12, TNF-α and TGF-β1 concentration

The levels of secreted cytokines in culture supernatants were quantified by ELISA according to manufactures' instructions. The concentration of IL-6, IL-8, IL-10, IL-12, TNF-α were determined using Mini ELISA Development Kits (PeproTech) while the amount of TGF-β1 in supernatants was quantified by DuoSet® ELISA development system (R&D systems). Concentrations were determined for, at least, five donors per condition (n=5-8) and the percentages of effect were calculated by normalizing the concentrations by the value obtained for the basal condition (0.4 mM Mg^{2+} without LPS or IL-10 stimuli). Of note, the 10 ng/mL of IL-10 used to polarize M2 macrophages was subtracted to the levels of IL-10 determined in the supernatants of those macrophages.

Isolation and culture of primary human bone marrow mesenchymal stem/stromal cells

Human bone marrow MSC (mesenchymal stem/stromal cell) were isolated and characterized according the international stem cell society criteria, as previously described by our team [22]. Cells were cultured in flasks with Dulbecco's Modified Eagle Medium (DMEM; GIbco), low-glucose, supplemented with glutamax, 10% FBS Hyclone (MSC qualified) and 1% P/S. Media was changed twice a week. Cells were passaged at 80% confluence by washing twice the culture with warm PBS and detaching cells by using 0.05% trypsin EDTA (Gibco) for 5 min at 37ºC. Complete medium was added to inhibit trypsin and cells were transferred to a tube and centrifuged at 300 g for 10 min. The viable cells were counted using trypan blue and plated at a density of 3000 cells/cm^2 in 150 cm2 tissue culture flasks (BD Falcon).

Osteogenic differentiation

MSC were used in passages 6 and 7. A total of $10x10^3$ cells were seeded on 24 well plate and incubated at 37ºC for 24 h in 10% FBS Hyclone and 1% P/S. Afterwards, medium was completely changed for DMEM 10% FBS Gibco and 1% P/S to stop MSC expansion and stablish conditions that allow cell differentiation. Four controls were used: positive control (osteogenic medium: DMEM with 10% FBS, 1% P/S, 100 mM dexamethasone, 0.05 mM ascorbic acid and 10 mM β-glicerophosphate), negative control (basal medium: DMEM with 10% FBS and 1% P/S) and basal media with Mg^{2+} concentration adjusted to 2.5 mM and 10 mM using $MgSO_4$, as previously performed for monocyte/macrophage cell culture. Conditioned media from day 13 of culture with macrophages, from six different donors, were diluted in basal medium 1:2. For each condition, four replicates were prepared for gene expression analysis while two replicates were made for colorimetric evaluation of ALP synthesis. Media was changed twice a week until day 7 (gene expression) or day 14 (ALP staining).

Gene expression analysis

MSCs were homogenized at day 7 using TRIzol® (Life Technologies) according to the manufacturer's instructions. The amount and quality of extracted total RNA were evaluated by Nanodrop ND-1000 (Thermo Fisher Scientific) and by running RNA samples in a 2 % agarose gel. Samples were then treated with TURBO DNA-free™ kit (Life Technologies) to remove contaminating DNA from RNA preparations. cDNA was obtained from 1.2 μg of DNAse-treated RNA with random hexamers (Invitrogen) using Superscript III kit (Invitrogen) according to

manufacturer instructions. All primers used in qRT-PCR were inter-exonic and included: β2M, sense, 5'-CCAGCGTACTCCAAAGATTCAG-3', anti-sense, 5'-AGTCAACTTCAATGTCGGATGG -3'; ALP, sense, 5'-GACGGACCCGTCACTCTC-3', anti-sense, 5'-GTGCCCGTGGTCAATTCT-3'; RUNX2, sense, 5'-CCTGAACTCTGCACCAAGTC-3', anti-sense, 5'-GAGGTGGCAGTGTCATCATC-3'; SOX-9, sense, 5'-TTCCTCCTGCCTTTGCTTGT-3', anti-sense, 5'-CGTGCTTGAAACATTCCCAGAAC-3'. β2 microglobulin (B2M) was used as reference gene. Relative gene expression levels were calculated using the quantification cycle (Cq) method, according to MIQE guidelines [23].

ALP staining

Previous to ALP staining at day 14, MSC were washed twice with PBS and fixed with 4% paraformaldehyde. Cells were then incubated for 45 min at room temperature with ALP substrate, composed by 4% Naphtol AS-MX phosphate alkaline solution in Fast Violet B solution (both from Sigma). Samples were washed twice and kept in PBS at 4ºC until being observed and photographed using a stereomicroscope (Olympus). The acquired images were analyzed using an algorithm developed in Matlab to quantify ALP staining, as previously described by our team [24]. In detail, ALP-positive regions were empirically defined as red > 76; red > 1.1 x green; green < 1.12 x blue and the number of pixels that fulfil those criteria were quantified over the total image area.

Statistical analysis

Statistical analysis was performed using Prism software. Normality of data was assessed by visual inspection of histograms and Kolmogorov-Smirnov test. Student's t-test or repeated measures ANOVA with Bonferroni Correction, or their non-parametric counterpart (Friedman with Dunn's Multiple Comparison) were used to analyze data with Gaussian distribution. Statistical significance was considered for $p < 0.05$ (*); $p < 0.01$ (**) and $p < 0.001$ (***).

Results

Magnesium supplementation induced elongated macrophage morphology

The potential of Mg^{2+} to modulate monocytes/macrophages was assessed by supplementing cell culture media with magnesium sulfate to increase Mg^{2+} concentration up to 2.5 mM and 10 mM. Macrophages exposed to 2.5 and 10 mM Mg^{2+} for 13 days presented altered morphologies in comparison to the control (0.4 mM Mg^{2+}). When observed by light microscopy, macrophages cultured in 0.4 mM Mg^{2+} were a mixed population of round and stretched cells (Figure 1A). The proportion of elongated cells was slightly augmented in the 2.5 mM Mg^{2+} (Figure 1B) and longer membrane extensions were observed for 10 mM Mg^{2+} (Figure 1C). These observations were confirmed after quantification of the cell area (Figure 1D) and elongation factor (Figure 1E), which were significantly altered in a dose-dependent manner in macrophages exposed to increased levels of Mg^{2+}.

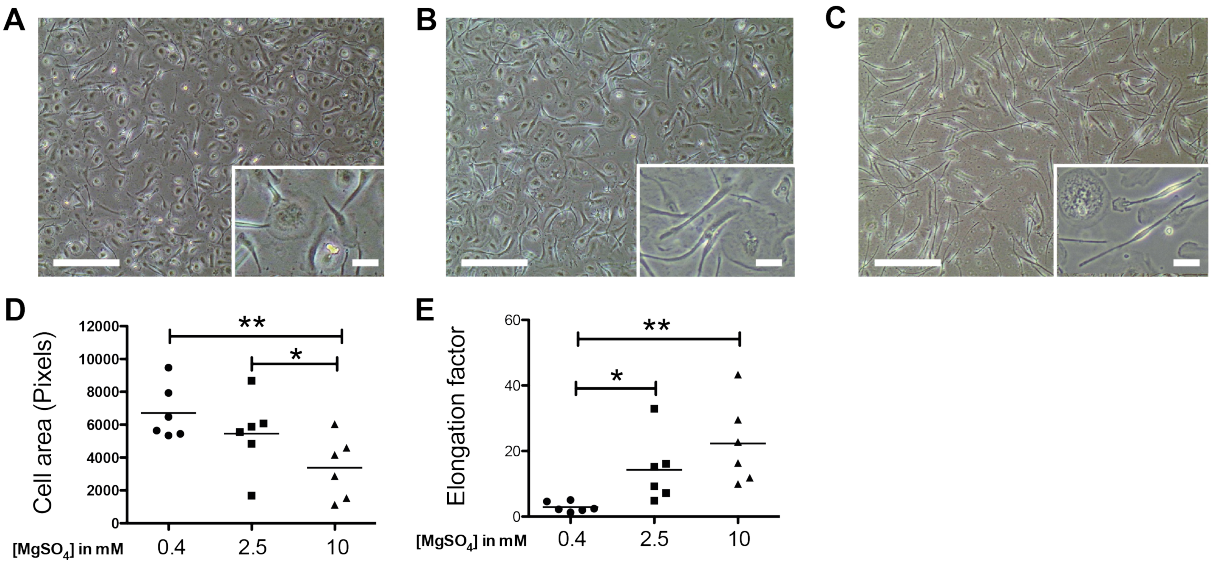

Figure 1. Macrophage elongation in response to increased levels of extracellular Mg^{2+}. **(A-C)** Light microscopy images of macrophages cultured along 13 days in presence of: **(A)** 0.4 mM, **(B)** 2.5 mM and **(C)** 10 mM Mg^{2+}. Results shown in A, B and C are representative of all donors tested (n=6). **(D)** Cell area and **(E)** elongation factor presented by macrophages in culture. Scale bars correspond to 300 μm while in small boxes value 30 μm. Results of all donors tested are presented (n=6). Repeated measures ANOVA with Bonferroni Correction was used to analyze data, *: $p<0.05$; **: $p<0.01$.

Macrophage survival was not affected by Mg^{2+} supplementation

To exclude possible cytotoxic effects induced by high levels of Mg^{2+}, we evaluated cell membrane integrity, apoptosis and metabolic activity presented by macrophages. The analysis of live/dead staining revealed similar number of dead cells (stained in red) for 0.4 mM, 2.5 mM and 10 mM Mg^{2+} (Figure 2A-C). Furthermore, similar percentages of apoptotic cells (Annexin V+ / PI -) and dead cells (PI +) were found for the three concentrations of Mg^{2+} (Figures 2D-F). When these were quantified over different donors, no significant differences were observed (Figure 2G). Moreover, the metabolic activity of macrophages cultured in Mg^{2+}-enriched media and activated with LPS or IL-10 was evaluated by measuring the fluorescence of resazurin reduced by cell mitochondria (Figure 2H). Data showed a significant increase of metabolic activity in macrophages exposed to 2.5 mM Mg^{2+}, but not to 10 mM Mg^{2+}, when compared to control (0.4 mM Mg^{2+}).

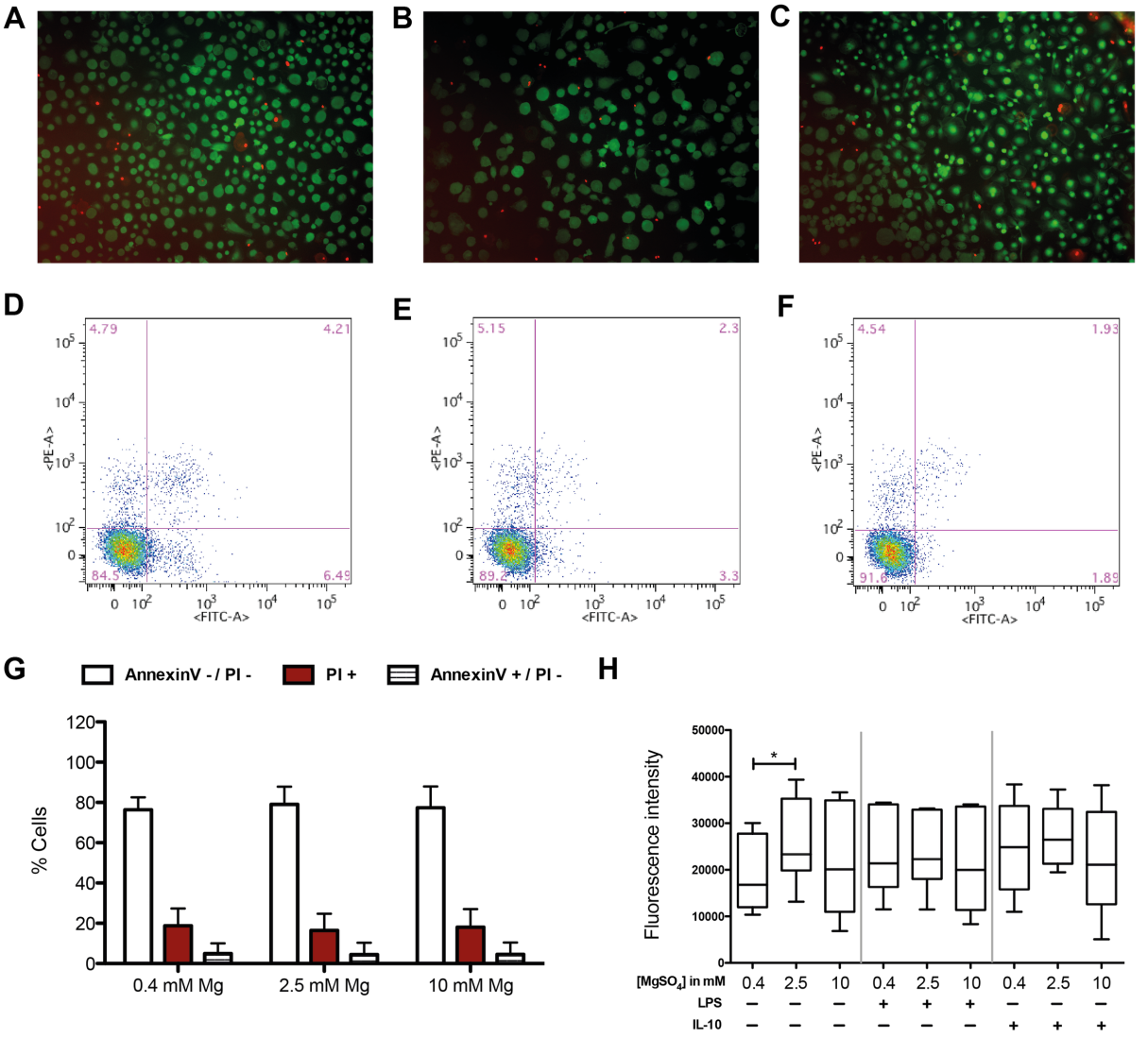

Figure 2. Mg^{2+}-enriched media did not induce cell apoptosis and death and 2.5 mM Mg^{2+} promotes higher metabolic activity. (A-C) Fluorescence microscopy images of macrophages cultured in 0.4 mM (A), 2.5 mM (B) and 10 mM Mg^{2+} RPMI (C) after calcein/propidium iodide staining at day 13. Live cells stained green while cells with damage membrane presented a red color. **(D-F)** Representative dot plots of macrophages stained with annexin V-FITC (X axis) and propidium iodide (Y axis) after exposure to 0.4 mM (D), 2.5 mM (E) and 10 mM Mg^{2+} levels (F). **(G)** Proportion of live (AnnexinV- / PI-), dead (PI+) and apoptotic (AnnexinV+ / PI-) cells determined by FACS analysis. **(H)** Metabolic activity of macrophages at day 13 analyzed by resazurin assay. Results of all donors tested are presented (n=6). Repeated measures ANOVA with Bonferroni Correction was used to analyze data, *: $p<0.05$).

Decreased CD86 expression on LPS-activated macrophages exposed to 2.5 mM and 10 mM Mg^{2+}

In order to evaluate the effect of increased levels of Mg^{2+} on macrophage polarization, cell surface markers associated to M1 (CD86 and HLA-DR) and M2 phenotypes (CD163 and CD206) were assessed at day 13. Results are illustrated in Figure 3A and show the changes in the different M1 and M2 markers with the polarization. When results were quantified across at least 7 different experiments (Figure 3B,C) we observed that exposure of unstimulated macrophages to increased levels of Mg^{2+} did not lead to significant changes in the cell surface expression of these molecules. Remarkably, the up-regulation of CD86 exhibited by M1 macrophages (LPS-activated cells) was significant decreased in macrophages exposed to 2.5 mM and 10 mM Mg^{2+} (Figure 3B). M1 macrophages also presented a tendency for up-regulation of HLA-DR and down-regulation of CD163, while no significant differences were observed for CD206 (Figure 3B,C). IL-10 stimulated macrophages presented a slight increase of CD163 expression, which was not affected by the Mg^{2+} treatment. Moreover, Mg^{2+} supplementation did not lead to important changes in cell surface molecules (CD86, HLA-DR and CD206) on M2 macrophages.

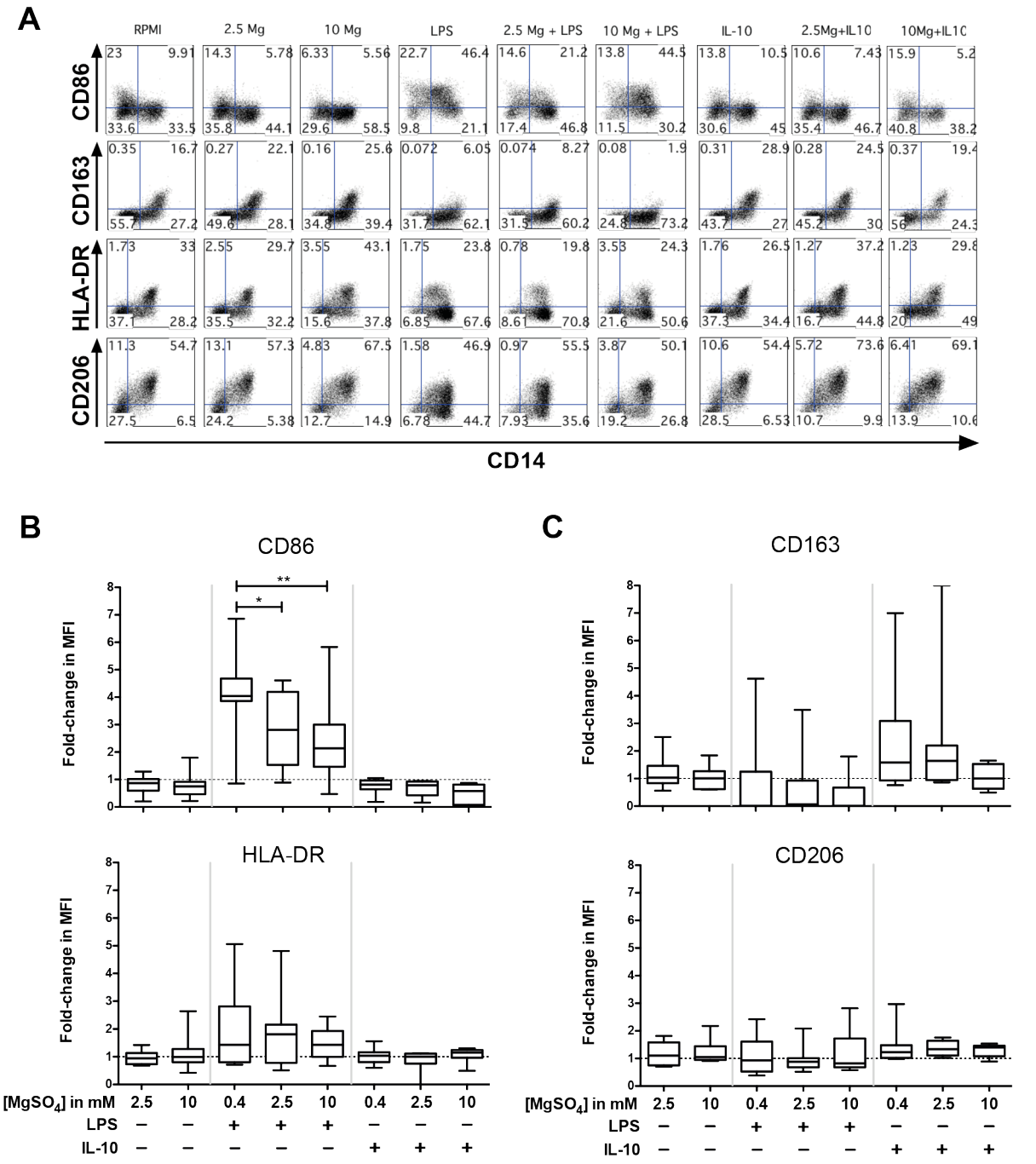

Figure 3. Magnesium supplementation induced downregulation of CD86 expression. Primary monocytes were isolated and cultured for 13 days, exposing cells to increased extracellular Mg^{2+} levels and different activation stimuli. **(A)** Dot plots of a representative donor, where values in each quadrant represent percentage of cells in that quadrant. **(B,C)** Mean fluorescence intensity (MFI) normalized by the control condition (non-stimulated macrophages/0.4mM Mg^{2+}) of M1 markers CD86 and HLA-DR (B) and M2 markers CD163 and CD206 (C). Results of all donors tested are presented (n=7-8). Repeated measures ANOVA with Bonferroni Correction was used to analyze data, *: $p<0.05$; **: $p<0.01$).

Macrophage cytokine production was influenced by the Mg^{2+} concentration

The soluble mediators produced by macrophage upon polarization were evaluated in cell culture supernatants at day 13. In order to minimize the influence of the inherent variability of response among donors, percentages of effect were calculated for the factors with detectable levels in the control condition (unstimulated macrophages 0.4 mM Mg^{2+}). The results are presented in Figure 4 and show that treatment of unstimulated macrophages with 2.5 mM and 10 mM Mg^{2+} media did not affect the secretion of the soluble factors tested in this study.

The production of TGF-β1 was down-regulated in M1 macrophages while increased levels of IL-10, IL-8, IL-6, IL-12 and TNF-α were found in the supernatants from those cells (Figure 4). The exposure of LPS-activated macrophages (M1) to 10 mM Mg^{2+}-enriched media seemed to rescue the secretion of TGF-β1 ($p=0.1046$) to similar concentration to the unstimulated macrophages (Figure 4A,B). Remarkably, the Mg^{2+} supplementation significantly damped the production of IL-8 (Figure 4C,D) induced by the activation with LPS. Similarly, a tendency to decreased secreted levels of IL-10 was observed in M1 macrophages exposed 10 mM Mg^{2+} (Figure 4E). No significant effect of Mg^{2+} treatment was registered regarding the secretion of IL-6, IL-12 and TNF-α (Figure 4F-H) in M1 macrophages.

The analysis of M2 macrophages showed a tendency for higher production of TGF-β1 in presence of 2.5 mM Mg^{2+}. Overall, this anti-inflammatory phenotype presented a similar cytokine profile to the unstimulated macrophages, with exception of the increased levels of IL-10 observed in those conditions.

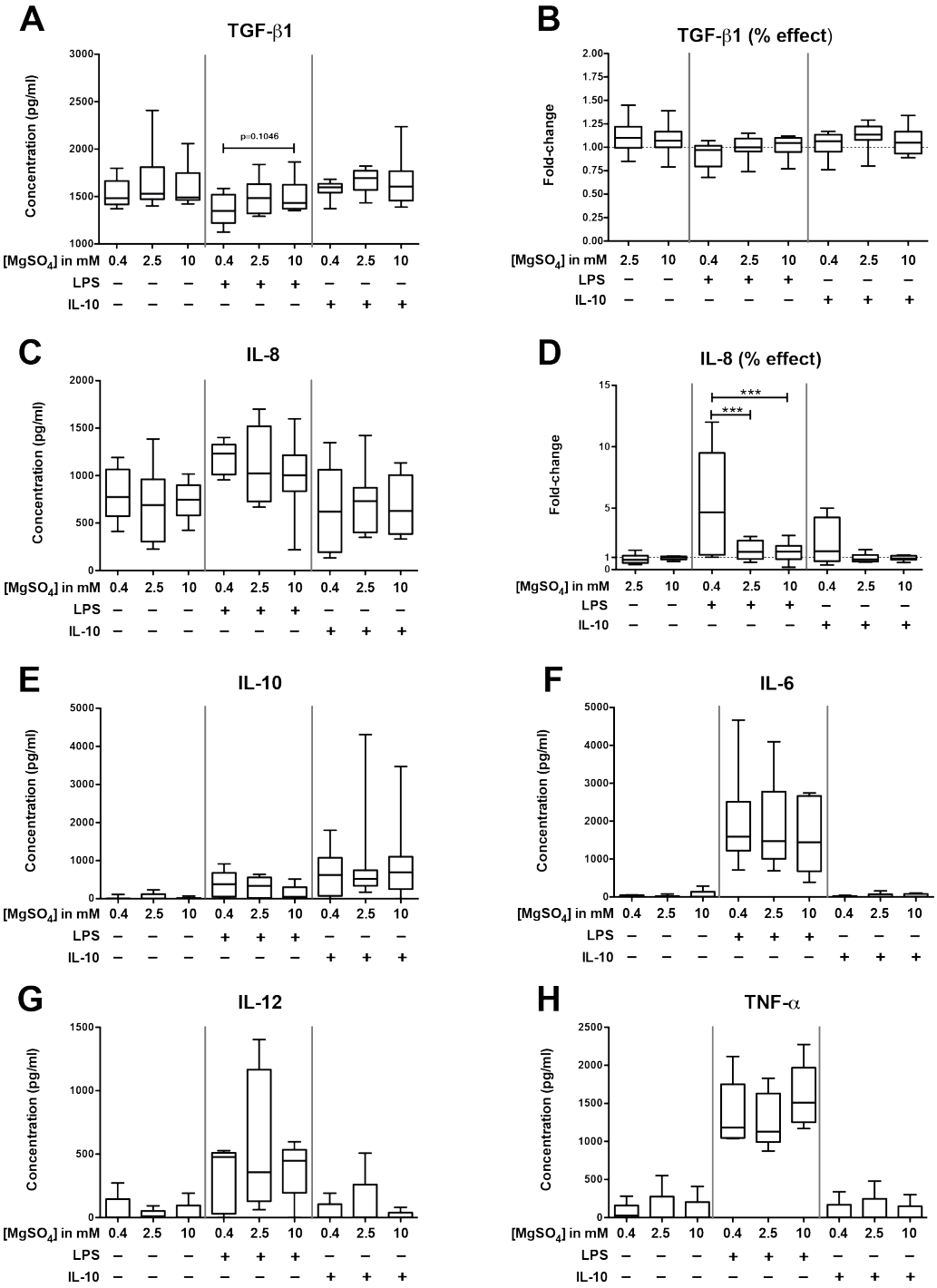

Figure 4. Cytokine profile was altered in macrophages cultured in 2.5 mM and 10 mM Mg^{2+} media. (A-B) TGF-β1, **(C-D)** IL-8, **(E)** IL-10, **(F)** IL-6, **(G)** IL-12 and **(H)** TNF-α release were determined by ELISA for, at least, five donors per condition (n=5-8), using cell culture supernatants from macrophages at day 13, three days after activation. Percentages of effect were calculated for cytokines with positive levels in control condition (non-stimulated macrophages in 0.4 mM Mg^{2+}) - TGF-β1 (B) and IL-8 (D). Repeated measures ANOVA with Bonferroni Correction (TGF-β1 and IL-8), or their non-parametric counterpart Friedman test with Dunn's Multiple Comparison test (IL-10, IL-6, IL-12 and TNF-α)were used to analyze data, ***: p<0.001).

Soluble factors produced by macrophages modulate MSC osteogenic differentiation

To evaluate the functional consequences of macrophage exposure to Mg^{2+} we investigated the potential of the secretome from macrophages exposed to the different conditions to promote MSC osteogenic differentiation. Moreover, MSCs were also culture in Mg^{2+}-enriched DMEM as control for the potential direct effect of Mg^{2+} on osteogenesis. MSC osteogenic differentiation was assessed in absence of other osteoinductive agents, namely ascorbic acid, β-glycerophosphate and dexamethasone. Unstimulated macrophages were able to promote ALP up-regulation in MSC while conditioned media (CM) from M1 macrophages induced a general down-regulation of ALP, RUNX2 and SOX9 (Figure 5A-C). Remarkably, the treatment of both unstimulated and M1 macrophages with 2.5 mM and 10 mM Mg^{2+} led to CM that increased mRNA levels of ALP on MSC. However, the quantification of ALP-stained areas showed that CM from non-stimulated macrophages led to an increased production of ALP in comparison to basal, being more intense for CM 0.4 mM Mg^{2+} and decreasing as the Mg^{2+} concentration increases (Figure 5D-I). A slight recovery of ALP staining was registered for MSCs cultured with CM from LPS-activated macrophages at 2.5 mM and 10 mM Mg^{2+} when compared to analogous condition at 0.4 mM Mg^{2+}.

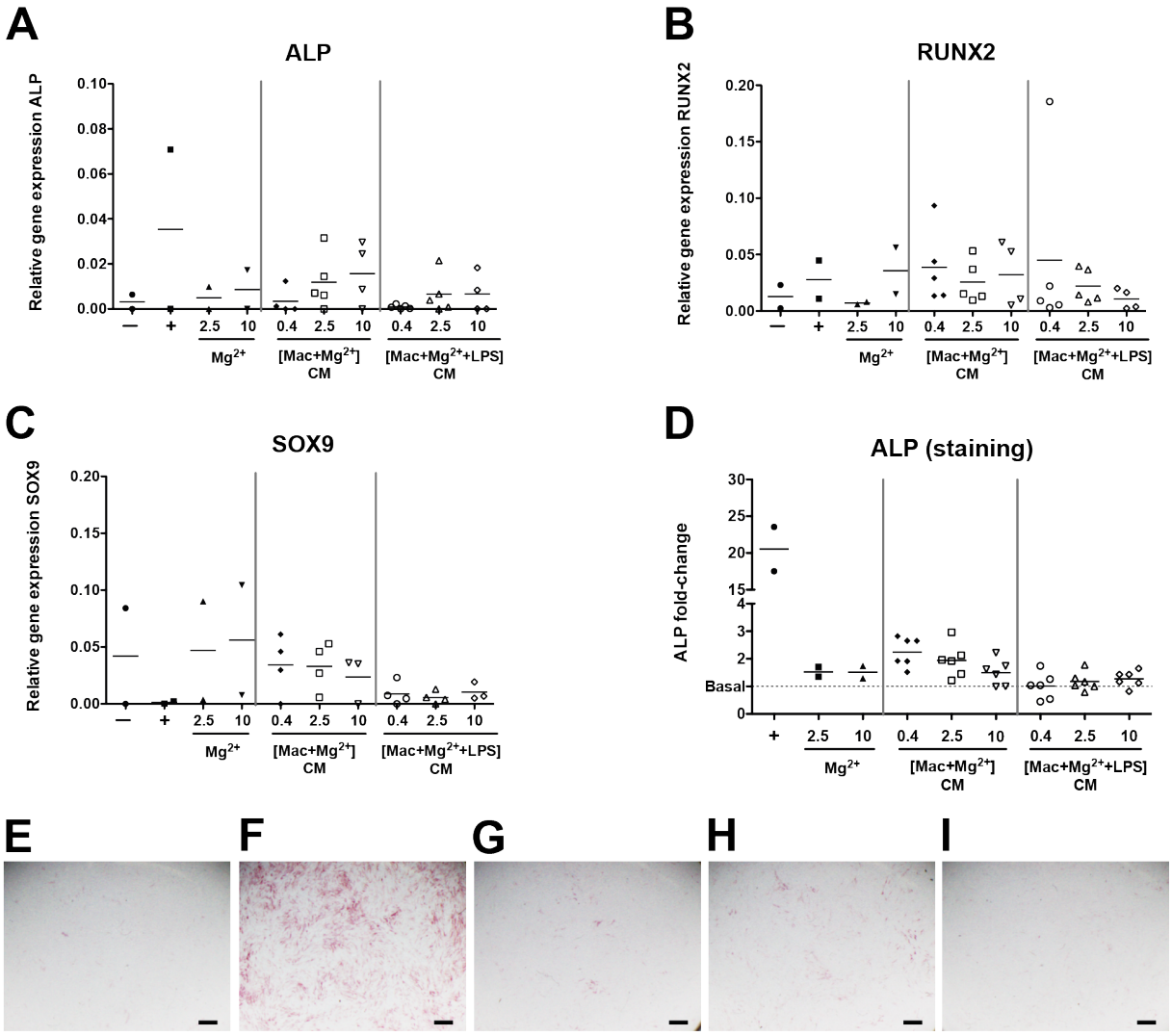

Figure 5. Conditioned media (CM) from macrophage culture promote the expression of key osteogenic markers. (A-C) ALP, RUNX2 and SOX9 mRNA levels were measured by qRT-PCR at day 7 for the following conditions: basal media (-), osteogenic media (+), Mg^{2+}-enriched DMEM, and media containing CM from macrophages differentiated in presence of increased levels of Mg^{2+} without [Mac+Mg^{2+}] or with LPS-induced activation [Mac+Mg^{2+}+LPS]. β2M gene was used as reference control (n=2-5). ALP staining was performed at day 14 of osteogenic differentiation assay. **(D)** ALP stained areas were quantified using Matlab and values were normalized by the basal condition (n=2-6). Representative pictures of ALP staining for the following conditions: **(E)** basal **(F)** osteogenic **(G)** 2.5 mM Mg^{2+} DMEM **(H)** CM 2.5 mM Mg^{2+} **(I)** CM 2.5 mM Mg^{2+} + LPS**.**

Discussion

In this study, we have found a positive effect of Mg^{2+} supplementation on macrophage behavior, leading to a decreased expression of pro-inflammatory markers. We believe that these findings are relevant in exploring the use of certain doses of Mg^{2+} as immunomodulatory.

The rational underlying this study was to understand to what extent Mg^{2+} influenced macrophage polarization towards M1 and M2 phenotypes, induced by LPS and IL-10, respectively. Moreover, biodegradable magnesium alloys for medical applications have gathered raising interest [7; 25]. In this context, the Mg^{2+} levels released by these biomaterials may constitute a promising approach to modulate implant-associated inflammation and promote tissue repair/regeneration.

The use of Mg^{2+} concentrations ranging from 2.5 mM to 10 mM has been previously explored at regulating immune responses involving NK cells [3], T cells [26] and monocytes/macrophages [5]. However, the role of those supraphysiological Mg^{2+} concentrations on macrophage polarization remained unclear. Moreover, since crosstalk between macrophages and MSCs likely plays a role in healing responses [18; 19; 27], this study also addressed the effect of macrophage CM on MSC behavior. Although the pro-osteogenic effect of Mg^{2+} in human MSCs has been described [14], little is known about the indirect effect of Mg^{2+} on MSC response, through the action of macrophages.

The analysis of cell morphology revealed a clear elongation and cell area reduction of the macrophages cultured in Mg^{2+}-enriched media. Morphological changes have been studied in the scope of macrophage polarization but controversial results are found in the literature [21; 28; 29]. Here, non-activated macrophages presented as a heterogeneous population with similar proportions of spindle-shaped fibroblastoid and large flat-round cells, in agreement with previous reports [28]. Human M1 macrophages are characterized by their elongate morphology while M2 macrophages are typically more round cells [28]. In our study, macrophages exposed to 2.5 mM and 10 mM Mg^{2+} media were predominantly elongated, resembling the M1 spindle-shaped fibroblastoid morphology. However, expression of cell surface receptors and secreted soluble factors revealed that non-activated macrophages treated with different Mg^{2+} concentrations presented similar profiles.

Therefore, the effect of Mg^{2+} is likely related to other mechanisms. Prescott and colleagues described Mg^{2+}-specific action on cell cytoskeleton, reporting disassembly of F-actin stress fibres by increasing intracellular Mg^{2+} levels with microinjections of 10 mM Mg^{2+} [30]. In a previous study, longer spindle-shaped fibroblasts were observed upon blockage of the transient receptor potential (TRPM7) [31], a key ion channel for Mg^{2+} homeostasis in the cell [32]. Considering that Mg^{2+}-enriched media will boost Mg^{2+} uptake and that intracellular Mg^{2+} levels negatively regulate TRPM7 activity [32], it is likely that the observed cell

morphologies are related to the interaction between Mg^{2+} and TRPM channels. It was previously reported the key role of TRPM7 in the differentiation of murine macrophages towards M2 phenotype through stimulation with IL-4 [33]. In detail, IL-4 promotes the activity of TRPM7 and the blockage of this ion channel led to loss of anti-inflammatory features, including the spindle-shaped morphology induced by IL-4 and M-CSF described by several authors for murine macrophages [21; 29]. Thus, interspecies difference regarding macrophage morphology may exist with murine macrophages presenting inverse morphologies for M1 and M2 phenotypes when compared to human cells.

Our study showed that the exposure to levels of Mg^{2+} up to 10 mM for 13 days does not impair macrophage survival. Moreover, macrophages cultured in 2.5 mM Mg^{2+} presented augmented metabolic activity, which is not associated to cell proliferation. As previously described, primary human macrophages have minimal mitotic activity *in vitro* [34] what is in line with the consistent number of cells observed throughout the 13 days of culture. Using cell lines, Feyerabend and colleagues [35] reported negative effects on cell viability in microenvironments with Mg^{2+} concentrations above 10-20 mM. Moreover, a prior study addressed *in vitro* the influence of Mg^{2+} supplementation on human osteoclasts, showing that levels of 5 and 10 mM Mg^{2+} led to increased metabolic activity at day 14 and higher expression of TRAP [36]. Taken together, those findings are in accordance to our data, confirming that, in certain doses, Mg^{2+} induces higher cell metabolic activity.

Magnesium exerts major effects on M1 macrophages induced upon activation with LPS. Both tested concentrations damped, at least in part, the pro-inflammatory action of LPS especially in the cell surface expression levels of co-stimulatory molecule CD86, and regarding the secretion of TGF-β1, IL-8 and IL-10. CD86 is a typical marker of the pro-inflammatory M1 phenotype, is involved in T cell activation and its highly expressed in response to metal ions such as nickel [37-39]. The selective decrease of CD86 expression in human monocytes/macrophages has been observed in clinical scenarios of immunotolerance [40; 41]. In detail, macrophages in decidual tissue, a region of immunological tolerance at the interface between the mother and the fetus, presented lower levels of CD86 in comparison to circulatory monocytes while CD80 and HLA-DR showed comparable values [40]. In agreement, diminished expression of CD86 was observed on monocytes from critical care patients with compensatory anti-inflammatory response syndrome [41]. The effect of Mg^{2+} supplementation on the expression of CD86 in LPS-activated macrophages was not addressed in previous studies. Therefore, our data on the profile of surface molecules on macrophages showed that Mg^{2+} seems to have a regulatory role in LPS activation, leading to immunological tolerance.

An immunoregulatory role has been attributed to Mg^{2+} mostly due to the up-regulation of pro-inflammatory cytokines such as TNF-α, IL-6 and MCP-1 in scenarios of Mg^{2+} deficiency [11]. Furthermore, previous studies reported that magnesium supplementation led to

decreased production of pro-inflammatory cytokines including IL-6 [5; 42], TNF-α [5; 10] as well as other LPS-induced immune mediators [10]. In overall, Mg^{2+} seems to promote immunoregulatory phenotypes, specially by decreasing IL-8, IL-10, but rescuing the secretion of TGF-β1 lost due to LPS activation.

Our findings showed that 2.5 mM and 10 mM Mg^{2+}-media did not deeply impact the behavior of IL-10-induced M2 macrophages. Although a significant increase in TGF-β1 secretion was observed in macrophages exposed to 2.5 mM Mg^{2+}, the three conditions stimulated with IL-10 presented similar expression of both surface molecules and soluble factors. So, the role of Mg^{2+} on the polarization of human macrophages seems to be mostly in reducing the M1 response, without inducing major changes in M2 phenotype.

The potential effect of Mg^{2+} on osteogenic differentiation through modulation macrophage behavior was assessed in this study. We have chosen to test MSC response in absence of other osteoinductive molecules to evaluate the capacity of Mg^{2+} modulate the differentiation of MSCs into osteoblasts. Overall, MSCs cultured with supernatants from Mg^{2+}-treated macrophages presented an up-regulation of ALP, which may be associated to the higher concentrations of TGF-β1 detected in the supernatants from those macrophage cultures. This finding is in line with a previous *in vitro* study reporting increased expression of ALP in human MSCs upon TGF-β1 supplementation [43]. Moreover, MSCs exposed to media with 4 mM Mg^{2+} revealed higher production of ALP at day 14 while pro-regenerative molecules TGF-β1, BMP-2 and SMAD4 were up-regulated in cells cultured for 3 days with Mg extracts [17]. Similarly, a study showed that 10 mM Mg^{2+} induce higher ALP activity in human MSCs cultured in osteogenic conditions during 3 weeks [14]. Additionally, the Mg^{2+} uptake to cell through TRPM7 was demonstrated as critical for *in vivo* biomineralization [44]. At day 7, a tendency for a small augment of the expression levels of RUNX2, a key transcription factor involved in osteogenic differentiation [45], was registered in CM conditions. Moreover, the expression of SOX9 was particularly low in presence of LPS-CM while high mRNA levels of SOX9 was registered in non-LPS CM conditions in comparison to osteogenic condition. SOX9 is a major regulator of chondrogenesis [46] and its expression is known to be strongly impaired by classical pro-inflammatory cytokines such as TNF-α [47], which was in high levels in LPS CMs. Additionally, the expression of SOX9 is known to be reduced in presence of low levels of Mg^{2+} [12]. Likewise, the ratio between SOX9 and RUNX2 was reported to decrease during healthy osteogenic differentiation of MSCs by other authors [45]. Therefore, our results show that tested Mg^{2+} concentrations modulate macrophages behavior to support MSC osteogenic differentiation. Those findings are in line with previous studies reporting improved chondrogenesis [15] and osteogenesis [48] in presence of Mg^{2+} levels ranging from 2.5 mM and 10 mM.

Conclusions

In conclusion, our findings have revealed a regulatory effect of Mg^{2+} in concentrations of 2.5 mM and 10 mM on human macrophages. This study suggests the use of Mg^{2+} to modulate macrophage phenotype as a therapeutic strategy, especially in scenarios involving the pro-inflammatory M1 phenotype and exacerbated expression of CD86 and secretion IL-8. Unstimulated and M2 macrophages maintained their phenotypic features when cultured in Mg^{2+}-enriched media. The use of concentrations of Mg^{2+} ranging 2.5 and 10 mM is a feasible strategy in clinics to dampen the M1 macrophages responses, without impairing tissue healing.

Acknowledgments

This work was funded by the project (NORTE-01-0145-FEDER-000012), supported by Norte Portugal Regional Operational Programme (NORTE 2020), under the PORTUGAL 2020 Partnership Agreement, through the European Regional Development Fund (ERDF). DMV was supported by a PhD fellowship SFRH/BD/87516/2012 from FCT - Fundação para a Ciência e a Tecnologia. The authors thank to the Immunohemotherapy service of Centro Hospitalar de São João E.P.E. for the kind donation of buffy-coats. Moreover, the authors acknowledge Raquel Gonçalves and Joana Ferreira for providing MSCs and Silvia Bidarra for kindly donate the hSOX-9 primers.

References

[1] - Vishwakarma, A., N. S. Bhise, M. B. Evangelista, J. Rouwkema, M. R. Dokmeci, A. M. Ghaemmaghami, N. E. Vrana, and A. Khademhosseini (2016), Engineering Immunomodulatory Biomaterials To Tune the Inflammatory Response, Trends Biotechnol, 34(6), 470-482.

[2] - Mourino, V., J. P. Cattalini, and A. R. Boccaccini (2012), Metallic ions as therapeutic agents in tissue engineering scaffolds: an overview of their biological applications and strategies for new developments, Journal of the Royal Society, Interface / the Royal Society, 9(68), 401-419.

[3] - Chaigne-Delalande, B., et al. (2013), Mg2+ regulates cytotoxic functions of NK and CD8 T cells in chronic EBV infection through NKG2D, Science, 341(6142), 186-191.

[4] - Lee, C. H., Z. H. Wen, Y. C. Chang, S. Y. Huang, C. C. Tang, W. F. Chen, S. P. Hsieh, C. S. Hsieh, and Y. H. Jean (2009), Intra-articular magnesium sulfate (MgSO4) reduces experimental osteoarthritis and nociception: association with attenuation of N-methyl-D-aspartate (NMDA) receptor subunit 1 phosphorylation and apoptosis in rat chondrocytes, Osteoarthritis Cartilage, 17(11), 1485-1493.

[5] - Sugimoto, J., A. M. Romani, A. M. Valentin-Torres, A. A. Luciano, C. M. Ramirez Kitchen, N. Funderburg, S. Mesiano, and H. B. Bernstein (2012), Magnesium decreases inflammatory cytokine production: a novel innate immunomodulatory mechanism, Journal of immunology, 188(12), 6338-6346.

[6] - Mami, A. G., J. Ballesteros, O. P. Mishra, and M. Delivoria-Papadopoulos (2006), Effects of magnesium sulfate administration during hypoxia on Ca(2+) influx and IP(3) receptor modification in cerebral cortical neuronal nuclei of newborn piglets, Neurochem Res, 31(1), 63-70.

[7] - Zhang, Y., et al. (2016), Implant-derived magnesium induces local neuronal production of CGRP to improve bone-fracture healing in rats, Nat Med, 22(10), 1160-1169.

[8] - Cheng, M. Q., T. Wahafu, G. F. Jiang, W. Liu, Y. Q. Qiao, X. C. Peng, T. Cheng, X. L. Zhang, G. He, and X. Y. Liu (2016), A novel open-porous magnesium scaffold with controllable microstructures and properties for bone regeneration, Sci Rep, 6, 24134.

[9] - Rochelson, B., O. Dowling, N. Schwartz, and C. N. Metz (2007), Magnesium sulfate suppresses inflammatory responses by human umbilical vein endothelial cells (HuVECs) through the NFkappaB pathway, Journal of reproductive immunology, 73(2), 101-107.

[10] - Dowling, O., P. K. Chatterjee, M. Gupta, H. B. T. Tam, X. Xue, D. Lewis, B. Rochelson, and C. N. Metz (2012), Magnesium sulfate reduces bacterial LPS-induced inflammation at the maternal-fetal interface, Placenta, 33(5), 392-398.

[11] - Tam Tam, H. B., O. Dowling, X. Xue, D. Lewis, B. Rochelson, and C. N. Metz (2011), Magnesium sulfate ameliorates maternal and fetal inflammation in a rat model of maternal infection, Am J Obstet Gynecol, 204(4), 364 e361-368.

[12] - Gruber, H. E., J. Ingram, H. J. Norton, L. Y. Wei, A. Frausto, B. G. Mills, and R. K. Rude (2004), Alterations in growth plate and articular cartilage morphology are associated with reduced SOX9 localization in the magnesium-deficient rat, Biotech Histochem, 79(1), 45-52.

[13] - Rude, R. K., H. E. Gruber, H. J. Norton, L. Y. Wei, A. Frausto, and J. Kilburn (2005), Dietary magnesium reduction to 25% of nutrient requirement disrupts bone and mineral metabolism in the rat, Bone, 37(2), 211-219.

[14] - Yoshizawa, S., A. Brown, A. Barchowsky, and C. Sfeir (2014), Magnesium ion stimulation of bone marrow stromal cells enhances osteogenic activity, simulating the effect of magnesium alloy degradation, Acta Biomater, 10(6), 2834-2842.

[15] - Shimaya, M., T. Muneta, S. Ichinose, K. Tsuji, and I. Sekiya (2010), Magnesium enhances adherence and cartilage formation of synovial mesenchymal stem cells through integrins, Osteoarthritis Cartilage, 18(10), 1300-1309.

[16] - Janning, C., E. Willbold, C. Vogt, J. Nellesen, A. Meyer-Lindenberg, H. Windhagen, F. Thorey, and F. Witte (2010), Magnesium hydroxide temporarily enhancing osteoblast activity and decreasing the osteoclast number in peri-implant bone remodelling, Acta Biomater, 6(5), 1861-1868.

[17] - Li, R. W., N. T. Kirkland, J. Truong, J. Wang, P. N. Smith, N. Birbilis, and D. R. Nisbet (2014), The influence of biodegradable magnesium alloys on the osteogenic differentiation of human mesenchymal stem cells, J Biomed Mater Res A, 102(12), 4346-4357.

[18] - Vasandan, A. B., S. Jahnavi, C. Shashank, P. Prasad, A. Kumar, and S. J. Prasanna (2016), Human Mesenchymal stem cells program macrophage plasticity by altering their metabolic status via a PGE2-dependent mechanism, Sci Rep, 6, 38308.

[19] - Lacey, D. C., P. J. Simmons, S. E. Graves, and J. A. Hamilton (2009), Proinflammatory cytokines inhibit osteogenic differentiation from stem cells: implications for bone repair during inflammation, Osteoarthritis Cartilage, 17(6), 735-742.

[20] - Oliveira, M. I., S. G. Santos, M. J. Oliveira, A. L. Torres, and M. A. Barbosa (2012), Chitosan drives anti-inflammatory macrophage polarisation and pro-inflammatory dendritic cell stimulation, Eur Cell Mater, 24, 136-152; discussion 152-133.

[21] - McWhorter, F. Y., T. Wang, P. Nguyen, T. Chung, and W. F. Liu (2013), Modulation of macrophage phenotype by cell shape, Proc Natl Acad Sci U S A, 110(43), 17253-17258.

[22] - Almeida, C. R., D. P. Vasconcelos, R. M. Goncalves, and M. A. Barbosa (2012), Enhanced mesenchymal stromal cell recruitment via natural killer cells by incorporation of inflammatory signals in biomaterials, Journal of the Royal Society, Interface / the Royal Society, 9(67), 261-271.

[23] - Bustin, S. A., et al. (2009), The MIQE guidelines: minimum information for publication of quantitative real-time PCR experiments, Clin Chem, 55(4), 611-622.

[24] - Almeida, M. I., A. M. Silva, D. M. Vasconcelos, C. R. Almeida, H. Caires, M. T. Pinto, G. A. Calin, S. G. Santos, and M. A. Barbosa (2016), miR-195 in human primary mesenchymal stromal/stem cells regulates proliferation, osteogenesis and paracrine effect on angiogenesis, Oncotarget, 7(1), 7-22.

[25] - Zhao, D., F. Witte, F. Lu, J. Wang, J. Li, and L. Qin (2017), Current status on clinical applications of magnesium-based orthopaedic implants: A review from clinical translational perspective, Biomaterials, 112, 287-302.

[26] - Li, F. Y., B. Chaigne-Delalande, C. Kanellopoulou, J. C. Davis, H. F. Matthews, D. C. Douek, J. I. Cohen, G. Uzel, H. C. Su, and M. J. Lenardo (2011), Second messenger role for Mg2+ revealed by human T-cell immunodeficiency, Nature, 475(7357), 471-476.

[27] - San Emeterio, C. L., C. E. Olingy, Y. Chu, and E. A. Botchwey (2017), Selective recruitment of non-classical monocytes promotes skeletal muscle repair, Biomaterials, 117, 32-43.

[28] - Cassol, E., L. Cassetta, C. Rizzi, M. Alfano, and G. Poli (2009), M1 and M2a polarization of human monocyte-derived macrophages inhibits HIV-1 replication by distinct mechanisms, Journal of immunology, 182(10), 6237-6246.

[29] - Schilling, T., F. Miralles, and C. Eder (2014), TRPM7 regulates proliferation and polarisation of macrophages, J Cell Sci, 127(Pt 21), 4561-4566.

[30] - Prescott, A. R., J. G. Comerford, R. Magrath, N. J. Lamb, and R. M. Warn (1988), Effects of elevated intracellular magnesium on cytoskeletal integrity, J Cell Sci, 89 (Pt 3), 321-329.

[31] - Su, L. T., W. Liu, H. C. Chen, O. Gonzalez-Pagan, R. Habas, and L. W. Runnels (2011), TRPM7 regulates polarized cell movements, Biochem J, 434(3), 513-521.

[32] - Schmitz, C., A.-L. Perraud, C. O. Johnson, K. Inabe, M. K. Smith, R. Penner, T. Kurosaki, A. Fleig, and A. M. Scharenberg (2003), Regulation of Vertebrate Cellular Mg2+ Homeostasis by TRPM7, Cell, 114(2), 191-200.

[33] - Compan, V., et al. (2012), Cell volume regulation modulates NLRP3 inflammasome activation, Immunity, 37(3), 487-500.

[34] - Keast, D., and G. D. Birnie (1969), Incorporation of [3H] uridine ad [3H] thymidine by murine peritoneal macrophages in vitro, Biochem J, 114(2), 42P.

[35] - Feyerabend, F., J. Fischer, J. Holtz, F. Witte, R. Willumeit, H. Drucker, C. Vogt, and N. Hort (2010), Evaluation of short-term effects of rare earth and other elements used in magnesium alloys on primary cells and cell lines, Acta Biomater, 6(5), 1834-1842.

[36] - Wu, L., B. J. Luthringer, F. Feyerabend, A. F. Schilling, and R. Willumeit (2014), Effects of extracellular magnesium on the differentiation and function of human osteoclasts, Acta Biomater, 10(6), 2843-2854.

[37] - Subauste, C. S., R. W. Malefyt, and F. Fuh (1998), Role of CD80 (B7.1) and CD86 (B7.2) in the Immune Response to an Intracellular Pathogen, The Journal of Immunology, 160, 1831-1840.

[38] - Mantovani, A., A. Sica, S. Sozzani, P. Allavena, A. Vecchi, and M. Locati (2004), The chemokine system in diverse forms of macrophage activation and polarization, Trends Immunol, 25(12), 677-686.

[39] - Manome, H., S. Aiba, and H. Tagami (1999), Simple chemicals can induce maturation and apoptosis of dendritic cells, Immunology, 98, 481-490.

[40] - Heikkinen, J., M. Mottonen, J. Komi, A. Alanen, and O. Lassila (2003), Phenotypic characterization of human decidual macrophages, Clin Exp Immunol, 131(3), 498-505.

[41] - Wolk, K., C. Hoflich, H. Zuckermann-Becker, W. D. Docke, H. D. Volk, and R. Sabat (2007), Reduced monocyte CD86 expression in postinflammatory immunodeficiency, Crit Care Med, 35(2), 458-467.

[42] - Amash, A., G. Holcberg, E. Sheiner, and M. Huleihel (2010), Magnesium sulfate normalizes placental interleukin-6 secretion in preeclampsia, J Interferon Cytokine Res, 30(9), 683-690.

[43] - Zhang, H., M. Ahmad, and G. Gronowicz (2003), Effects of transforming growth factor-beta 1 (TGF-beta1) on in vitro mineralization of human osteoblasts on implant materials, Biomaterials, 24(12), 2013-2020.

[44] - Nakano, Y., M. H. Le, D. Abduweli, S. P. Ho, L. V. Ryazanova, Z. Hu, A. G. Ryazanov, P. K. Den Besten, and Y. Zhang (2016), A Critical Role of TRPM7 As an Ion Channel Protein in Mediating the Mineralization of the Craniofacial Hard Tissues, Front Physiol, 7, 258.

[45] - Loebel, C., E. M. Czekanska, M. Bruderer, G. Salzmann, M. Alini, and M. J. Stoddart (2015), In vitro osteogenic potential of human mesenchymal stem cells is predicted by Runx2/Sox9 ratio, Tissue Eng Part A, 21(1-2), 115-123.

[46] - Pan, Q., Y. Yu, Q. Chen, C. Li, H. Wu, Y. Wan, J. Ma, and F. Sun (2008), Sox9, a key transcription factor of bone morphogenetic protein-2-induced chondrogenesis, is activated through BMP pathway and a CCAAT box in the proximal promoter, Journal of cellular physiology, 217(1), 228-241.

[47] - Murakami, S., V. Lefebvre, and B. de Crombrugghe (2000), Potent inhibition of the master chondrogenic factor Sox9 gene by interleukin-1 and tumor necrosis factor-alpha, J Biol Chem, 275(5), 3687-3692.

[48] - Wu, L., F. Feyerabend, A. F. Schilling, R. Willumeit-Romer, and B. J. Luthringer (2015), Effects of extracellular magnesium extract on the proliferation and differentiation of human osteoblasts and osteoclasts in coculture, Acta Biomater, 27, 294-304.

CHAPTER V

Concluding Remarks and Future Perspectives

The original proposal for the Doctoral dissertation presented herein was the modulation of the immune response induced by implantable biomaterials. This topic reflects the growing interest and the shift from inert implants to immunomodulatory biomaterials, ongoing in the field [1; 2]. In fact, orthopedic implants fail mostly due to biological factors, highly associated to the inability of those biomaterials at promoting tissue healing. In this context, new solutions to modulate the biological response to biomaterials are required.

Although fibrinogen and metal ions have been perceived as exclusive pro-inflammatory agents [3; 4], they may exert immunomodulation when applied in controlled doses and/or arrangements. Hence, we aimed at exploring new therapies based on fibrinogen and metal ions that mitigate the drawbacks presented by the orthopedic devices currently used in clinical practice. Our objectives have been to (1) identify key immune cell populations and molecules involved in the immune response induced by hip implant, (2) develop a new protein-based biomaterial with immunomodulatory properties for bone regeneration, (3) test the regulatory effect of magnesium ions on macrophages behavior as a therapeutic application of biodegradable magnesium alloys.

Hip prostheses fail mostly due to aseptic loosening (AL) [5], a pathological bone resorption induced by an exacerbated immune response against prosthetic debris. In an effort to understand this immune response, the synovial tissues and blood collected from both osteoarthritis (OA) and AL patients were analyzed by histological and molecular techniques. Artificial hip joints constitute a good clinical model and together with laboratorial studies shed light on cellular mechanisms underlying prosthetic debris toxicity and immune response in presence of high levels of particles and ions [6; 7].

This study revealed that macrophages are the most prevalent immune cell type within a foreign body response underlying aseptic loosening. In this clinical scenario, both M1 and M2 macrophage phenotypes were observed while in OA macrophages were in lower number and mostly confined to the synovial membrane. Conversely, the expression of classical immune mediators in synovial tissues were found similar in OA and AL patients, which was, at least in part, unexpected. According to the literature, the pro-inflammatory cytokines TNF-α, IL-1β and IL-6 have been considered the key mediators involved in aseptic loosening [8; 9]. However, recent publications report findings in line with our data [10], and have clarified the role of other molecules such as IFN-γ and TLR4 in aseptic loosening [11]. Our strategy addressed molecules previously pointed out as targets by other authors using *in vitro* assays [8; 9] and working with animal models [12]. Although this focused approach likely missed changes in the levels of other molecules, which are also important in the assessed pathologies, our work provides a different view on the inflammatory status of synovial tissues in both OA and AL. In the future, the use of high-throughput technologies may provide valuable insights on biological events that have been poorly explored in the context of AL, namely the neuro-immune axis.

Additionally, the standardization of synovial tissue retrieval is challenging yet critical for the accuracy of the obtained results. The use of samples from OA patients allows to overcome the lack of access to healthy synovial tissue. However, the use of OA tissues as control is a limitation of the majority of studies because two different immune responses are being compared in a pathological context. Due to the number of factors influencing the immune response involved in AL, further studies must include more defined populations, by applying more strict inclusion criteria, namely regarding the presence of relevant comorbidities with impact on the immune system. Additionally, future works should focus more on the ratio between mediators than in their absolute level of expression. This has been evident as recently described in a study revealing the importance of the relative concentration of IFN-γ in the pathophysiology of AL [11] while earlier reports did not found significant differences of IFN-γ levels between AL and control groups [10; 13].

The significant changes regarding the expression of TGF-β1 in AL patients led us to evaluate the levels of this mediator in the bloodstream. The identification of systemic biomarkers of early aseptic loosening and osteolysis has been explored by many research groups with the objective of developing new diagnostic tools. However, there is no solid evidence that support the use of molecules as biomarkers for early implant failure [14]. In our study, both OA and AL groups showed concentrations of TGF-β1 ranging between similar intervals, as well as the proportions of monocytes, lymphocytes and neutrophils in circulation. Therefore, we believe that in humans the pathological responses occurring at the hip seem to be mostly confined to the joint [15].

The immune response against particles and ions released by implants has a central role in aseptic loosening. While major efforts have been done by manufacturers to reduce the amount of prosthetic debris produced over time, the development of therapies to modulate the immune response is still limited to research. The promising results obtained by the use of immunomodulator drugs such as methotrexate [16], IL-4 [17] and NF-kB decoy oligos [18] in treating particle-induced osteolysis support further development of immunomodulatory biomaterials to mitigate aseptic loosening.

Unbalanced immune responses in the context of joint replacement are undesirable and the therapeutic alternatives to treat hip failure still lead to poor clinical outcomes [19; 20]. The gold standard solution in managing aseptic loosening is revision surgery, which involves the replacement of one component, typically the acetabular cup [21], or both faulty implants. However, this approach does not aim at solving the ongoing immune response to the released prosthetic debris [22]. Additionally, orthopedic surgeons are often challenged with the lack of bone tissue at the site of the implant, which impairs implant fixation [20]. Therefore, revision

surgeries are technically demanding and, even when bone graft materials are used, periprosthetic bone repair and proper implant fixation are difficult to achieve [23].

Inspired in these challenges faced by orthopedic surgeons, we proposed the development of an immunomodulatory biomaterial capable of promoting bone repair/regeneration. Implants made of pure fibrinogen (Fg-3D) were prepared and stabilized without the use of enzymes, and then implanted in a femoral critical bone defect. This innovative biomimetic approach aimed to establish a pro-regenerative environment by modulating the inflammatory response. Fg-3D presented a structure somewhat similar to the blood clot formed during the first days of bone healing response. Fg-3D implantation led to accelerated formation of granulation tissue at the injury site, visible 6 days post-implantation. Locally, Fg-3D did not potentiate the inflammatory response induced by bone injury but promoted significant changes in the proportions of key immune cell populations at systemic level. Bone healing with periosteal repair was observed in animals implanted with Fg-3D at 8 weeks post-implantation. The reduction of Mac-1 receptor (CD11b/CD18)-expressing cells systemically lead us to speculate that those cells may be found locally, but this could not be confirmed either by histology or gene expression analysis. Although Fg has been classically perceived as a pro-inflammatory molecule [3; 24], the rearrangement of the molecule in a 3D structure (Fg-3D) induces molecular changes with impact upon the biological response. In detail, a recent study demonstrated a distinct macrophage response to fibrin and soluble Fg, with fibrin gels promoting an M2-like phenotype [25]. Earlier studies had also shown differential responses when human monocytes and dendritic cells were exposed to soluble or adsorbed Fg [24; 26]. Our group has been exploring different ways of presenting Fg, namely adsorbed to Ch substrates. We previously reported that human monocytes interact with the Fg adsorbed on Ch surfaces through TLR4, inducing increased expression of BMP-2 [27]. In presence of same substrates, macrophages increased production of pro-healing factors, such as BMP-7, platelet-derived growth factor, TGF-β3, IGF and VEGF [28].

Our study is one the first reports showing the systemic nature of the response to bone injury and the implantation of biomaterials. Recently, another group has promoted the repair of muscle tissue by modulating the host adaptive immune system after applying an immunomodulatory biomaterial [29]. Increasing efforts have been applied in the development of new biomaterials engineered for immunomodulation and tissue regeneration [30]. The Fg-3D scaffolds presented in this Thesis offer several advantages in comparison to other materials already used in the clinical arena. The porous structure of Fg-3D turns cell migration and proliferation within the biomaterial easier than in the hydrogel-structure of fibrin sealants, which have been tested for tissue engineering purposes [31; 32]. Moreover, Fg-3D provides a biomimetic matrix to close tissue defects providing pro-regenerative signals along the healing response. As a biodegradable biomaterial, Fg-3D avoids foreign body response in the long

term and improves integration and promote tissue regeneration. Therefore, we envisage that Fg-3D may be used as an immunomodulatory biomaterial, as a delivery system or even as a coating for conventional biomaterials in order to improve their early biological response.

Fibrinogen-based systems integrate the orthobiologic strategies, an emerging field that includes protein therapeutics, cell-based regenerative therapies and biomimetic matrixes. Although promising, orthobiologics are still in their infancy but novel products will likely emerge from exploring the new cellular and molecular targets, that result from the increasing knowledge on osteoimmunology. Furthermore, the combination of orthobiologic tools with conventional biomaterials might mitigate some of the drawbacks related to their soft mechanical properties. The fibrinogen biomimetic material presented in this Thesis constitutes a promising approach to modulate host biological response but its application in Orthopedics in limited to confined and relative small bone defects. Although the mechanical properties of Fg-3D may be reinforced by its combination with metals and ceramics, the application of these immunomodulatory biomaterials could be explored in other contexts such as soft tissue lesions. Moreover, Fg-3D may have a role in cancer immunotherapy due to its systemic reduction of Mac-1+ myeloid cells, which was previously show to improve tumor response to radiotherapy [33].

Also in the context of this Thesis, we proposed to explore the use of metal ions to modulate macrophage response. In this context, magnesium ions (Mg^{2+}) may constitute an interesting tool due to its immunomodulatory and pro-regenerative effects. Certain doses of Mg^{2+} have been associated to regulatory effects on some immune populations [34] but the role of Mg^{2+} in macrophage polarization remained unclear. Therefore, the differentiation of human macrophages was assessed in presence of extracellular levels of Mg^{2+} up to 10 mM. Our findings showed that Mg^{2+} has an anti-inflammatory effect, particularly in presence of M1 polarizing stimuli, such as LPS, leading to decreased cell surface expression of CD86 and secretion of IL-8, IL-10 and secretion of higher levels of TGF-β1. Unstimulated and IL-10-activated macrophages did not present significant changes in Mg^{2+}-enriched media. This study clarified the immunoregulatory effect of Mg^{2+} upon macrophages supporting its use in clinical scenarios of exacerbated M1 macrophages response.

Although few reports have addressed the effect of Mg^{2+} on macrophages, the existing literature seems to corroborate, at least in part, the behavior observed by us for this immune cell population. Sugimoto and colleagues reported anti-inflammatory effects of 2.5 mM Mg^{2+} on primary human macrophages with decreased production of TNF-α and IL-6. These findings contrast with the secreted levels of TNF-α and IL-6 observed by us for M1 macrophages exposed to basal (0.4 mM), 2.5 mM or even 10 mM Mg^{2+}. While we measured TNF-α and IL-6 concentrations by ELISA, Sugimoto determined the percentage of positive cells after

intracellular staining for those targets and measured their expression at mRNA level 2-4 hours after stimulating the cells with LPS. We believe that the differences between the two approaches, perhaps allied to the inherent differences among individuals and populations, may account for the dissimilarities to the results previously reported. Moreover, in line with Sugimoto's report, levels of Mg^{2+} between 2 and 3 mM Mg^{2+} reduced the placental secretion of IL-6 in pre-eclampsia [35]. However, other cell populations may be responding to Mg^{2+} treatment. Our major findings upon macrophage secretome were a dampening effect of Mg^{2+} on IL-8 and IL-10 secretion. A similar reduction of IL-8 was previously reported for decidual cells [36] while the decrease of IL-10 levels may be related to the up-regulation induced by LPS activation. Overall, Mg^{2+} has an immunomodulatory role on macrophages but further studies, combining laboratorial and clinical observations, are required to clarify the complete effects of this ion.

Magnesium is currently used in clinical practice in different ways. In Obstetrics, magnesium sulfate up to 3 mM is administrated in preeclamptic women to control seizures and inflammation, protecting the fetus from neurological damage. Conversely, in Orthopedics biodegradable magnesium alloys are applied in bone fracture fixation. However, the application of controlled levels of Mg^{2+} for modulating the response of immune cells to biomaterials remains widely unexplored. Although fundamental studies on the influence of Mg^{2+} on various cell populations are lacking, new therapies may be envisaged taking profit from the immunoregulatory effects of Mg^{2+}. In this context, this Thesis supports the use of a patch made from Fg, for example, to deliver controlled concentration of Mg^{2+} into soft tissue lesions or attached to orthopedic prostheses.

The lessons learned from conventional implants highlighted the instrumental role of the immune system in the well-functioning of medical devices. Thus, a next generation of implantable medical devices should provide adequate biological signals to the host, benefiting from new biomaterials engineered to modulate immune responses and healing processes. In this sense, this Doctoral thesis clarified the macrophage-driven response underlying hip prosthesis failure and proposed two strategies, which can be combined for immunomodulation using fibrinogen and metal ions.

References

[1] - Franz, S., S. Rammelt, D. Scharnweber, and J. C. Simon (2011), Immune responses to implants - a review of the implications for the design of immunomodulatory biomaterials, Biomaterials, 32(28), 6692-6709.

[2] - Hotaling, N. A., L. Tang, D. J. Irvine, and J. E. Babensee (2015), Biomaterial Strategies for Immunomodulation, Annu Rev Biomed Eng, 17, 317-349.

[3] - Ryu, J. K., et al. (2015), Blood coagulation protein fibrinogen promotes autoimmunity and demyelination via chemokine release and antigen presentation, Nat Commun, 6, 8164.

[4] - Konttinen, Y. T., and J. Pajarinen (2013), Adverse reactions to metal-on-metal implants, Nat Rev Rheumatol, 9(1), 5-6.

[5] - Graves, S. (2011), National Joint Replacement Registry Annual Report 2011*Rep.*, Australian Orthopaedic Association.

[6] - Revell, P. A. (2008), The combined role of wear particles, macrophages and lymphocytes in the loosening of total joint prostheses, J R Soc Interface, 5(28), 1263-1278.

[7] - Antonios, J. K., Z. Yao, C. Li, A. J. Rao, and S. B. Goodman (2013), Macrophage polarization in response to wear particles in vitro, Cell Mol Immunol, 10(6), 471-482.

[8] - Landgraeber, S., M. Jager, J. J. Jacobs, and N. J. Hallab (2014), The pathology of orthopedic implant failure is mediated by innate immune system cytokines, Mediators Inflamm, 2014, 185150.

[9] - Caicedo, M. S., P. H. Pennekamp, K. McAllister, J. J. Jacobs, and N. J. Hallab (2010), Soluble ions more than particulate cobalt-alloy implant debris induce monocyte costimulatory molecule expression and release of proinflammatory cytokines critical to metal-induced lymphocyte reactivity, J Biomed Mater Res A, 93(4), 1312-1321.

[10] - Jamsen, E., V. P. Kouri, J. Olkkonen, A. Cor, S. B. Goodman, Y. T. Konttinen, and J. Pajarinen (2014), Characterization of macrophage polarizing cytokines in the aseptic loosening of total hip replacements, J Orthop Res, 32(9), 1241-1246.

[11] - Jamsen, E., V. P. Kouri, M. Ainola, S. B. Goodman, D. C. Nordstrom, K. K. Eklund, and J. Pajarinen (2017), Correlations between macrophage polarizing cytokines, inflammatory

mediators, osteoclast activity, and toll-like receptors in tissues around aseptically loosened hip implants, J Biomed Mater Res A, 105(2), 454-463.

[12] - Mediero, A., S. R. Frenkel, T. Wilder, W. He, A. Mazumder, and B. N. Cronstein (2012), Adenosine A2A receptor activation prevents wear particle-induced osteolysis, Sci Transl Med, 4(135), 135ra165.

[13] - Loria, M. P., et al. (2004), Role of cytokines in gonarthrosis and knee prosthesis aseptic loosening, J Orthop Sci, 9(3), 274-279.

[14] - Sumner, D. R., R. Ross, and E. Purdue (2014), Are there biological markers for wear or corrosion? A systematic review, Clin Orthop Relat Res, 472(12), 3728-3739.

[15] - Glyn-Jones, S., A. J. Palmer, R. Agricola, A. J. Price, T. L. Vincent, H. Weinans, and A. J. Carr (2015), Osteoarthritis, Lancet 386(9991), 376-387.

[16] - Mediero, A., M. Perez-Aso, T. Wilder, and B. N. Cronstein (2015), Brief Report: Methotrexate Prevents Wear Particle-Induced Inflammatory Osteolysis in Mice Via Activation of Adenosine A2A Receptor, Arthritis Rheumatol, 67(3), 849-855.

[17] - Rao, A. J., C. Nich, L. S. Dhulipala, E. Gibon, R. Valladares, S. Zwingenberger, R. L. Smith, and S. B. Goodman (2013), Local effect of IL-4 delivery on polyethylene particle induced osteolysis in the murine calvarium, J Biomed Mater Res A, 101(7), 1926-1934.

[18] - Goodman, S. B., et al. (2014), Novel biological strategies for treatment of wear particle-induced periprosthetic osteolysis of orthopaedic implants for joint replacement, J R Soc Interface, 11(93), 20130962.

[19] - Postler, A. E., F. Beyer, T. Wegner, J. Lutzner, A. Hartmann, I. Ojodu, and K. P. Gunther (2016), Patient-reported outcomes after revision surgery compared to primary total hip arthroplasty, Hip Int, 0.

[20] - Beswick, A., and A. W. Blom (2011), Bone graft substitutes in hip revision surgery: a comprehensive overview, Injury, 42 Suppl 2, S40-46.

[21] - Watts, C. D., M. P. Abdel, A. D. Hanssen, and M. W. Pagnano (2016), Anatomic Hip Center Decreases Aseptic Loosening Rates After Total Hip Arthroplasty with Cement in Patients with Crowe Type-II Dysplasia: A Concise Follow-up Report at a Mean of Thirty-six Years, J Bone Joint Surg Am, 98(11), 910-915.

[22] - Mihalko, W. M., M. A. Wimmer, C. A. Pacione, M. P. Laurent, R. F. Murphy, and C. Rider (2014), How have alternative bearings and modularity affected revision rates in total hip arthroplasty?, Clin Orthop Relat Res, 472(12), 3747-3758.

[23] - Gross, C. E., J. Huh, C. Green, S. Shah, J. K. DeOrio, M. Easley, and J. A. Nunley, 2nd (2016), Outcomes of Bone Grafting of Bone Cysts After Total Ankle Arthroplasty, Foot Ankle Int, 37(2), 157-164.

[24] - Kuhns, D. B., D. A. Priel, and J. I. Gallin (2007), Induction of human monocyte interleukin (IL)-8 by fibrinogen through the toll-like receptor pathway, Inflammation, 30(5), 178-188.

[25] - Hsieh, J. Y., T. D. Smith, V. S. Meli, T. N. Tran, E. L. Botvinick, and W. F. Liu (2017), Differential regulation of macrophage inflammatory activation by fibrin and fibrinogen, Acta Biomater, 47, 14-24.

[26] - Thacker, R. I., and G. S. Retzinger (2008), Adsorbed fibrinogen regulates the behavior of human dendritic cells in a CD18-dependent manner, Exp Mol Pathol, 84(2), 122-130.

[27] - Oliveira, M. I., M. L. Pinto, R. M. Goncalves, M. C. Martins, S. G. Santos, and M. A. Barbosa (2017), Adsorbed Fibrinogen stimulates TLR-4 on monocytes and induces BMP-2 expression, Acta Biomater, 49, 296-305.

[28] - Maciel, J., M. I. Oliveira, E. Colton, A. K. McNally, C. Oliveira, J. M. Anderson, and M. A. Barbosa (2014), Adsorbed fibrinogen enhances production of bone- and angiogenic-related factors by monocytes/macrophages, Tissue Eng Part A, 20(1-2), 250-263.

[29] - Sadtler, K., et al. (2016), Developing a pro-regenerative biomaterial scaffold microenvironment requires T helper 2 cells, Science, 352(6283), 366-370.

[30] - Vishwakarma, A., N. S. Bhise, M. B. Evangelista, J. Rouwkema, M. R. Dokmeci, A. M. Ghaemmaghami, N. E. Vrana, and A. Khademhosseini (2016), Engineering Immunomodulatory Biomaterials To Tune the Inflammatory Response, Trends Biotechnol, 34(6), 470-482.

[31] - Kim, B. S., H. J. Kim, J. G. Choi, H. K. You, and J. Lee (2015), The effects of fibrinogen concentration on fibrin/atelocollagen composite gel: an in vitro and in vivo study in rabbit calvarial bone defect, Clin Oral Implants Res, 26(11), 1302-1308.

[32] - Kim, B. S., and J. Lee (2015), Enhanced bone healing by improved fibrin-clot formation via fibrinogen adsorption on biphasic calcium phosphate granules, Clin Oral Implants Res, 26(10), 1203-1210.

[33] - Ahn, G. O., D. Tseng, C. H. Liao, M. J. Dorie, A. Czechowicz, and J. M. Brown (2010), Inhibition of Mac-1 (CD11b/CD18) enhances tumor response to radiation by reducing myeloid cell recruitment, Proc Natl Acad Sci U S A, 107(18), 8363-8368.

[34] - Chaigne-Delalande, B., et al. (2013), Mg2+ regulates cytotoxic functions of NK and CD8 T cells in chronic EBV infection through NKG2D, Science, 341(6142), 186-191.

[35] - Amash, A., G. Holcberg, E. Sheiner, and M. Huleihel (2010), Magnesium sulfate normalizes placental interleukin-6 secretion in preeclampsia, J Interferon Cytokine Res, 30(9), 683-690.

[36] - Makhlouf, M. A., and H. N. Simhan (2006), Effect of tocolytics on interleukin-8 production by human amniotic and decidual cells, J Reprod Immunol, 69(1), 1-7.